POCKET-TYPE REINFORCED BRICKWORK RETAINING WALLS

John Tellett, B.Sc.

A thesis submitted for the Degree of
Doctor of Philosophy

Department of Engineering Science,
The University of Warwick.

The experimental work was carried out in the laboratories of the British Ceramic Research Association Ltd. and the theoretical work was carried out at the University of Warwick.

April, 1984.

SYNOPSIS

From the literature survey it is clear that reinforced brickwork pocket type retaining walls are a well established form of construction in the USA, however, only a small number have been built in the UK. This is surprising since cost studies have consistently indicated that pocket type construction is more economical than fair-faced concrete walls. The available and forthcoming design guidance on reinforced brickwork is reviewed. The main aim of this research was to investigate the structural performance of pocket type walls in relation to the requirement of the Draft Code for Reinforced Masonry.

Reported within are the method and results of an experimental research programme. In all six walls and fifteen beams were tested. The parameters examined were brick type, percentage of reinforcement, slenderness and shear span ratio. Flexural failure occurred in all the walls and in the medium-lightly reinforced beams whilst only the heavily reinforced beams failed in shear. The experimental results were predicted accurately when analysed using the flexural design equations in the Draft Code. However the Code requirements for shear appear to be unduly conservative.

Concurrent with the experimental work a finite element program was developed to analyse pocket type walls. In spite of the many assumptions made in the modelling of material properties there was good agreement between analytical and experimental results.

Subsequently a parametric survey was undertaken. The variables selected for examination were slenderness, pocket spacing, panel thickness percentage of reinforcement and arching action in the panels. Both rectangular and flanged sections were investigated. The results indicated that the Draft Code gave good predictions when flexural failure of the stem occurred. But when panel failure developed neither yield line analysis nor arching theory was able to predict collapse. Guidance is given on the sizing of panels.

It is concluded that pocket type walls, when designed to the requirements of the Draft Code, perform adequately at serviceability and ultimate design loads for pocket spacings upto 1.0m. Further experimental work is nessecary to establish whether the guidance given in the Code is applicable to walls with pocket spacings greater than 1.0m.

CONTENTS

LIST OF PLATES

NOTATION

A_s	Area of tension reinforcement
a	Shear span
a',b'	Dimensions of plate element in x and y directions respectively.
[B]	Matrix which relates internal displacements to nodal strains.
b	breadth
b_e	Effective breadth
[C]	Matrix relating $\{\alpha\}$ to $\{\delta^e\}$
C_{ij}	Elasticity coefficients in [D] matrix
[D]	Material property matrix
d	Effective depth to tension reinforcement
E_b	Elastic modulus of brickwork
E_s	Elastic modulus of steel
f_c	Uniaxial compressive strength of brickwork
f_k	Characteristic compressive strength of brickwork
f_s	Uniaxial tensile strength of steel reinforcement
f_t	Uniaxial tensile strength of brickwork
f_v	Characteristic shear strength of brickwork
f_y	Charactristic tensile strength of steel reinforcement
h	Height
I	Second moment of area of a section
I_{cr}	Second moment of area of a cracked section
[K]	Global stiffness matrix
$[K^e]$	Element stiffness matrix

l	length
l_p	pocket spacing
M	Bending moment
M_d	Design moment of resistance of a section
M_p, N_p	Bending moment and normal force per unit length
n	Neutral axis depth
$\{P\}$	Load vector
$[Q]$	Matrix relating $[C]$ to $[B]$
$R_{ij}, S_{ij}, T_{i/}$	Elastic properties of eccentric plate element
$S_o S_n$	Measure of potential energy in previous and present iterations respectively
t_f	Flange thickness
u, v, w	components of displacement in the x,y & z directions respectively
V	Shear force
v	Shear stress
W_n, W_m	Weigthing function for Gauss quadrature
x, y, z	Cartesian coordinate axes
Z_1, Z_2	Distance from reference surface to top and bottom layers of element
z^1	Lever arm
α	Aspect ratio, h/l_p
$\{\alpha\}$	vector of coefficients $\alpha_1 - \alpha_{24}$
β	Degree of tension stiffening
$\gamma_f, \gamma_{mm}, \gamma_{ms}, \gamma_{mv}$	Partial safety factors for loads, brickwork, steel and shear
Δ	Displacement

$\{\delta\}$	Displacement vector
ε_1-ε_4	Transition strains
$\varepsilon_x, \varepsilon_y$	Normal strains in x and y directions
$\{\varepsilon\}$	Strain vector
η	Acceleration scalar
ν	Poisson's ratio
ρ	Density
θ	Rotation
σ, τ	Stress
σ_n, σ_p	Stress
σ	Stress resultant vector
τ_{xy}	Shear stress
ϕ_D, ϕ_R, ϕ_F	Convergence tolerances for iterations
χ	Curvature
ψ	Tolerance for η

Superscripts

$[\ ]^{-1}$	Inverse of matrix
$[\ ]^T$	Transpose of matrix
e	Element

Subscripts

b	Brickwork
ex	Excess
i, j	i th row and j the column of a matrix
m, m+1	Iterative vectors and scalars

o,n	old and new
s	steel
x,y,z	coordinate axes

POCKET-TYPE REINFORCED BRICKWORK RETAINING WALLS

John Tellett, B.Sc.

A thesis submitted for the Degree of

Doctor of Philosophy

Department of Engineering Science,

The University of Warwick.

The experimental work was carried out in the laboratories of the British Ceramic Research Association Ltd. and the theoretical work was carried out at the University of Warwick.

April, 1984.

SYNOPSIS

From the literature survey it is clear that reinforced brickwork pocket type retaining walls are a well established form of construction in the USA, however, only a small number have been built in the UK. This is surprising since cost studies have consistently indicated that pocket type construction is more economical than fair-faced concrete walls. The available and forthcoming design guidance on reinforced brickwork is reviewed. The main aim of this research was to investigate the structural performance of pocket type walls in relation to the requirement of the Draft Code for Reinforced Masonry.

Reported within are the method and results of an experimental research programme. In all six walls and fifteen beams were tested. The parameters examined were brick type, percentage of reinforcement, slenderness and shear span ratio. Flexural failure occurred in all the walls and in the medium-lightly reinforced beams whilst only the heavily reinforced beams failed in shear. The experimental results were predicted accurately when analysed using the flexural design equations in the Draft Code. However the Code requirements for shear appear to be unduly conservative.

Concurrent with the experimental work a finite element program was developed to analyse pocket type walls. In spite of the many assumptions made in the modelling of material properties there was good agreement between analytical and experimental results.

Subsequently a parametric survey was undertaken. The variables selected for examination were slenderness, pocket spacing, panel thickness percentage of reinforcement and arching action in the panels. Both rectangular and flanged sections were investigated. The results indicated that the Draft Code gave good predictions when flexural failure of the stem occurred. But when panel failure developed neither yield line analysis nor arching theory was able to predict collapse. Guidance is given on the sizing of panels.

It is concluded that pocket type walls, when designed to the requirements of the Draft Code, perform adequately at serviceability and ultimate design loads for pocket spacings upto 1.0m. Further experimental work is nessecary to establish whether the guidance given in the Code is applicable to walls with pocket spacings greater than 1.0m.

Acknowledgements

I am grateful to Don Foster for suggesting that the research I was about to undertake at the British Ceramic Research Association would be an interesting subject for a thesis. Indeed this proved to be the case.

I am indebted to the British Ceramic Research Association for allowing me to publish the experimental work which forms part of their research programme into the structural behaviour of brickwork. In particular I would like to thank Dr. G. J. Edgell for his advice and guidance and also the technical staff without whom this would not have been possible.

My gratitude extends to my supervisor, Dr. I. M. May for his guidance and appraisal, to Structural Clay Products Ltd. for allowing me to complete the theoretical work and to Mrs. Trudy Foster for typing the manuscript.

Finally I dedicate this thesis to my wife, Rachel, for her support and encouragement during the last four and a half years.

Declaration

In collaboration with others the author has published a number of articles relating to aspects of the work reported within. All the experimental and theoretical work was carried out under the supervision of Dr. I.M. May and Dr. G.J. Edgell. The publications were as follows:

1. Tellett J "Tests on reinforced pocket-type retaining walls", Proc. of the C.I.B. working commission W23A on Bearing Walls held at the British Ceramic Research Assocn., Stoke-on-Trent, pp71-81, Sept 1981.

2. Tellett J, Edgell G J and West H W H "Research into the structural behaviour of pocket-type retaining walls", B.Ceram.R.A., Tech Note 329, March 1982.

3. Edgell G J, Tellett J and West H W H "research into the behaviour of reinforced pocket-type retaining walls" Proc. 3rd North American Masonry Symposium, August 1982.

4. Tellett J and Edgell G J "The structural behaviour of reinforced brickwork pocket-type retaining walls" B.Ceram.R.A., Tech Note 353, Sept. 1983.

5. May I M and Tellett J "Non-linear finite element analysis of reinforced and unreinforced brickwork" Preprints of the 8th Int. Symp. on Loadbearing Brickwork, London, Nov. 1983.

1. REVIEW OF THE LITERATURE ON REINFORCED BRICKWORK

1.1 Introduction.

Reinforced brickwork, as the name implies, consists of brickwork in which lengths of suitable material, normally steel, are embedded and so placed that the brickwork will have a greatly increased resistance to forces producing tensile, shearing and compressive stresses. Thus it is a structural material which may be used to construct rationally designed elements such as walls, columns, beams and slabs.

Although reinforced brickwork was first used over 150 years ago, it is only during the last 60 years that systematic testing of reinforced brickwork structures has been carried out to determine their behaviour under load. These tests have mainly been performed abroad, notably in the U.S.A.. The results from these tests have shown that there is very little difference between the behaviour of reinforced brickwork and reinforced concrete structures.

Reinforced brickwork has been adopted widely abroad, especially in areas liable to seismic action, thereby testifying to its economic application, but until recently its use in this country has been very limited. The main reason for this may have been the lack of relevant design information available to structural engineers together with the inadequate guidance given in the current Code of Practice, CP111:1970[1]. A prerequisite to

improving this situation is to assertain in greater detail the structural performance of reinforced brickwork. During the last decade, as part of this process, a substantial amount of research data has been accumulated and this is being used to produce a new Code of Practice for reinforced masonry[3].

The research reported within this thesis is part of the research effort that currently is being undertaken into the performance of reinforced brickwork. It is hoped that in the near future this will ensure reinforced brickwork is again considered as an important structural material.

1.2.1. History

It is well known that the use of reinforced brickwork had its inception in this country in 1825 when Sir Marc Isambard Brunel used it for the construction of the caissons on each side of the Wapping-Rotherhithe Thames tunnel. Following this, at various times during the next 100 years, engineers world-wide, showed interest in this form of construction.

However it was not until 1923 that the most significant development occurred when a report by Sir Alexander Brebner was published[2] in India. It contained the results of extensive tests on reinforced brickwork structures carried out over a two year period. These tests were the first organised research on reinforced brickwork and they are generally recognised as marking the first stage of its modern development.

Following this work the use of reinforced brickwork increased particularly in India, New Zealand, U.S.A. and Japan. Severe earthquakes occur in all these countries thus it is necessary to design buildings with a high resistance to lateral forces. In the U.S.A. the Brick Manufacturers' Association of America sponsored further research through their National Brick Manufacturers' Research Foundation. This work formed the basis of the currently accepted design practices relating to reinforced brickwork in the U.S.A. and several other countries. Much additional information has been and still is being obtained through research, experience of construction and the monitoring of completed stuctures.

Interest in reinforced brickwork in this country was not apparent until about 1938 when some work was carried out at the Building Research Station. The outbreak of war brought to a halt further developments and interest was not shown again until about 1963, with much greater enthusiasm during the last fifteen years by both brick manufacturers and structural engineers. This has resulted in the publication in 1981 of the draft code on reinforced masonry[3] which is written in limit state terminology. Hopefully this should mark a new era for reinforced brickwork as a structural material.

The sections below relate to the literature on reinforced brickwork retaining walls. A wider and more general review of the literature on reinforced brickwork is given by Tellett[4].

1.2.2. Retaining walls

There are four types of brickwork retaining wall in use, the oldest of which is the mass brickwork wall which relies on its self weight for its stability. The resultant thrust at the base is generally designed to be within the middle third of the wall, thereby ensuring no tensile stresses develop. A consequence of this design method is that these walls are often extremely thick compared to their height.

If reinforcement is introduced to resist tensile forces the thickness of the retaining wall can be reduced greatly giving a more economic construction. The three types of reinforced brickwork retaining wall that have evolved are usually known as grouted cavity, Quetta bond and pocket-type construction, Figure 1.1. Of these the pocket-type wall is the most efficient in resisting lateral earth pressure. Where reversals of load are likely to occur, such as in a line of storage bins, grouted cavity or Quetta bond contruction is better.

1.2.3 Pocket-type retaining walls

1.2.3.1 General

A pocket-type retaining wall contains reinforcement concentrated in pockets formed in the brickwork at regular intervals along the loaded face. The pockets are formed by leaving whole bricks out of the bonding pattern . Steel reinforcement is placed in the

pockets and these are subsequently filled with a high slump conrete to create a composite constrution.

There are the three variations of wall recommended by Grogan and Plummer[5]. Figure 1.2 shows the pocket wall in its simplest form as a rectangular section in plan with the pockets usually spaced at 1.0-1.3 m centres. The type of wall shown in Figure 1.3 is a 'T'-section in plan which has the advantages of requiring less materials and no formwork. The third variation is a combination of the others, Figure 1.4, with the practical advantage that the flange thickness may be kept constant up the full wall height. It would be usual for the other wall types to have a reduction in thickness at intervals up their height, Figure 1.5. This form of construction is referred to as a stepped pocket wall.In the present study only the simplest type of wall, Figure 1.2, is investigated experimentally although the 'T'-section is considered in the analysis.

1.2.3.2. Sources of design information

Until recently there was only a limited amount of design information available in the U.K. for the designer intending to use pocket-type construction. The current British Standard relating to reinforced brickwork is CP111:1970[1]. This contains a few paragraphs only on reinforced brickwork, which are based on permissible stress philosophy, however for design principles the Standard refers the user to the reinforced concrete Code CP114:1969[6] which recommends the use of elastic analysis with

Figure 1.1 Types of reinforced brickwork retaining wall (plans)

pocket-type

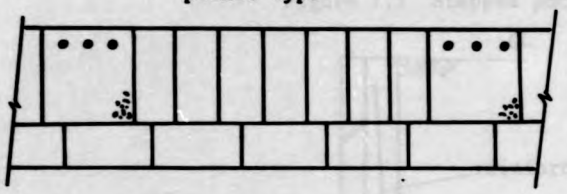

grouted cavity

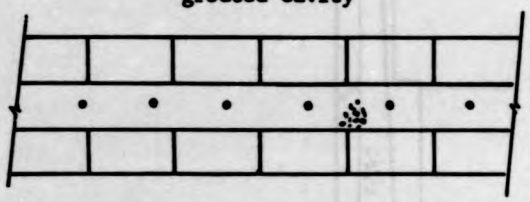

Quetta bond

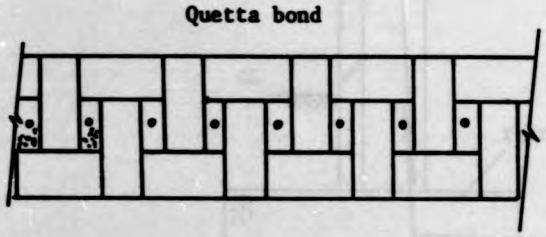

Figure 1.2 Simple rectangular wall

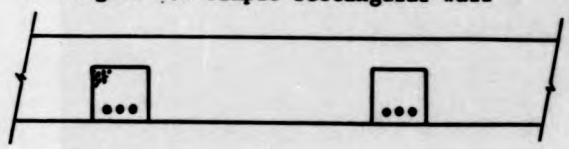

Figure 1.3 'T' shaped wall

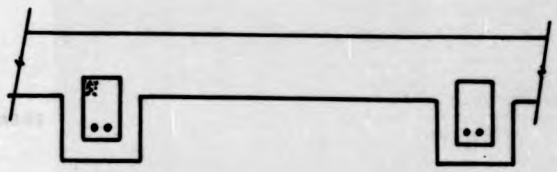

Figure 1.4 Composite pocket wall

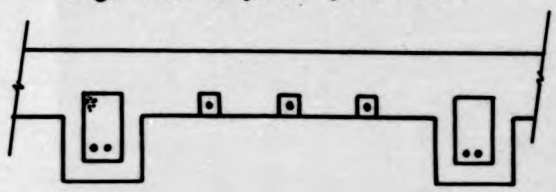

Figure 1.5 Stepped pocket wall

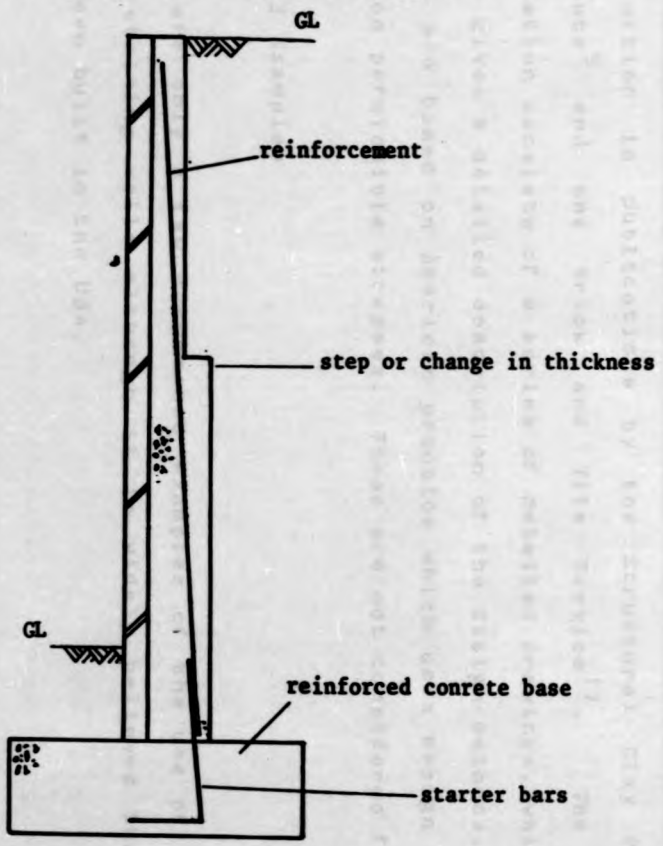

section

maximum stresses limited at working loads.

As the British Codes were not very helpful publications have been produced in the last decade by the Brick Development Association[7], the British Ceramic Research Association[8] and Structural Clay Products Ltd.[9-16] to give design guidance on reinforced brickwork. More recently a Draft Code has been issued by the British Standards Institution[3] for public comment and it is at present being redrafted. The design methods proposed in this document are discussed more fully in Chapter 2.

In the USA guidance has been available on pocket-type construction in publications by the Structural Clay Products Institute[5] and the Brick and Tile Service[17]. The latter publication consists of a series of detailed drawings, whilst the former gives a detailed description of the design methods. These guides are based on American practice which uses design methods based on permissible stresses. These are not considered further.

1.2.3.3 Examples

There are only a few documented examples of the use of pocket-type retaining walls, although it is widely believed that many have been built in the USA.

One example of the design and construction of a 7m high pocket-type retaining wall in the USA is described by Abel & Cochran[18] although there is no indication of where or when it

was built. Recent correspondence[19] has resulted in three further examples being discovered; these are situated at Fayetteville, Hickory and Raleigh, North Carolina, USA. They were constructed about 1970 and formed part of road developments.

At present there are two documented examples in this country. The first[13] is a 4.2m high earth retaining wall built in the mid 1970's with the intention of examining the feasibility of pocket-type construction, the economics and performance. The second[20], which is also an earth retaining wall, is upto 2.5m high and forms part of a road development in Dartford.

During 1982 three more pocket-type walls have been constructed[21] in the UK. These were a 3.37m high wall at Biggin Hill, Kent for a private house, a 4.8m high flanking wall to a pedestrian subway in the London Borough of Haringey and a 2.5m high wall which formed part of bridge abutments at Dilham, Norfolk.

1.2.3.4 Cost considerations

The economic feasibility of pocket-type walls was studied by Maurenbrecher et al[10], Haseltine and Tutt[7] and Drinkwater and Bradshaw[22]. In each case comparisons are made between reinforced concrete walls and reinforced brickwork walls including pocket-type construction.

Maurenbrecher et al presented the results of a cost study done in 1972-3 which was based on an actual job. They showed that for walls up to 6.0m high a pocket-type wall was more economical than a comparable reinforced concrete wall with a ribbed finish. For walls greater than 6.0m high reinforced concrete walls become more economical, Figure 1.6.

The cost study reported by Haseltine and Tutt was undertaken in 1975. It compared grouted cavity, mass brickwork, Quetta bond, stepped and plain pocket-type walls with two types of reinforced concrete walls (one with a ribbed finish, the other with a brick-faced finish). Table 1.1 gives the results which indicated that reinforced brickwork pocket-type retaining walls are the most economical construction for heights greater than 1.0m. Wall heights up to 4.0m were considered, however Haseltine and Tutt suggested that similar results would be obtained for walls greater than 4.0m high. The cheapest of the reinforced concrete walls was the one with the ribbed finish which was between 30%-49% more expensive than pocket-type construction, depending on height.

The most recent cost comparison between the various types of retaining walls was completed in 1982[22]. It was financed by George Armitage & Sons, a brick company in the North of England. The results are presented graphically in Figure 1.7 and an itemised breakdown of the costs[23] is given in Table 1.2. The results show that pocket-type construction is the most economical form of reinforced brickwork retaining walls for wall heights

Figure 1.6 Cost comparison of brickwork retaining walls presented by Maurenbrecher et al[10]

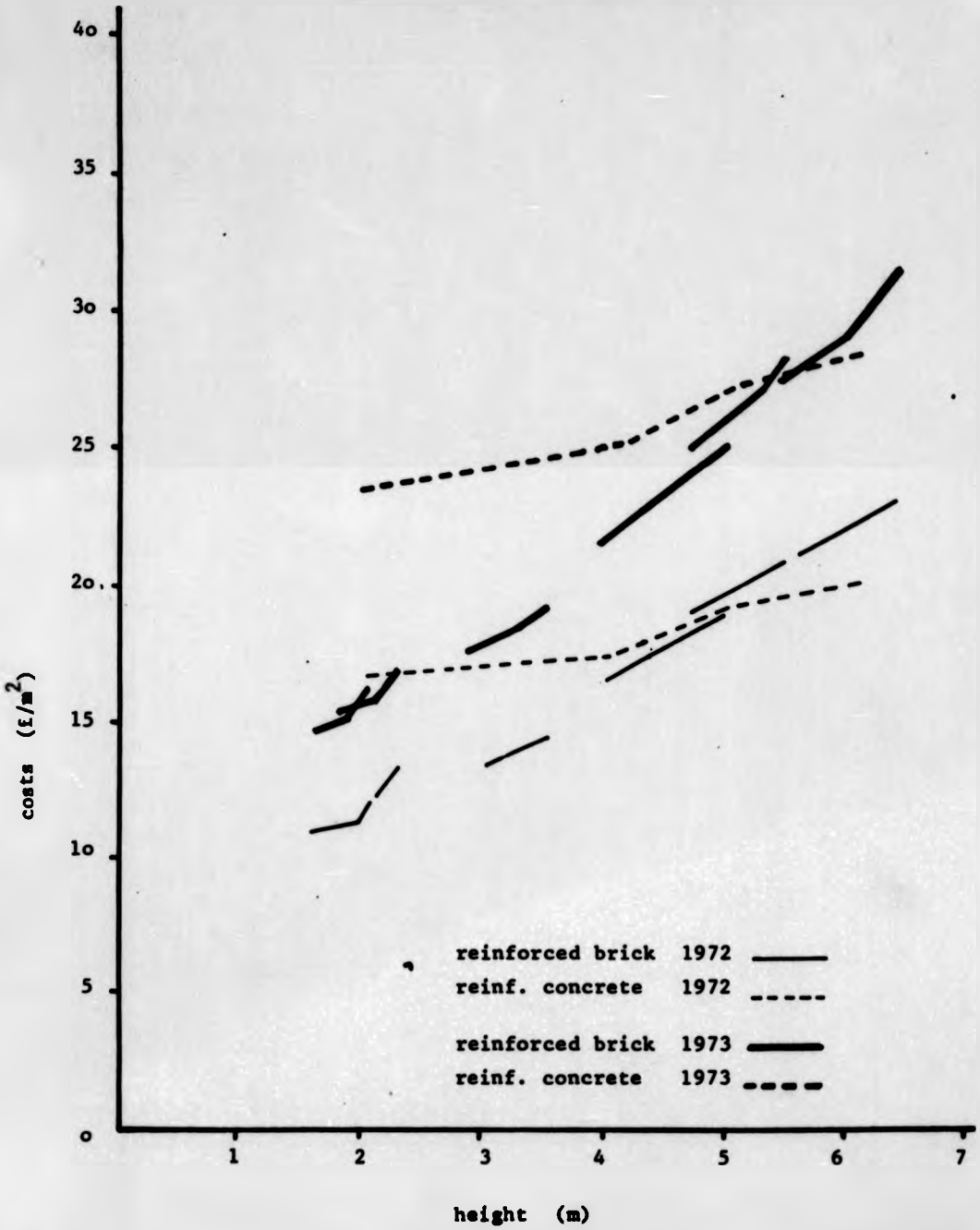

TABLE 1.1 COST COMPARISON OF BRICKWORK RETAINING WALLS TO REINFORCED CONCRETE RETAINING WALLS carried out in 1975, reported by Haseltine & Tutt

height (m)	grouted cavity	mass brick wall	Quetta bond wall (330mm)	Pocket wall (plain stem)		Pocket wall (stepped stem)		Ribbed finish concrete	brick-faced concrete
				Pocket centres 900 mm	1800 mm	900 mm	1800 mm		
1.0	101	100	-	-	-	-	-	106	122
2.0	128	-	120	106	100	-	-	149	169
3.0	136	-	107	118	115	104	100	134	149
4.0	138	-	-	110	111	100	102	130	142

Figure 1.7 Results of a cost study on retaining walls presented by Drinkwater and bradshaw[22]

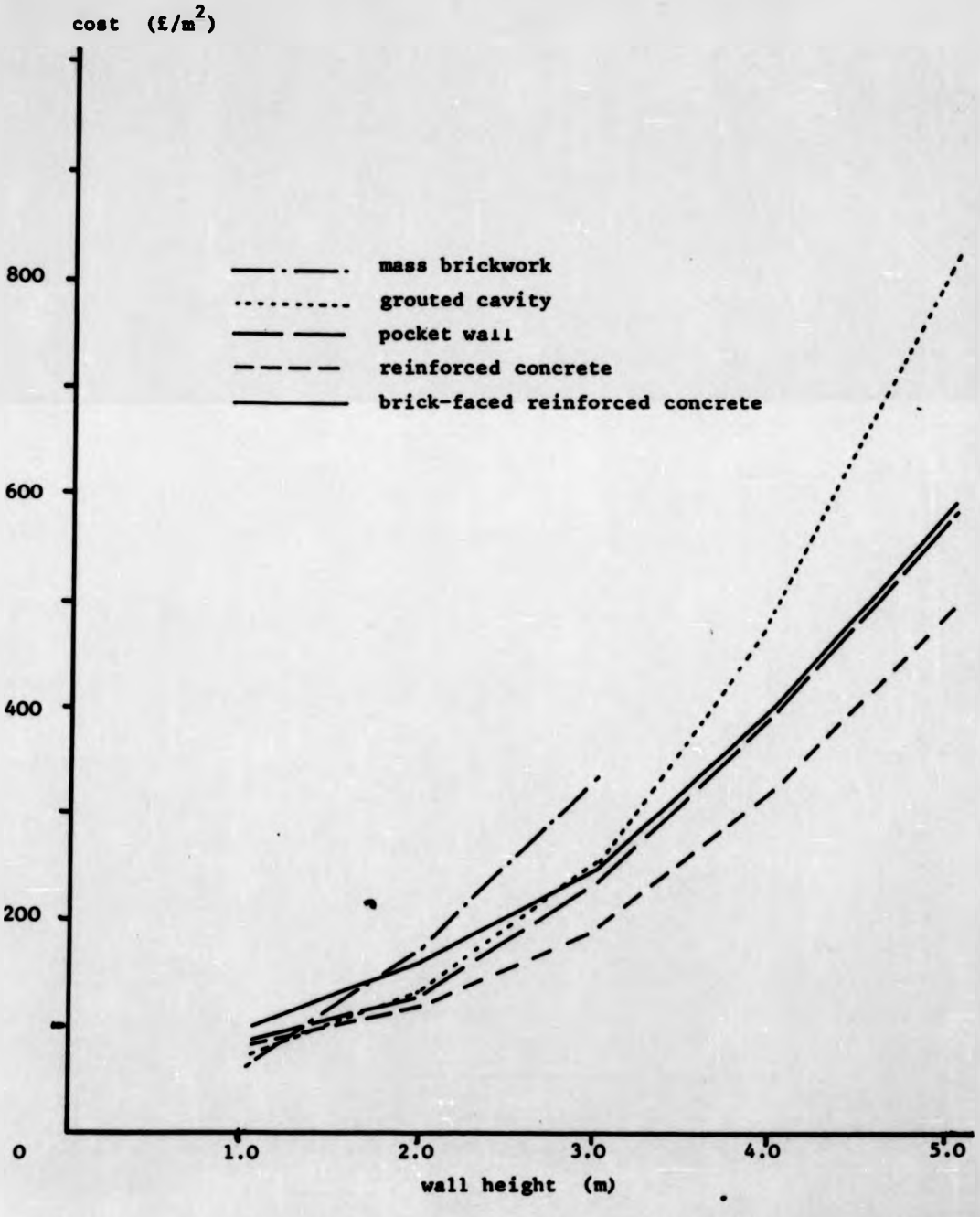

TABLE 1.2 ITEMISED ACCOUNT OF A COST STUDY DONE IN 1982
on behalf of GEORGE ARMITAGE & SONS

Wall height	Wall type	Foundation Costs (£/m)					Wall Costs (£/m)							total cost (£/m)
		excavation	concrete	reinforcement	formwork	sub total	concrete	reinforcement	formwork	brickwork	scaffolding	expansion joints & sundries	sub total	
1.050	MB[1]	1.19	5.27	0.83	-	7.29	-	-	-	58.95	-	3.24	62.19	69.48
	GC[2]	1.75	5.08	1.60	6.50	14.93	5.27	5.36	-	44.78	-	3.27	58.68	73.61
	Pocket[3]	3.84	11.80	2.38	12.00	30.02	2.16	1.29	5.99	40.70	-	3.10	53.24	83.26
	RC[4]	3.63	10.82	2.22	12.00	28.67	9.75	5.73	34.16	-	-	0.99	50.63	79.30
	RC & B[5]	3.63	10.82	2.22	12.00	28.67	8.85	5.73	29.20	26.51	-	2.27	72.56	101.23
2.025	MB	2.85	11.41	1.44	-	15.70	-	-	-	145.21	4.00	7.39	156.60	172.30
	GC	3.26	10.29	5.53	6.50	25.58	10.14	9.70	-	79.57	4.00	5.89	109.30	134.88
	Pocket	3.61	11.41	5.83	6.50	27.25	4.73	3.71	11.58	77.47	4.00	6.13	107.62	134.87
	RC	3.22	10.04	5.49	6.50	25.25	20.79	13.28	59.64	-	4.00	1.34	99.05	124.30
	RC & B	3.22	10.04	5.49	6.50	25.25	19.71	13.28	52.72	44.24	4.00	4.05	138.00	163.25
3.000	MB	4.82	19.91	2.51	-	26.88	-	-	-	290.26	6.00	13.10	309.00	336.24
	GC	5.85	20.64	9.05	12.50	48.04	15.02	12.72	-	164.50	6.00	9.57	207.81	255.85
	Pocket	5.73	17.67	7.87	12.50	43.77	10.39	13.40	17.12	135.07	6.00	9.90	191.88	235.65
	RC	4.97	14.82	7.84	12.50	40.13	42.01	19.90	84.86	-	6.00	2.10	154.87	195.00
	RC & B	4.97	14.82	7.84	12.50	40.13	40.50	19.90	76.00	64.30	6.00	6.26	212.96	253.09
4.050	GC	10.83	34.96	15.12	23.00	83.91	20.25	23.45	-	341.02	8.00	15.45	408.17	492.08
	Pocket	10.97	35.59	13.92	23.00	83.48	21.74	19.91	23.12	229.39	8.00	14.30	316.46	399.94
	RC	10.97	35.58	15.08	23.00	84.63	75.71	38.04	113.48	-	8.00	5.38	240.61	324.24
	RC & B	10.97	35.58	15.08	23.00	84.63	73.74	38.04	102.30	85.80	8.00	10.87	318.74	403.37
5.025	GC	24.57	73.46	25.82	30.00	153.85	37.72	46.88	-	553.18	10.00	22.08	669.86	823.71
	Pocket	23.19	67.97	27.05	29.50	147.71	34.15	25.93	28.70	326.39	10.00	17.93	443.10	590.81
	RC	24.66	73.46	32.69	30.00	160.81	120.28	62.79	140.92	-	10.00	7.82	341.81	502.62
	RC & B	24.66	73.46	32.69	30.00	160.81	117.73	62.79	127.78	160.04	10.00	14.61	438.95	599.76

NOTES: 1 = Mass brickwork 2 = Reinforced grouted cavity brickwork

3 Reinforced brickwork pocket type 4 = Reinforced concrete (no finish)

5 = Reinforced concrete with brick face

above 2.0m. When compared with brick-faced reinforced concrete walls up to 5.0m high pocket walls are cheaper, however for greater heights there is little to choose between them.

The results of these cost studies show that over a ten year period the relative cost of pocket-type retaining walls compares favourably with reinforced concrete construction. This suggests more use should be made of pocket-type construction, however this may be a reflection on the reticence of the construction industry to change or the lack of design guidance or, more likely, a combination of these factors.

1.2.3.5 Potential applications

In the USA reinforced brickwork has been employed for approximately half a century in various forms of structures such as basement walls, bridge abutments, grain and crop storage bins, railway embankments, reservoirs and dams[24-25]. As the concept of pocket-type construction was not developed until the mid 1960's it is assumed that most of these structures were built using grouted cavity construction. All these structures are required to resist lateral earth pressure from one direction only hence a more economic use of these materials would be achieved if pocket-type construction were employed. Thus it is reasonable to assume that structures similar to those above, particularly those which require curves or changes in level, are potential applications for pocket-type construction.

Sutherland[26] has suggested that prefabrication of pocket-type retaining wall sections is a feasible method of construction which could keep up with the requirements of a highway contract. Indeed he cited some work carried out by a brick company that demonstrated the feasibility of such a project.

1.3 Specific aims of the research project

It is clear from the literature that the information relating to the design and structural performance of reinforced brickwork is incomplete. Prior to the tests reported within this thesis only one pocket-type wall[11] had been tested and this failed before the theoretical load capacity had been reached due to poor detailing of the reinforcement at a change in wall thickness. It was therefore necessary to investigate experimentally the structural performance of this form of construction before recommending its adoption in this country. Furthermore, the full potential of pocket-type construction has yet to be realised, since the majority of the examples have close pocket spacings, usually about 1.0m centres; whereas wider pocket spacings are more economic[7].

The aims of this research project are therefore:-

(i) To investigate the behaviour upto collapse of pocket-type walls under flexural and shear forces.

(ii) To examine the combined effects of shear and flexure at the

base of the wall.

(iii) To determine the effect on performance of the wall of different pocket spacings.

(iv) To investigate the behaviour upto collapse of a stepped wall under flexural and shear forces.

(v) To compare the results with the current proposals in the Draft Code for reinforced masonry.

It was originally envisaged that all the above aims would be examined experimentally using full scale test structures. However it was realised that this would be very expensive, thus to complement the test programme a theoretical study was required to reduce the amount of testing. Thus the sixth aim is:-

(vi) To develop a computer program based on the finite element method which is capable of analysing a pocket-type retaining wall.

During the course of this research work the Draft Code was being compiled and it became clear that the shear requirements were onerus for pocket-type walls. In fact trial calculations indicated that shear was the governing design criterion for all but the most lightly reinforced walls. However the initial test results failed in flexure with no signs of shear failure. Therefore it became a priority to determine the shear performance

of pocket-type sections and aims (iii) and (iv) were abandonned in favour of aim (vii) below:-

(vii) To examine the effect of shear forces on pocket-type sections tested as beams under four point loading.

2. REINFORCED BRICKWORK DESIGN

2.1 General

The two design philosophies currently used in the design of reinforced brickwork structures are permissible stress design, based on elastic theory and limit state design. Conceptually the latter approach is more soundly based. For this reason the main emphasis of this research is concentrated on limit state philosophy.

2.2 Permissible stress design

Probably the first guidance available in the UK for the design of reinforced brickwork was given in BS.1146:1943[27]. It was drafted in permissible stress terms but no design equations were given, instead the designer was instructed to use the same general principles as for reinforced concrete. Scant regard was paid to the possibility of corrosion and no attention was given to serviceability performance, although a large section on the properties of bricks, mortar, grout and reinforcement was included. This Standard was originally issued as a interim measure pending the publication of a Code of Practice for reinforced brickwork.

Eventually this was issued in 1948 as CP.111: "Structural Recommendations for Loadbearing Walls" but it contained only a small section on reinforced brickwork. The first revision was

carried out in 1964 when the main change was that the permissible stresses were increased; a subsequent revision made in 1970[1] converted all values into S.I units. This is the current Standard available for the use in the design of reinforced brickwork. In it the user is referred to CP.114:1969 "The Structural use of Reinforced Concrete for Buildings"[6] for advice on design equations whilst for guidelines covering workmanship the user is referred to CP.121: Part 1:1973[28].

Haseltine and Tutt[7] give an example of a reinforced brickwork retaining wall designed according to CP.111. This well written guide collates much of the dispersed information regarding durability detailing and workmanship aspects. In addition sensible advice on concrete cover to the reinforcement is given.

2.3 Limit state design

2.3.1 Background.

In view of the limited guidance available for the design of reinforced brickwork, a committee of the British Ceramic Research Association commenced work in 1972 on a Design Guide for Reinforced and Prestressed brickwork, published in 1977 as SP.91[8]. It marked a significant advance since it was the first guide drafted in limit state philosophy that applied to the design of brickwork. Partly as a result of this guide an increased interest has been shown recently in reinforced brickwork.

A revised version of CP.111 was published in 1978 as BS.5628:Part 1:1978 "Structural use of Masonry - Unreinforced"[29]. It was drafted in limit state philosophy. A draft version[3] of Part 2 for the design of reinforced and prestressed masonry was issued in 1981 for public comment. Subsequently some of the proposals made in the draft have been altered. The recommendations and design equations given below are those currently accepted by the code committee at the time of writing but discussion still continues. *

2.3.2. Design Philosophy.

The philosophy of limit state design may be defined as the achievement of acceptable probabilities that the structure will perform adequately and will not become unfit for use during its lifetime. Two limit states are recognised:-

(i) the ultimate limit state where the ultimate flexural strength, shear strength or overturning capacity should not be reached, and

(ii) the serviceability limit state where deflection and cracking should not adversely affect the appearance or the behaviour of the stroture.

For retaining walls the ultimate limit state is of prime importance whilst serviceability is of secondary or in some

* *Many of the issues raised in this thesis have been adopted and the draft has been amended, in particular the section on characteristic shear strength.*

cases, no importance. This is because deflection is rarely a governing design criterion for retaining walls.

2.3.3 Design to the Draft Code[3].

In the derivation of the design equations the following conditions are assumed:-

(i) The strain distribution in the section is linear. This assumes that plane sections remain plane.

(ii) The stress distribution in the brickwork is rectangular with an intensity of f_k/γ_{mm} taken over the whole of the compression zone. γ_{mm} is given the value appropriate to the limit state under consideration, where f_k is the characteristic compressive strength of brickwork and γ_{mm} is the partial safety factor for brickwork.

(iii) The maximum compressive strain in the outer-most compression fibre is 0.0035.

(iv) The tensile strengths of brickwork and concrete are ignored

(v) The characteristic strengths of steel reinforcement, f_y, are given in Table 2.1 and the assumed stress-strain relationships in Figure 2.1.

(vi) The span to effective depth ratio of the member is greater

Figure2.1 Short-term design stress-strain curve for reinforcement

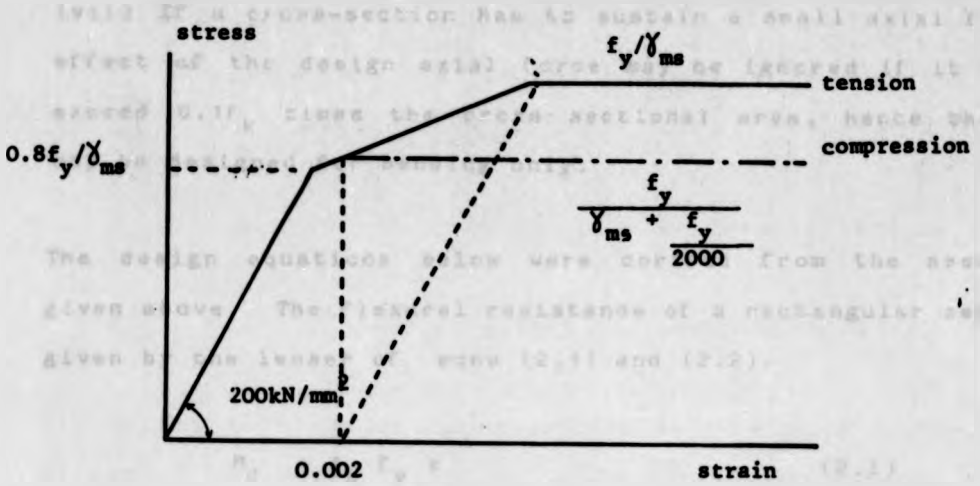

Figure 2.2 Characteristic compressive strength of brickwork, f_k

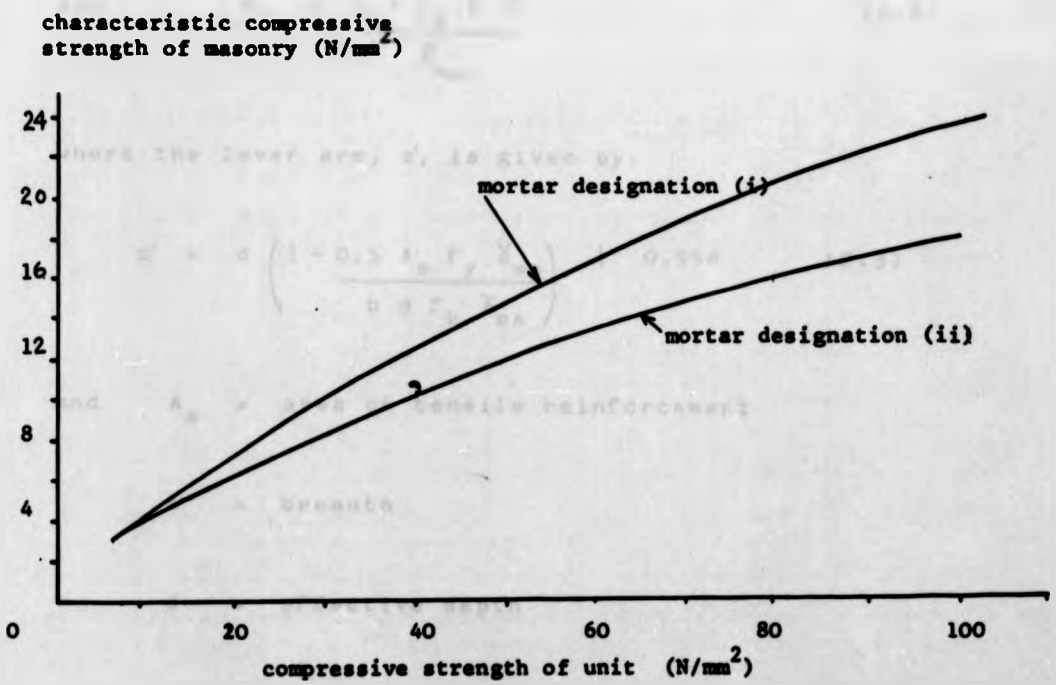

than 1.5.

(vii) If a cross-section has to sustain a small axial force the effect of the design axial force may be ignored if it does not exceed $0.1f_k$ times the cross sectional area, hence the member may be designed for bending only.

The design equations below were derived from the assumptions given above. The flexural resistance of a rectangular section is given by the lesser of eqns (2.1) and (2.2).

$$M_d = \frac{A_s f_y z}{\gamma_{ms}} \qquad (2.1)$$

and

$$M_d > \frac{0.4 f_k b d^2}{\gamma_{mm}} \qquad (2.2)$$

where the lever arm, z', is given by

$$z' = d\left(1 - \frac{0.5 A_s f_y \gamma_{mm}}{b d f_k \gamma_{ms}}\right) \leq 0.95d \qquad (2.3)$$

and A_s = area of tensile reinforcement

b = breadth

d = effective depth

f_k = characteristic compressive strength of masonry given in Table 2.2 or Figure 2.2

f_y = characteristic tensile strength of reinforcing steel given in Table 2.1.

γ_{mm} = partial safety factor for strength of masonry (=2)

γ_{ms} = partial safety factory for strength of steel (=1.15)

The effect of these design equations is to ensure the section is always under reinforced, that is the steel is designed to yield before the brickwork crushes.

The draft code treats members in which the reinforcement is concentrated locally as a flanged section. These should be designed using the recommendations given below. Pocket-type sections are generally considered as flanged sections.

The design moment of resistance is given by the lesser of eqns (2.4) and (2.5).

$$M_d = \frac{A_s f_y (d - 0.5t_f)}{\gamma_{ms}} \qquad (2.4)$$

$$M_d > \frac{f_k b\, t_f (d - 0.5t_f)}{\gamma_{mm}} \qquad (2.5)$$

where t_f is the flange thickness which should be taken as the

TABLE 2.1 CHARACTERISTIC STRENGTH OF REINFORCING STEEL, f_y

Designation	Nominal size (mm)	Characteristic tensile strength (N/mm^2)	Characteristic compressive strength (N/mm^2)
Hot rolled steel grade 460/425 (BS.4449)	Up to and including 16ϕ	460	372
	over 16ϕ	425	353
Hot rolled steel grade 250 (BS449)	all	250	208
Cold worked steel grade 460/425 (BS.4461)	up to and including 16ϕ	460	372
	over 16ϕ	425	353

TABLE 2.2 CHARACTERISTIC COMPRESSIVE STRENGTH OF BRICKWORK, f_k CONSTRUCTED WITH STANDARD UNITS

mortar designation	compressive strength of unit (N/mm^2)								
	5	10	15	20	27.5	35	50	70	100
(i)	2.5	4.4	6.0	7.4	9.2	11.4	15.0	19.2	24.0
(ii)	2.5	4.2	5.3	6.4	7.9	9.4	12.2	15.1	18.2

TABLE 2.4 CHARACTRISTIC SHEAR STRENGTH OF REINFORCED BRICKWORK f_v N/mm^2

$\frac{100 A_s}{bd}$	Up to 0.15	0.5	1.0	1.5	2.0
f_v	0.35	0.45	0.55	0.60	0.65

lesser of:-

(i) 0.5d at the level considered

or

(ii) for a pocket-type wall the thickness of brickwork on the compressive side of the pocket, Figure 2.3

or

(iii) for a reinforced hollow blockwork wall the thickness of masonry between the ribs, Figure 2.3

Implicit in clause (ii) is that the flange thickness is limited to the width of the unit or multiples thereof whilst clause (iii) is a more logical and generous specification as indicated by Figure 2.3. Of these clauses the author suggests that the latter should be adopted for all non-rectangular plan pocket-type construction, whatever the material.

The flange width, b, should be taken as the lesser of

(i) for pocket-type walls the width of the pocket or rib plus 12 times the flange thickness

or

(ii) the spacing of the pockets or ribs

or

(iii) one third of the height of the wall

The effect of these clauses is to limit the width of the reinforced section in the design equations, however the pocket spacing may exceed the flange width provided that the panel is

Figure 2.3 Examples of recommended flange widths

(a) pocket walls

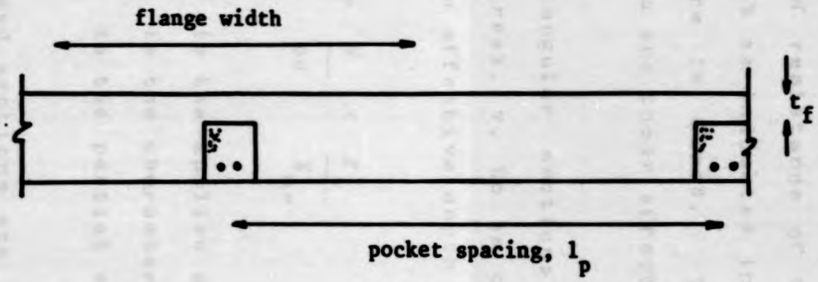

(b) reinforced hollow block walls

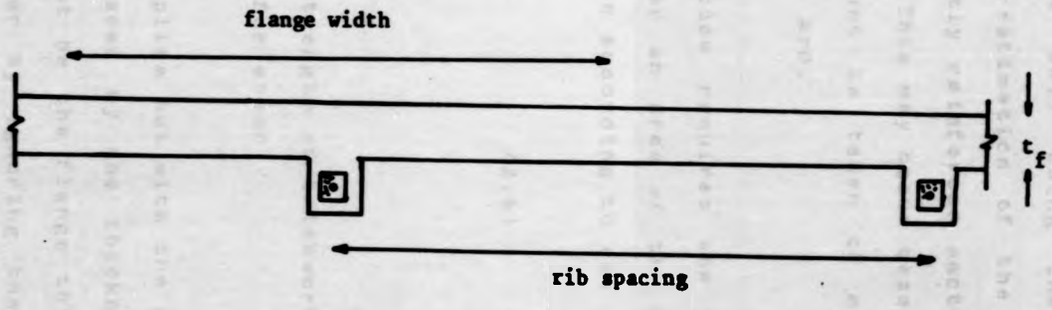

able to span horizontally between the pockets. This should be checked using BS.5628:Part 1:1978[29].

Design of a rectangular pocket-type wall using the above recommendations may lead to an underestimation of the design moment of resistance of the most lightly reinforced sections of up to 25% as indicated in Table 2.3. This may occur because the lever arm is fixed. Thus no account is taken of material strengths and their effect on the lever arm.

For rectangular sections the draft code requires the average shear stress, v, to be calculated over an area of the breadth times the effective depth of the section according to eqn (2.6)

$$v = \frac{V}{bd} < \frac{f_v}{\gamma_{mv}} \qquad (2.6)$$

where V is the applied shear force

f_k is the characteristic shear strength of brickwork

γ_{mv} is the partial safety factor for shear

For flanged sections eqn (2.6) also applies but with the proviso that the effective depth, d, is replaced by the thickness of masonry between the ribs. This may not be the flange thickness as indicated by Figure 2.3. Moreover by ignoring the shear capacity of the pocket the design method is conservative.

If the average shear stress, eqn (2.6), exceeds the

TABLE 2.3 COMPARISON OF LEVER ARMS IN FLANGE AND RECTANGULAR SECTIONS

Wall details	wall plan	flanged section lever arm (mm) $Z=(d-0.5t_f)$	rectangular section lever arm (mm) $Z = 0.95d$	% difference in lever arms
t = 215 d = 170 t_f = 100	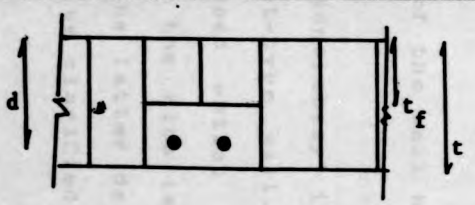	120.0	161.5	25.6
t = 327 d = 280 t_f = 100	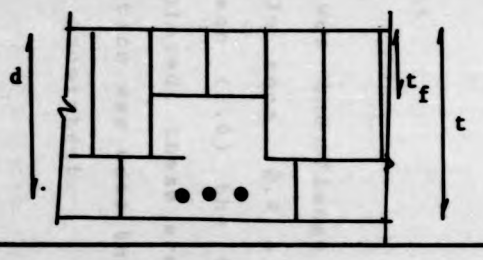	230.0	266.0	13.5
t = 440 d = 280 t_f = 215	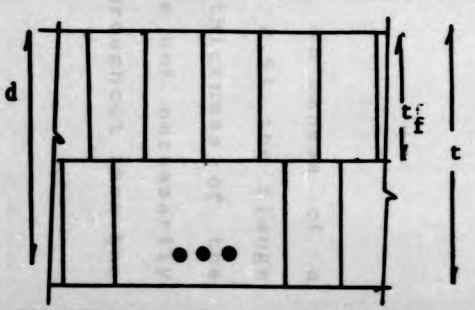	293.0	380.0	23.0

characteristic shear stress, f_v, divided by the partial safety factor for shear, γ_{mv}, then shear reinforcement should be provided to sustain the entire shear force. Values of f_v are given in Table 2.4.

There are two inconsistencies in the draft code requirements relating to the shear and flexural design equations. The first concerns the breadth of the section, b, which is defined as the flange width in eqns (2.4&2.5) but in eqns (2.1-2.3, &2.6) it is defined as the section width. These are not necessarily the same, especially if wide pocket spacings are used. To resolve the situation it is suggested that for pocket walls the effective width, b_e, should be used which is the lesser of:

(i) the pocket spacing

or

(ii) one third of the wall height

The second inconsistecy involves the flange thickness of a brickwork pocket-type wall. In eqns (2.4 & 2.5) the flange thickness is used whilst in eqn (2.6) the thickness of the masonry between the ribs is employed, these are not necessarily the same. If the latter definition was used throughout then the situation would be clarified and consistent.

2.3.4 Design specification

The draft code[3] gives detailed guidance on durability, reinforcement detailing, spacing of movement joints, drainage, waterproofing and construction sequence for pocket-type construction. None of these aspects is considered to be an ultimate limit state although each will have an effect on the serviceability limit state if inadequate design details are employed. No further consideration is given to these aspects because they are outside the scope of this research.

2.4 Design loads

A recent review[31] stated that the classical earth pressure theories of Coulomb and Rankine are still widely used by the practising engineer. Indeed these theories are utilised in the Earth Retaining Structures Code CP2:1951[34] which is still the current document for the design of earth retaining walls. The design guides[7,15] use the Rankine approach to assertain earth pressures.

Coulomb's method assumes a rupture surface in the retained soil from which the thrust on the wall is evaluated by consideration of the equilibrium of the soil mass. To simplify the analysis a plane rupture surface is assumed although in practice it may be curved. This method requires a trial and error method to determine the maximum thrust.

Rankine's method was devloped nearly a century later in 1857. It is perhaps the most popular design method since it is easier to apply and arguably it is subject to fewer pit-falls. It consists of examining the lateral earth pressures due to the self weight of the soil mass.

Although both methods involve approximations they have served the civil engineering profession well because the majority of retaining walls designed by these methods are still performing satisfactorily after more than one hundred years. However, there are some examples of failures which are primarily due to inadequate assessment of the design loads [35-38]; these failures were due to compaction by modern mechanical machines which generated very high lateral earth pressures and effectively over-consolidating the fill. Ingold [39-40] has studied this problem in depth and he has proposed a design method which seems to give a reasonable assessment of the magnitude of lateral earth pressure under these circumstances.

When limit state design is employed the actual loads have to be multiplied by a partial safety factor for loads, γ_f, to obtain the design loads. Generally γ_f is 1.6 for live loads such as earth loads.

3. EXPERIMENTAL APPROACH

3.1 Tests on pocket-type retaining walls

3.1.1 Programme

An ambitious programme was originally considered which set out to examine the effect of the six parameters given below on the performance of the wall:-

(i) brick strength

(ii) wall slenderness

(iii) percentage of tensile reinforcement

(iv) pocket spacing

(v) shear reinforcement

(vi) 'stepped' pocket-type walls

Of these only the first three parameters were subsequently investigated; expense precluded examination of the rest. Two brick types, two wall slendernesses and four different percentages of reinforcement were examined in six full scale tests. Table 3.1 gives details of the walls tested.

The programme relected the current techniques used in the construction of pocket walls which are generally upto 3m high, of uniform thickness and have a pocket spacing of 1.0m. A low strength common brick and a high strength facing brick were assumed to be representative of the wide range of bricks

TABLE 3.1 TEST PROGRAMME FOR RETAINING WALLS

Wall Number	1	2	3	4	5	6
Height (mm)	3000	3000	3000	3000	3000	3000
Width (mm)		2000	2000	2000	2000	2000
Thickness (mm)	327	327	327	327	215	215
Brick Type	A	B	B	A	B	B
Reinforcement (%)	0.92	0.92	0.28	0.28	1.44	1.25
Pocket Spacing (mm)	1000	1000	1000	1000	1000	1000
No. Pockets	2	2	2	2	2	2

TABLE 3.2 COMPRESSIVE STRENGTH OF BRICKS TESTED ON THE BED FACE IN ACCORDANCE WITH BS.3921:1974

Wall No		RW 1	RW 2	RW3,5 & 6	RW 4
Brick Type		A	B	B	A
Spec. No	1	109.4	22.8	24.4	64.6
	2	78.8	22.9	24.1	56.5
	3	91.4	22.9	21.4	69.1
	4	75.0	23.0	25.4	62.5
	5	73.4	20.5	27.1	71.1
	6	85.2	18.8	27.4	65.4
	7	82.1	21.8	28.1	65.9
	8	101.7	22.0	26.8	61.0
	9	84.4	19.4	25.0	68.7
	10	66.9	21.7	24.1	61.9
Mean		84.8	21.6	25.4	64.7
C.V.%		14.6	7.0	7.9	6.7

Units? X

available in the UK both in material qualities and in terms of brick sales. Between them they account for approximately 50% of the total number of brick sales in this country; the common alone having 40% market share. Two pockets per wall were used in order to examine whether arching of the brickwork between the pockets was an important criterion. Slenderness ratios (height/effective depth) of approximately 11 and 18 and reinforcement percentages of 0.28-1.44 were both considered to cover the likely range for pocket-type walls.

3.1.2 Materials

3.1.2.1 Bricks and Brickwork

Two brick types were used in the test walls. Type A was a multi-perforated, wire cut, high strength, low water absorption, clay facing brick which meets the specification of a class B engineering brick. Type B was a deep frogged, semi-dry pressed, low strength, high water absorption clay brick that required docking or wetting with water prior to laying in accordance with the specification given in SP.56[41]. The properties of each brick type were determined according to the requirements of BS.3921:1974[42] and they are given in Tables 3.2 and 3.3. Generally each wall was built with bricks from different batches; properties were determined for each batch.

For each wall one or two sets of ten, four course high, one brick square prisms were built concurrent with wall construction.

TABLE 3.3 DETERMINATION OF THE INITIAL RATE OF ABSORPTION AND WATER ABSORPTION

	Initial Rate of Absorption ($kg/m^2/min$)				Absorption, Weight after 5hr boil[2] %			
Wall No.	RW1	RW2	RW3,5 & 6	RW4	RW1	RW2	RW3, 5 & 6	RW4
Brick Type	A	B	B	A	A	B	B	A
Spec. No. 1	0.23	1.47	3.49	0.55	4.6	22.4	22.5	5.2
2	0.23	2.42	1.54	0.72	5.0	27.8	22.0	5.9
3	0.58	1.60	1.81	0.72	6.9	27.0	22.0	5.9
4	0.23	3.56	2.29	0.67	4.1	26.0	21.5	5.6
5	0.17	2.81	3.19	0.73	4.2	23.8	19.1	5.7
6	0.23	2.47	2.77	0.60	5.0	24.3	21.6	5.7
7	0.30	3.48	2.85	0.60	5.1	19.1	21.1	5.4
8	0.17	1.42	3.90	0.61	3.9	18.3	22.0	5.4
9	0.23	3.11	3.22	0.55	5.1	21.1	22.3	5.0
10	0.17	1.86	3.03	0.67	4.3	22.2	22.4	5.2
Mean -1	0.25	2.42	2.81	0.64	4.8	23.2	21.65	5.5
CV %	47.0	33.5	26.0	10.7	17.7	13.7	4.6	5.6

1. In accordance with SP56
2. In accordance with BS 3921:1974

These were cured under a polythene sheet for 28 days and their compressive strength was determined subsequently in a 500 tonne Avery universal machine. The prisms were usually capped with a sheet of 6mm thick cardboard, however in some cases two sets of prisms were tested, one with cardboard, the other with a 12mm thickness of fibreboard (Tentest) packing. The results are presented in Table 3.4.

3.1.2.2 Mortar

A high strength 1:1/4:3 cement:lime:sand mortar by volume, batched by weight was used in the construction of all walls. This mortar is the stronger of the two types recommended in the Draft Code[3]. Ordinary Portland cement conforming to BS:12[43] was obtained directly from the manufacturers, whilst hydrated lime to BS:890[44] was supplied by a builders' merchant. Building sand was obtained from a local quarry and it met the requirements of BS:1200[46], Table 3.5. From each mix 100mm mortar cubes were made and subsequently stored under water for 28 days prior to testing.

The consistency of the mortar was adjusted by the bricklayer to suit his requirements. No attempt was made to regulate the amount of water added to the mix, however the results of the cube tests, given in Table 3.6, indicate from their small variation that a uniform compressive strength was achieved.

TABLE 3.4 COMPRESSIVE STRENGTH OF FOUR COURSE HIGH, 215mm SQUARE BRICKWORK PRISMS TESTED ON THE BED FACE

	Compressive Strength (N/mm^2)						
Wall No	RW1	RW2	RW3	RW4	RW5	RW6	RW6
Brick type	A	B	B	A	B	B	B
Packing	CB	CB	CB	CB	CB	CB	FB
Pier No. 1	13.0	7.0	5,7	12.4	7.4	5.9	11.2
2	17.5	7.7	9.0	19.8	6.0	10.7	10.8
3	15.4	5.9	6.6	18.8	11.4	6.4	8.4
4	19.1	8.1	9.7	19.2	8.0	10.5	8.8
5	17.4	7.9	10.0	22.0	9.1	8.4	13.4
6	16.7	5.4	6.0	14.3	8.5	9.2	13.7
7	16.5	6.3	8.1	13.8	8.9	8.4	9.4
8	13.5	6.3	8.8	12.9	7.6	11.1	9.0
9	15.5	5.7	12.0	19.4	7.9	9.9	10.1
10	16.8	8.6	8.0	15.2	6.3	9.7	14.3
Mean	16.1	6.9	8.4	16.8	8.1	9.0	10.9
CV %	11.3	16.3	23.4	20.3	18.9	19.5	20.0

CB = cardboard

FB = fibreboard (tentest)

TABLE 3.5 GRADING OF BUILDING SAND FROM CHEADLE

BS Sieve Size	% passing by weight Typical Analysis Oct 1981	Analysis Feb 1982	BS.1200 Table 1
5.00mm	100	100	100
2.36mm	100	99	90-100
1.18mm	98	95	70-100
600um	94	90	40-100
300um	66	57	5- 70
150um	15	7	0-15
75um	4	2	-

TABLE 3.6 COMPRESSIVE STRENGTH OF 100mm 1:1/4:3 MORTAR CUBES

	COMPRESSIVE STRENGTH (N/mm^2)					
WALL NO	RW 1	RW 2	RW 3	RW 4	RW 5	RW 6
CUBE NO. 1	11.0	15.11	14.77	13.32	13.85	14.19
2	11.92	15.93	15.64	13.22	14.77	14.24
3	11.78	14.48	14.38	12.50	12.55	12.45
4	12.55	12.55	14.24	14.14	12.50	13.03
5	11.97	13.32	14.87	13.85	11.82	13.18
6	12.69	12.21	14.96	13.76	12.45	13.03
7	11.97	13.22	15.35	13.76	12.50	13.47
8	10.67	12.55	15.20	13.80	14.91	13.27
9	11.10	10.91	14.38	12.16	13.13	14.00
10	11.65	13.18	15.54	12.45	15.11	14.38
11	-	13.80	-	-	13.76	14.58
12	-	13.61	-	-	15.93	14.53
13	-	12.55	-	-	13.18	-
14	-	12.93	-	-	13.95	-
15	-	14.82	-	-	14.24	-
16	-	12.69	-	-	-	-
17	-	15.01	-	-	-	-
MEAN	11.73	13.46	14.93	13.30	13.64	13.70
C.V.%	5.5	9.4	3.3	5.2	8.7	5.2

Note these are the 28 day strengths

3.1.2.3 Concrete

A nominal grade 25N/mm^2 concrete with a 30mm minimum cover to the main reinforcement was chosen to meet the durability requirements of

CP:110[46]. Moderate exposure conditions were assumed to exist on the tension face of retaining walls

A 1:2:3, cement:sand:aggregate, mix by weight with a water cement ratio of 0.6 met these conditions. The concrete had a slump of 80-120mm and a mean concrete cube compressive strength of greater than 25N/mm^2 was always achieved as indicated in Table 3.7. Ordinary Portland cement was used. The aggregate consisted of clean rounded pebbles with a maximum size of 20mm. Presented in Table 3.8 are the results of a wet sieve analysis carried out on the 'concreting' sand which shows the sand lies within grading zone 3 of BS:1200[45].

3.1.2.4 Reinforcing Steel

High-yield ribbed steel reinforcement bars conforming to BS:4449[47] with a type 2 bond classification were incorporated in the walls. Summarised in Table 3.9 are the results of tests carried out by the reinforcement manufacturer on bar specimens that were representative of those used in the retaining walls. The mean yield strength was always greater than the characteristic yield stress specified in the code[3].

TABLE 3.7 COMPRESSIVE STRENGTH OF 100mm CONCRETE CUBES

	COMPRESSIVE STRENGTH (N/mm^2)					
WALL NO.	RW.1	RW.2	RW.3	RW.4	RW.5	RW.6
CUBE NO.1	30.89	36.68	27.02	34.94	31.18	32.43
2	37.65	36.00	35.43	35.91	36.87	34.75
3	33.50	38.42	39.09	28.08	33.21	30.89
4	33.98	27.32	33.30	34.27	37.07	34.56
5	39.38	38.70	32.63	31.47	40.35	31.27
6	34.94	31.90	34.27	30.40	38.42	31.47
7	31.08	47.49	28.96	27.70	37.16	25.87
8	-	37.94	32.34	32.63	39.87	27.22
9	-	-	-	34.36	36.20	28.28
10	-	-	-	31.66	42.86	25.39
11	-	-	-	29.05	38.61	-
12	-	-	-	33.11	40.83	-
MEAN	34.06	36.8	32.88	31.97	37.72	30.21
C.V %	9.1	15.8	11.3	8.5	8.6	11.2

W/C ratio 0.575

TABLE 3.8 GRADING OF CONCRETING SAND FROM CHEADLE

Sieve Size	% passing by weight	
	Concrete Sand	Grading Zone 3[1]
10.0mm	100	100
5.0mm	98.7	90 - 100
2.36mm	89.6	85 - 100
1.18mm	79.4	75 - 100
600um	69.2	69 - 79
300um	38.3	12 - 40
150um	5.8	0 - 10

1 requirement of BS.882:Part 2:1973

TABLE 3.9 SUMMARY OF MATERIAL PROPERTIES FOR WALLS

wall number	1	2	3	4	5	6
Brick type	A	B	B	A	B	B
Mean brick strength (N/mm^2)	84.8	21.6	25.4	64.7	25.4	25.4
Mean initial suction rate of brick ($kg/m^2/min$)	0.25	2.42	2.81	0.64	2.81	2.81
Mean water absorption of brick, 5h boil (%)	4.8	23.2	21.6	5.5	21.6	21.6
Mean water cube strength* (N/mm^2)	11.7	13.5	14.9	13.3	13.6	13.7
Mean concrete cube strength+ (N/mm^2)	34.1	38.6	32.9	32.0	37.7	30.2
Mean brickwork pier strength‡ (N/mm^2)	16.2	6.9	8.4	16.8	8.1	10.9
Mean steel yield strength** (N/mm^2)	443	443	480	480	451	451
Mean steel ultimate strength (N/mm^2)	620	620	643	643	622	622
Code characteristic brickwork strength (N/mm^2)	21.6	7.8	8.8	18.1	8.8	8.8
Code characteristic steel strength (N/mm^2)	425	425	460	460	425	425

* Mortar mix 1:¼:3 cement:lime:sand by volume

\+ Nominal grade 25 N/mm^2 to CP110:1972

‡ 4-course-high one-brick-equare capped piers

** High-yield deformed bars

3.1.3 Construction

The walls were built off a reuseable steel base to which the reinforcement was anchored. In order to provide a good key for the bottom mortar bed expanded steel gauze was bolted to the base and subsequently a propriety bonding agent was applied. The brickwork was built in English bond. Around the reinforcement vertical pockets were formed by omitting whole or half bricks from the bond, Plate 3.1. No more than twenty courses were laid in a day. When the brickwork was completed wooden shuttering was clamped to the rear face of the wall. Concrete was poured into the pockets and subsequently compacted by a poker vibrator to prevent air pockets forming. Usually the concrete was placed in one day in two 1.5m high lifts. The walls were cured for 28 days, under a polythene sheet, prior to testing.

3.1.4 Test Rig

The test rig comprised two items, namely the steel base, on which the wall was built, and the steel reaction frame which carried the loading equipment. A general view of the rig is shown in Plate 3.2.

The reaction frame consisted of three, 3.5m high, triangular, steel reaction frames, spaced at 1.2m centres, bolted to the strong floor. Each frame was connected to its neighbour by a series of horizontal cross beams on which the hydraulic loading cylinders were mounted.

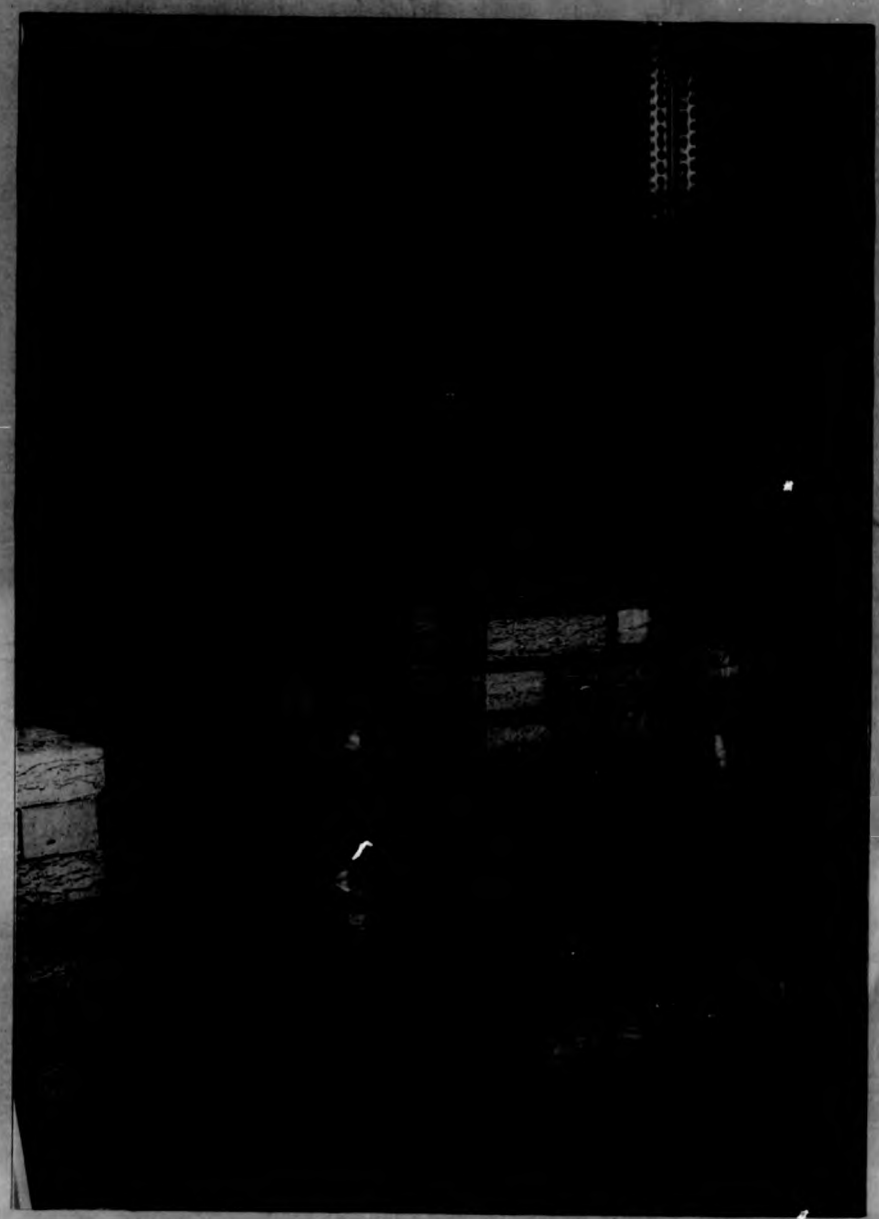

PLATE 3.1 Pocket-type wall under construction

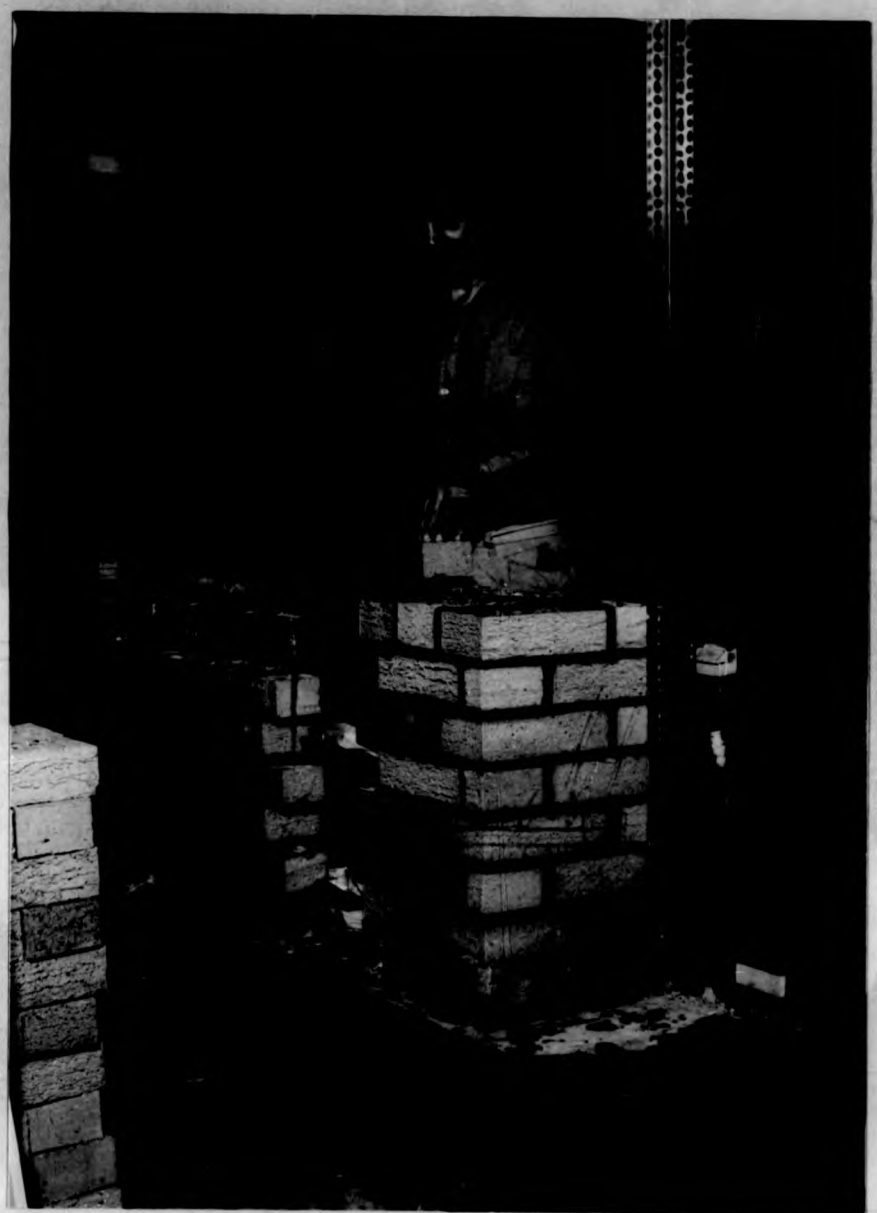

PLATE 3.1 Pocket-type wall under construction

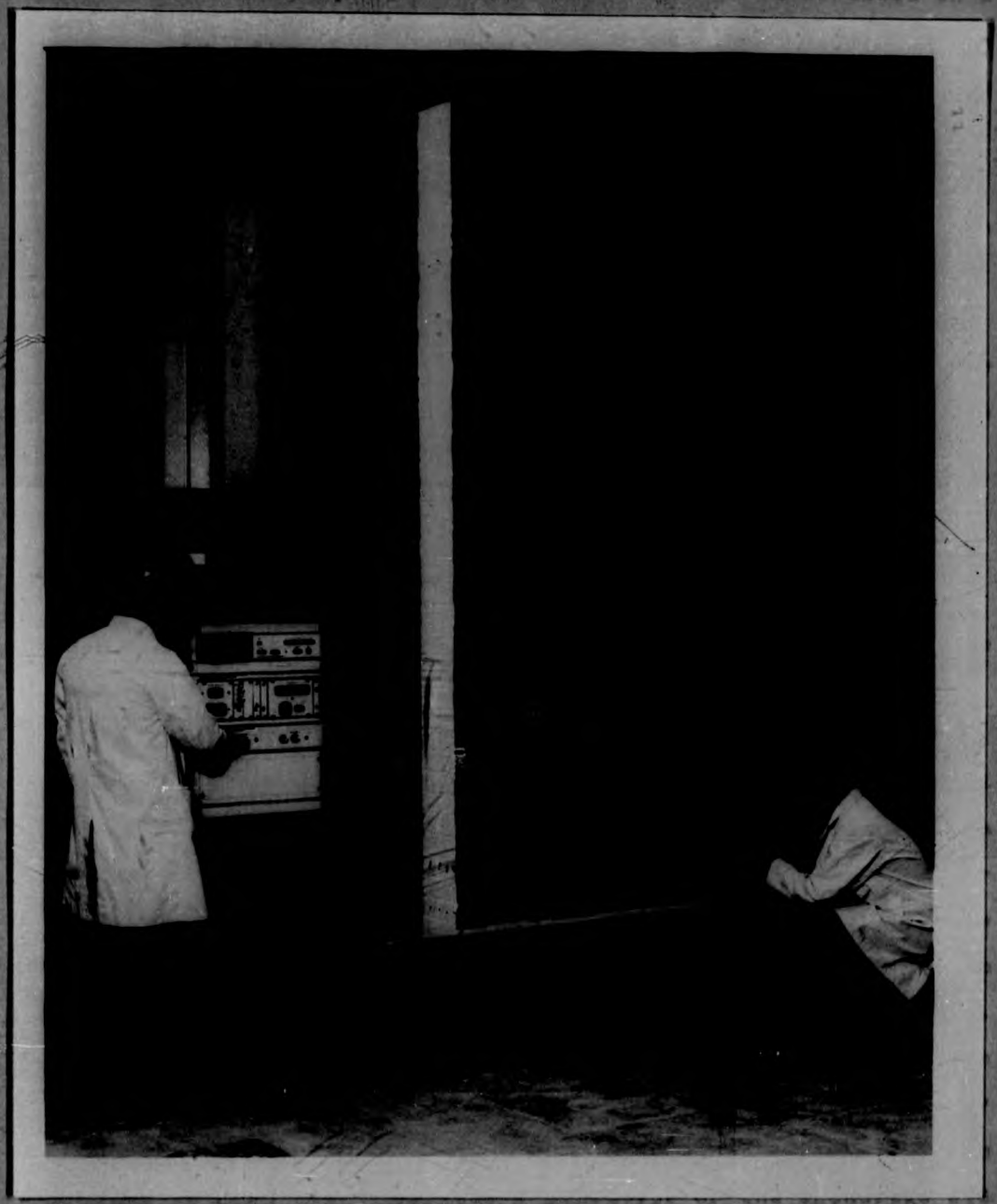

PLATE 3.2 General view of a pocket-type wall under test

PLATE 3.2 General view of a pocket-type wall under test

Under field conditions a retaining wall would be constructed on a reinforced concrete base around the starter bars, however in the laboratory a steel base was found to be advantageous for the reasons outlined below:-

(i) Starter bars would make the behaviour of the walls at the base and the analysis more difficult to interpret.

(ii) The base was required to be reuseable; therefore a steel base used because it could be easily repaired, whereas if a concrete base was damaged it would need to be replaced.

(iii)It is easier to anchor a steel base to the strong floor.

(iv) A steel base could be designed to allow the position of the reinforcement to be varied.

In view of these circumstances it was apparent that the steel base offered the most economic solution. The base comprised a grillage of channel sections welded together to which a cover plate was bolted. This is shown in Figures 3.1 and 3.2. The reinforcement was anchored to the base in one of two ways : In the first test high strength friction grip bolts were used, Fig. 3.3 but these allowed slip in the anchorage of upto 2mm, in subsequent tests the reinforcement was welded to an inverted 'T' section which was bolted to the underside of the steel base as indicated in Fig. 3.4. Tests on a prototype of the anchorage did not detect any slip with this system.

Figure 3.1 Plan of steel base

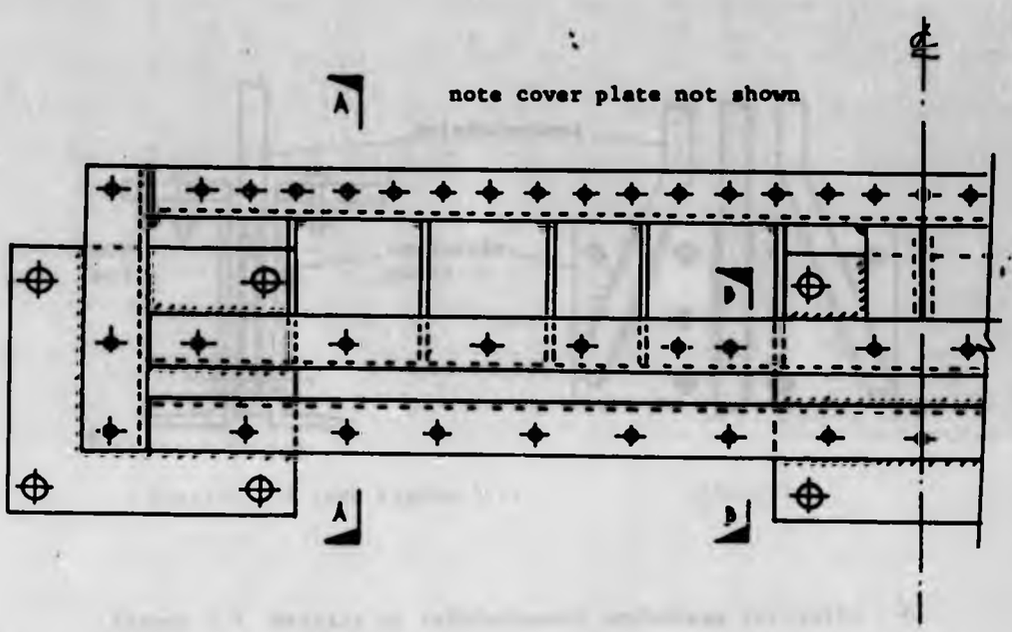

Figure 3.2 Section through wall and base

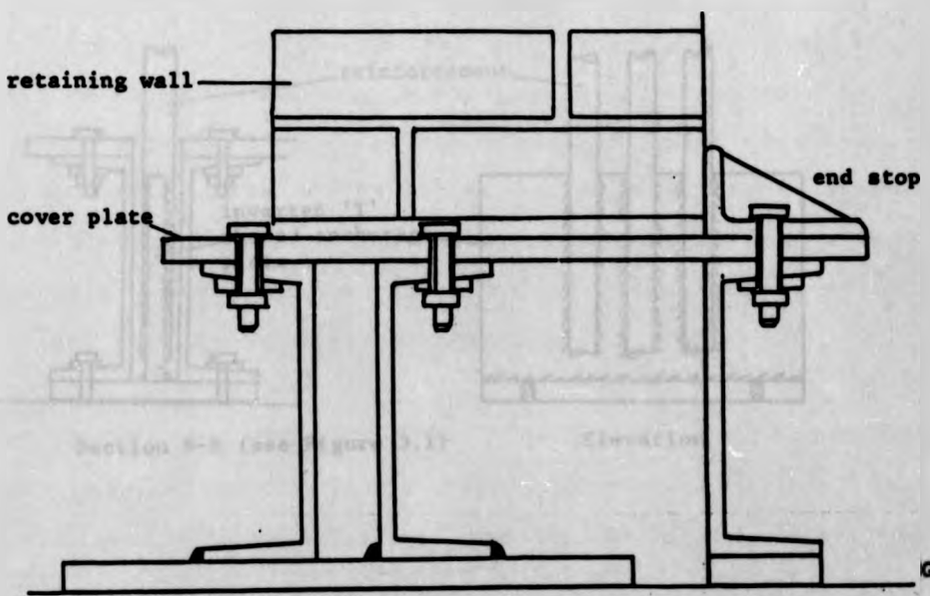

section A-A (see Figure 3.1)

Figure 3.3 Details of reinforcement anchorage for wall 1.

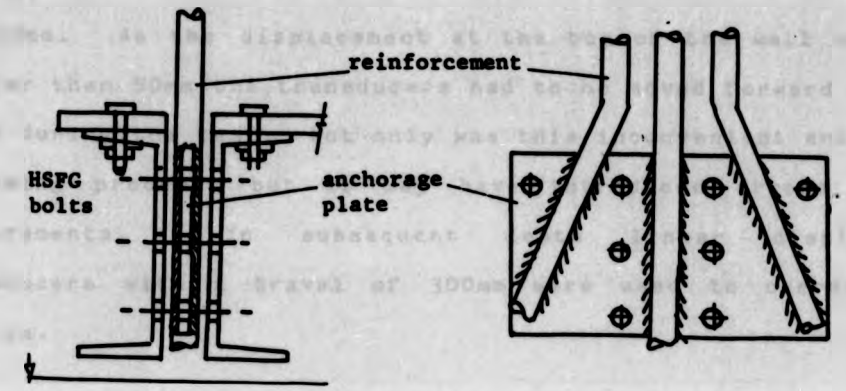

Figure 3.4 Details of reinforcement anchorage for walls 2-6.

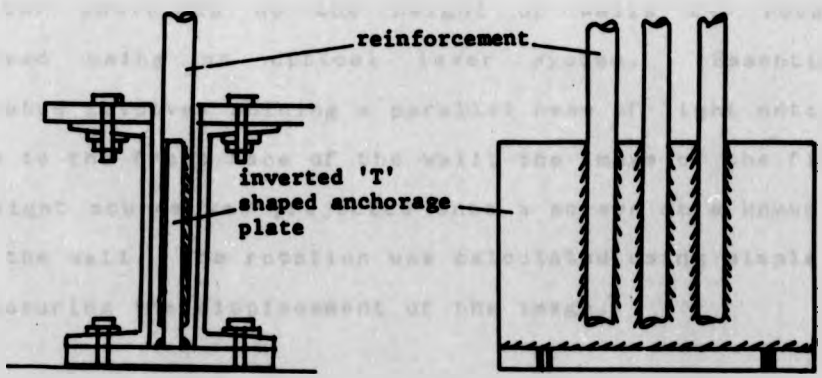

3.1.5 Instrumentation

For the first test displacements were measured using linear voltage displacement transducers with a maximum travel of 25mm and 50mm. As the displacement at the top of the wall was much greater than 50mm the transducers had to be moved forward several times during the test. Not only was this inconvenient and a time consuming process, but it may have introduced errors in the measurements. In subsequent tests linear displacement transducers with a travel of 300mm were used to overcome the problem.

The displacement at the top of the wall was monitored manually during the test using a plumb bob. This enabled a check on the behaviour of the wall during the test and it also acted as a safeguard should the electronic equipment have failed.

At four positions up the height of walls 2-6 rotation was measured using an optical lever system. Essentially the apparatus involves shining a parallel beam of light onto a mirror glued to the front face of the wall; the image of the filament in the light source was projected onto a screen at a known distance from the wall. The rotation was calculated using simple geometry by measuring the displacement of the image.

Strains in the reinforcement were measured using electrical resistance strain gauges bonded onto a prepared surface on the bar. Two gauges were stuck on each bar at a height of 150mm

above the base and placed diametrically opposite. From these the mean strain in each bar was obtained. In the first test four core wire, screened, PVC covered cable was used as the lead wire. This gave problems in the interpretation of the results as moisture permeated the cable affecting the resistance. In subsequent tests an impervious PTFE covered cable was used; the results were no longer affected and they were considered to be reliable for walls 2-6.

The strains in the brickwork were measured manually with a 150mm demec extensometer. Strains were measured around the base of the wall at the same height as the strain gauges on the reinforcement, with most readings being taken on the compression face. In the first test readings were taken at several positions up the height of the wall. These indicated that the brickwork was lightly strained at heights greater than 300mm above the base. Subsequently it was decided to take readings only at the base of the wall for walls 2-6. The strain readings were generally reliable with an accuracy of approximately ± 10μs. However the process of taking readings was a slow one.

Polyester mould embedment electrical resistance strain gauges were built into the compression face of the brickwork in walls 5 and 6. The results of these gauges compared favourably with the manually read demec gauge results from a similar area of the wall Generally the embedment gauges gave lower strains. The main advantages of the embedment gauges were speed of taking readings and that strains could be measured upto failure , unlike the

manual readings. It is recommended that further experience of the use of embedment gauges should be gained before they can be used to replace manual demec readings, until then both methods should be used together.

The load was measured in two ways. The first involved recording the oil pressure in the hydraulic system supplying the jacks using a standard calibrated pressure gauge and the second method used involved load cells placed behind the jacks. There was a good correlation between the two methods. In addition an attempt was made to measure the friction in the jacks, however this was found to be very small and highly variable.

3.1.6 Loading System

In the design of an earth retaining wall the simplest and most often used design load is based on an assumed triangular pressure distribution. A loading arrangement was chosen which gave a proportion of bending momement to shear force at the base of the wall similar to that given by a triangular pressure distribution. The loading arrangement, illustrated schematically in Figure 3.5, comprised three sets of hydraulic jacks at various levels up the wall. The jacks were mounted horizontally on a substantial steel reaction frame, with load cells placed behind the jacks.

The initial loading arrangement was found to be inadequate during the second loading cycle of the test on wall 1 due to insufficient stroke on the jacks at the upper level. These were

Figure 3.5 Loading arrangement, shear force and bending moment diagrams for wall 1,load cycles 182.

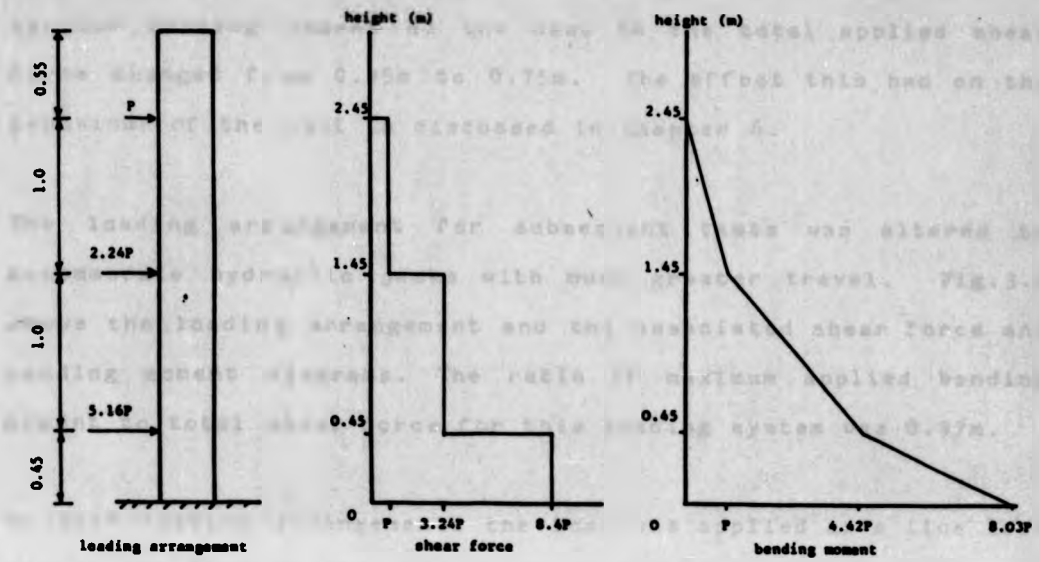

Figure 3.6 Loading arrangement, shear force and bending moment diagrams for walls 2-6.

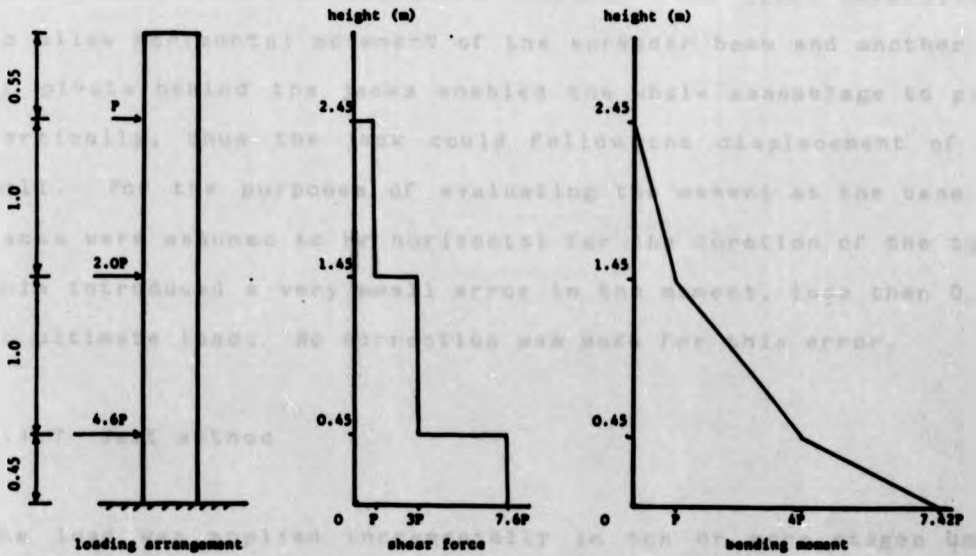

disconnected for the third load cycle, thus the "ratio" of applied bending moment at the base to the total applied shear force changed from 0.95m to 0.75m. The effect this had on the behaviour of the wall is discussed in Chapter 6.

The loading arrangement for subsequent tests was altered to accommodate hydraulic jacks with much greater travel. Fig.3.6 shows the loading arrangement and the associated shear force and bending moment diagrams. The ratio of maximum applied bending moment to total shear force for this loading system was 0.97m.

In both loading arrangements the load was applied as a line load across the face of the wall by three evenly spaced jacks at each load level as illustrated in Fig. 3.7. A hydraulic bolster was placed between the spreader beam and the wall to distribute the load evenly over the brickwork surface. The jacks were pivoted to allow horizontal movement of the spreader beam and another set of pivots behind the jacks enabled the whole assemblage to pivot vertically, thus the jack could follow the displacement of the wall. For the purposes of evaluating the moment at the base the jacks were assumed to be horizontal for the duration of the test. This introduced a very small error in the moment, less than 0.3%, at ultimate load. No correction was made for this error.

3.1.7 Test method

The load was applied incrementally in ten or more stages until failure occurred. Each load increment took about five minutes to

Figure 3.7 Plan of loading arrangement

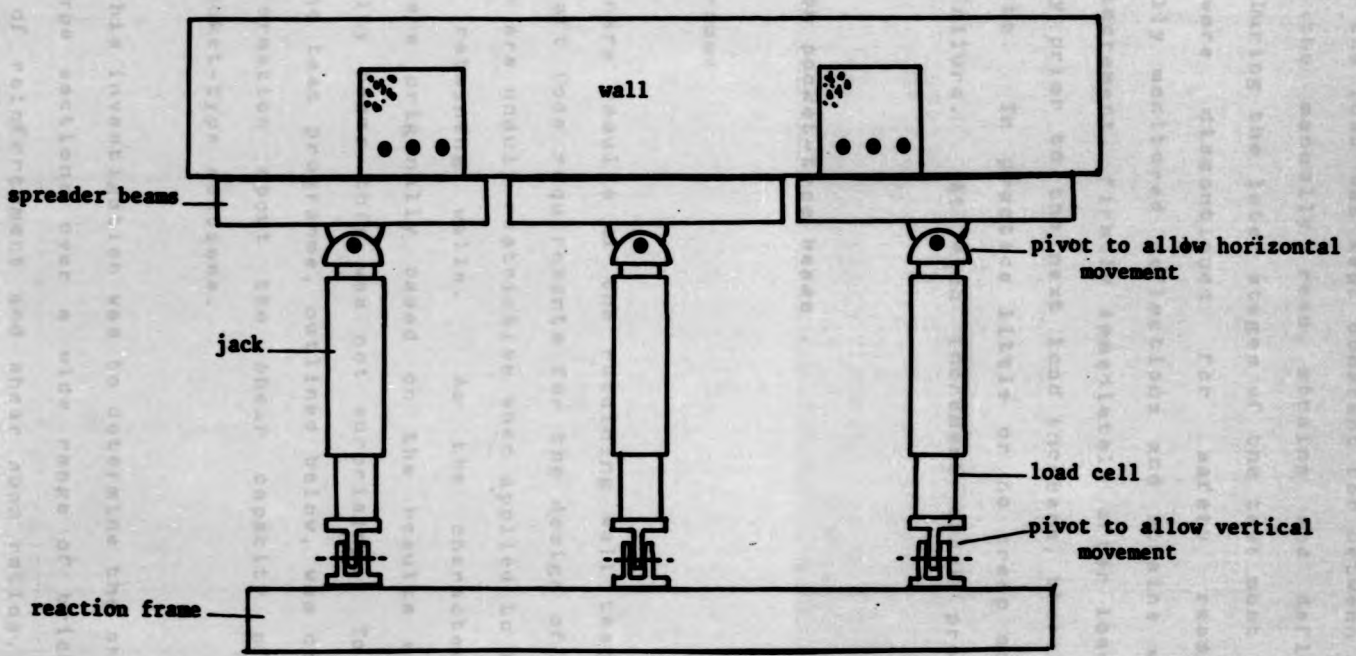

apply, then the load was kept constant for between 15-25 minutes until all the manually read strains and deflections were recorded. During the later stages of the test most of the manual readings were discontinued for safety reasons. The electronically monitored deflections and strains were recorded each load increment, firstly immediately after load application and secondly prior to the next load increase, thereby monitoring creep effects. In practice little or no creep occurred until close to failure. At each increment crack propagation was monitored.

3.2 Tests on pocket-type beams

3.2.1 Programme

The preliminary results of the retaining wall tests suggested that the Draft Code requirements for the design of brickwork to resist shear are unduly restrictive when applied to the design of pocket-type retaining walls. As the characteristic shear strengths were originally based on the results of reinforced grouted cavity beams this was not surprising. To clarify the situation the test programme, outlined below, was carried out to provide information about the shear capacity of reinforced brickwork pocket-type sections.

The aim of this investigation was to determine the shear strength of pocket-type sections over a wide range of brick strengths, percentages of reinforcement and shear span ratios. Table 3.10

TABLE 3.10 BEAM TEST PROGRAMME

Reinforcement %	Span / Effective Depth Ratio 1	2	3	4	5
0.27		C		C	A,B,C
0.53					C
0.88		A,B,C			A,B,C
1.40		C			B,C

NOTE: 1. All beams had nominal dimensions of 1m wide, effective depth 270 and an overall depth 327mm Each beam had a centrally located pocket

2. Brick Type A= 14 hole perforated facing brick
B= deep frogged semi-dry pressed common
C= solid class A engineering brick

TABLE 3.10 BEAM TEST PROGRAMME

Reinforcement %	Span / Effective Depth Ratio 1	2	3	4	5
0.27		C		C	A,B,C
0.53					C
0.88		A,B,C			A,B,C
1.40		C			B,C

NOTE: 1. All beams had nominal dimensions of 1m wide, effective depth 270 and an overall depth 327mm Each beam had a centrally located pocket

2. Brick Type A= 14 hole perforated facing brick
B= deep frogged semi-dry pressed common
C= solid class A engineering brick

gives details of the test programme.

A simply supported beam under two point loading was considered to be the best specimen to be tested in order to examine shear strength because within the beam there is a region of constant maximum bending moment and zero shear force at the centre, whilst at each end there is a constant shear force with a linearly varying bending moment as illustrated in Fig. 3.8. This situation allows an easier understanding of the failure mechanism in that failure may be attributed to either shear forces or flexural forces or a combination of both. This is not possible in a cantilever because both shear force and bending moment are greatest at the base, thus it was considered to be difficult to isolate the cause of failure.

3.2.2 Materials

Generally the materials used in the construction of the walls and beams were similar, therefore the material properties are not reported in detail, but a summary of the mean properties is given in Table 3.11.

A third brick, type C, was used in this investigation. It was a solid, very high strength, low water absorption, class A engineering[42] brick. This brick was not used in the retaining wall series.

The 28 day, compressive strength of four course high (300mm)

Figure 3.8 General arrangement of test beams

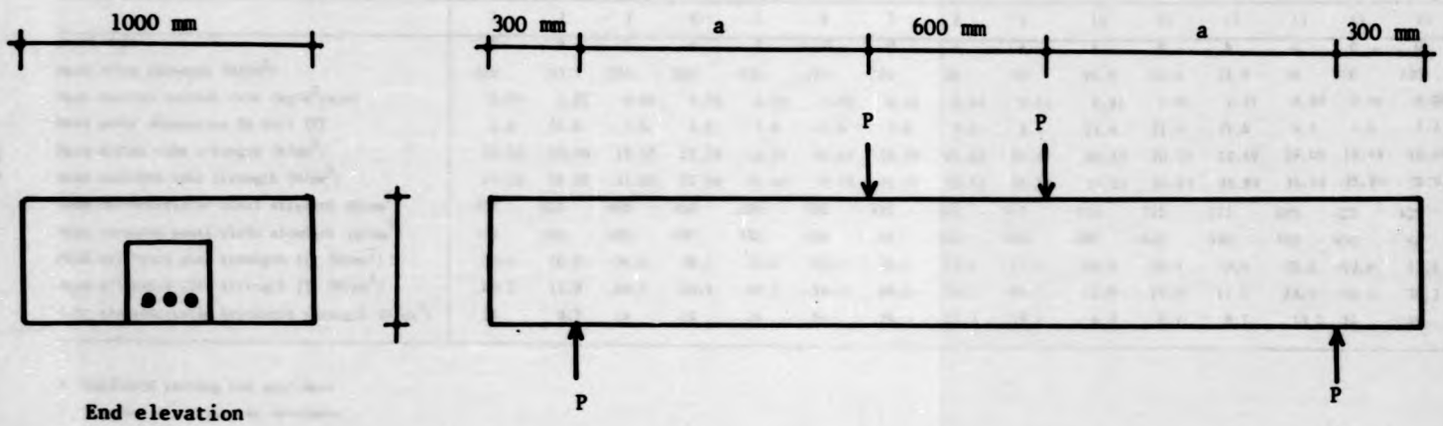

beam nos	shear span a (mm)
5,12-15	560
4	1100
1-3,6-11	1400

TABLE 3.11 MATERIAL PROPERTIES FOR BEAMS

	Beam Number														
	1	2	3	4	5	6	7	8	9	10	11	12	13	14	15
Brick type	C	B	C	C	C	C	C	A	A	B	B	B	A	C	C
Mean brick strength (N/mm^2)	220	25.4	220	220	220	220	220	70	70	25.4	25.4	25.4	70	220	220
Mean initial suction rate ($kg/m^2/min$)	0.06	2.81	0.06	0.06	0.06	0.06	0.06	0.62	0.62	2.81	2.81	2.81	0.62	0.06	0.06
Mean water absorption 5h boil (%)	1.6	21.6	1.6	1.6	1.6	1.6	1.6	5.4	5.4	21.6	21.6	21.6	5.4	1.6	1.6
Mean mortar cube strength (N/mm^2)	13.10	13.10	12.59	12.59	12.59	20.15	18.51	21.42	21.42	20.15	20.15	18.49	18.49	18.49	18.49
Mean concrete cube strength (N/mm^2)	29.16	29.16	31.50	21.50	31.50	37.13	40.31	35.51	35.51	37.13	37.13	35.93	35.93	35.93	35.93
Code characteristic steel strength (N/mm^2)	425	425	460	460	460	425	425	425	460	460	425	425	425	425	425
Mean measured steel yield strength (N/mm^2)	450	450	480	480	480	450	NA	450	480	480	425	450	450	450	NA
Mean brickwork pier strength (1) (N/mm^2) *	36.1	10.8	36.1	36.1	36.1	43.4	36.1	17.4	17.4	10.4	10.4	10.4	18.2	43.4	43.4
Mean brickwork pier strength (2) (N/mm^2) +	60.2	11.8	60.2	60.2	60.2	50.3	60.2	21.1	21.1	11.8	11.8	11.8	23.4	50.3	50.3
Code characteristic brickwork strength (N/mm^2)	24	8.7	24	24	24	24	24	19.2	19.2	8.7	8.7	8.7	19.2	24	24

* Cardboard packing, ten specimens

+ Fibreboard packing, ten specimens

brick square (215mm) brickwork prisms that were built concurrently with beam construction using the same materials are given in Table 3.12.

3.2.3 Construction

The beams were constructed vertically to ensure the workmanship achieved was similar to that for the retaining wall test series. The beams were half the width of the walls (1000mm) and the same depth as the first four walls (327mm). On completion of the brickwork the reinforcement was placed in a centrally located pocket formed by omitting bricks from the bonding pattern and it was accurately positioned by tying it to small diameter bars that spanned the pocket; these were built into the brickwork at intervals up the height of the beam. English bond was again used. Formwork was placed against the beam and the pocket was concreted in one lift. This removed any possibility of a weak construction joint near the centre of the beam. No problems of segregation of the aggregate or bleeding occurred.

3.2.4 Test Rig

The test rig consisted of two items, namely the steel supports at each end of the beam and a steel portal frame which was bolted to the strong floor and carried the loading equipment. A general view of the test arrangement is shown in Plate 3.3.

The load was applied through a pivoted spreader beam onto rollers

TABLE 3.12 COMPRESSIVE STRENGTH OF FOUR COURSE HIGH, 215mm square BRICKWORK PRISMS TESTED ON THE BED FACE

	Compressive Strength (N/mm^2)											
Beam No	1,3,4, & 5		2		8 & 9		10,11,12		13		6,14, 15	
Brick	C		B		A		B		A		C	
Packing	CB[1]	FB[2]	CB	FB	CB	FB	CB	FB	CB	FB	CB	FB
No. 1	43.2	50.0	8.3	13.1	12.3	23.9	7.6	10.1	23.0	24.4	42.9	55.8
No. 2	30.5	62.6	7.6	10.5	16.6	20.6	9.7	12.7	21.0	20.3	43.1	49.8
3	47.0	72.0	13.9	12.3	20.8	25.0	13.7	11.9	19.5	24.8	40.6	57.4
4	36.3	51.6	8.2	12.5	17.0	25.5	10.5	12.1	15.5	20.6	41.8	44.3
5	30.0	70.7	14.5	11.7	11.5	17.2	11.4	12.7	15.2	23.1	40.5	47.3
6	31.2	52.6	12.6	13.2	23.0	17.7	9.2	10.8	19.5	24.2	45.8	56.9
7	41.9	57.0	10.7	11.5	14.6	19.1	6.6	9.5	12.3	29.4	48.0	40.8
8	33.0	72.7	12.3	10.1	20.5	20.1	12.0	11.4	14.5	28.3	52.4	35.0
9	36.1	58.7	11.3	12.8	17.4	22.5	13.0	11.7	22.3	17.9	29.8	53.8
10	31.4	54.5	8.4	10.4	19.9	19.5	10.5	14.9	18.8	21.2	49.4	61.7
Mean	36.1	60.2	10.8	11.8	17.4	21.1	10.4	11.8	18.2	23.4	43.4	50.3
C.V %	16.7	14.5	23.5	9.7	21.7	14.0	21.5	12.8	19.7	15.3	14.3	16.7

NOTE: 1 CB = cardboard
2 FB = fibreboard (Tentest)

which rested on a 100mm wide, 10mm thick, steel plate bedded onto the beam with ciment fondu. This enabled the load to be applied across the full width of the beam. A similar arrangement was used at the supports. The load was applied by a servo-controlled hydraulic jack which contained a built-in load cell.

3.2.5 Instrumentation

The instrumentation that was used for the beams is illustrated in Fig.3.9. Deflections were measured using linear displacement voltage transducers. The mean strain in each reinforcing bar at mid-span was determined using two high yield electrical resistance strain gauges (120Ω) bonded diametrically opposite to each other. One gauge faced the tension face, the other faced the compression face. Brickwork strains were measured at various positions using a 150mm gauge length demec extensometer.

3.2.6 Method

The beams were tested horizontally under two point loading using the equipment illustrated in Plate 3.2. In order to prevent anchorage bond failure of the reinforcement the beams extended beyond the ends of the supports by at least 300mm as indicated in Fig.3.7. The loading points were spaced 600mm (8 courses) apart.

Usually the beams were loaded in ten or more equal load increments until failure occurred. Failure was defined when the beam was unable to sustain an increase in load.

Figure 3.9 Instrumentation on beams

(a) short beams, a/d=2

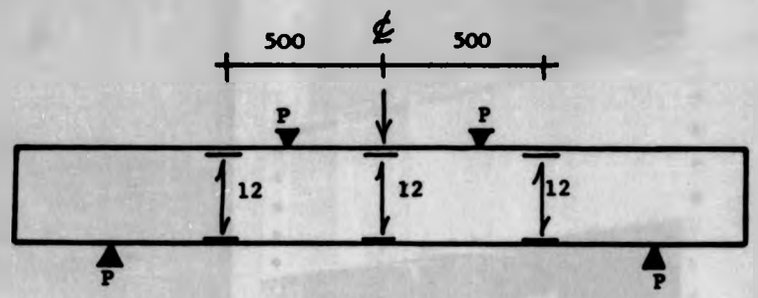

(b) long beams, a/d=4 or 5

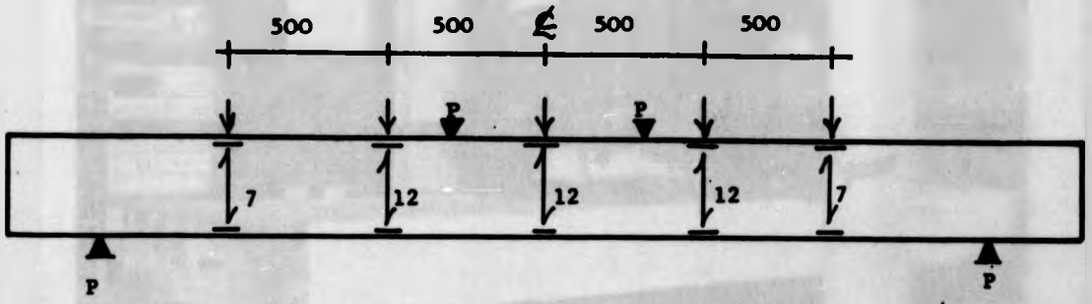

12 position of demec points at the following depths 0,20,40,60,80,100,120,150,200,250,280,320 mm.

7 position of demec points at the following depths 0,40,80,120,150,280,320,

position of linear voltage displacement transducers

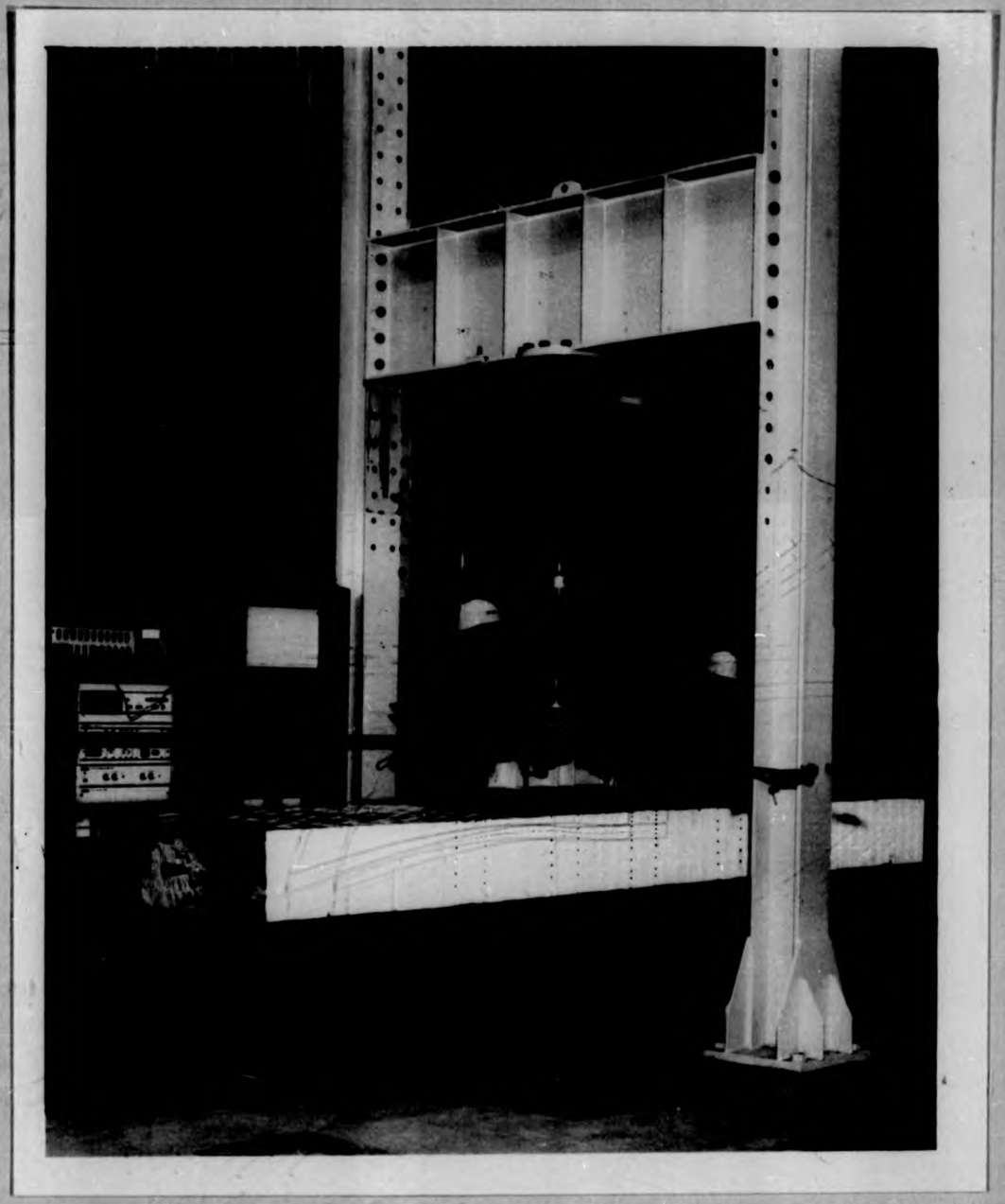

PLATE 3.3 General view of a pocket-type beam under test

PLATE 3.3 General view of a pocket-type beam under test

The procedure used to record information at each load increment was to scan automatically on a data logger the deflections and steel strains, then to read manually the brickwork strains, which took approximately 10 minutes and finally to scan the deflections and steel strains again. This system was used to detect whether the beam was creeping under load; it was found that creep was very small until close to failure. At each load increment the position of cracks was marked.

4. THE FINITE ELEMENT METHOD

4.1 Introduction

It is possible to carry out a simple analysis to evaluate the shear and flexural stresses in a pocket type wall using the design equations in Chapter 2. However the finite element method offers a more sophisticated approach that allows the more complicated aspects of behaviour of a pocket wall to be investigated.

The problem presented by pocket type construction is one of biaxial bending in which the wall spans vertically from the base whilst the brickwork panels span horizontally between the reinforced pockets, Fig.4.1. This situation may be considered analogous to a rectangular two-way spanning slab, supported on three sides with the two parallel supported sides able to cantilever off the third support.

The principal advantage of the finite element method is that it offers a quick and comparatively cheap way of investigating the effects of varying parameters on the performance of a pocket type wall. Thus it is a useful analytical tool for indicating areas where full scale tests are necessary.

4.2 Review of the literature

Many researchers[48-53] have employed the finite element method to

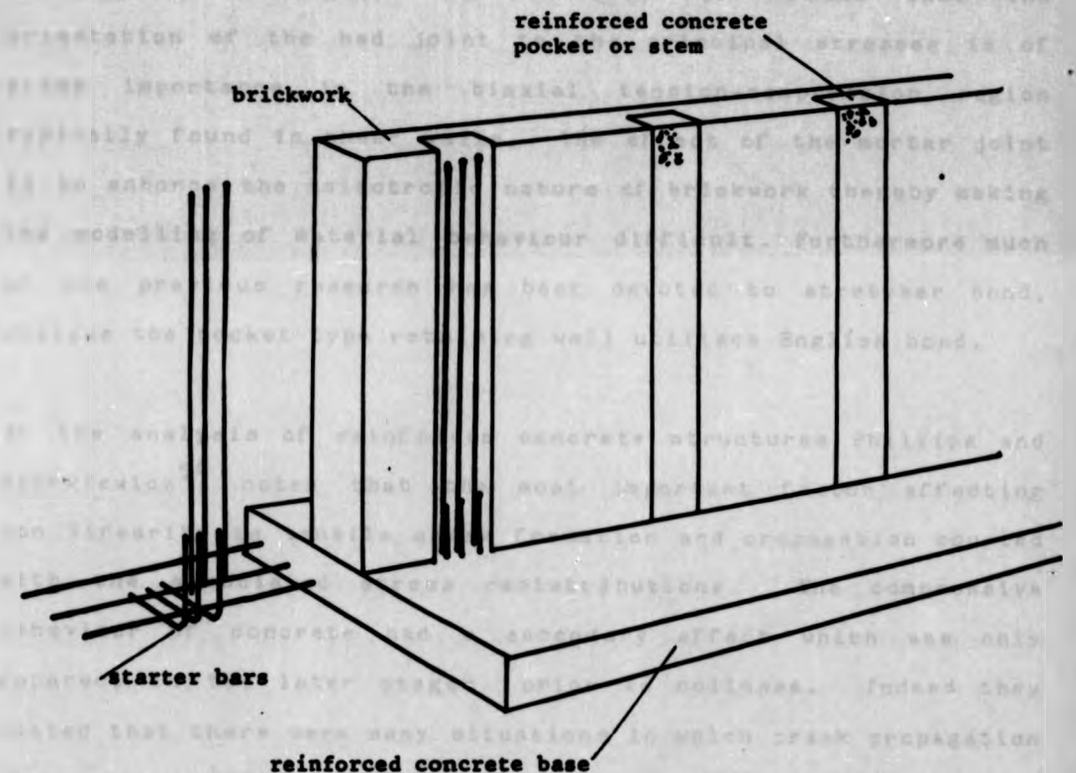

Figure 4.1 Pocket-type reinforced brickwork retaining wall

solve various problems in the design, analysis and research of masonry. The types of problem examined include axially loaded walls, diaphragm walls and shear walls; additionally the theoretical determination of some biaxial constitutive relationships has been performed . A major factor in many of these investigations was the influence of the mortar joint. For example, Samarasinghe, Page and Hendry[51] found that the orientation of the bed joint to the principal stresses is of prime importance in the biaxial tension-compression region typically found in shear walls. The effect of the mortar joint is to enhance the anisotropic nature of brickwork thereby making the modelling of material behaviour difficult. Furthermore much of the previous research has been devoted to stretcher bond, whereas the pocket type retaining wall utilises English bond.

In the analysis of reinforced concrete structures Phillips and Zienkiewicz[54] noted that the most important factor affecting non linearity is tensile crack formation and propagation coupled with the associated stress redistributions. The compressive behaviour of concrete had a secondary effect which was only apparent in the later stages prior to collapse. Indeed they stated that there were many situations in which crack propagation alone was sufficient to predict structural behaviour under applied loading.

Phillips and Zienkiewicz[54] also found that the constant stiffness technique suffered from slow rates of convergence in highly non-linear problems. They considered the best approach

was to update the stiffness matrix at regular intervals, but not every increment. Thus a combination of variable stiffness and constant stiffness approach was feasible because it lead to fast rates of convergence; the main disadvantge is the time required to recompile the stiffness matrix. Crisfield[55,56] found the line search technique, a type of accelerator, offered a considerable improvement on the rate of convergence when a constant stiffness approach was employed. Furthermore it is a simple procedure to implement and uses very little computer time. For these reasons Crisfield's method was employed in this analysis.

4.3. Material constitutive relationships

4.3.1 General

The purpose of this section is to state explicity the assumed properties for brickwork, concrete, reinforcement and the reinforced brickwork composite. However it is understood that these assumptions can only be approximations to the actual behaviour of the reinforced brickwork. Brickwork and concrete are subject to creep, shrinkage, cracking, strength variation with age and strength variation within a member. Brickwork has the additional problem of non-linear highly anisotropic behaviour , for example the compressive, flexural and shear strength vary considerably and are dependent on the orientation of the applied force to the bed joint. Inclusion of reinforcement introduces the additional problems of bond, anchorage and bond slip, which

for the purposes of simplicity have been ignored in the finite element analysis.

4.3.2 Brickwork

Powell and Hodgkinson[57] found that the uniaxial, compressive, stress-strain relationship for brickwork with the load applied on the bed face was a parabola with a falling branch, Fig.4.2. However a literature review[58] indicates that other researchers have not obtained the falling branch. When the load is applied across the head faces (on end) or the stretcher face there is only a limited amount of information [59,60], which suggests that the σ - ε relationship is parabolic but without a falling branch. Moreover the tangential modulus of elasticity and the ultimate stress were markedly lower in the head face and stretcher face directions compared with bed face values. Thus there is a considerable degree of anisotropy. The main problem of incorporating it into a finite element model is the lack of information although it is known that bond pattern, brick type (e.g. solid, frogged or perforated units) specimen shape and orientation of the applied compressive force all have an effect. However Dhanasekar et al [61] have shown that under biaxial stress brickwork using solid units may be regarded as isotropic, contrary to the uniaxial behaviour described above.

The tensile strength of brickwork is usually determined from flexural tests on small walls[62], Fig.4.3, although attempts have been made to measure it directly from brick couplets.

Figure 4.2 Uniaxial stress-strain relationship for brickwork after Powell and Hodgkinson[57]

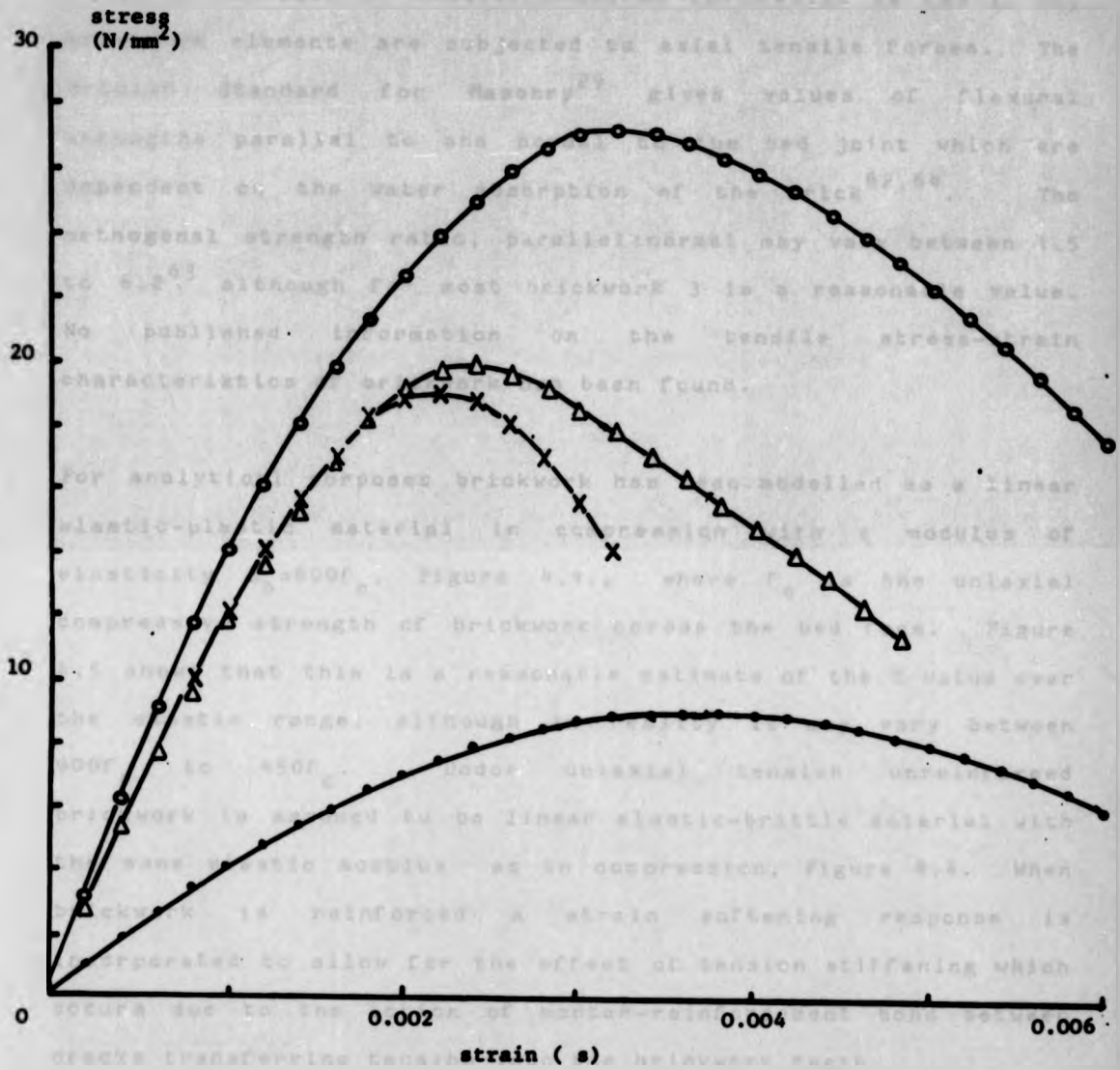

Flexural strength is usually required for design as few if any brickwork elements are subjected to axial tensile forces. The British Standard for Masonry[29] gives values of flexural strengths parallel to and normal to the bed joint which are dependent on the water absorption of the brick[62,64]. The orthogonal strength ratio, parallel:normal may vary between 1.5 to 6.2[63] although for most brickwork 3 is a reasonable value. No published information on the tensile stress-strain characteristics of brickwork has been found.

For analytical purposes brickwork has been modelled as a linear elastic-plastic material in compression with a modulus of elasticity $E_b=600f_c$, Figure 4.4., where f_c is the uniaxial compressive strength of brickwork across the bed face. Figure 4.5 shows that this is a reasonable estimate of the E value over the elastic range, although in reality it may vary between $900f_c$ to $450f_c$. Under uniaxial tension unreinforced brickwork is assumed to be linear elastic-brittle material with the same elastic modulus as in compression, Figure 4.4. When brickwork is reinforced a strain softening response is incorporated to allow for the effect of tension stiffening which occurs due to the action of mortar-reinforcement bond between cracks transferring tension into the brickwork teeth.

Biaxial constitutive relationships for brickwork have received little attention from researchers although Page has examined both the tension-tension[53] range and compression-compression[65] range whilst Samarasinghe and Hendry [66] have studied the

Figure 4.3 Flexural tests on wallettes

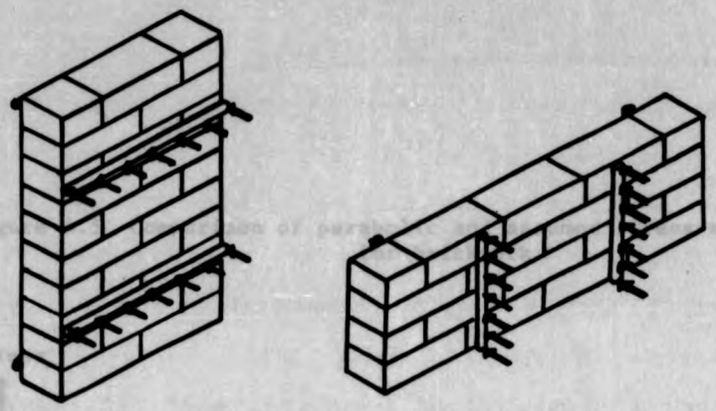

(a) parallel to bed joints (b) normal to bed joints

Figure 4.4 Assumed uniaxial stress-strain relationship for brickwork

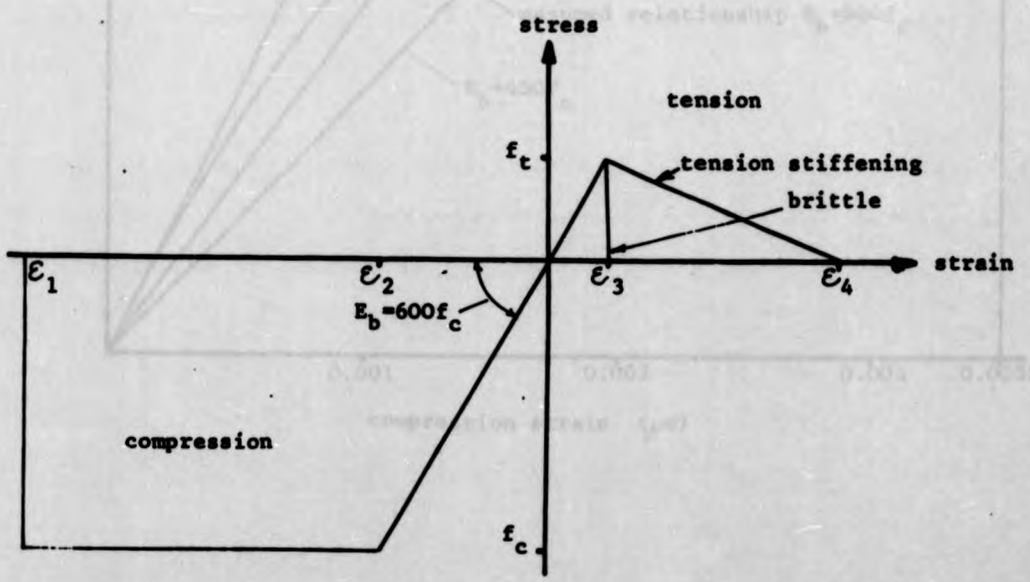

Figure 4.5 Comparison of parabolic and assumed stress-strain curves for brickwork.

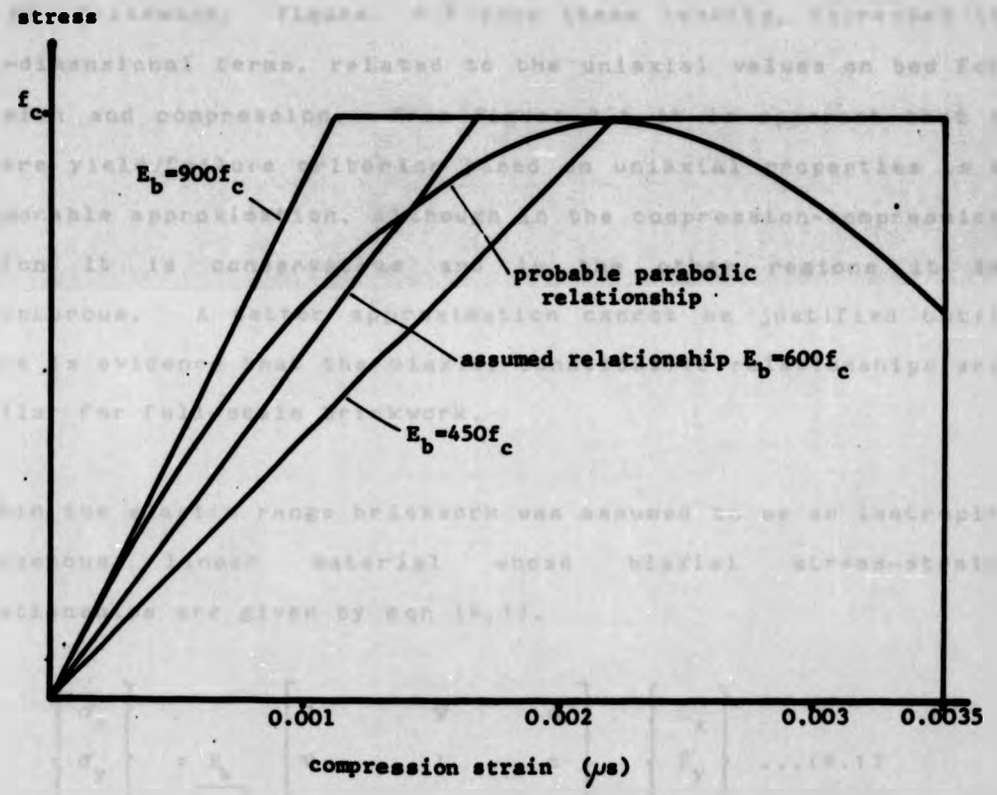

tension-compression range. In each investigation two factors were important, namely the ratio of the principal stresses and their orientation with respect to the bed joint. As all this work was based directly or indirectly on tests on 1/2 or 1/6th scale brickwork using one type of brick mortar combinations then care must be exercised before assuming that these results apply to all brickwork. Figure 4.6 show these results, expressed in non-dimensional terms, related to the uniaxial values on bed for tension and compression. From Figure 4.6 it is apparent that a square yield/failure criterion based on uniaxial properties is a reasonable approximation, although in the compression-compression region it is conservative and in the other regions it is adventurous. A better approximation cannot be justified until there is evidence that the biaxial constitutive relationships are similar for full-scale brickwork.

Within the elastic range brickwork was assumed to be an isotropic homogenous linear material whose biaxial stress-strain relationships are given by eqn (4.1).

$$\begin{Bmatrix} \sigma_x \\ \sigma_y \\ \tau_{xy} \end{Bmatrix} = \frac{E_b}{1-\nu^2} \begin{bmatrix} 1 & \nu & 0 \\ \nu & 1 & 0 \\ 0 & 0 & \frac{1-\nu}{2} \end{bmatrix} \begin{Bmatrix} \varepsilon_x \\ \varepsilon_y \\ \gamma_{xy} \end{Bmatrix} \quad \ldots(4.1)$$

Brickwork is defined as cracked when the strain within the element is algebraically greater than the transition strain, ε_3, from the uniaxial stress-strain curve, Figure 4.4. Cracks are

Figure 4.6 Comparison of the experimental biaxial relationship for brickwork with the square yield/failure criterion.

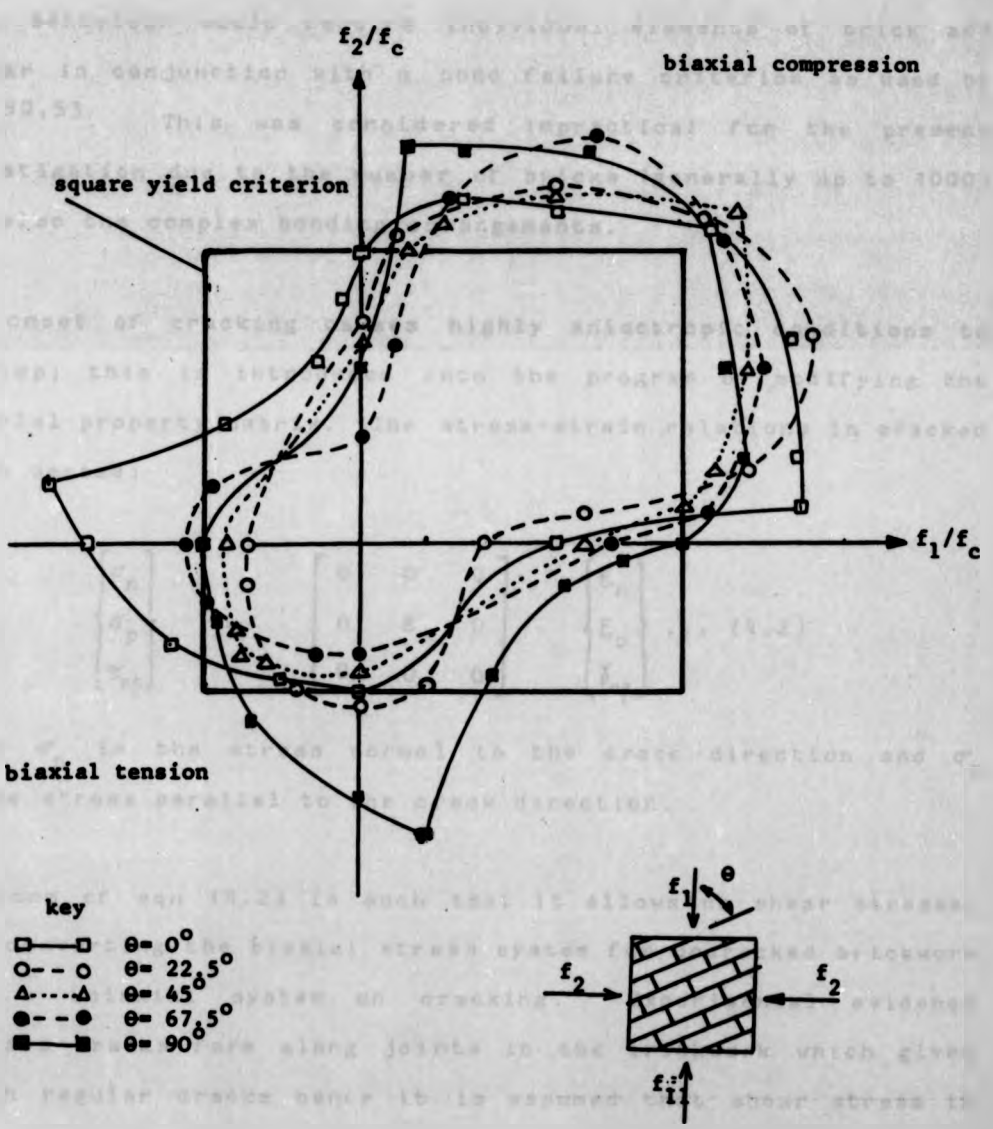

assumed to form perpendicular to the principal tensile stress in the brickwork. This may not be strictly true as Samarasinghe, Page and Hendry[51] and Edgell, Tellett and Hodgkinson[67] have shown that cracking generally occurs along the brick-mortar interface rather than through the brick unit. However to model this behaviour would require individual elements of brick and mortar in conjunction with a bond failure criterion as used by Page[50,53]. This was considered impractical for the present investigation due to the number of bricks (generally up to 1000) and also the complex bonding arrangements.

The onset of cracking causes highly anisotropic conditions to develop; this is introduced into the program by modifying the material property matrix. The stress-strain relations in cracked zones become:

$$\begin{Bmatrix} \sigma_n \\ \sigma_p \\ \tau_{np} \end{Bmatrix} = \begin{bmatrix} 0 & 0 & 0 \\ 0 & E & 0 \\ 0 & 0 & 0 \end{bmatrix} \begin{Bmatrix} \varepsilon_n \\ \varepsilon_p \\ \gamma_{np} \end{Bmatrix} \quad \ldots (4.2)$$

where σ_n is the stress normal to the crack direction and σ_p is the stress parallel to the crack direction.

The form of eqn (4.2) is such that it allows no shear stresses thus converting the biaxial stress system for uncracked brickwork into a uniaxial system on cracking. Experimental evidence suggests cracks form along joints in the brickwork which gives smooth regular cracks hence it is assumed that shear stress is

not transferred across the crack.In practice cracks form randomly at discrete points which is difficult to model because it requires either many small elements or a very large number of sampling points. Either way, the process involves a considerable additional number of calculations with an associated increase in execution time. Thus smeared properties are assumed in which the properties at the sampling points represent the average of those for a portion of the element. Hence a crack in the analysis may represent two or more closely spaced but narrower cracks. Cracks are allowed to open and close at will during the analysis with no control exercised over the orientations of successive openings and closures.

4.3.3 Concrete

Concrete is usually assumed to be a material with a parabolic stress-strain relationship under uniaxial stress. In this respect it is similar to brickwork. Moreover the biaxial properties of concrete as determined by Kupfer, Hilsdorf and Rush[68] may be represented by a square yield criterion.

Hence to simplify the analysis and reduce the number of elements concrete has been assumed to have identical properties to those assumed for brickwork, section 4.3.2.

However there is one major aspect of concrete behaviour which differs from brickwork, that is the ability of cracked concrete to carry shear stresses across a cracked boundary due to the

irregular nature of the cracks. It has been suggested [54,69] that a shear retention factor should be included to cater for this phenomenon. It was considered that the proportion of shear transference across the cracked concrete was small compared with the total shear on a pocket-type retaining wall, hence no allowance was made for this effect.

4.3.4 Steel reinforcement

Individual reinforcement bars cannot be modelled easily with the chosen element. Instead a bar element lying parallel to the appropriate co-ordinate axis with smeared uniaxial properties and no bending or shear stiffness was developed to model the reinforcement.

The assumed uniaxial stress-strain relationship for the reinforcement is linear elastic up to yield stress f_y then plastic as illustrated in Figure 4.7 .

If the strain in the element lies between the transition strains ε_2 and ε_3, Figure 4.7, the reinforcement is elastic and eqn (4.3a) or (4.3b) applies for the x-direction and y-direction respectively.

$$\sigma_x = E\,\varepsilon_x \qquad \ldots(4.3a)$$

$$\sigma_y = E\,\varepsilon_y \qquad \ldots(4.3b)$$

Figure 4.7 Assumed uniaxial stress-strain relationship for steel reinforcement.

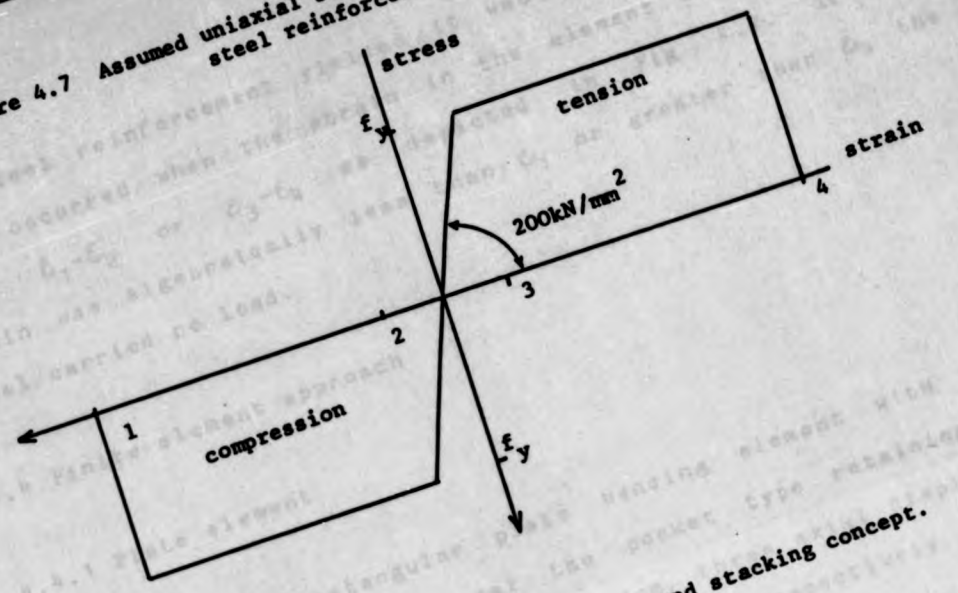

Figure 4.8 Element coordinate system and stacking concept.

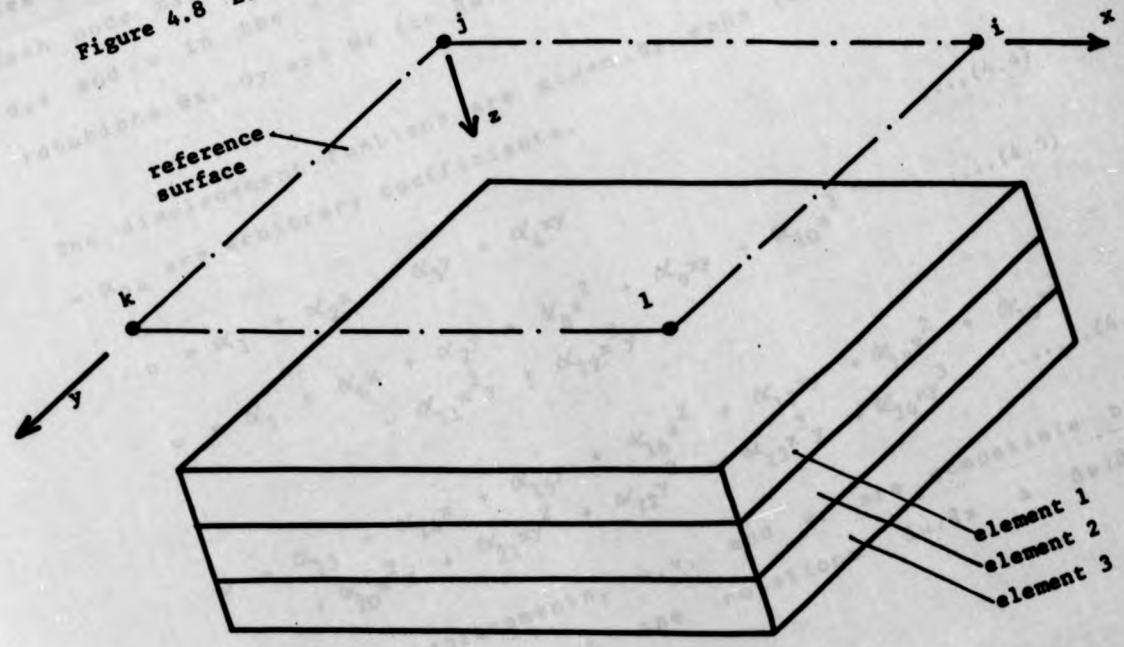

When steel reinforcement yielded it was assumed to be plastic which occurred when the strain in the element was within the range ε_1-ε_2 or ε_3-ε_4 as depicted in Fig 4.7. If the strain was algebraically less than ε_1 or greater than ε_4 the steel carried no load.

4.4 Finite element approach

4.4.1 Plate element

A four noded rectangular plate bending element with offset axes[70] was chosen to model the pocket type retaining wall. Each node has six degrees of freedom, three axial displacements u,v and w in the x y and z directions respectively and three rotations θx, θy and θz (ie ∂w/∂y, - ∂w/∂x and ∂v/∂x).

The displacement funtions are given by eqns (4.4-4.6) where α_1 - α_{24} are arbitrary coefficients.

$$u = \alpha_1 + \alpha_2 x + \alpha_3 y + \alpha_4 xy \qquad \ldots.(4.4)$$

$$v = \alpha_5 + \alpha_6 x + \alpha_7 y + \alpha_8 x^2 + \alpha_9 xy + \alpha_{10} x^3 + \alpha_{11} x^2 y + \alpha_{12} x^3 y \qquad \ldots.(4.5)$$

$$w = \alpha_{13} + \alpha_{14} x + \alpha_{15} y + \alpha_{16} x^2 + \alpha_{17} xy + \alpha_{18} y^2 + \alpha_{19} x^3 + \alpha_{20} x^2 y + \alpha_{21} xy^2 + \alpha_{22} y^3 + \alpha_{23} x^3 y + \alpha_{24} xy^3 \qquad \ldots.....(4.6)$$

The three displacements, u,v, and w, are compatible between adjacent elements but the rotations ∂w/∂x & ∂w/∂y are

incompatible, therefore the element is classed as non-conforming. As the rotations are discontinuous the element may have greater flexibility than that actually possessed by the continuum. There may also be discontinuity of stresses at element boundaries except at the nodes where equilibrium of the forces from adjacent elements is achieved. However this may be counteracted by the displacement function which restricts the deformed shape of the element.

A feature of this element is that the displacement in the x direction given by eqn (4.4) varies linearly between two nodes whilst in the y direction a cubic variation of displacement may occur, hence the element is more flexible in the y direction. Therefore it is important to consider carefully the element discretisation when investigating the structural behaviour of a member because if insufficient elements are used the deflections in the x direction may be under estimated.

By definition the edges of the element are parallel to the x & y axes as indicated in Figure 4.8. Thus by coupling of the flexural and extensional behaviour it becomes possible to stack elements or divide elements into layers, each element having a common reference surface which may be offset from the mid plane of the element.

Hand et al[69] give an excellent description of the layering concept in which a simpler plate bending element was used. Instead of stacking elements they used a single element with

variations in material properties through the depth simulated by splitting the element into layers, each layer corresponding to a change in material properties. The present study uses the analogous stacking concept, each stacked element modelling a change in material properties or perhaps a change in section. Thus it is possible to model 'I', 'L', 'T' sections. The assumed material properties for brickwork concrete and steel are outlined in Section 4.3.

The main advantage of stacking elements is that a three dimensional problem can be examined using a two dimensional analysis without incurring the cost associated with three dimensional analysis. Furthermore it is only necessary to incorporate biaxial constitutive relationships. The main disadvantage is that the shear stress through the depth is not taken into account in the analysis.

4.4.2 Method

The finite element method is described briefly below and in more detail by Zienkiewicz[71]. A program was specifically written to examine the behaviour under load of a pocket-type retaining wall. The procedure employed in obtaining a solution to the non-linear problem is outlined by a flow chart in Figure 4.9. A constant stiffness approach was adopted with non-linearity being introduced through material properties and rapid convergence was achieved using an accelerator.

Figure 4.9. Non-linear solution procedure

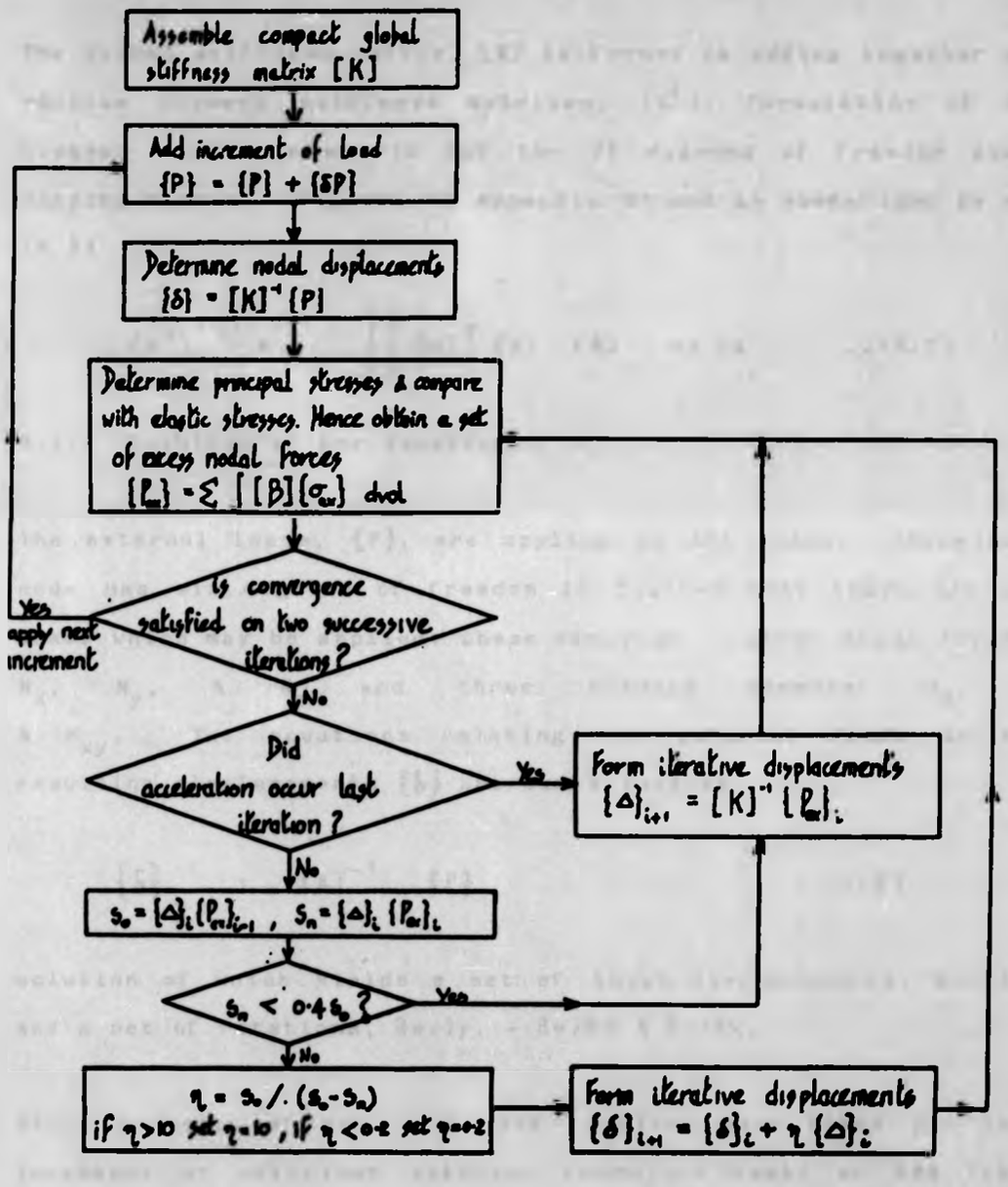

4.4.3 Global Stiffness Matrix

The global stiffness matrix, [K] is formed by adding together the various element stiffness matrixes, $[K^e]$. Formulation of the element stiffness matrix for the 24 degrees of freedom plate bending element is given in Appendix A1 and is summarised by eqn (4.7)

$$[K^e] = \iint [B]^T [D] [B] \, dx \, dy \qquad ..(4.7)$$

4.4.4 Solution of the Equations

The external loads, $\{P\}$, are applied to the nodes. Since each node has six degrees of freedom it follows that there are six loads which may be applied: these comprise three axial forces, N_x, N_y, & N_z and three bending moments, M_x, M_y & M_{xy}. The equations relating the external loads to the resulting displacements $\{\delta\}$ are summarised as

$$\{\delta\} = [K]^{-1} \{P\} \qquad ...(4.8)$$

solution of which yields a set of axial displacements, u,v & w and a set of rotations, $\partial w/\partial y$, $-\partial w/\partial x$ & $\partial v/\partial x$.

Since solution of eqn (4.8) was required many times per load increment an efficient solution technique based on the Crout method was adopted. The technique, described in detail by Zienkiewicz [71] requires decomposition (factorisation) of the

upper triangular part of the global stiffness matrix, which is subsequently stored.

4.4.5. Stresses

The stresses within an element are computed from the strains using equ (4.10), however it is first necessary to determine the strains from eqn (4.9)

$$\{\varepsilon\} = [B]\{\delta\} \qquad \ldots(4.9)$$

$$\{\sigma\} = [D]\{\varepsilon\} \qquad \ldots(4.10)$$

Where $\{\varepsilon\}$, [B], $\{\delta\}$, $\{\sigma\}$, & [D] are defined in Appendix A.1.

Within the element the strains and curvatures are calculated at the Gauss points because these give the best estimation of the variation in the stress resultants across the element for a given number of sampling points [71]. This is a form of numerical integration in which a weighting function is applied to the strains at the Gauss points. A two point integration scheme in the x and y directions (2x2), Figure 4.10, was chosen by considering how the strains may vary across the element. Differetiation of the displacement functions, eqns (4.4, 4.5, & 4.6), gives the strains and curvatures.

$$\varepsilon_x = \frac{\partial u}{\partial x} = \alpha_2 + \alpha_4 y \qquad \ldots.(4.11a)$$

$$\varepsilon_y = \frac{\partial v}{\partial y} = \alpha_7 + \alpha_9 x + \alpha_{11} x^2 + \alpha_{12} x^3 \qquad (4.11b)$$

Figure 4.10 Integration scheme for element.

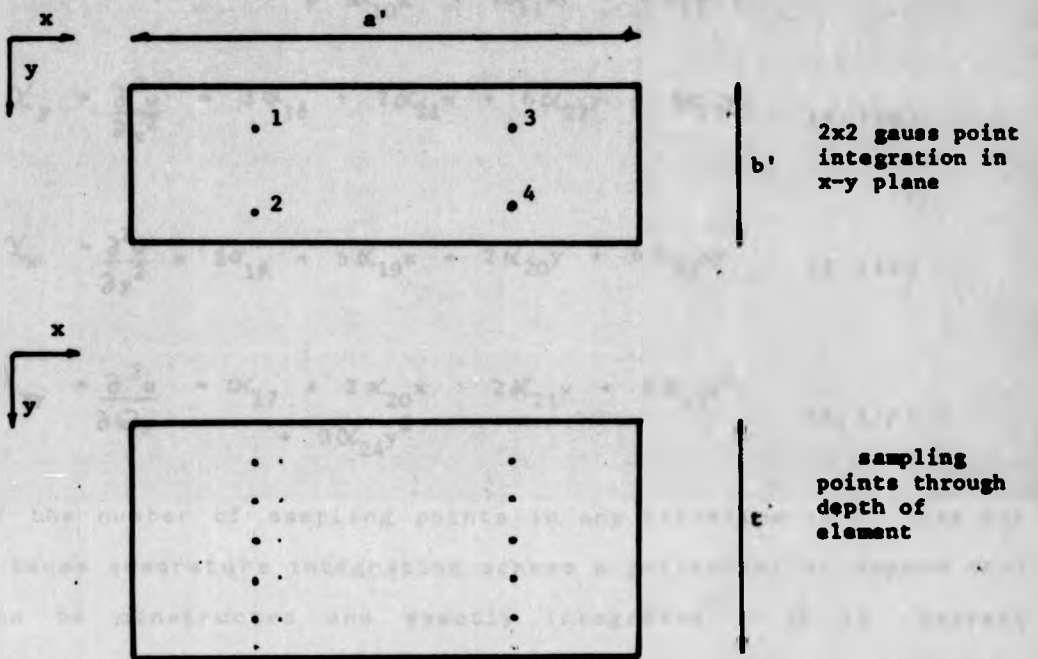

Figure 4.11 A one dimensional problem showing the acceptable range of the acceleration scalar, η.

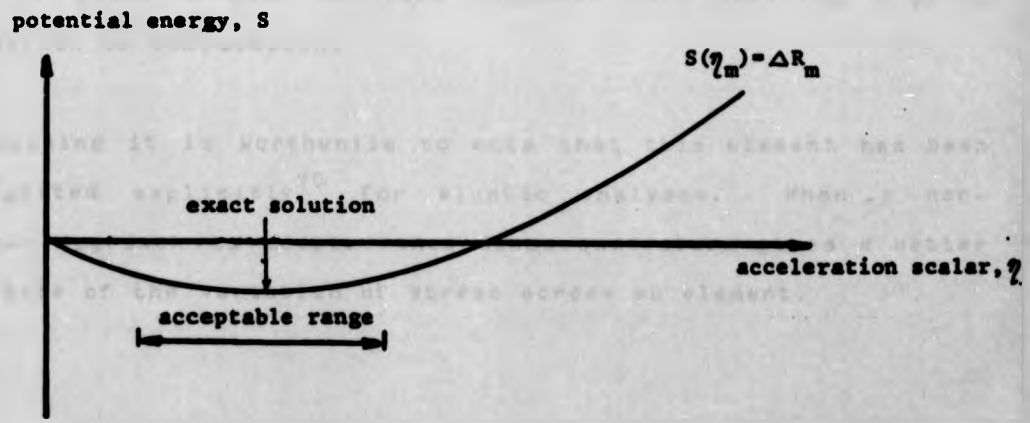

$$\gamma_{xy} = \frac{\partial u}{\partial y} + \frac{\partial v}{\partial x} = \alpha_3 + \alpha_4 x + \alpha_6 + 2\alpha_8 x + \alpha_9 y + 3\alpha_{10}x^2 + 2\alpha_{11}xy + 3\alpha_{12}x^2 y \quad (4.11c)$$

$$\chi_y = \frac{\partial^2 w}{\partial x^2} = 2\alpha_{16} + 2\alpha_{21}x + 6\alpha_{22}y + 6\alpha_{23}xy \quad (4.11d)$$

$$\chi_x = \frac{\partial^2 w}{\partial y^2} = 2\alpha_{18} + 6\alpha_{19}x + 2\alpha_{20}y + 6\alpha_{23}xy \quad (4.11e)$$

$$\chi_{xy} = \frac{\partial^2 w}{\partial x \partial y} = \alpha_{17} + 2\alpha_{20}x + 2\alpha_{21}y + 3\alpha_{23}x^2 + 3\alpha_{24}y^2 \quad (4.11f)$$

If the number of sampling points in any direction is n, then for a Gauss quadrature integration scheme a polynomial of degree 2n-1 can be constructed and exactly integrated[71]. It is apparent from eqn (4.11b) that the highest order polynomial expressions is the cubic variation of x, hence for E_y to be determined exactly it is necessary to employ a two point integration scheme in each direction. Furthermore it has been shown that a 2x2 scheme is more suitable than a 3x3 scheme because it converges more rapidly and it gives a more accurate response thus offering a great reduction in computation.

In passing it is worthwhile to note that this element has been integrated explicitly[70] for elastic analyses. When a non-linear approach is adopted then Gauss quadrature gives a better estimate of the variation of stress across an element.

In addition to sampling the strains on the x-y plane, they were sampled at various stations through the depth of the element (out of plane) . These are required to detect non-linear behaviour. Usually five equally spaced stations were employed to facilitate interpretation of the results, Figure 4.10. Thus in each element strains were sampled at twenty (4x5) positions, although only four of these are independent. The rest are related to the distance from the reference surface, Appendix A1.

4.4.6 Evaluation of Excess Nodal Forces

Non linear material behaviour develops within an element when the principal strains at the sampling points exceed the elastic strains on stress strain curve, Figs 4.4 & 4.7 . This results in an imbalance between the internal nodal forces and the external applied loads which manifest itself as a set of excess or residual forces. These simulate degradation in the stiffness of the structure due to non-linear material properties; as such they are considered to be ficticious. To evaluate them it is necessary to calculate the principal strains at the sampling points. If the principal strain, ε_p, is inside the plastic range of the stress strain curve then the actual stress is f_c or f_t and the difference between the actual and elastic stress is the excess principal stress, σ_{ex}, noting that tension is positive.

The excess principal stress is converted into excess principal stress resultant by eqns 4.12.a & 4.12.b which are subsequently

resolved into components along the coordinate axes.

$$N_p = \sigma_{ex} t \qquad \ldots.(4.12.a)$$

$$M_p = \sigma_{ex} t\, z \qquad \ldots.(4.12.b)$$

where t is the thickness of the stations and z is the distance from the refernce surface to the sampling points.

The excess nodal forces, $\{P_{ex}\}$, are obtained by integrating through the depth of the station and by applying weighting functions, W_m and W_n, across the area of the element in the x and y directions as given in eqn (4.13)

$$\{P_{ex}\} = \sum_{m=1}^{n_x} \sum_{n=1}^{n_y} W_m W_n \int_0^t [B]^T \begin{Bmatrix} N \\ M_{ex} \end{Bmatrix} dx.dy\, dz \qquad \ldots(4.13)$$

where $\begin{Bmatrix} N \\ M_{ex} \end{Bmatrix}$ is the out of balance excess stress resultant vector.

4.4.7 Line Search Technique

The constant stiffness approach is a reliable but uneconomical method of obtaining a solution to a non-linear problem. To improve this situation the program incorporates an accelerator whose effect is to reduce the number of iterations at any given

load level. The method is based on a line search technique[56] and is illustrated in Figure 4.9.

The iterative procedure is given by eqn (4.14) where the trial displacements $\{\delta\}_m$ are updated to $\{\delta\}_{m+1}$ using an iterative displacement vector $\{\delta_{ex}\}_m$ and an accelerating scalar η_m.

$$\{\delta\}_{m+1} = \{\delta\}_m + \eta \{\delta_{ex}\} \quad \ldots.(4.14)$$

where $$\{\delta_{ex}\}_m = [K]^{-1} \{P_{ex}\}_m \quad \ldots.(4.15)$$

For non-linear analysis of problems involving cracking Crisfield[56] has shown that it is advantageous to apply a line search to find the optimum or near optimum value of the acceleration scalar. Effectively the line search process tries to find a stable equilibrium state by choosing a value of η_m such that the out of balance forces in the next iteration are zero. In practice the program does not set out to achieve this exactly but allows a range of values wich are considered acceptable; for a one dimensional problem the concept is illustrated in Figure 4.11.

The following simplified approach was employed to obtain a suitable estimate of the acceleration scalar. Firstly assume $\eta_m = 1$ from which eqns (4.16 & 4.17) are derived where S_o and S_n are a measure of the potential energy in the system in sucessive iterations.

$$S_o = \{\delta_{ex}\}_m^T \{P_{ex}\}_{m-1} \quad \ldots.(4.16)$$

$$S_n = \{\delta_{ex}\}_m^T \{P_{ex}\}_m \quad \ldots.(4.16)$$

Secondly interpolate linearly to determine the acceleration scalar for the next iteration, η_{m+1} , using eqn. (4.17). A tolerance, ψ , is placed on the range of acceptable values of η_{m+1} according to eqn (4.18). It may be quite slack at ψ=0.8 or quite tight at ψ=0.4 as incorporated in the program. Crisfield [56] showed the latter tolerance gives the better results. If eqn. (4.18) is not satisfied then the procedure reverts to the unaccelerated constant stiffness approach.

$$\eta_{m+1} = \eta_m \frac{S_o}{S_o + S_n} \quad \ldots(4.17)$$

where $$\frac{S_o}{S_n} < \psi \quad \ldots(4.18)$$

Moreover limits are placed on the magnitude of the accelerating scalar to prevent numerical difficulties. For instance if η_{m+1} is greater than η_m the process involves extrapolation which may result in over-acceleraton whereas if η_{m+1} was very small the change in displacements and rotations would be small and the next excess force vector $\{P_{ex}\}_{m+1}$ would be nearly the same as the current one $\{P_{ex}\}_m$; hence the procedure may fail to converge. The limits below, used successfully by Crisfield, were incorporated into the program.

if $\eta_{m+1} < 0.2$ set $\eta_{m+1} = 0.2$

and if $\eta_{m+1} > 10$ set $\eta_{m+1} = 10$

4.4.8 Convergence

A convergence criterion is necessary to determine when the residual or out of balance forces have reached an acceptable value. This situation arises from the iterative procedure involved in trying to achieve an equilibrium state between the externally applied forces and the internal nodal forces. In practice equilibrium is unlikely to be achieved exactly in a non-linear analysis, thus the method is an approximation which for its accuracy is dependent on the convergence criterion adopted.

Two criteria were tried, the first was a dual criteria based on a residual displacement norm, eqn. (4.19a) and a residual rotation norm, eqn. (4.19b). Both of these had to be satisfied before convergence was deemed to have been achieved. The tolerances ϕ_D and ϕ_R were both equal and a value of 0.001 was found to be adequate. Occasionally, at large displacements near failure, this criterion gave a spurious set of converged displacements whilst large residual forces remained. This occurred with very large total displacements because the incremental displacements were comparatively small; thus convergence was achieved.

$$\phi_D > \sqrt{\frac{\Sigma(\text{incremental displacements})^2}{\Sigma(\text{total displacements})^2}} \qquad \ldots.(4.19a)$$

$$\phi_R > \sqrt{\frac{\Sigma(\text{incremental rotations})^2}{\Sigma(\text{total rotations})^2}} \qquad \ldots.(4.19b)$$

The second criterion utilized the residual force norm based solely on the out of plane (z direction) nodal forces, eqn (4.20).

Previously Cope and Rao[72] had successfully used this technique with a similar plate bending element. They found that a tolerance ϕ_F=0.02 was generally satisfactory. This criterion performed better than the displacement norm near to failure, although it required slightly more iterations to achieve convergence at low loads. Prior to failure when tight tolerences were used both criteria gave almost identical analyses.

$$\phi_F > \sqrt{\frac{\Sigma(\text{out of plane reidual forces})^2}{\Sigma(\text{applied out of plan nodal forces})^2}} \qquad \ldots.(4.20)$$

On balance the residual force norm was considered to be the better criterion since it was reliable at failure. Subsequently it was employed for the majority of analyses reported herein.

4.5 Application of the finite element method

4.5.1 Introduction

This section considers briefly the performance of the technique and element in relation to published experiental and theoretical work. Problems specifically examined include one-way and two-way reinforced concrete slabs, reinforced brickwork retaining walls, unreinforced and reinforced brickwork panels, arching action in unreinforced, one-way, brickwork panels. Element discretisation matrial prcperties and convergence tolerances are also studied. Load control was used for all the analyses.

4.5.2 A one-way reinforced concrete slab

A one-way reinfcrced concrete slab tested by Jain and Kennedy[73] was analysed using the material properties given in Figure 4.12. This slab which is effectively a beam was analysed four times with the convergence tolerance, ϕ_p, varied from 0.02 to 0.005. In Figure4.12 the results may be compared with the experimental solution and another finite element solution[56] which used the same element discretisation of the problem. It can be seen that the program gave a reasonable approximation to the experimental behaviour. Although the theoretical responses were more flexible than the experimental results an improvement in the theoretical response occurred when allowance was made for tension stiffening effects by assuming β=8.

Figure 4.12 Load deflection behavior of a one-way slab

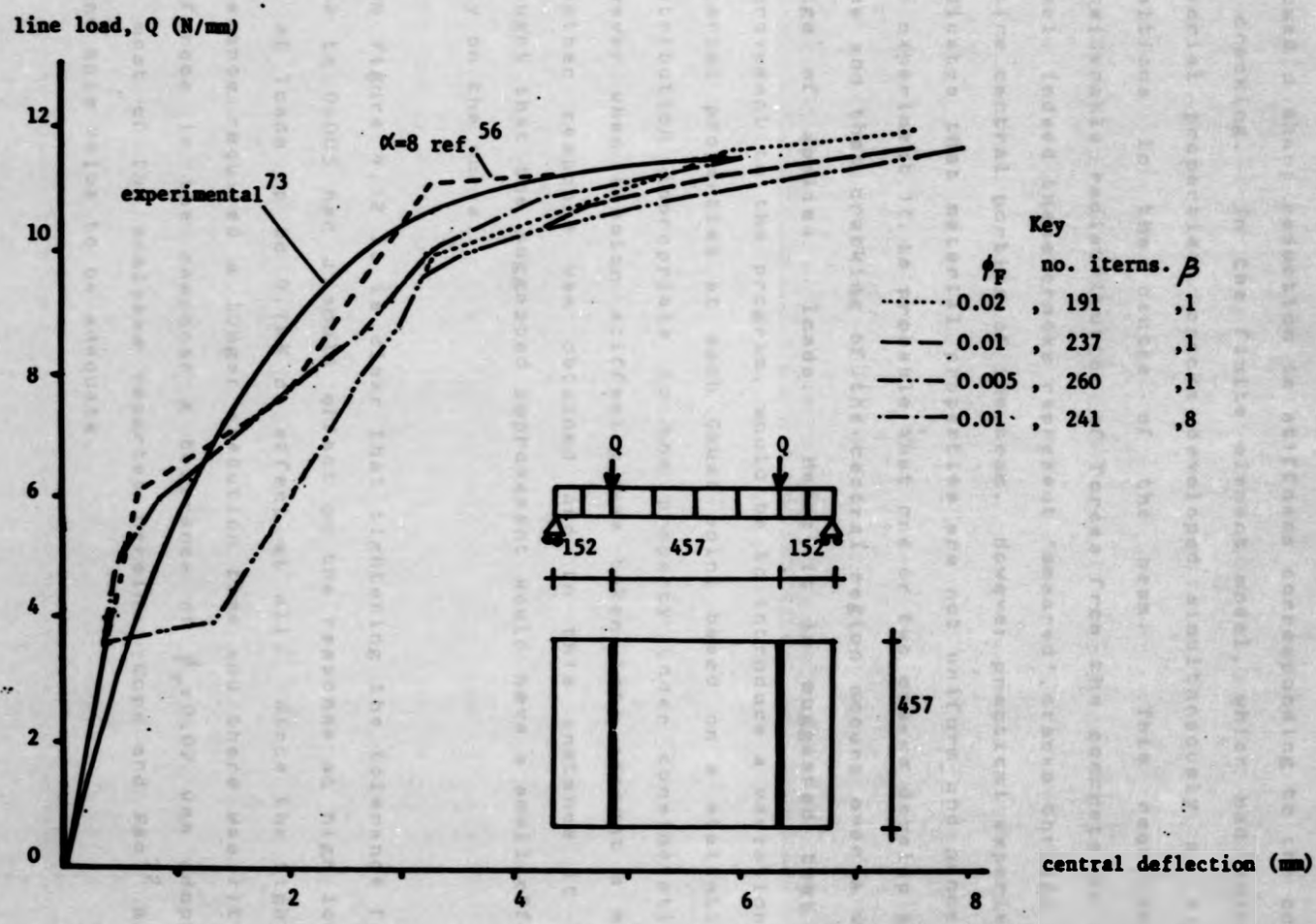

When tension stiffening was not incorporated, β=1, the responses showed a sharp reduction in stiffness corresponding to the onset of cracking. In the finite element model, which had uniform material properties, cracks developed simultaneously at eight positions in the centre of the beam. This required a considerable redistribution of forces from the concrete to the steel. Indeed these cracks represent 'smeared' cracks through the entire central portion of the beam. However practical experience indicates that material properties are not uniform and hence in the experiment it is probable that one or two cracks develop at a time and that cracking of the central region occurs over a wide range of applied loads. Hence it is suggested that an improvement to the program, would be to introduce a variation in material properties at each Gauss point based on a statistical distribution appropriate to the property under consideration. However when tension stiffening was taken into account a much smoother response was obtained and in this instance it was thought that the suggested improvement would have a small effect only on the curve.

From Figure 4.12 it is clear that tightening the tolerance from 0.02 to 0.005 had a small effect on the response at high loads and at loads up to 9.7kN no effect at all. Since the tighter tolerance required a longer execution time and there was little differece in the response a tolerance of ϕ_r=0.02 was adopted for most of the analyses reported herein. Cope and Rao[72] also found this value to be adequate.

4.5.3 A two-way reinforced concrete slab

It was considered important to examine the performance of the finite element model when analysing two-way action in slabs. The example chosen was a two-way reinforced concrete slab simply supported on its corners which was tested by McNiece[74] . This problem has been analysed by many researchers, the majority of whom used a 6x6 element discretisition of a quarter of the slab.

The effects of element discretisation are illustrated by the load-deflection curves shown in Figure 4.13. The analysis using the 1x1 element mesh did not indicate failure until a load of 28kN, thus the mesh was inadequate, probably because there were insufficient points at which the stresses were sampled. Both the 3x3 and 6x6 meshes gave satisfactory results, there being little difference between them, however the 6x6 mesh required an eight fold increase in execution time. Failure occurred at 22kN for the 3x3 mesh and at 19.2kN for the 6x6 mesh. Hence a relatively coarse mesh, such as the 3x3, should be adequate for analysis of slabs and panels.

Also shown is the experimental result of McNiece[74] and the theoretical result of Crisfield[56] who also used a 3x3 , mesh to analyse this problem . The main differences between Crisfield's analysis and this study were the integration schemes through the depth, the solution procedure and the modelling of the material properties. It is probably the latter with accounts for most the difference since Crisfield employed a Von Mises

Figure 4.13 Load-deflection behaviour of a two-way slab

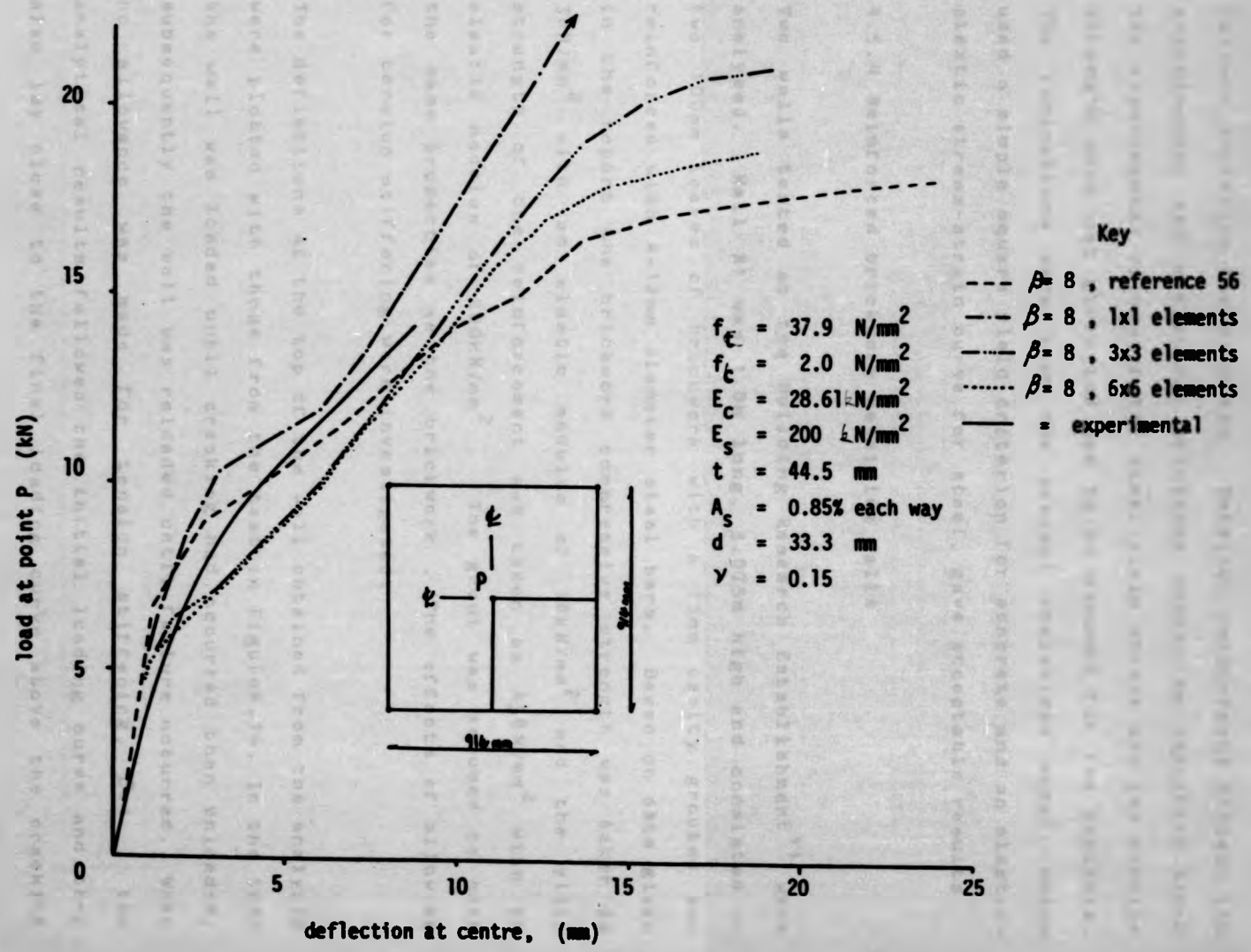

failure criterion for concrete. Detailed comparisons between the experimental and analytical solutions cannot be justified since the experimental values of the steel yield stress and the tensile strength were not given and had to be assumed for the analysis. The indications were that the present analytical model, which used a simple square yield criterion for concrete and an elastic-plastic stress-strain curve for steel, gave acceptable results.

4.5.4 Reinforced brickwork retaining walls

Two walls tested at the Building Research Establishment[11] were analysed. Wall R1 was 1.0m long, 3.075m high and consisted of two 100mm leaves of brickwork with a 75mm cavity grouted and reinforced with 4-12mm diameter steel bars. Based on data given in the report the brickwork compressive strength was taken as $38N/mm^2$ with an elastic modulus of $18kN/mm^2$ and the yield strength of the reinforcement was taken as $436N/mm^2$ with an elastic modulus of $200kN/mm^2$. The grout was assumed to have the same properties as the brickwork . The effects of allowing for tension stiffening were investigated.

The deflections at the top of the wall obtained from the analysis were plotted with those from the test in Figure4.14. In the test the wall was loaded until cracking had occurred then unloaded, subsequently the wall was reloaded until failure occurred. When no allowance was made for tension stiffening, $\beta=1$, the analytical results followed the initial loading curve and they also lay close to the final loading curve above the cracking

Figure 4.14 Load deflection behavior of reinforced brickwork wall R1[11]

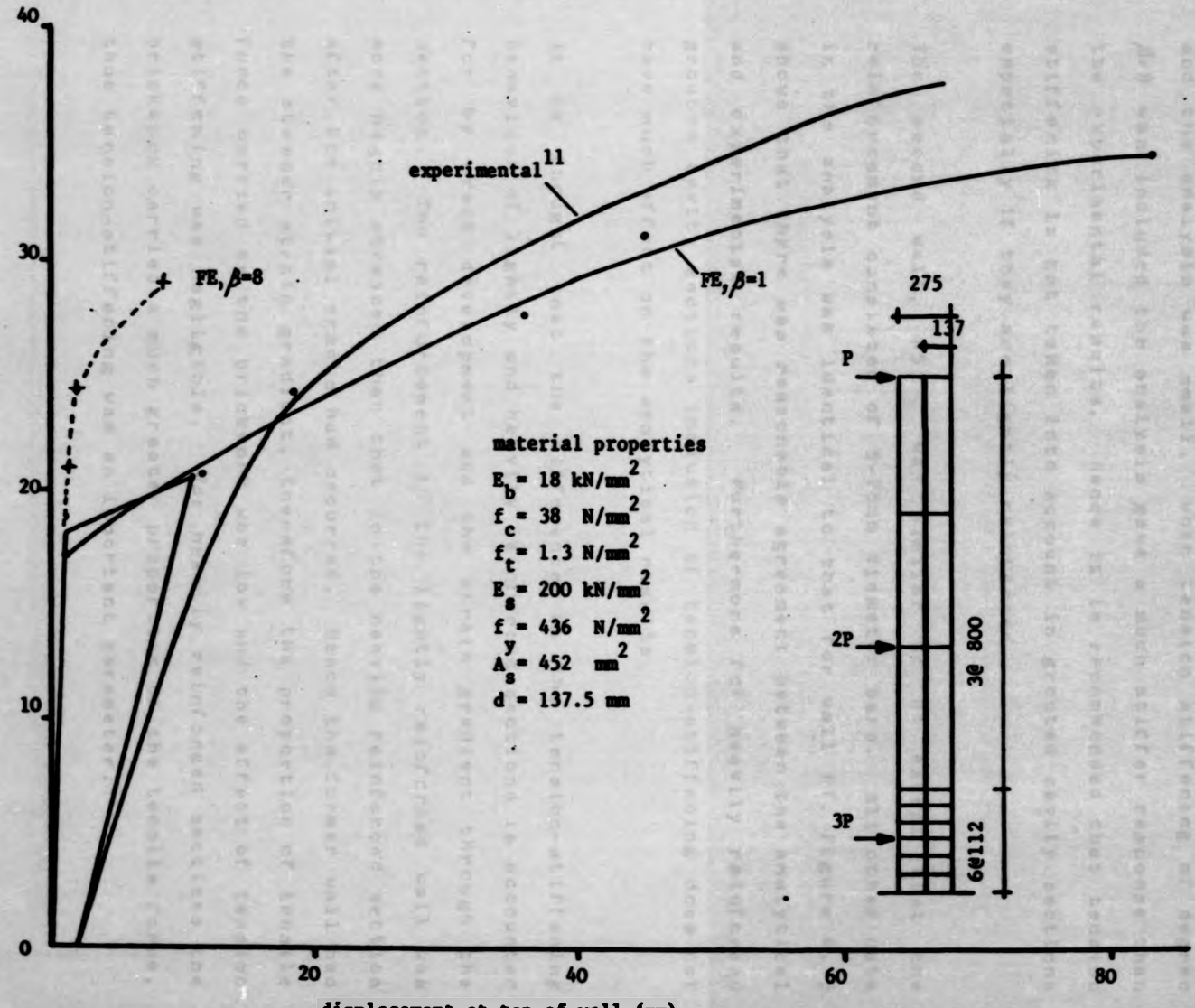

load. The difference between the collapse loads from the test and the analysis was small. when tension stiffening of degree β=8 was included the analysis gave a much stiffer response than the experimental results. Hence it is recommended that tension stiffening is not taken into account in grouted cavity sections especially if they are lightly reinforced.

The second wall, R5 , was similar to R1 except that the reinforcement consisted of 5-25mm diameter bars. All other data in the analysis was identical to that for wall R1. Figure 4.15 shows that there was reasonable agreement between the analytical and experimental results. Furthermore for heavily reinforced grouted cavity sections inclusion of tension-stiffening does not have much effect on the analytical results.

It is thought that the difference in the tension-stiffening behaviour of lightly and heavily reinforced sections is accounted for by crack development and the strain gradient through the section. The reinforcement in the lightly reinforced wall was more highly stressed than that in the heavily reinforced section after the initial cracks had occurred. Hence the former wall had the steeper strain gradient, therefore the proportion of tensile force carried by the brickwork was low and the effect of tension stiffening was negligible. For heavily reinforced sections the brickwork carried a much greater proportion of the tensile force, thus tension-stiffening was an important parameter.

Figure 4.15 Load deflection behavior of reinforced brickwork wall R5[11]

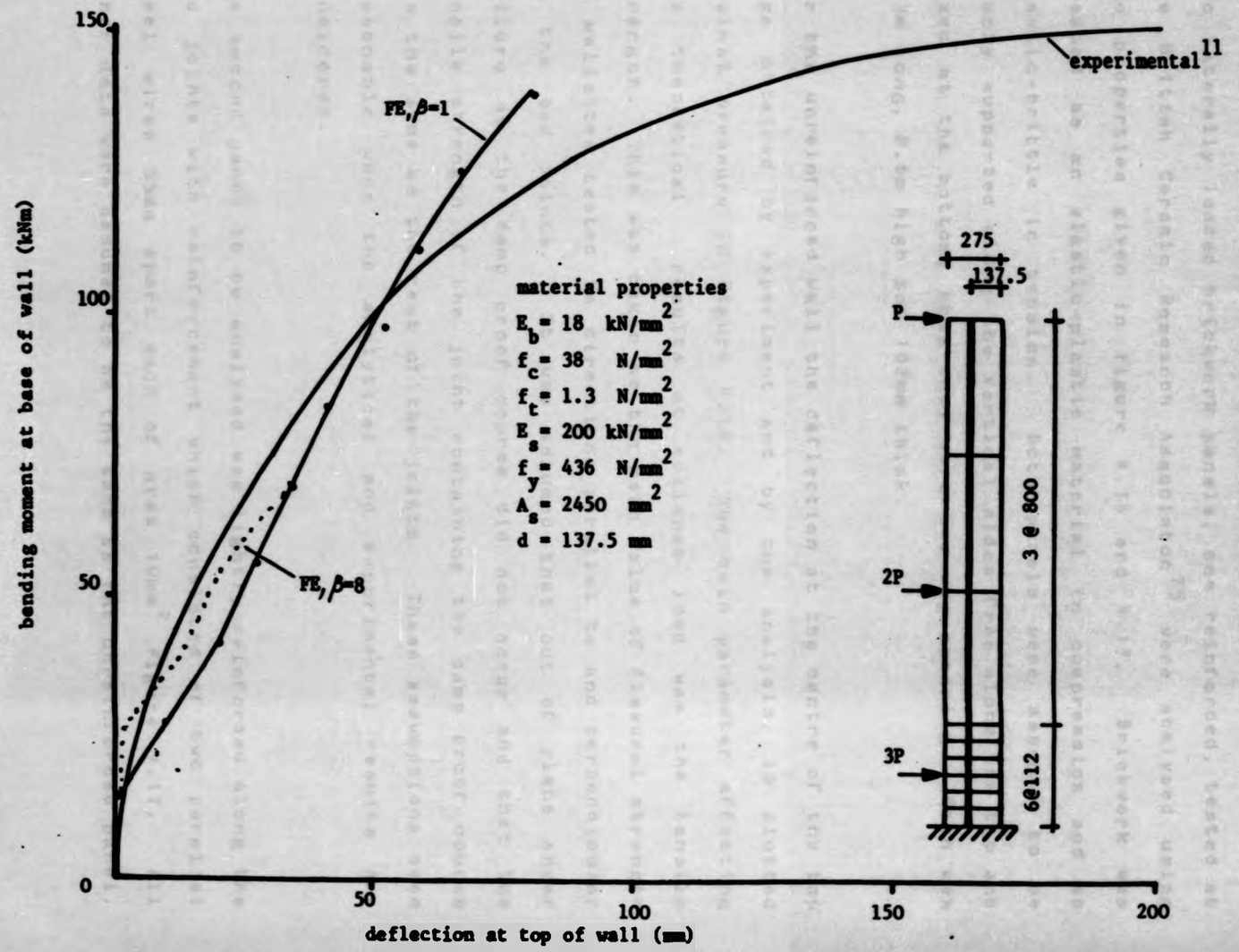

4.5.5 Two-way brickwork panels

Two laterally loaded brickwork panels, one reinforced, tested at the British Ceramic Research Associaton[75] were analysed using the properties given in Figure 4.16 and 4.17. Brickwork was treated as an elastic-plastic material in compression and as elastic-brittle in tension. Both panels were assumed to be simply supported along the vertical sides free along the top and fixed at the bottom, thus they were two-way spanning. Each was 4.3m long, 2.6m high and 102mm thick.

For the unreinforced wall the deflection at the centre of the top edge obtained by experiment and by the analysis, is plotted against pressure in Figure 4.16. The main parameter affecting the theoretical results at collapse load was the tensile strength. This was taken as the mean value of flexural strength of wallettes tested in directions parallel to and perpendicular to the bed joints. It was assumed that out of plane shear failure at the damp proof course did not occur and that the tensile strength of the joint containing the damp proof course was the same as the rest of the joints. These assumptions seem reasonable when the analytical and experimental results are considered.

The second panel to be analysed was lightly reinforced along the bed joints with reinforcement which consisted of two parallel steel wires 55mm apart each of area 10mm^2 Figure 4.17. All other data were assumed to be the same as the unreinforced panel.

Figure 4.16 Load deflection behavior of an unreinforced brickwork panel.

material properties

E_b = 9 kN/mm^2

f_t = 1.4 N/mm^2

f_c = 10 N/mm^2

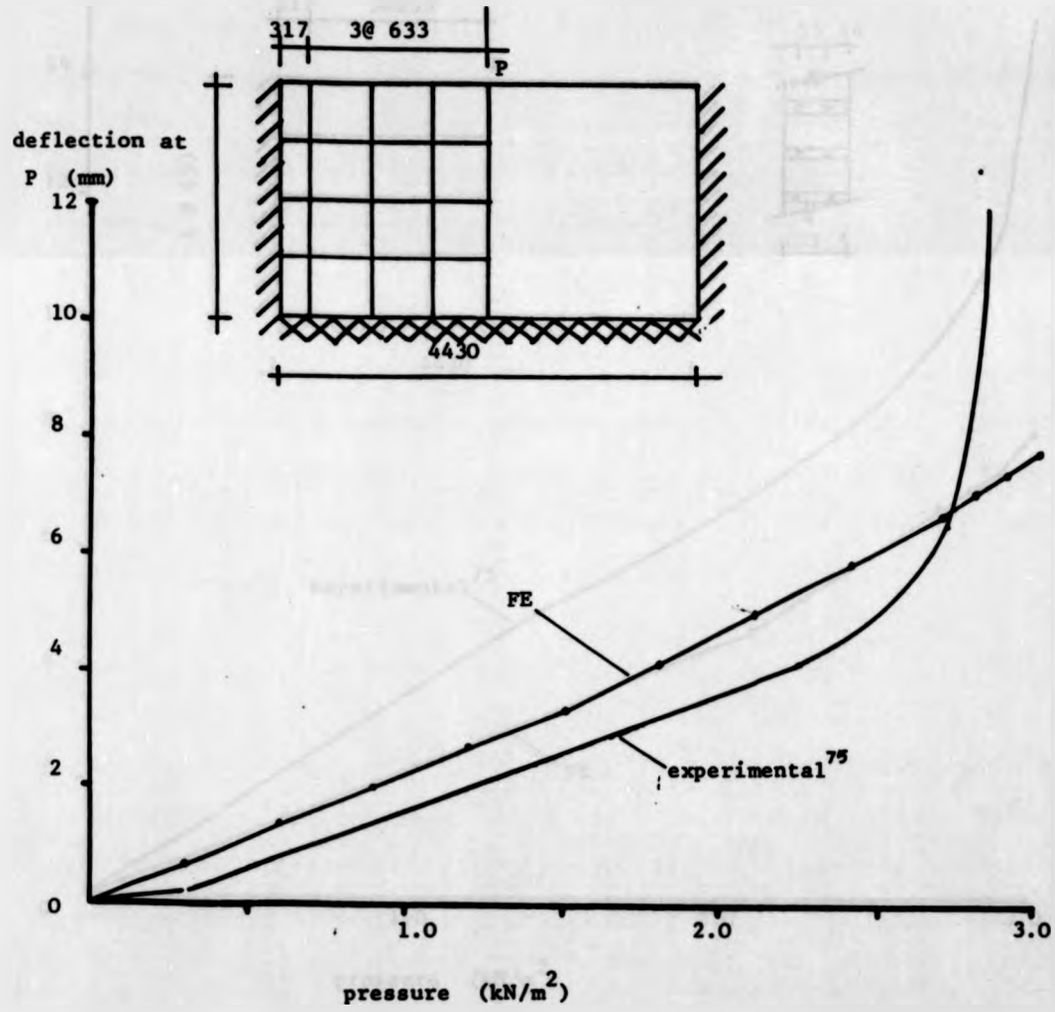

Figure 4.17 Load deflection behavior of a reinforced brickwork panel[75].

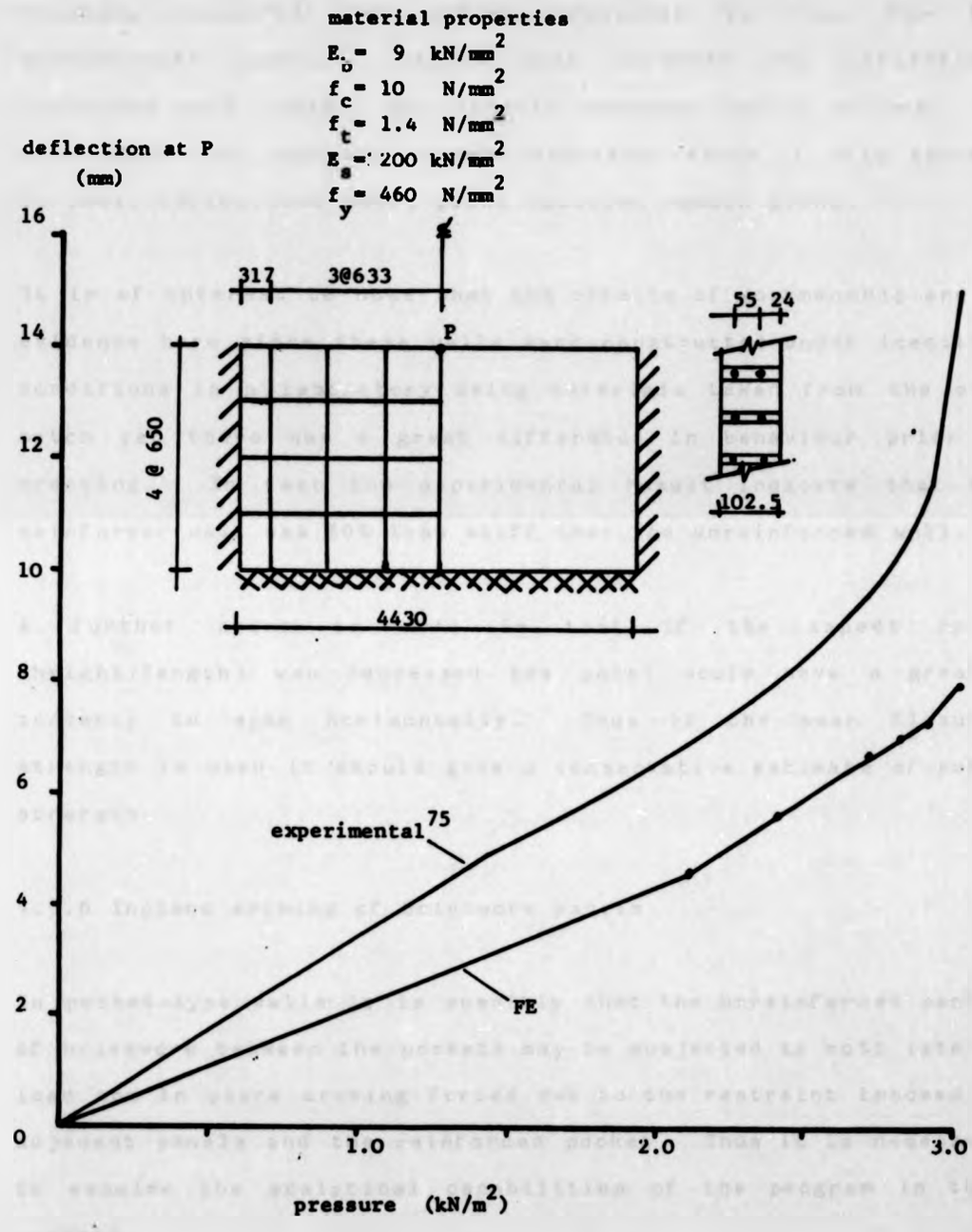

The behaviour up to a pressure of 3.0kN/m at which extensive cracking occurred was almost identical to that for the unreinforced panel. Beyond this pressure the deflections increased very rapidly and tensile membrane action occurs. At this stage the analysis became unsuitable since it only applied to small deflections where plane sections remain plane.

It is of interest to note that the effects of workmanship are in evidence here since these walls were constructed under identical conditions in a laboratory using materials taken from the same batch yet there was a great difference in behaviour prior to cracking. In fact the experimental result indicate that the reinforced wall was 50% less stiff than the unreinforced wall.

A further point to note is that if the aspect ratio (height/length) was decreased the panel would have a greater tendency to span horizontally. Thus if the mean flexural strength is used it should give a conservative estimate of panel strength.

4.5.6 Inplane arching of brickwork panels

In pocket-type walls it is possible that the unreinforced panels of brickwork between the pockets may be subjected to both lateral load and in plane arching forces due to the restraint imposed by adjacent panels and the reinforced pocket. Thus it is necessary to examine the analytical capabilities of the program in this respect.

A series of tests on one-way spanning panels built up to rigid abutments and loaded laterally were reported by Hodgkinson et al [76]. One of these walls, No 979, was analysed using the program. It was 2.72, wide. 1.68m high and 102.5mm thick and was loaded uniformly. Figure 4.18 shows the element discretisation of the problem and the results of the analyses. The material properties were assumed as insufficient data were given in the reference. However the brick type was the same as type A brick used in the retaining wall tests thus a reasonable estimate of the compressive strength was made.

For Analysis 1 of the elastic modulus was assumed to be $900f_c$ and the tensile strength was taken as zero. In Analysis 2 similar properties were assumed except the tensile strength was taken as $0.1f_c$ whilst in Analysis 3 zero tensile strength and an elastic modulus of $600f_c$ was assumed.

The deflection at the centre of the panel obtained from the analysis generally followed the experimental results, Figure 4.17. The inclusion of tensile strength increased the stiffness of the initial response but at pressures greater than $15kN/m^2$ it had a negligible effect. It is likely that that the initial values employed in the analyses for the elastic modulus and the tensile strength were not high enough. At high loads Analyses 1 and 2 under-estimated deflections however Analysis 3 gave a better estimate. It is probable that the stress-strain curve is of the form shown in Figure 4.5, hence the curves used in the analyses were likely to provide bounds to the correct curve. The

Figure 4.18 Arching action in restrained unreinforced brickwork panels

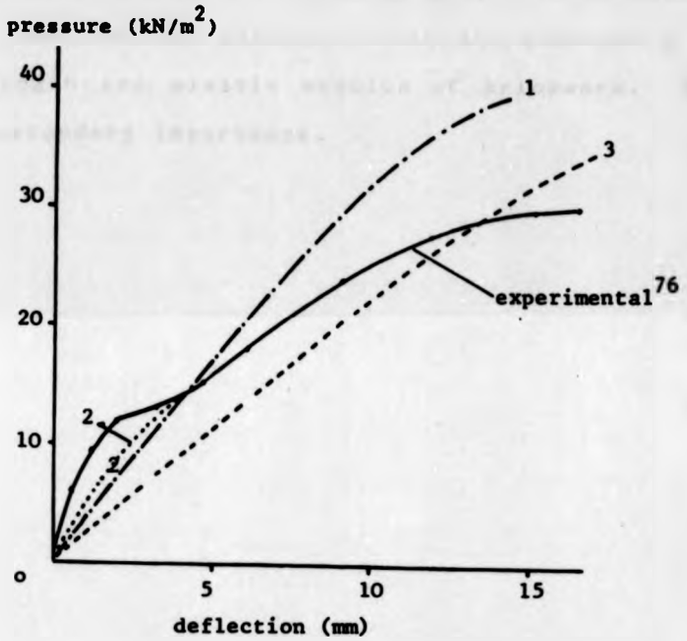

last pressure at which convergence was obtained in Analysis 1 was 39.9kN/m^2 and in Analysis 3 was 34.6kN/m^2 both of which compare reasonably with the experimental collapse load of 36.5kN/m^2 .

These analyses indicate that for arching action to be adequately predicted it is important to obtain an accurate assessment of the compressive strength and elastic modulus of brickwork. Tensile strength is of secondary importance.

5. EXPERIMENTAL RESULTS

5.1 Retaining walls

5.1.1 General

The wall details and test results are summarised in Table 5.1 whilst the material properties are given in section 3.1.2.

All the walls failed in flexure due to either the reinforcement reaching its yield stress or by the brickwork crushing. There were no signs of shear failure in any of the tests. Walls 1,3 & 4 failed by the steel yielding, whilst walls 5 & 6 failed by crushing of the brickwork. Wall 2 failed as a balanced section with both yielding and crushing occurring together. There was no indication that arching of the brickwork panels between the reinforced pockets took place.

5.1.2 Deflection

Figure 5.1 indicates how the lateral deflection at the top of the wall varied with applied bending moment at the base; this includes all the load cycles for walls 1 & 2 . These deflection results should be used for comparative purposes only because it was discovered at the end of the test programme that the measured deflections included the effects of base rotation. A reconsideration of the wall deflections is given in Appendix A2.

TABLE 5.1 WALL DETAILS AND RESULTS

	wall number					
	1	2	3	4	5	6
Breadth (mm)	1900	1995	1990	2000	2000	2005
depth (mm)	330	332	330	325	215	215
effective depth (mm)	275	263	289	289	167	167
percentage of reinforcement %	0.92	0.92	0.28	0.28	1.44	1.25
brick type	A	B	B	A	B	B
failure moment (KN m)	412	503	222	221	254	224
shear force at failure (KN)	550	519	229	228	262	231
failure mode*	T	T+C	T	T	C	C

* T = steel yield, C = brickwork crushing

Figure 5.1 Experimental load deflection behavior of walls 1-6.

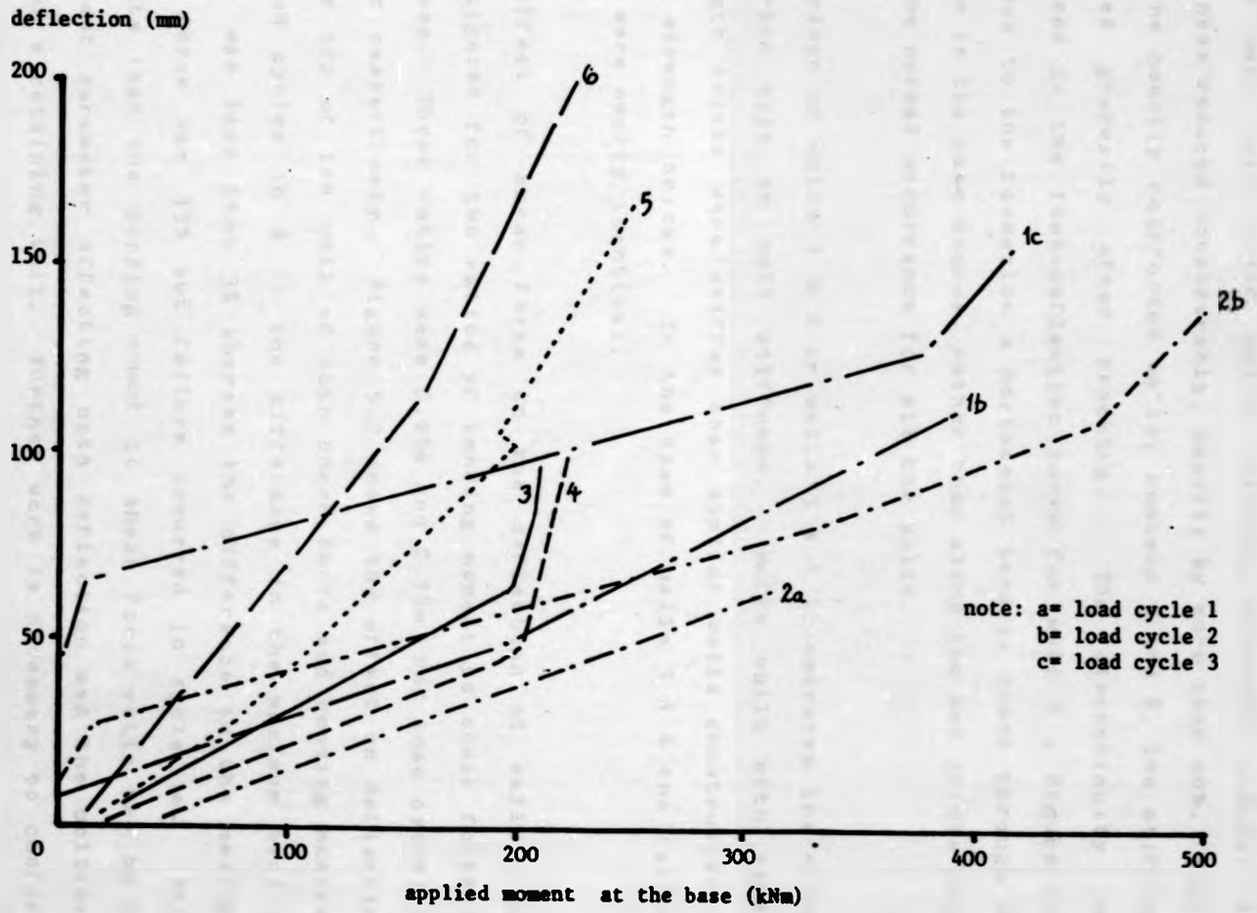

All the load-deflection curves were non-linear. Initially the walls were very stiff until cracking occurred whereon the stiffness reduced considerably, usually by more than 20%. Except for the heavily reinforced walls, numbers 5 and 6, the stiffness reduced gradually after cracking. The discontinuity that occurred in the load-deflection curve for wall 5 , Figure 5.1, was due to the formation a horizontal tensile crack through the bricks in the base course, rather than along the bed joints which was the normal occurrence for all the walls.

Comparison of walls 1 & 2 or walls 3 & 4 illustrates the effect of brick type on wall stiffness. Walls built with higher strength bricks were stiffer than similar walls constructed of lower strength bricks. In the case of walls 3 & 4 the failure loads were nearly identical.

The effect of shear force on the deflection of wall 1 was investigated for two ratios of bending moment to shear force at the base. These ratios were 0.95m and 0.75m for load cycles 1b and 1c respectively. Figure 5.2 shows the effect on deflection at the top of the wall of both shear force and bending moment. In load cycles 1b & 1c the difference in the maximum bending moment was less than 3% whereas the difference in the maximum shear force was 33% but failure occurred in cycle 1c. This suggests that the bending moment to shear force ratio may be an important parameter affecting both deflection and the collapse load of a retaining wall. Further work is necessary to confirm this point.

Figure 5.2 Effect of moment and shear on wall 1.

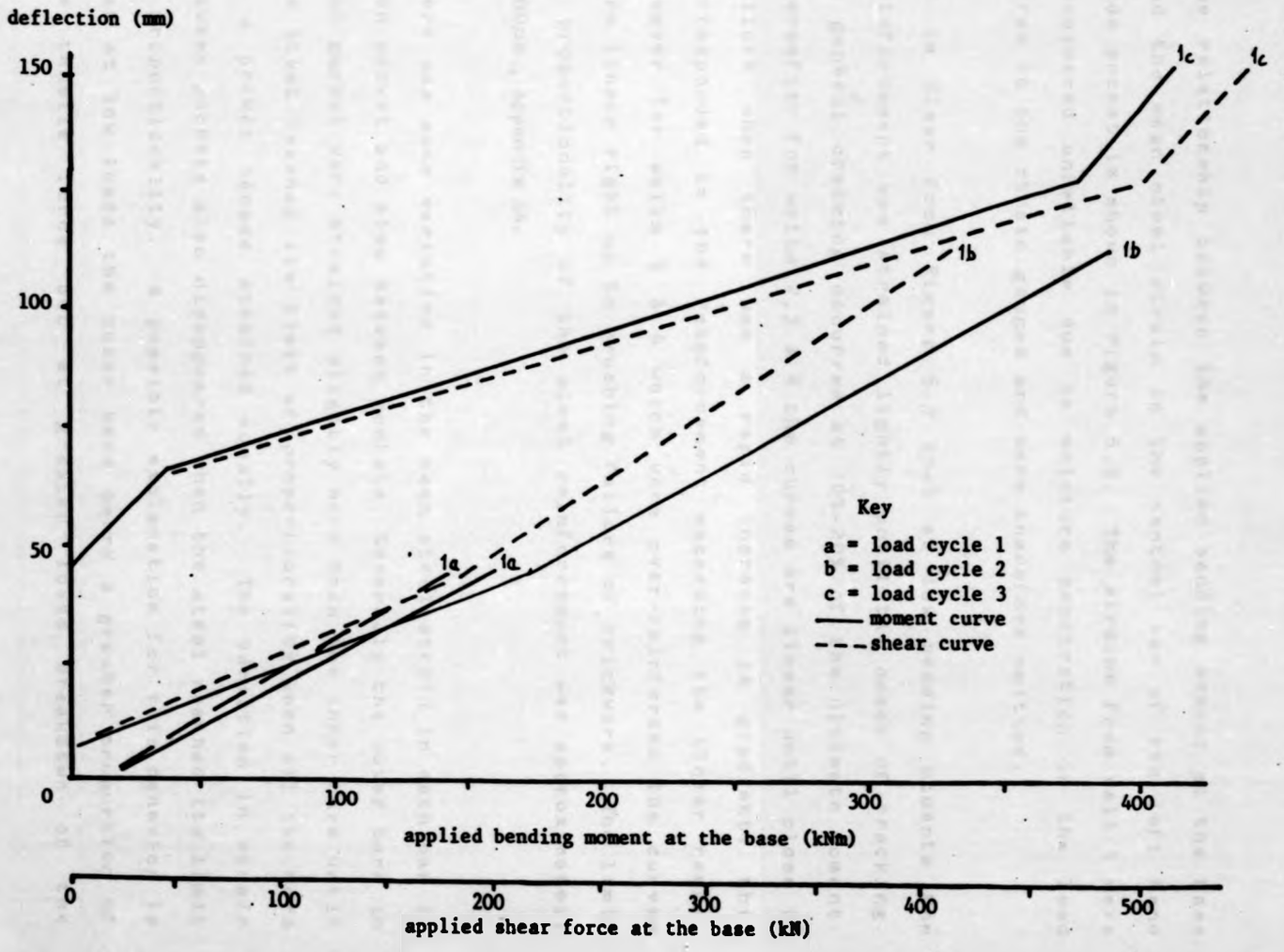

5.1.3 Steel strain

The relationship between the applied bending moment at the base and the mean steel strain in the central bar of the left hand side pocket is shown in Figure 5.3. The strains from wall 1 were considered unreliable due to moisture penetration in the lead wires to the strain gauges and were therefore omitted.

It is clear from Figure 5.3 that at low bending moments the reinforcement was strained lightly until the onset of cracking. In general cracking occurred at 10%-20% of the ultimate moment. Thereafter for walls 2,3 & 4 the curves are linear until close to failure when there was a rapid increase in gradient: this corresponded to the reinforcement exceeding its linear range. However for walls 5 & 6 which were over-reinforced the curves were linear right up to crushing failure of brickwork. The limit of proportionality of the steel reinforcement was approximately 2100μs., Appendix A4.

There was some variation in the mean steel strain in each bar in each pocket and also between pockets. Generally the outer bars in each pocket were strained slightly more than the inner bars until the steel reached its limit of proportionality when all the bars in a pocket became strained equally. The variation in strain between pockets also disappeared when the steel reached its limit of proportionality. A possible explanation for this behavior is that at low loads the outer bars carry a greater proportion of the tensile force but at greater loads breakdown of the

Figure 5.3 Variation of mean steel strain with applied load for walls 2-6.

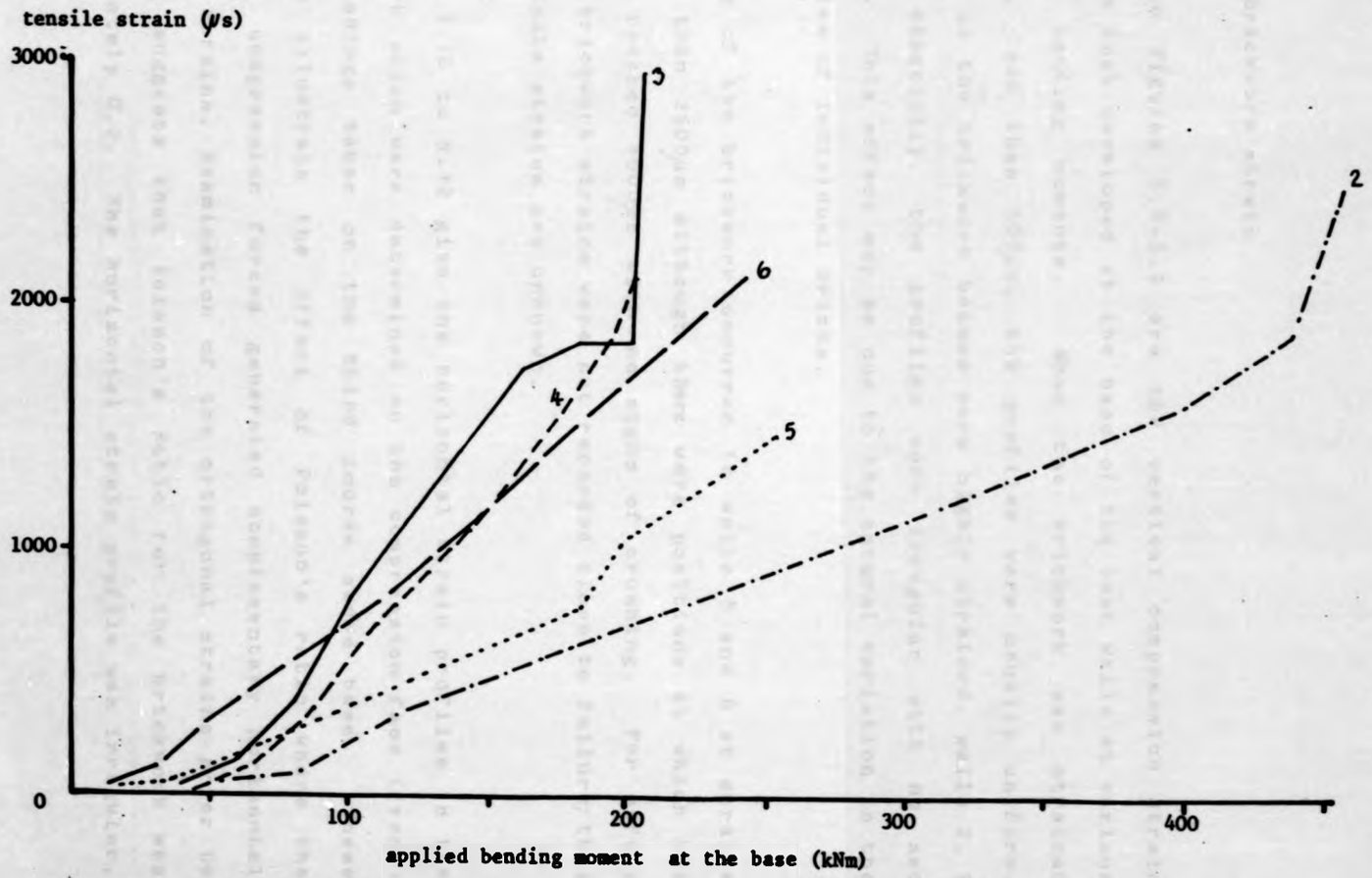

concrete/steel bond occurs causing redistribution of the tensile force.

5.1.4 Brickwork strain

Shown in Figures 5.4-5.9 are the vertical compression strain profiles that developed at the base of the test walls at various applied bending moments. When the brickwork was strained lightly, less than 500μs, the profiles were usually uniform. However as the brickwork became more highly strained, walls 2, 5 and 6 especially, the profiles were irregular with no set pattern. This effect may be due to the natural variation in the properties of individual bricks.

Crushing of the brickwork occurred in walls 5 and 6 at strains greater than 2500μs although there were positions at which the strains reached 4000μs with no signs of crushing. For safety reasons brickwork strains were not recorded close to failure; thus the ultimate strains are unknown.

Figures 5.10 to 5.12 give the horizontal strain profiles in the brickwork which were determined on the compression face (front) from readings taken on the third course above base. These profiles illustrate the effect of Poisson's ratio where the vertical compression forces generated complementary horizontal tensile strains. Examination of the orthogonal strains prior to cracking suggests that Poisson's Ratio for the brickwork was approximately 0.2. The horizontal strain profile was irregular,

Figure 5.4 Vertical strain profiles along base of wall 1

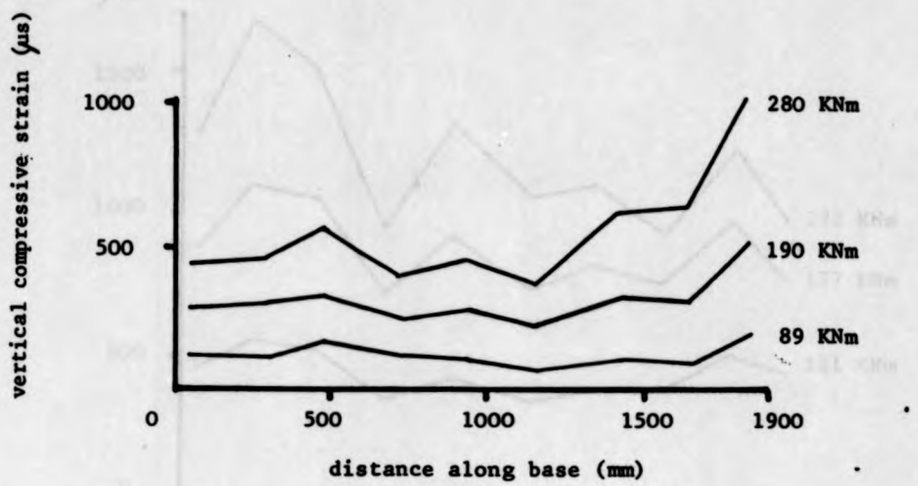

Figure 5.5 Vertical strain profiles along base of wall 2

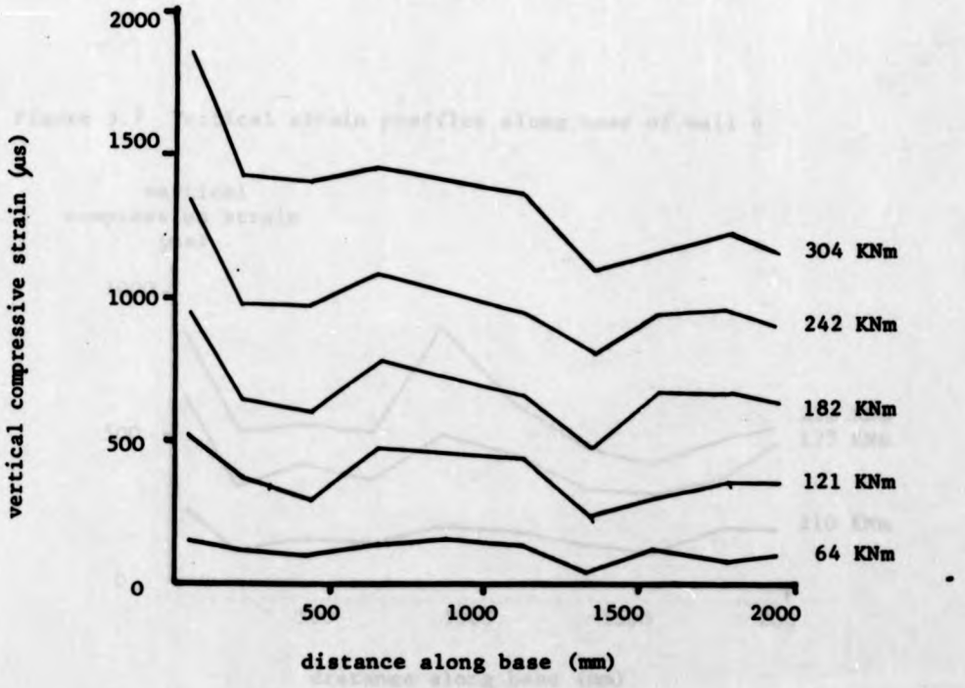

Figure 5.6 Vertical strain profiles along base of wall 3

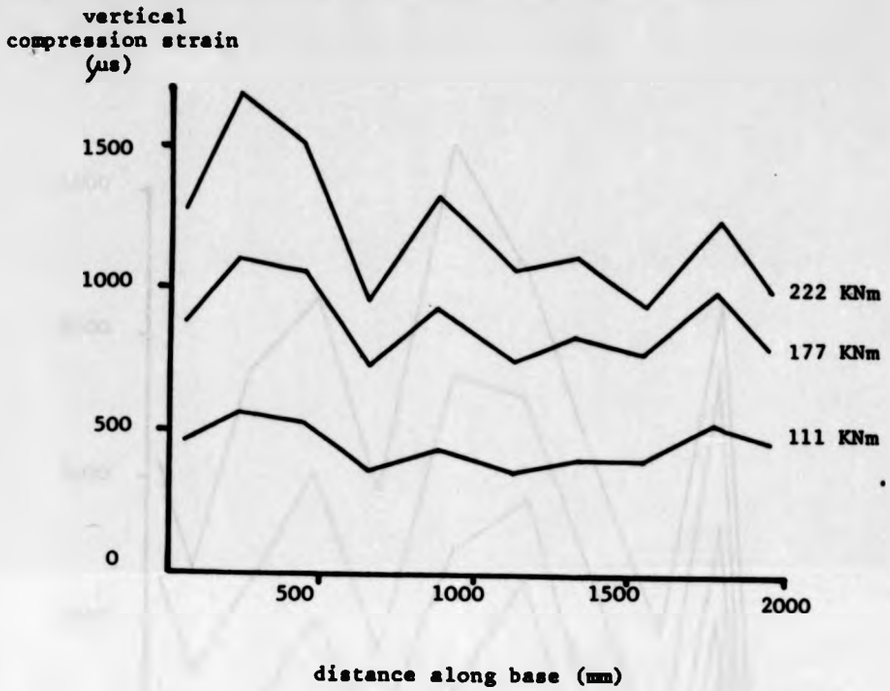

Figure 5.7 Vertical strain profiles along base of wall 4

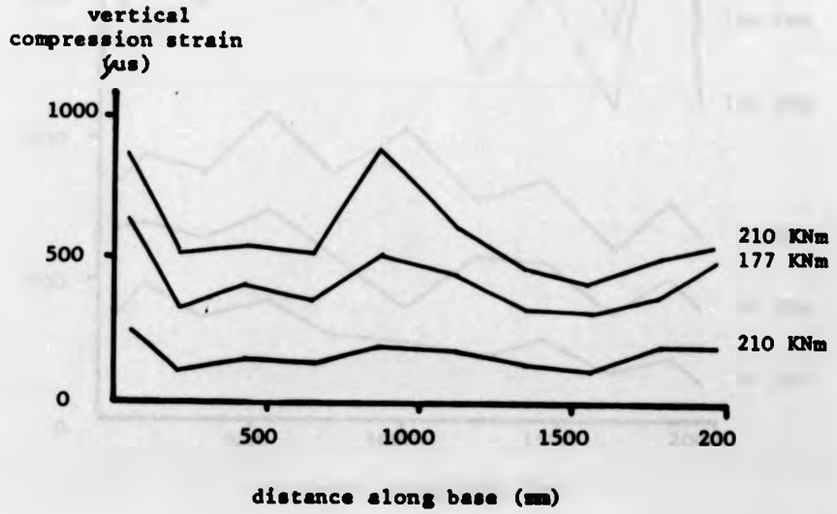

Figure 5.8 Vertical strain profiles along base of wall 5

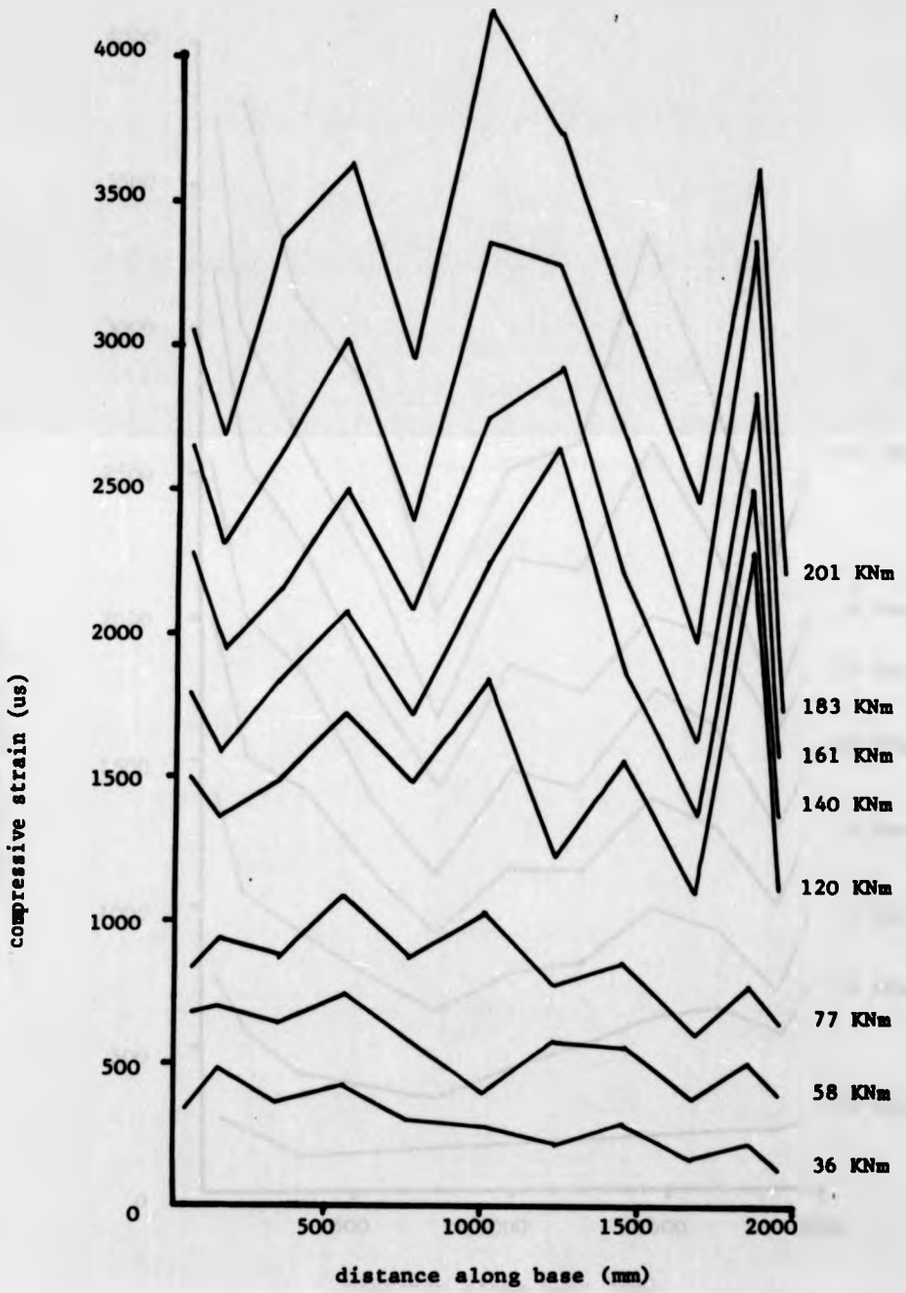

Figure 5.9 Vertical strain profiles along base of wall 6

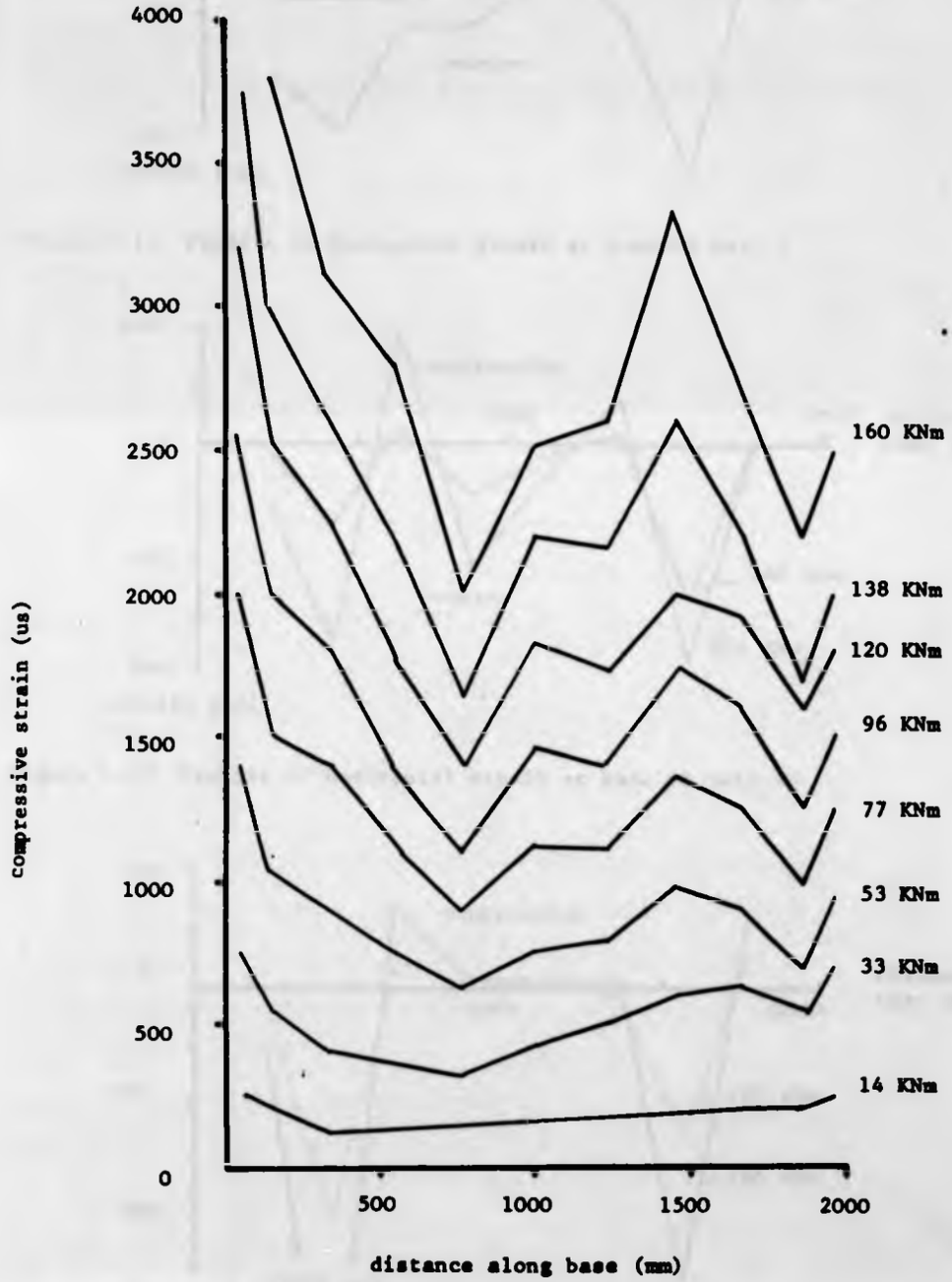

Figure 5.10 Profile of horizontal strain at base of wall 4

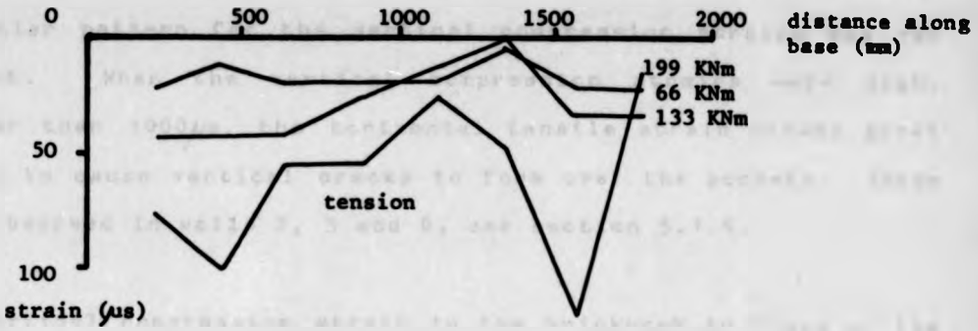

Figure 5.11 Profile of horizontal strain at base of wall 5

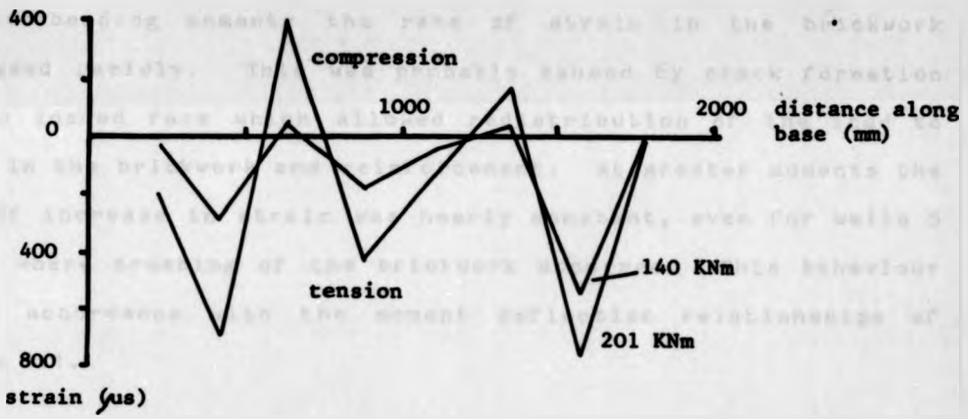

Figure 5.12 Profile of horizontal strain at base of wall 6

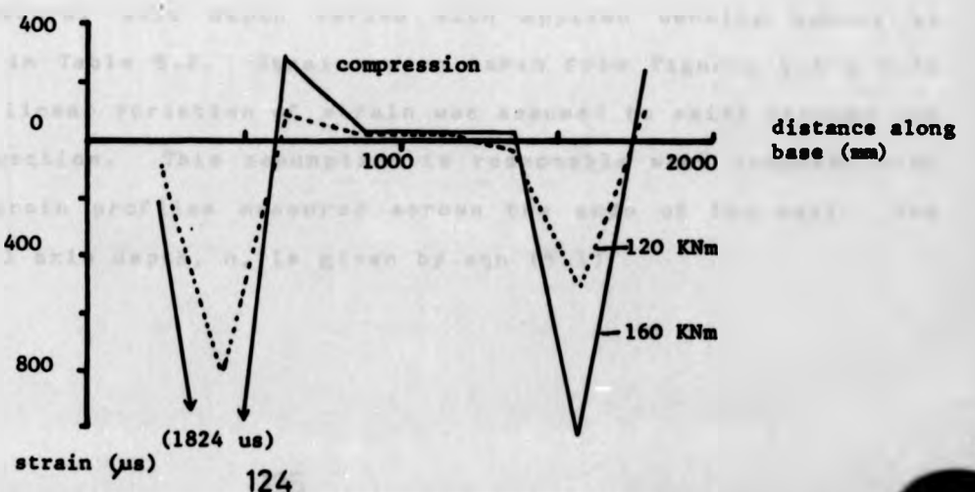

the greatest tensile strains occurred over the pockets. However a similar pattern for the vertical compression strains was not evident. When the vertical compression strains were high, greater than 1000μs, the horizontal tensile strain became great enough to cause vertical cracks to form over the pockets. These were observed in walls 2, 5 and 6, see section 5.1.6.

The vertical compressive strain in the brickwork in front of the centreline of the left hand side pocket is related to the applied bending moment at the base by the curves shown in Figure 5.13. At low bending moments the rate of strain in the brickwork increased rapidly. This was probably caused by crack formation on the loaded face which allowed redistribution of the load to occur in the brickwork and reinforcement. At greater moments the rate of increase in strain was nearly constant, even for walls 5 and 6 where crushing of the brickwork occurred. This behaviour is in accordance with the moment deflection relationships of Figure 5.1.

5.1.5 Neutral Axis Depth

The neutral axis depth varied with applied bending moment as shown in Table 5.2. Strains were taken from Figures 5.3 & 5.13 and a linear variation of strain was assumed to exist through the wall section. This assumption is reasonable when compared with the strain profiles measured across the ends of the wall. The neutral axis depth, n, is given by eqn (5.1)

Figure 5.13 Variation of vertical strain in brickwork with applied load for walls 1-6

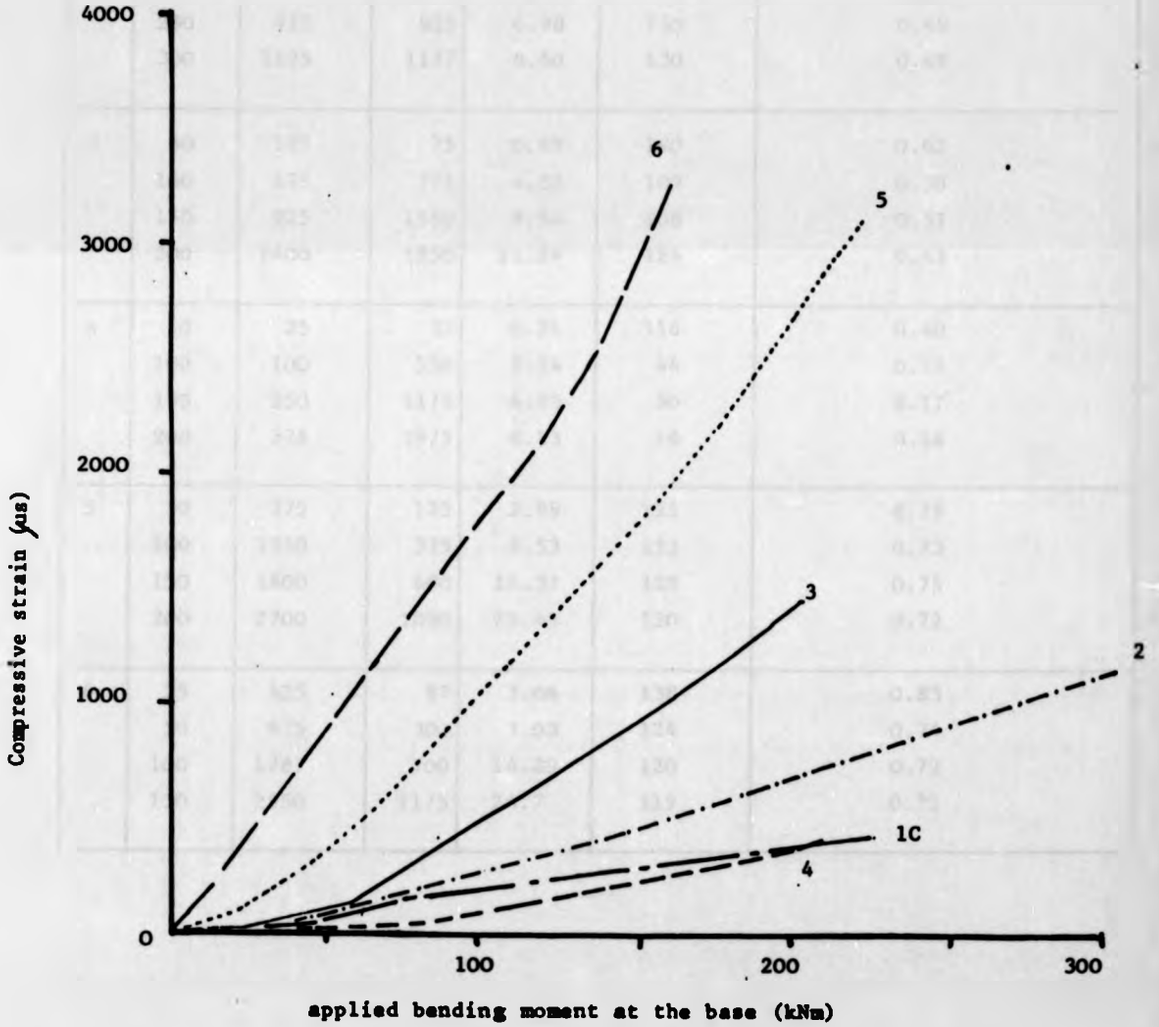

TABLE 5.2 Variation of neutral axis depth with applied bending moment at the base of the wall

Wall No	Bending Moment kNm	Brickwork Strain us	Steel Strain us	Strain Gradient. mm^{-1}	Neutral Axis Depth mm	Ratio Neutral Axis Depth to Effective Depth
2	50	150	37	0.71	211	0.80
	100	275	200	1.80	152	0.57
	150	462	500	3.65	126	0.48
	200	787	700	5.65	139	0.53
	250	912	925	6.98	130	0.49
	300	1125	1137	8.60	130	0.49
3	50	125	75	0.69	180	0.62
	100	475	775	4.32	109	0.38
	150	925	1550	8.56	108	0.37
	200	1400	1850	11.24	124	0.43
4	50	25	37	0.21	116	0.40
	100	100	550	2.24	44	0.15
	150	250	1175	4.93	50	0.17
	200	375	1975	8.13	46	0.16
5	50	375	125	2.99	125	0.75
	100	1050	375	8.53	123	0.73
	150	1800	600	14.37	125	0.75
	200	2700	1050	22.45	120	0.72
6	25	425	87	3.06	138	0.83
	50	875	300	7.03	124	0.74
	100	1787	700	14.89	120	0.72
	150	2950	1175	24.7	119	0.71

$$n = \frac{\varepsilon_b d}{\varepsilon_b + \varepsilon_s} \quad \ldots(5.1)$$

where ε_b is the compression strain in the brickwork and ε_s is the steel strain.

For each wall the neutral axis depth was constant except during the initial load stages when cracks were developing at the base of the wall causing the neutral axis depth to decrease.

The ratio of the neutral axis depth to the effective depth, n/d, may be used to assess whether a section is over-reinforced, balanced or under-reinforced. In order to find the ratio which defines the balanced section the limiting strain (or the strain at peak stress) of brickwork and steel are substituted into equation (5.1).The draft code assumes they are 0.0035 and 0.0042 respectively, hence for a balanced section n/d = 0.45, whilst for an over-reinforced section n/d > 0.45 and for an under-reinforced section n/d < 0.45. These values are only approximate because in practice the limiting strains were not reached.

Thus the n/d ratio in Table 5.2 imply that wall 2 was a balanced section, walls 3 & 4 were under-reinforced and walls 5 and 6 were over-reinforced. These implications are confirmed by Figures. 5.3 and 5.13 and by observations made during the test.

5.1.6 Crack Patterns

The crack patterns at failure of walls 1-6 are illustrated in

Figures 5.14-5.22. Numbers besides the cracks refer to the bending moment at the base when the crack was first observed. The under-reinforced walls (1,3 & 4) all had similar crack patterns on the tension face, Figures 5.14, 5.16 & 5.17. Generally the cracks ran horizontally along the bed joints, with the first crack forming at the base at a low bending moment. As the load increased several more cracks formed along the bed joints at approximately equal distances higher up the wall.

The over-reinforced walls (5 & 6) and wall 2, which was a balanced section, have similar crack patterns on the tension face as indicated by Figures 5.20-5.22 respectively. Initially cracking proceeded in the way outlined above, however in the later stages at large bending moments additional horizontal cracks formed between those already formed. Immediately prior to failure diagonal cracks formed which ran upwards from the brickwork into the pockets and at failure vertical cracks formed in the concrete over the reinforcement.

The local bond stresses between the reinforcement and concrete were calculated according to the requirements given in CP110[45]. At ultimate load these were 3.08,3.22,1.91,1.91,2.60 and 2.47N/mm^2 for walls 1-6 respectively . According to CP110 the ultimate local bond stress for type 2 deformed bars in a grade 25 concrete subjected to tension is 3.0N/mm^2 which includes an factor of safety that is presumed to be 1.5 . This suggests that the vertical cracks over the reinforcement bars may be caused by local bond failure. Furthermore it seems that the

Figure 5.14 Crack pattern of the base of the tensile face of wall 1

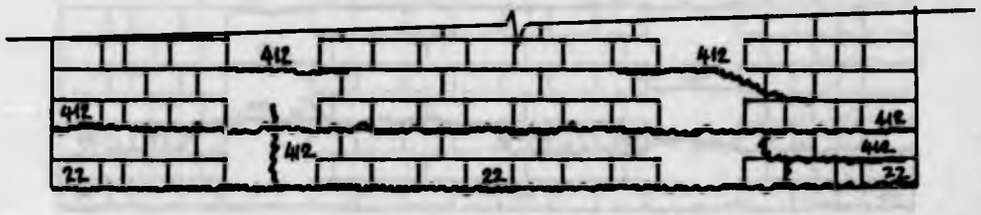

base course

note: the numbers refer to the applied moment at the base when the crack was observed

Figure 5.15 Crack pattern at the base of the tensile face of Wall 2

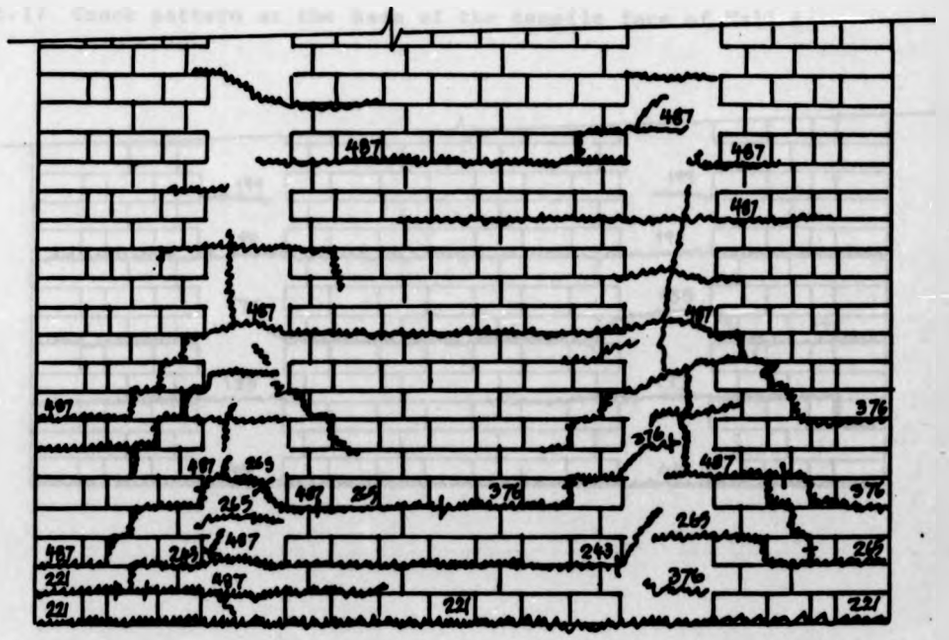

base course

Figure 5.16 Crack pattern at the base of the tensile face of Wall 3

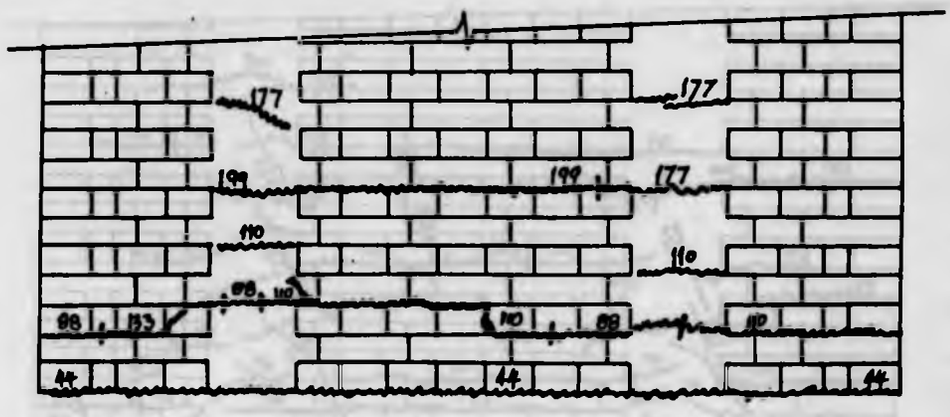

base course

note: the numbers refer to the applied moment at the base when the crack was observed

Figure 5.17 Crack pattern at the base of the tensile face of Wall 4

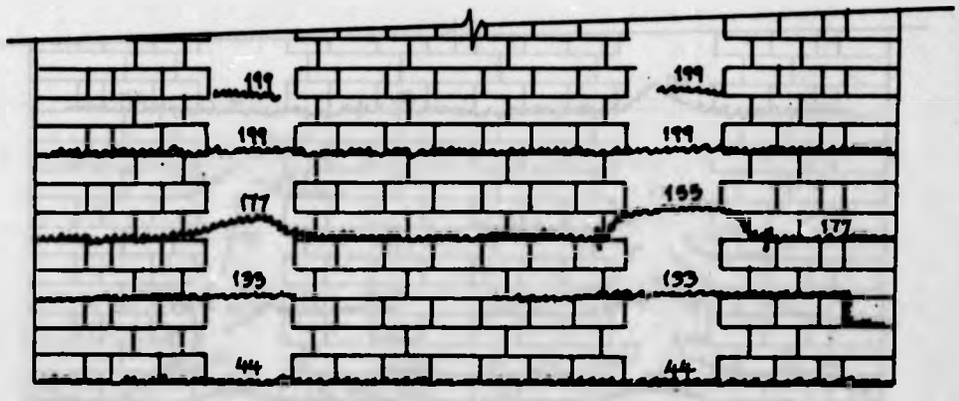

base course

Figure 5.18 Crack pattern at the base of the tensile face of Wall 5

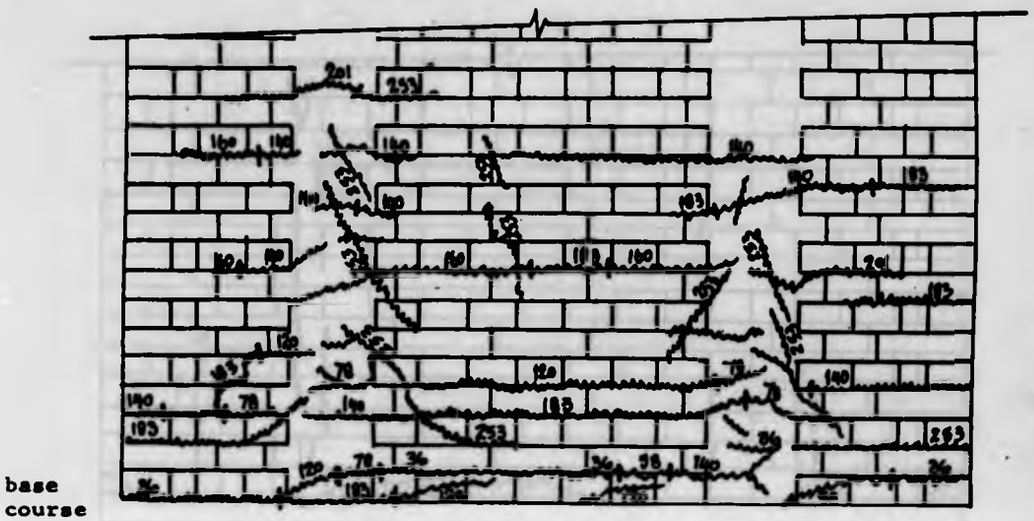

Figure 5.19 Crack pattern at the base of the tensile face of Wall 6

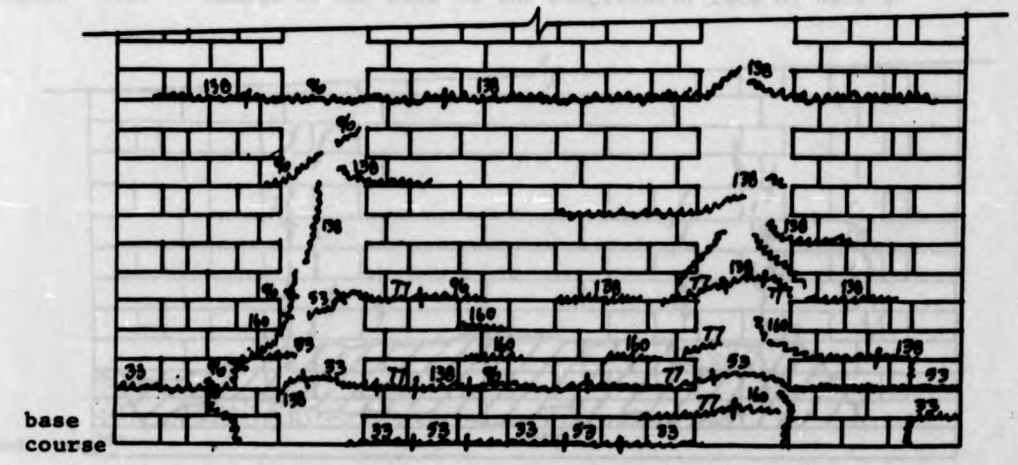

Figure 5.20 Damage at the base of the compressive face of Wall 2

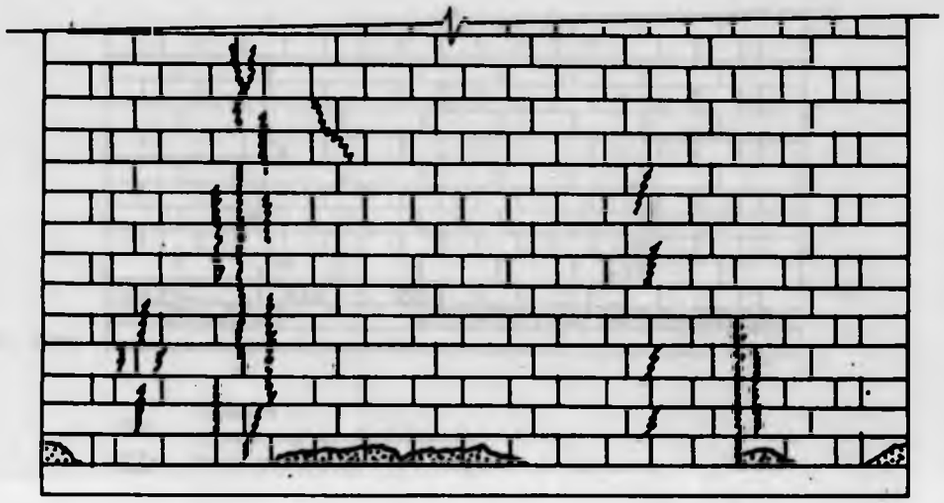

end stop restraining base course

Figure 5.21 Damage at the base of the compressive face of Wall 5

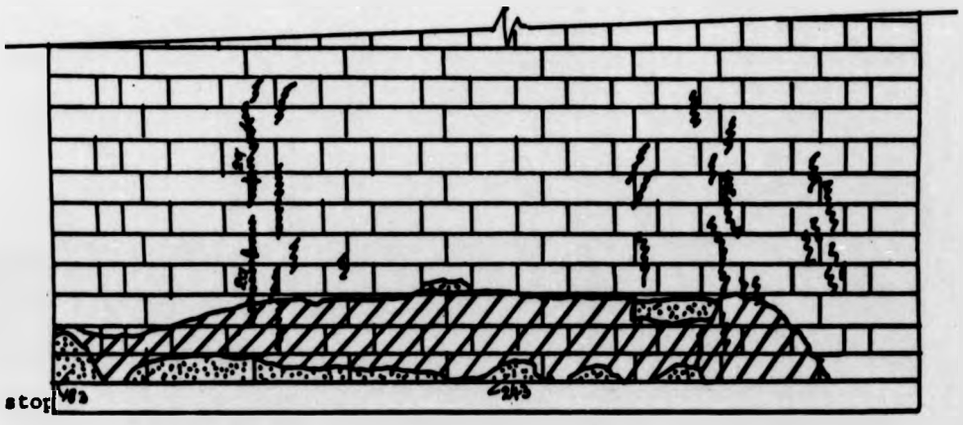

end stop

note: cracked brickwork
crushed brickwork
hollow sound when tapped

Figure 5.22 Damage at base of the compressive face of Wall 6

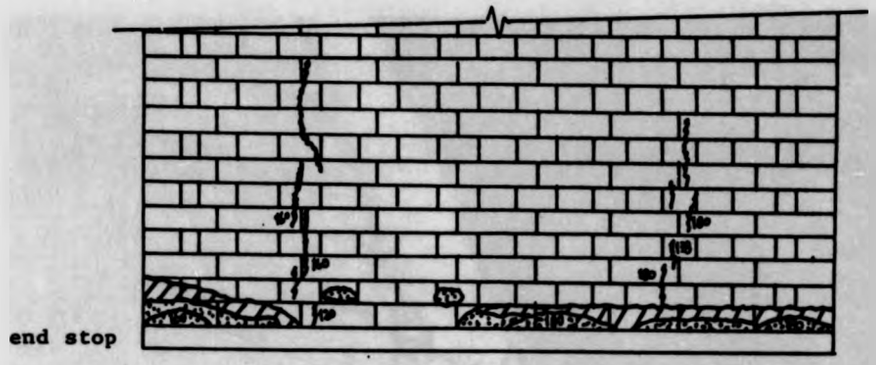

cracks
crushing of brickwork
hollow sound when tapped

PLATE 5.1 Crushing of the brickwork at the base of wall 6

PLATE 5.1 Crushing of the brickwork at the base of wall 6

ultimate bond stress given in CP110 may be too high for heavily reinforced sections and concentrations of reinforcement.

In addition to cracks on the tension face, damage was observed on the compression face in walls 2,5 & 6 as shown in Figures 5.16, 5.20 & 5.21 respectively. The damage consisted of crushing of the brickwork Plate 5.1, predominantly in the second course, with areas above which sounded hollow when tapped thereby indicating the presence of internal fractures. Also vertical cracks were observed, walls 2, 5 and 6, over the pockets in courses 3-14.

5.2 Beams

5.2.1 General

The beam details and results are summarised in Table 5.3. All beams failed by either steel yield or shear failure. Although there were no compression failures there were some signs of localised crushing under the load points after shear failure had occurred. Prior to failure there was no crushing.

5.2.2. Deflection

Figure 5.23 shows how the deflection at the centre of the beam varied with the bending moment at the centre. It is clear that the shape of the curve conforms to a set pattern depending on the mode of failure that occurs. Beams that fail in flexure due to steel yield had a moment deflection behaviour which approximated

TABLE 5.3 Beam Details and Results

Beam Number	1	2	3	4	5	6	7	8	9	10	11	12	13	14	15
Length (mm)	3960	3970	3950	3372	2196	3995	3980	4010	3985	3995	3980	2152	2140	2190	2580
Breadth (mm)	1010	1005	1025	1050	1004	1020	1010	1010	1005	1010	1007	1005	1000	1005	1002
Depth (mm)	332	327	330	330	328	330	330	327	330	327	330	327	327	330	330
Span (mm)	3400	3400	3400	2800	1700	3400	3400	3400	3400	3400	3400	1680	1680	1680	1680
Effective Depth (mm)	275	280	295	280	280	275	265	270	280	270	265	270	270	285	275
Span/Effective Depth	5.09	5.00	4.75	3.93	2.0	5.09	5.28	5.18	5.00	5.18	5.28	2.0	2.0	1.89	1.96
Reinforcement	3Y25	3Y32	4Y16	4Y16	4Y16	3Y32	3Y40	3Y32	4Y16	4Y16	3Y40	3Y32	3Y32	3Y32	3Y40
Percentage Reinforcement (%)	0.53	0.86	0.27	0.28	0.28	0.87	1.42	0.89	0.28	0.29	1.42	0.89	0.89	0.84	1.37
Failure Moment [1] (KN m)	170	240	117	129	123	305	326	263	121	121	281	132	208	172	257
Total shear force [1] (KN)	253	352	178	240	451	446	476	384	182	182	403	493	720	617	956
Failure Mode [2]	T	T+S	T	T	T+S+L	T+S+L	S+L	T+S+L	T	T	S+L	S+L	S+L	S+L	S

Note: 1 includes the self weight of the beam

2 T = steel yield S = shear failure, L = longitudinal cracking along pocket boundary

Figure 5.23 Bending moment vs displacement plots for beams

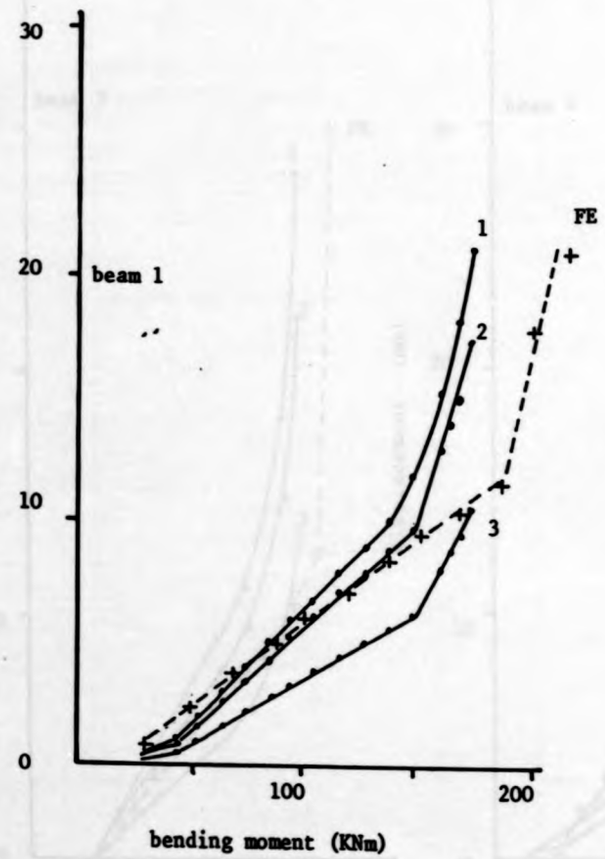

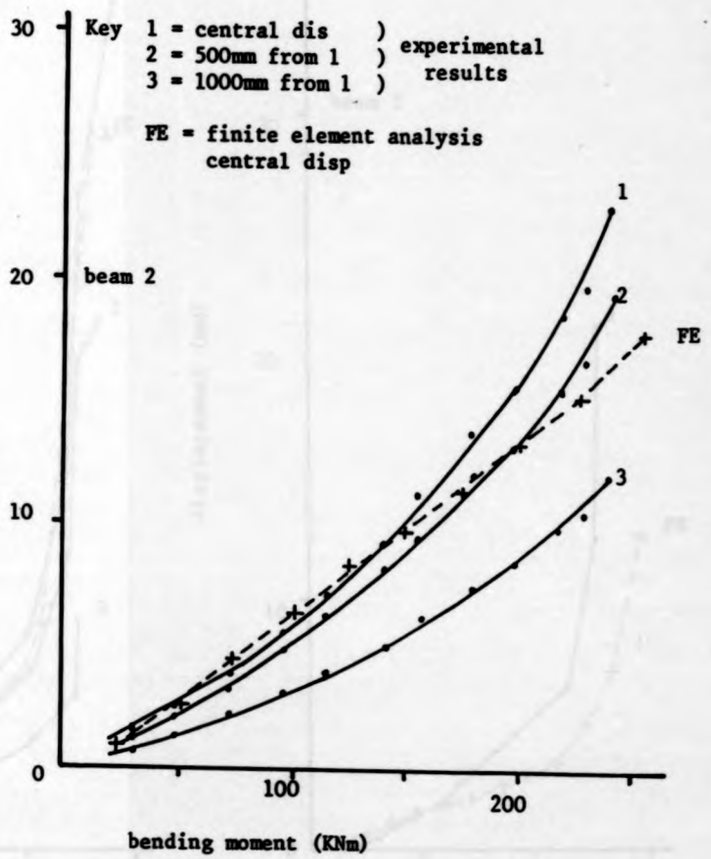

Figure 5.23 (contd)

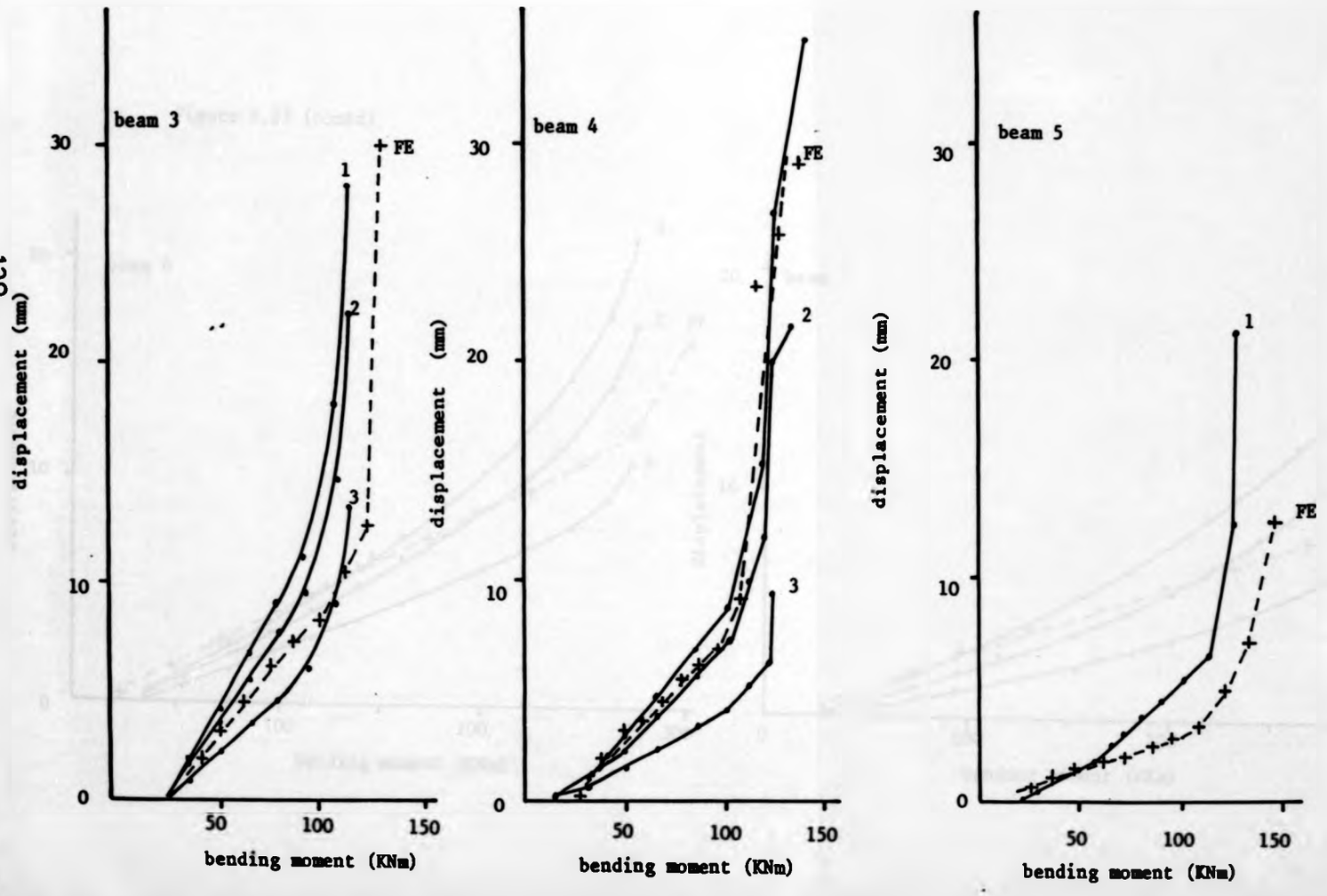

Figure 5.23 (contd)

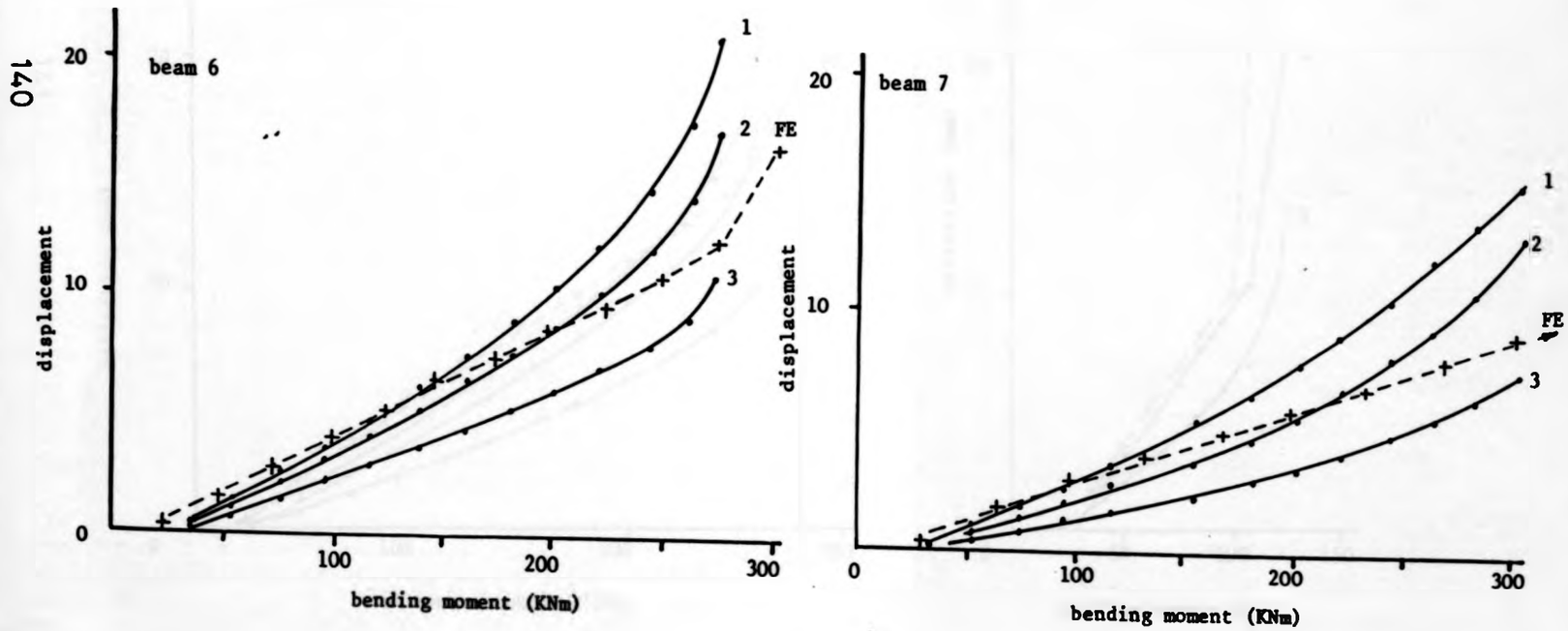

Figure 5.23 (contd)

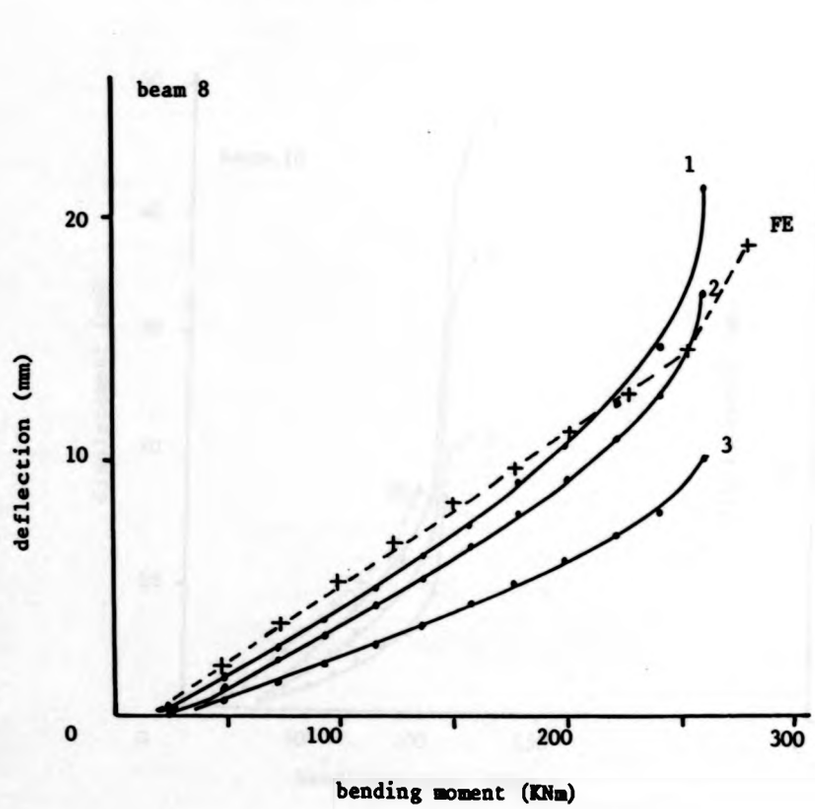

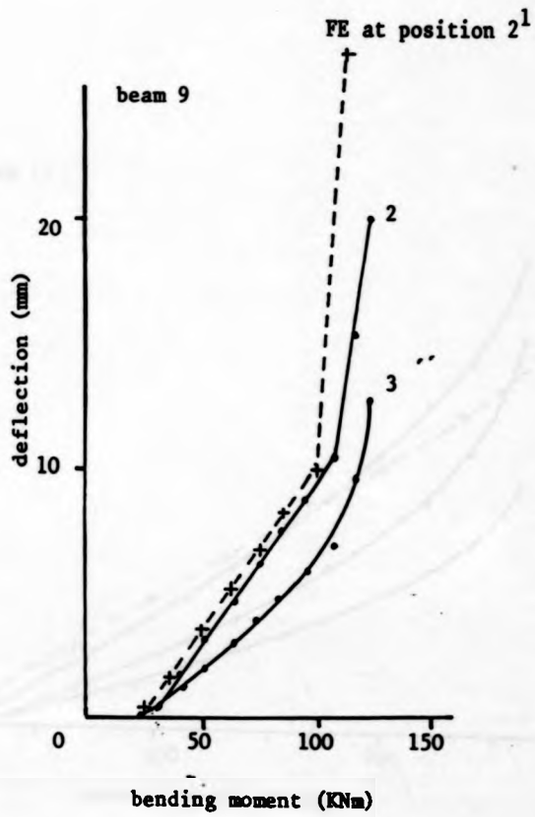

Figure 5.23 (contd)

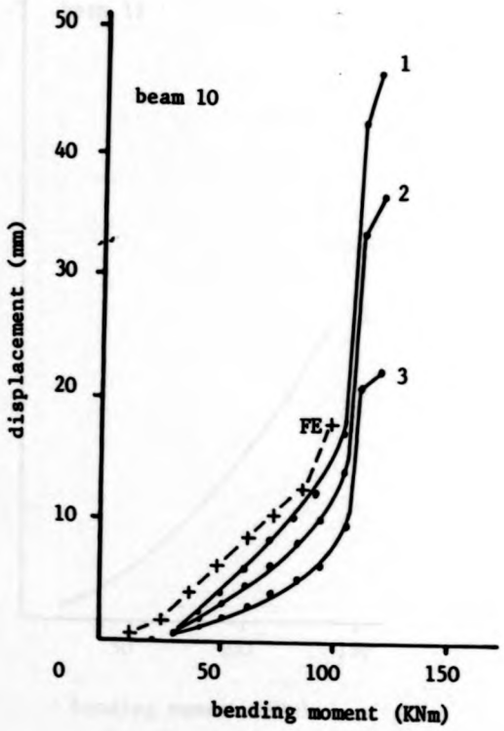

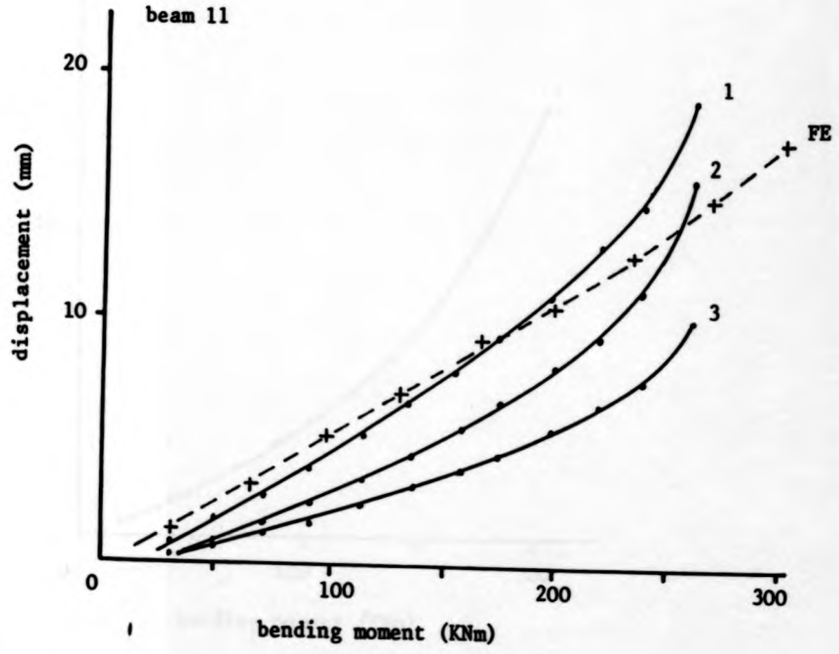

Figure 5.23 (contd)

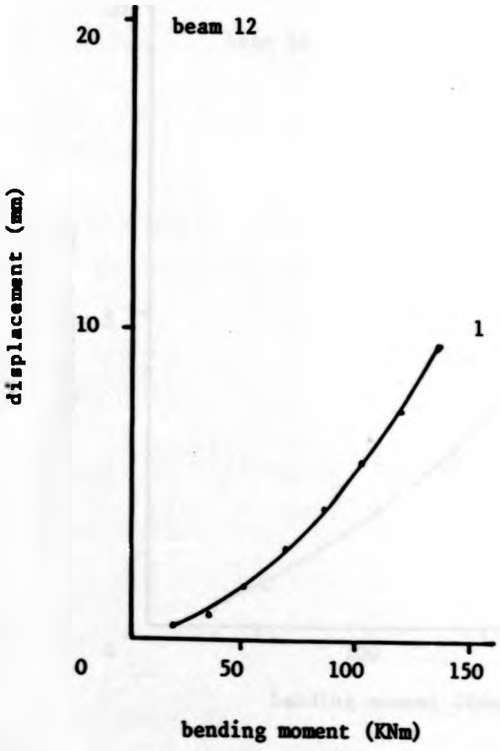

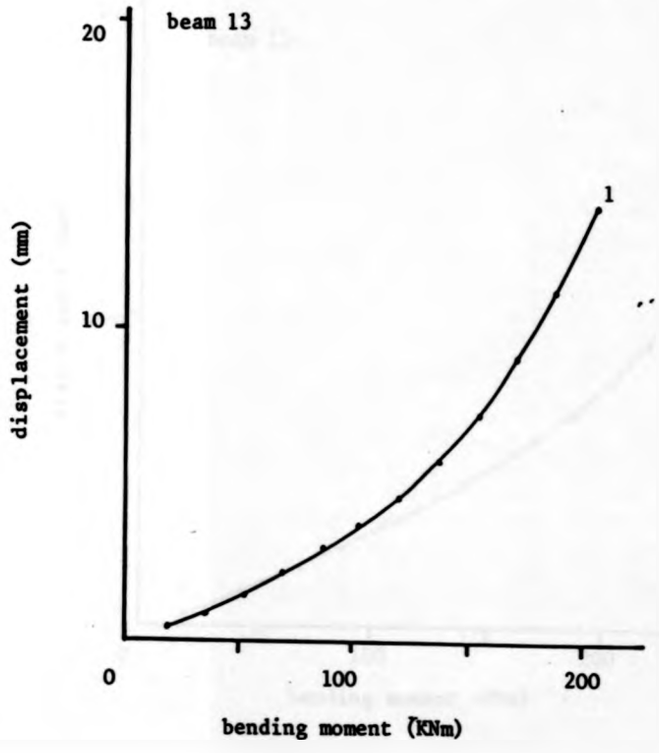

Figure 5.23 (contd)

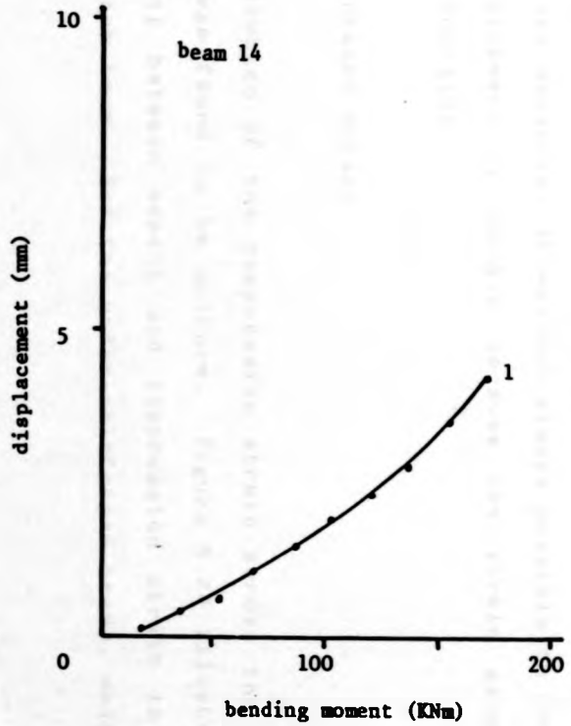

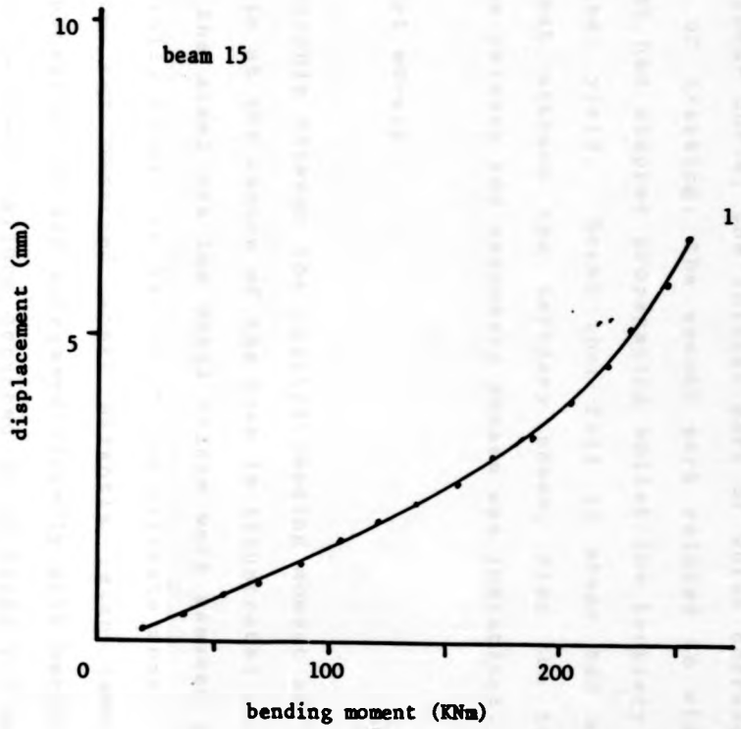

to a trilinear curve, the initial part of which corresponded to the onset of cracking, the second part related to widening of cracks that had stopped propagating whilst the tertiary part was due to steel yield. Beams that fail in shear had a similar response but without the tertiary phase, also the transition between the primary and secondary phases was indistinct.

5.2.3 Steel strain

The relationship between the applied bending moment and the mean steel strain at the centre of the beam is illustrated in Fig5.24. Strain in the steel was low until cracks were assumed to occur; these generally formed at 5%-20% of the ultimate moment although cracks were not observed until slightly later (see section 5.2.6). Thereafter strain increased linearly with bending moment until either a shear failure occurred as in beams 2,7 and 11-15, or the steel exceeded its limit of proportionality at about 2100μs. Beyond this limit there was a rapid increase in strain until failure occurred. It was not always possible to follow this rapid development of strain because the strain gauges often ceased to function.

5.2.4 Brickwork strain

The distribution of the compressive strain across the width of the beam was found to be uniform. Figure 5.24 illustrates the relationship between moment and compression strain in the top fibre of each beam. For the under-reinforced beams, which always

Figure 5.24 Bending moment vs strain in steel and brickwork (contd)

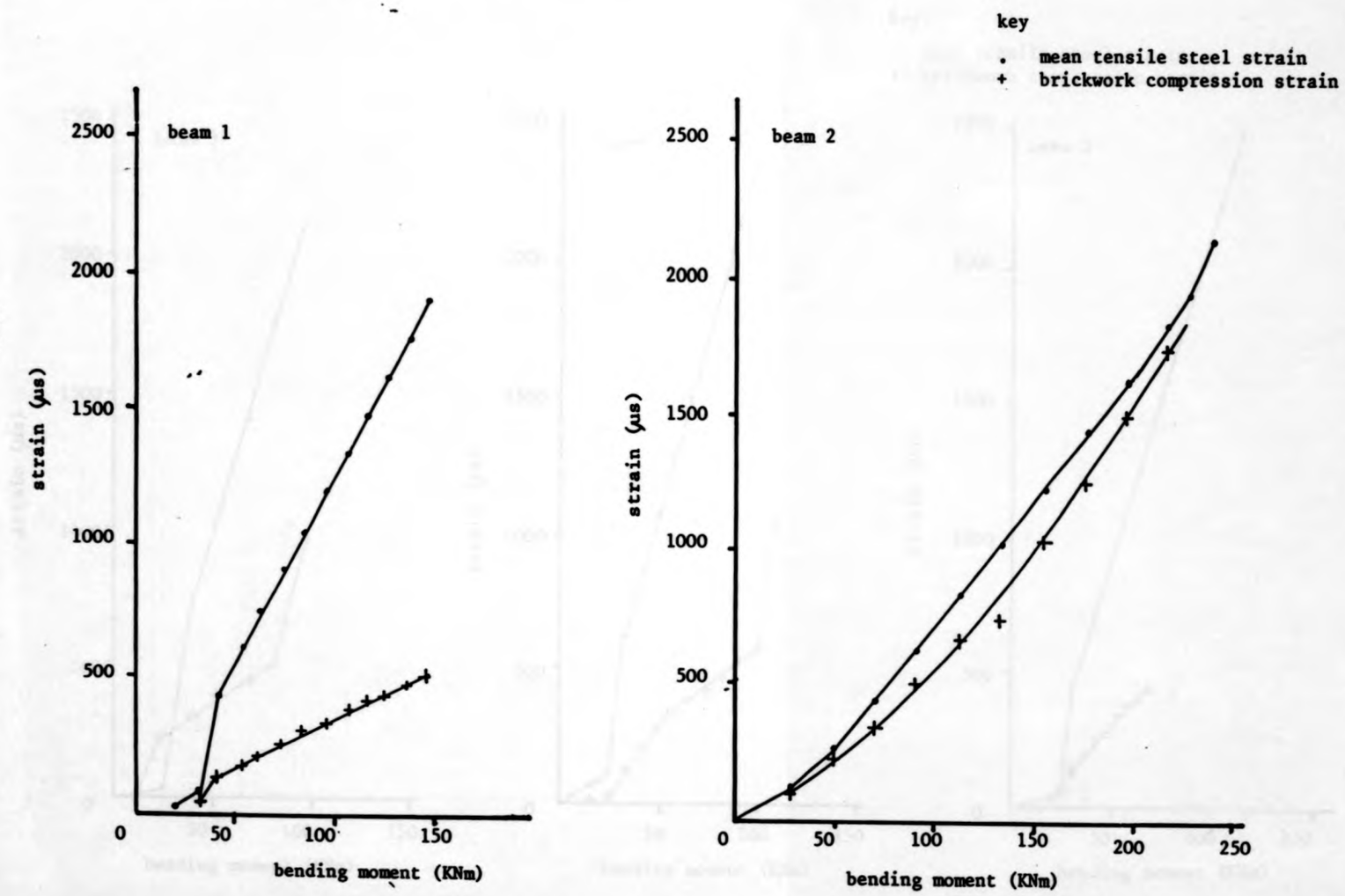

Figure 5.24 Bending moment vs strain in steel and brickwork (contd)

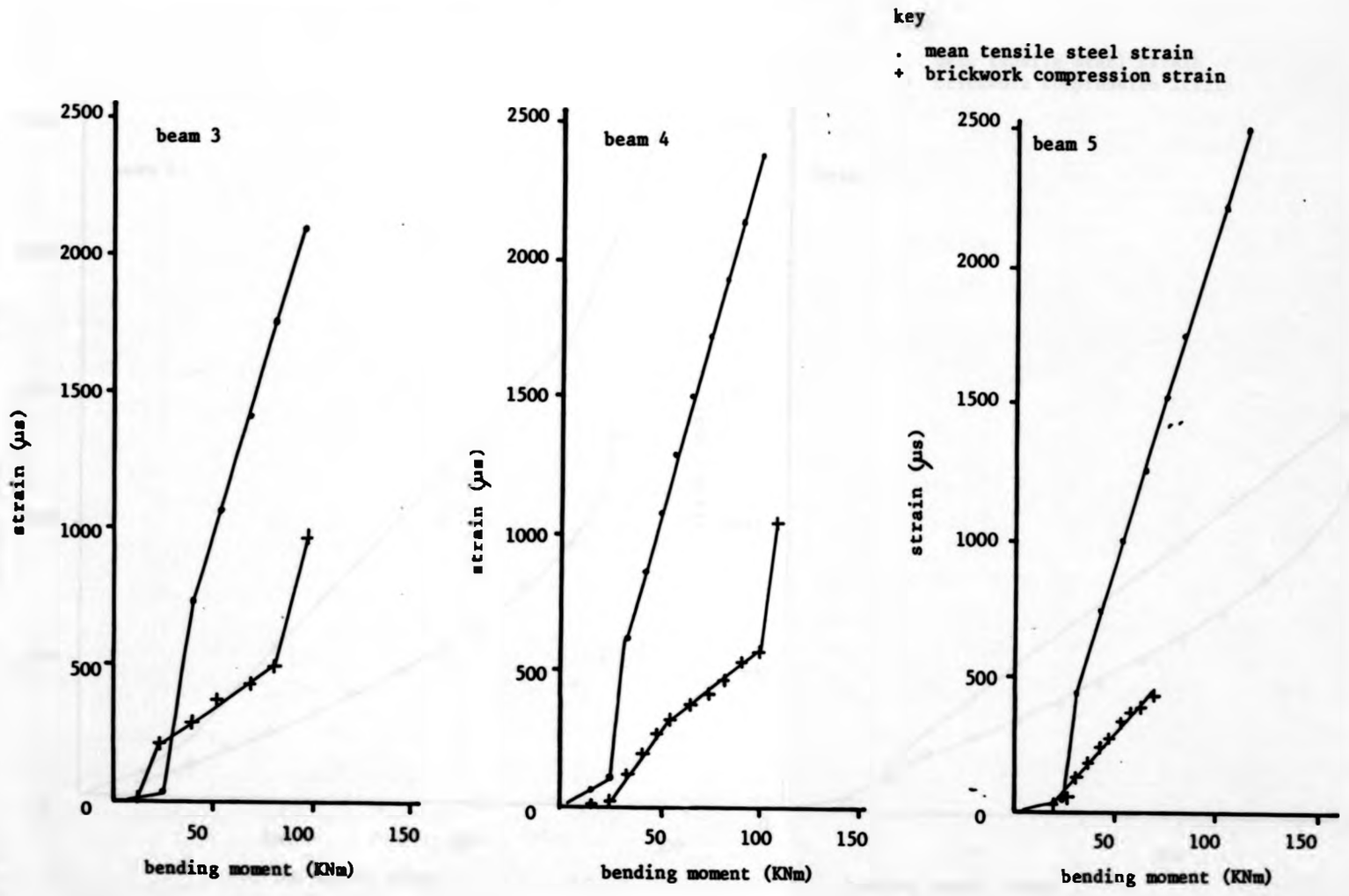

Figure 5.24 Bending moment vs strain in steel and brickwork (contd)

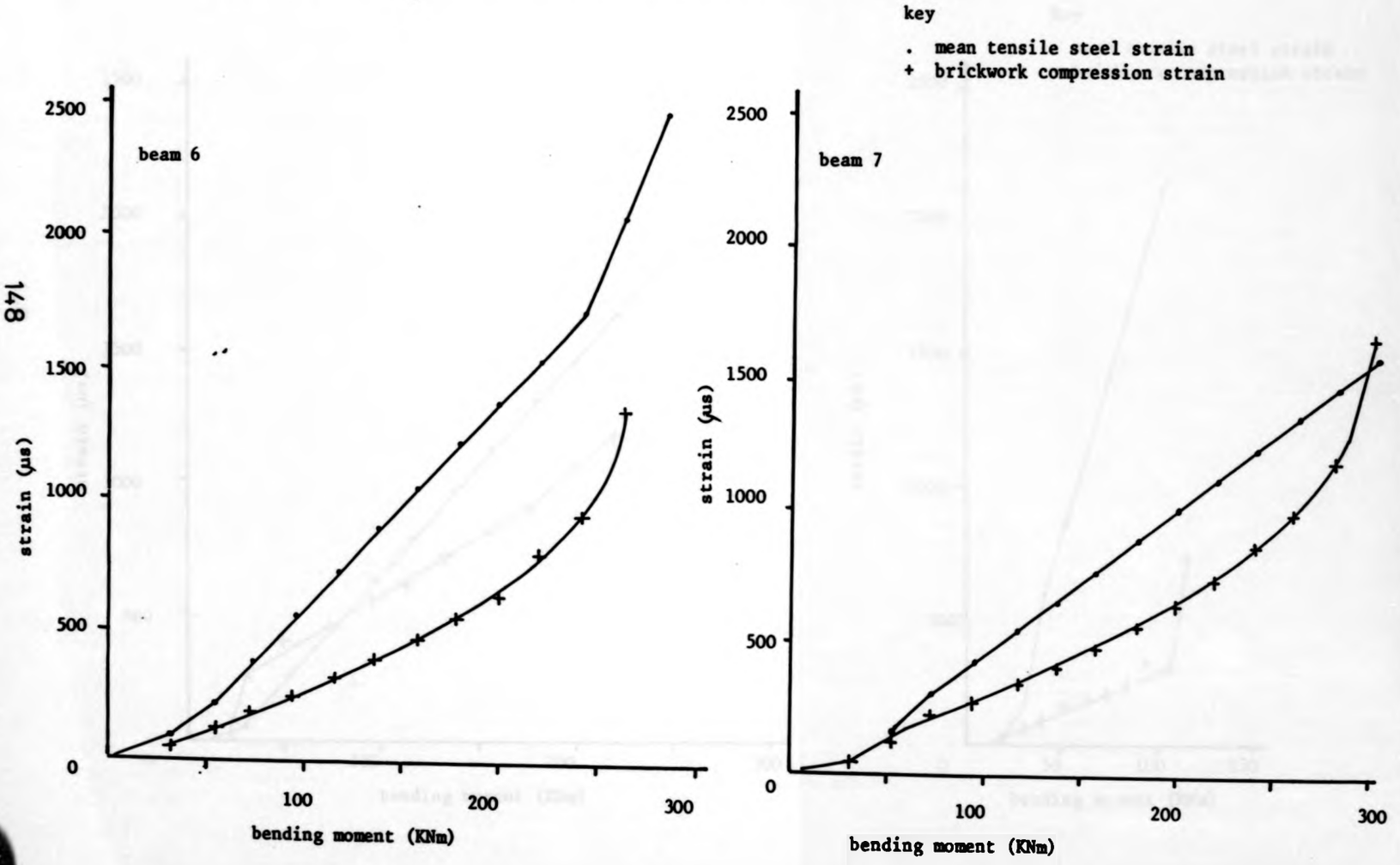

Figure 5.24 Bending moment vs strain in steel and brickwork

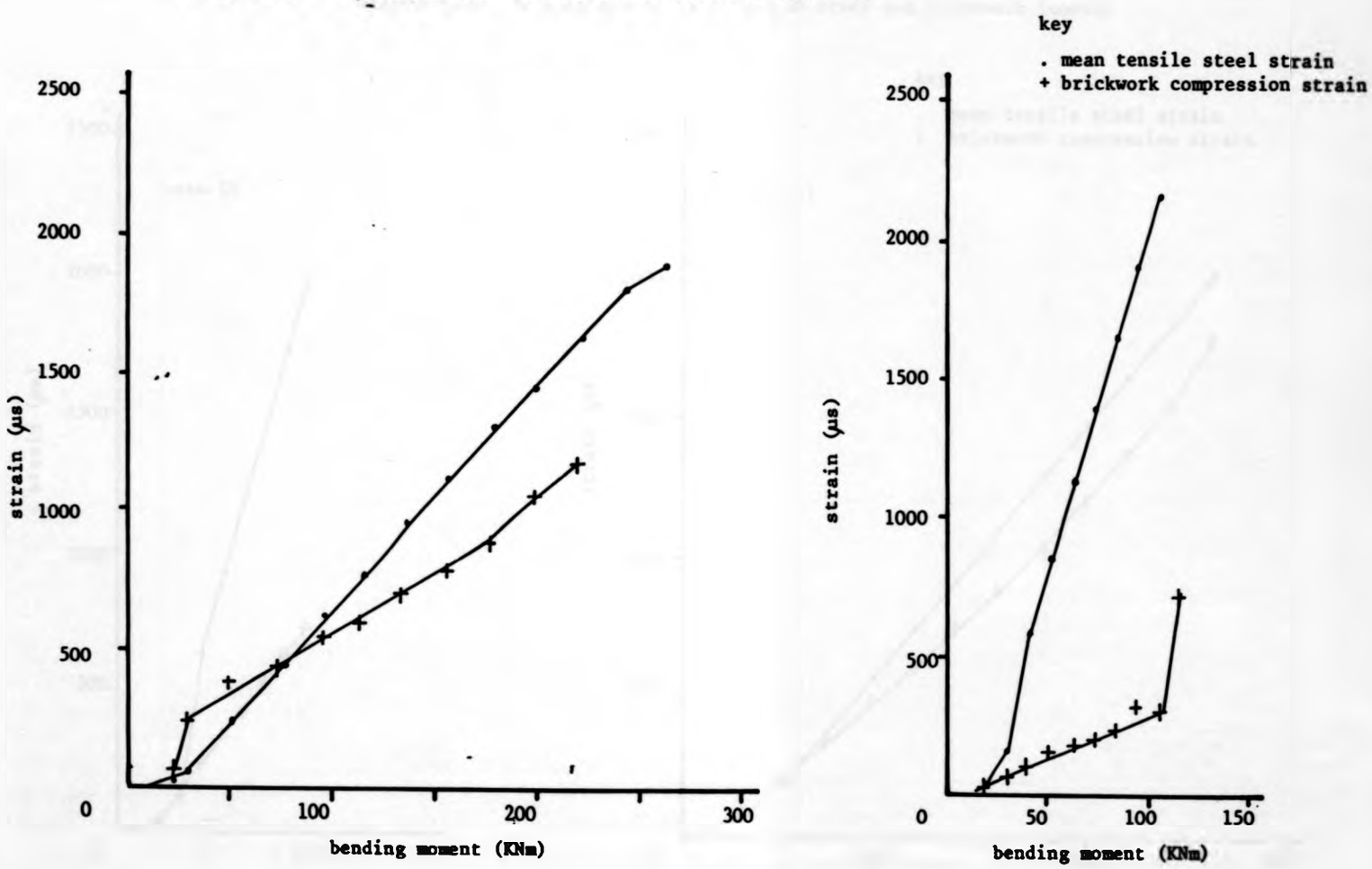

Figure 5.24 Bending moment vs strain in steel and brickwork (contd)

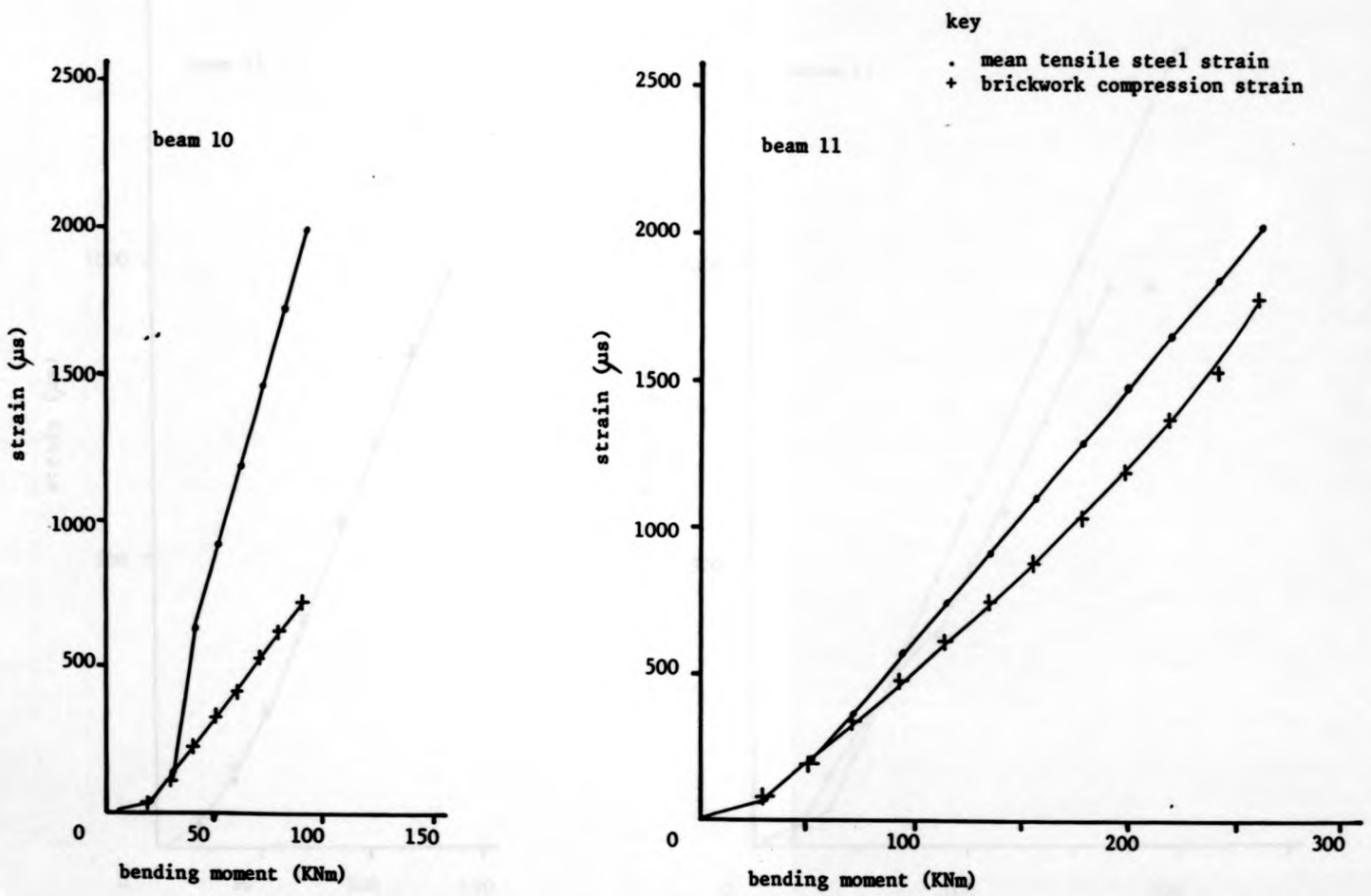

Figure 5.24 Bending moment vs strain in steel and brickwork (contd)

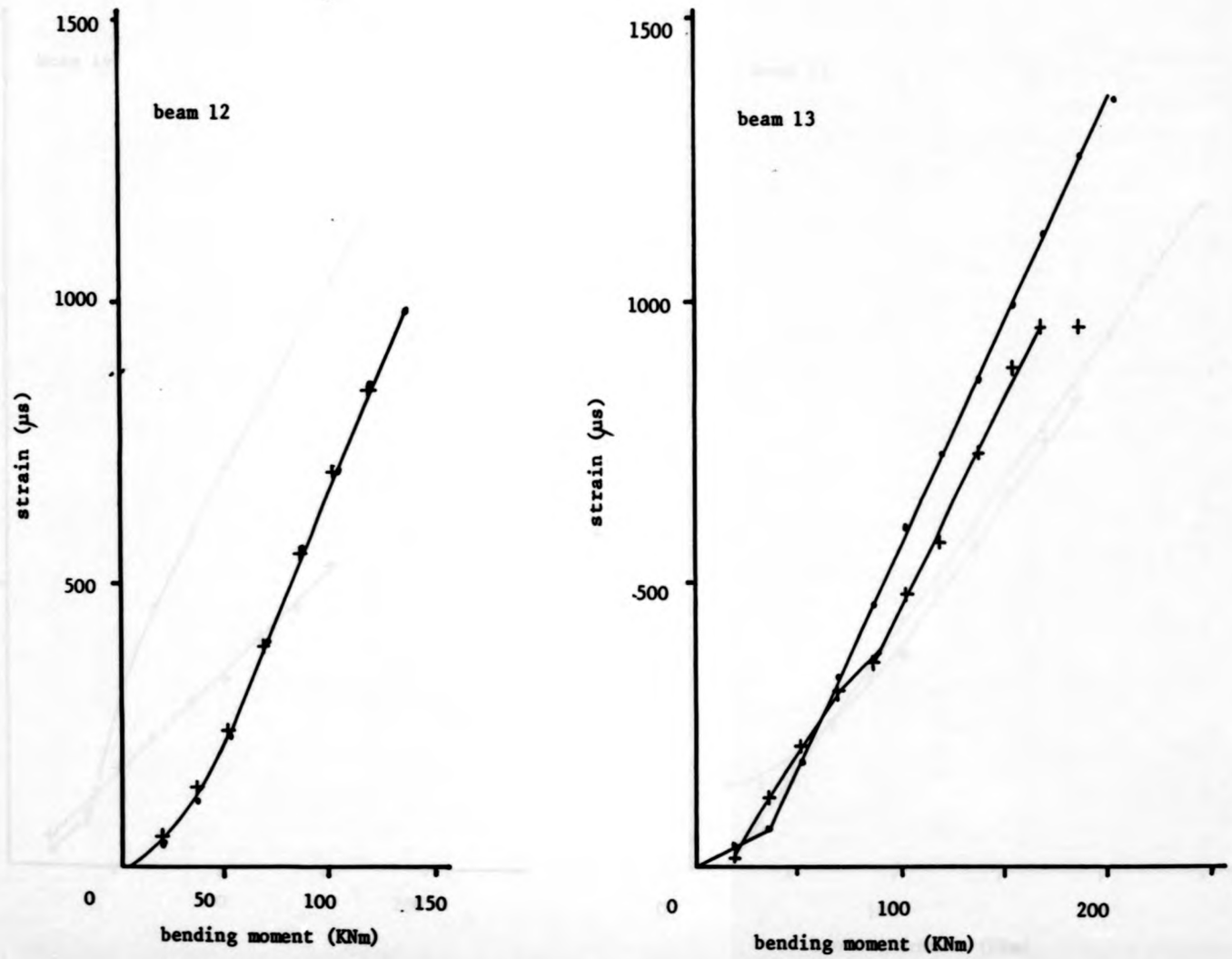

Figure 5.24 Bending moment vs strain in steel and brickwork

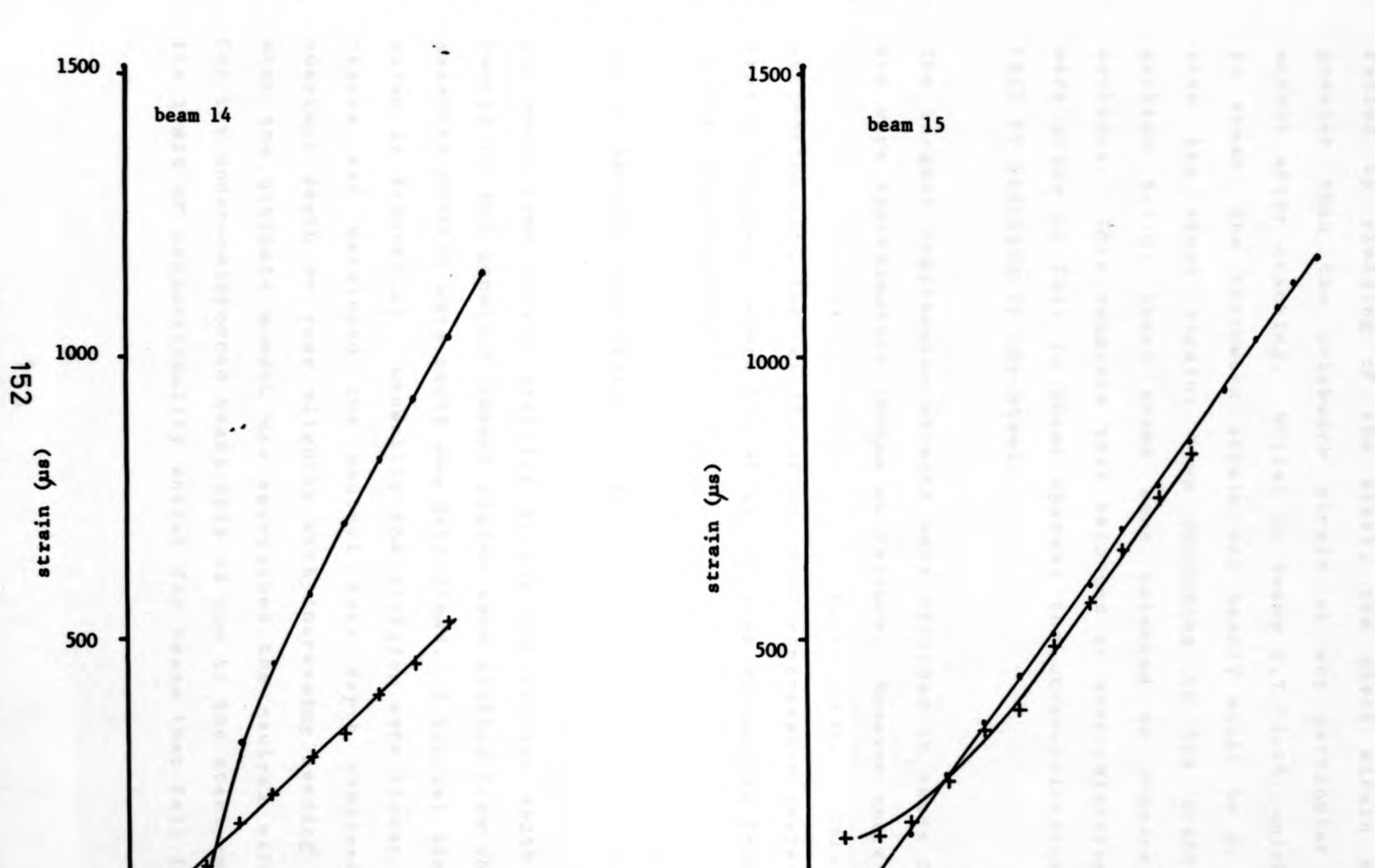

failed by yielding of the steel, the steel strain was much greater than the brickwork strain at any particular bending moment after cracking. Whilst in beams 2,7,11-15, which failed in shear, the brickwork strain was nearly equal to or greater than the steel strain: thus according to the Draft Code[3], section 5.1.5, these beams were balanced or over-reinforced sections. This suggests that balanced or over-reinforced beams were prone to fail in shear whereas the under-reinforced beams fail by yielding of the steel.

The largest compression strains were recorded in beams 2 and 11 and were approximately 1900μs at failure. However there were no signs of compression failure in either beam. This is in accordance with the results of uniaxial compression tests on this type of brickwork where the strain at peak stress was found to be 3800μs approximately[57].

5.2.5 Neutral axis depth

For each beam strain profiles across the section depth at the centre of the constant moment region were plotted from which the measured neutral axis depth was determined. A typical example is given in Figure5.25. Generally the profiles were linear. After cracks had developed the neutral axis depth remained at a constant depth or rose slightly with increasing bending moment. When the ultimate moment was approached the neutral axis rose: for the under-reinforced beams this is due to the steel exceeding its limit of proportionality whilst for beams that fail in shear

Figure 5.25 Typical profile of brickwork strain through depth of beam

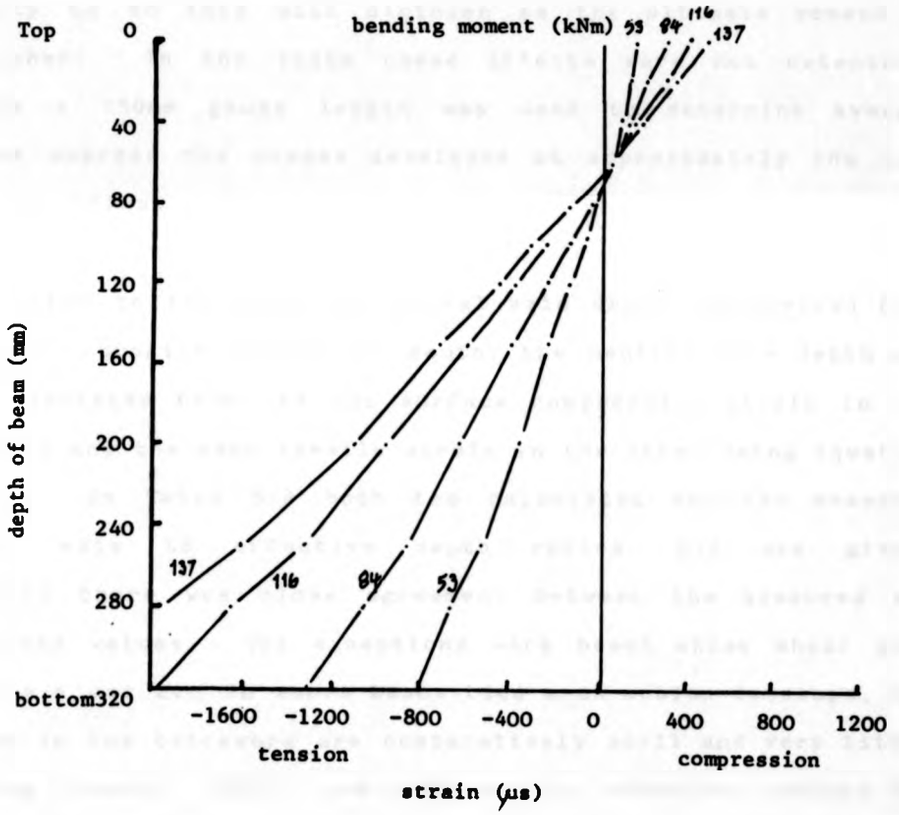

it was because diagonal rather than flexural cracks reduced the depth of the compression zone.

It is to be expected that in the constant moment region the neutral axis depth is unlikely to remain constant at any given moment but it is dependent on the depth and position of the cracks. Between the cracks it will increase slightly due to the tension stiffening effect of the uncracked brickwork and its capacity to do this will diminish as the ultimate moment is approached. In the tests these effects were not detectable because a 150mm gauge length was used to determine average strains whereas the cracks developed at approximately the same distance, 150mm.

In addition to the measured neutral axis depth, determined from the strain profile across the depth, the neutral axis depth was also calculated from the top surface compression strain in the brickwork and the mean tensile strain in the steel using equation (5.1) . In Table 5.4 both the calculated and the measured neutral axis to effective depth ratios, n/d are given. Generally there was close agreement between the measured and calculated values. The exceptions were beams whose shear span ratios a/d was 2. In short beams tied arch action develops, the strains in the brickwork are comparatively small and very little cracking occurs. Thus it was difficult to determine, within the accuracy of the demec gauge, the exact neutral axis depth from the strain profile. Hence for short shear spans the calculated neutral axis depth was considered to be more accurate since it

TABLE 5.4 NEUTRAL AXIS RATIOS IN BEAMS

Beam No	Measured [1] ratio n/d	Calculated [2] ratio n/d
1	0.23	0.21
2	0.53	0.48
3	0.15	0.19
4	0.19	0.19
5	0.14	0.23
6	0.24	0.35
7	0.34	0.44
8	0.32	0.42
9	0.12	0.12
10	0.29	0.26
11	0.41	0.43
12	0.29	0.53
13	0.17	0.42
14	0.19	0.34
15	0.18	0.40

Note: 1. minimum neutral axis depth evaluated from strain profiles on edge of beams.

2. neutral axis depth determined using eqn (5.1) from measured strains in steel and on top surface of beam.

compared favourably with those from similar beams with greater shear span ratios.

5.2.6 Crack patterns

Crack patterns of each beam are illustrated in Figure 5.26. Plates 5.2-5.5. show the cracks in beams 2,5,8 & 12. Generally the first cracks to form were the flexural cracks in the constant moment region which were observed at 20% - 40% of the ultimate load. As the load increased, flexural cracks developed in the shear spans, all cracks gradually widened and propagated towards the neutral axis of the beam. The beams that failed in shear usually showed few signs of impending failure until diagonal shear cracks developed explosively in the shear span. This behaviour contrasts with the slow ductile flexural failures which were associated with an increasing rate of deflection of the beam.

In many of the beams that failed in shear, longitudinal cracks developed in the compression face over the pocket boundary immediately prior to failure. These started in the constant moment region and propagated rapidly to the supports, in each case they extended through the depth of the beam. Plate 5.5 shows the longitudinal cracks after failure in beam 12. It is not known whether imminent shear failure induced longitudinal cracking but the results of beams 2 and 15 which both failed in shear without longitudinal cracking suggests that this was the case.

Figure 5.26 Crack patterns for beams

note: 1 All figures on the beams are the total applied load when the crack was first observed
2 Dotted lines represent the cracks that developed at failure

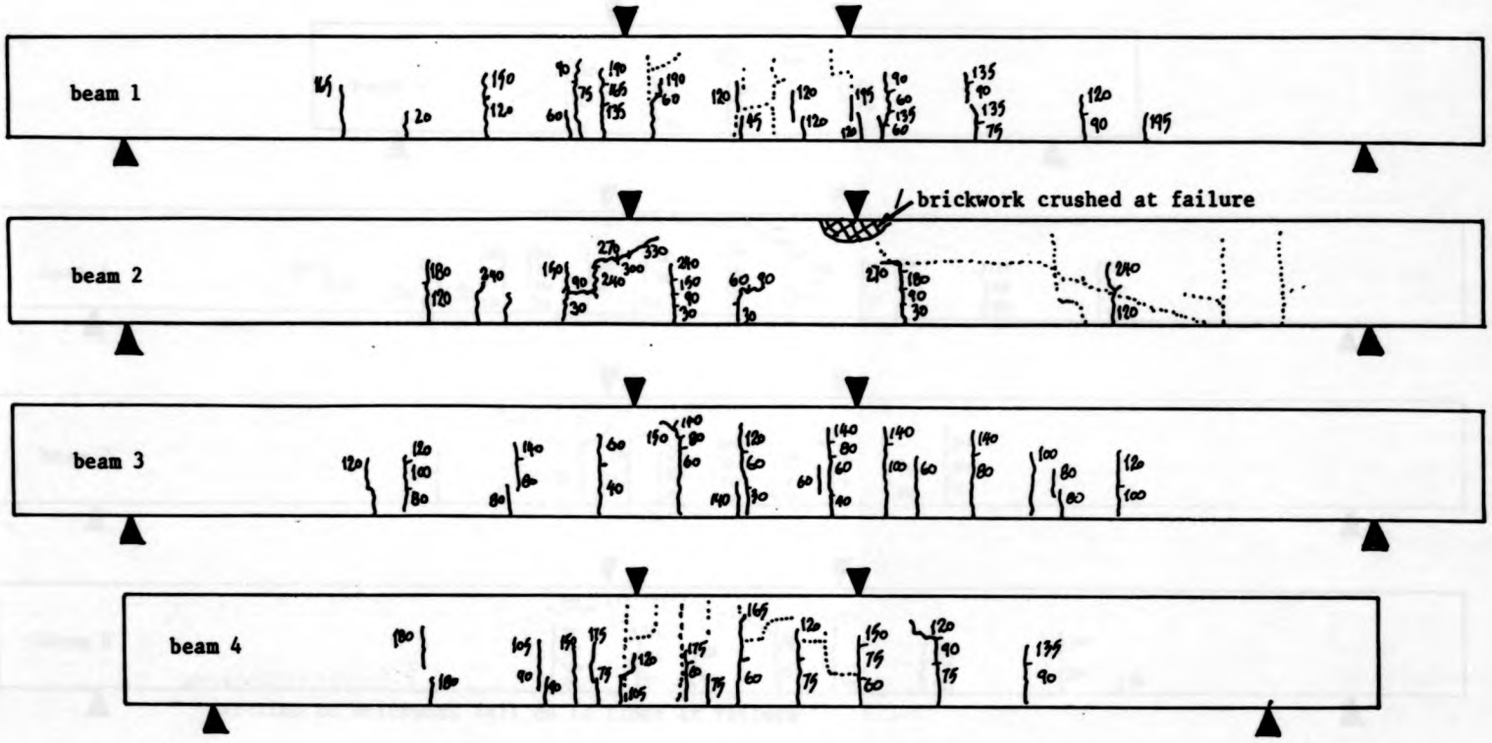

Figure 5.26 Crack patterns of beams (contd)

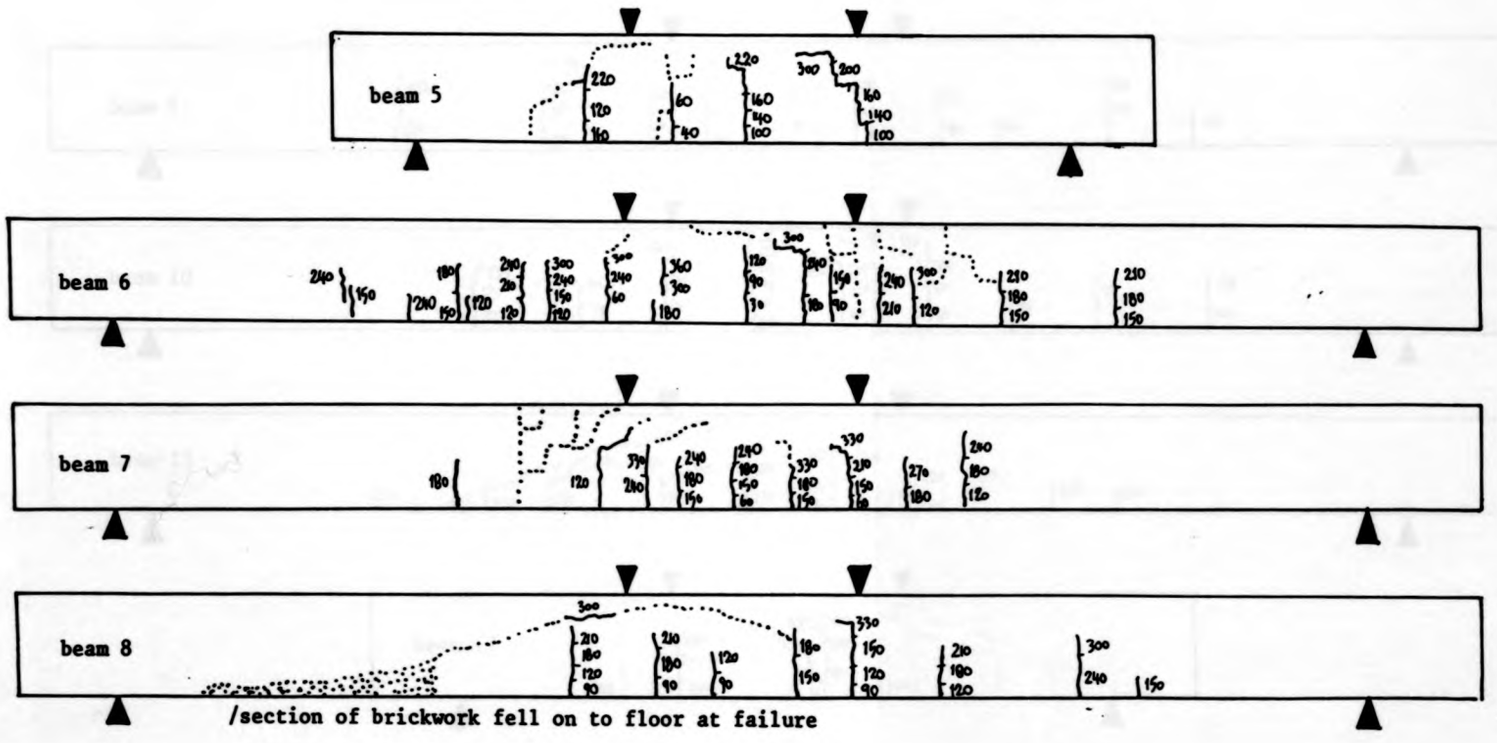

Figure 5.26 Crack patterns of beams (contd)

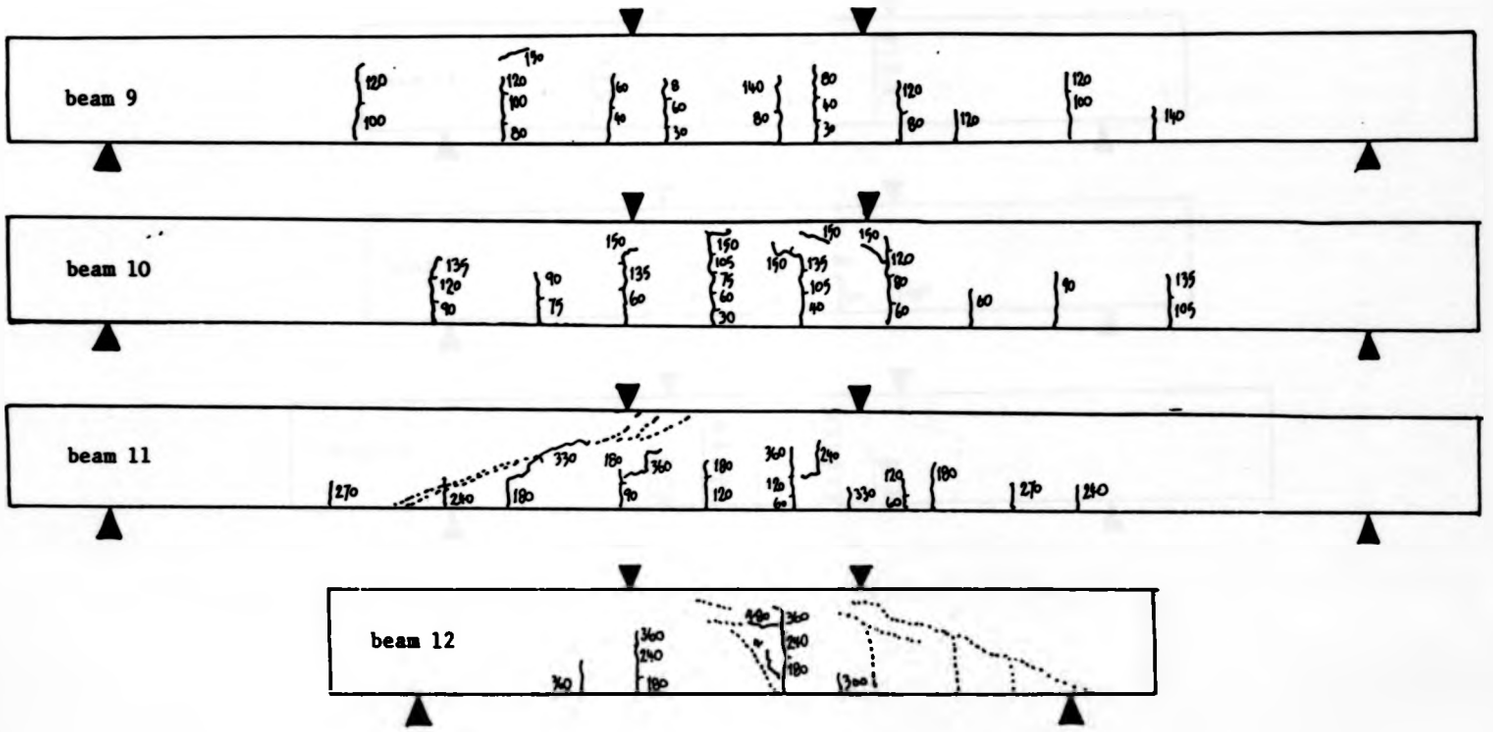

Figure 5.26 Crack patterns (contd)

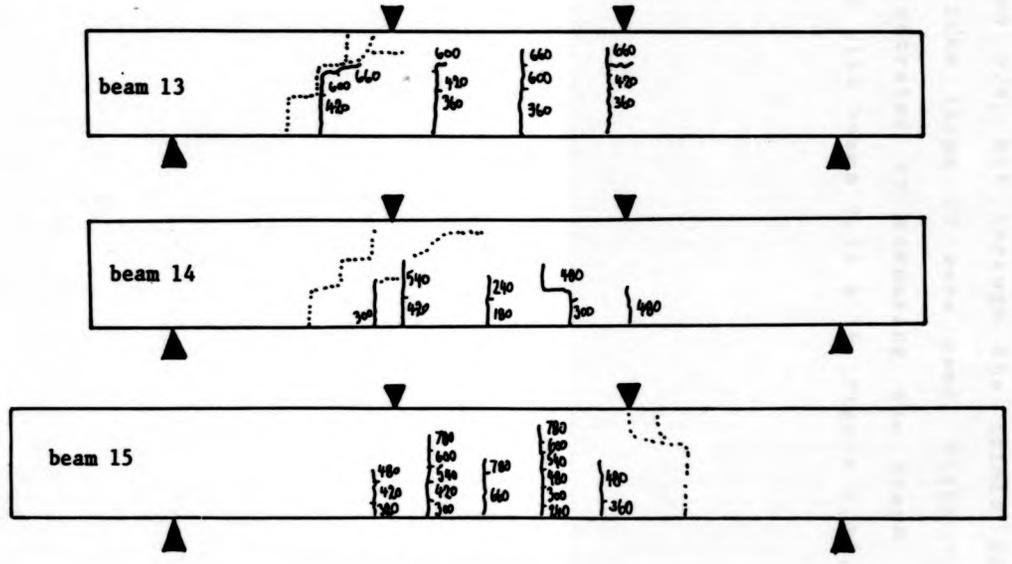

When shear failure occurred there was a tendency whereby cracks developed through both the joints and the units when low strength (type B) and high strength (type A) bricks were used, Plates 5.2, 5.3 and 5.4, but through the joints only when very high strength bricks (type C) were used, Plate 5.2. This is also clearly illustrated by comparing the crack patterns of beams 2,8,11 & 12 with beams 7,14 & 15, Figure 5.26.

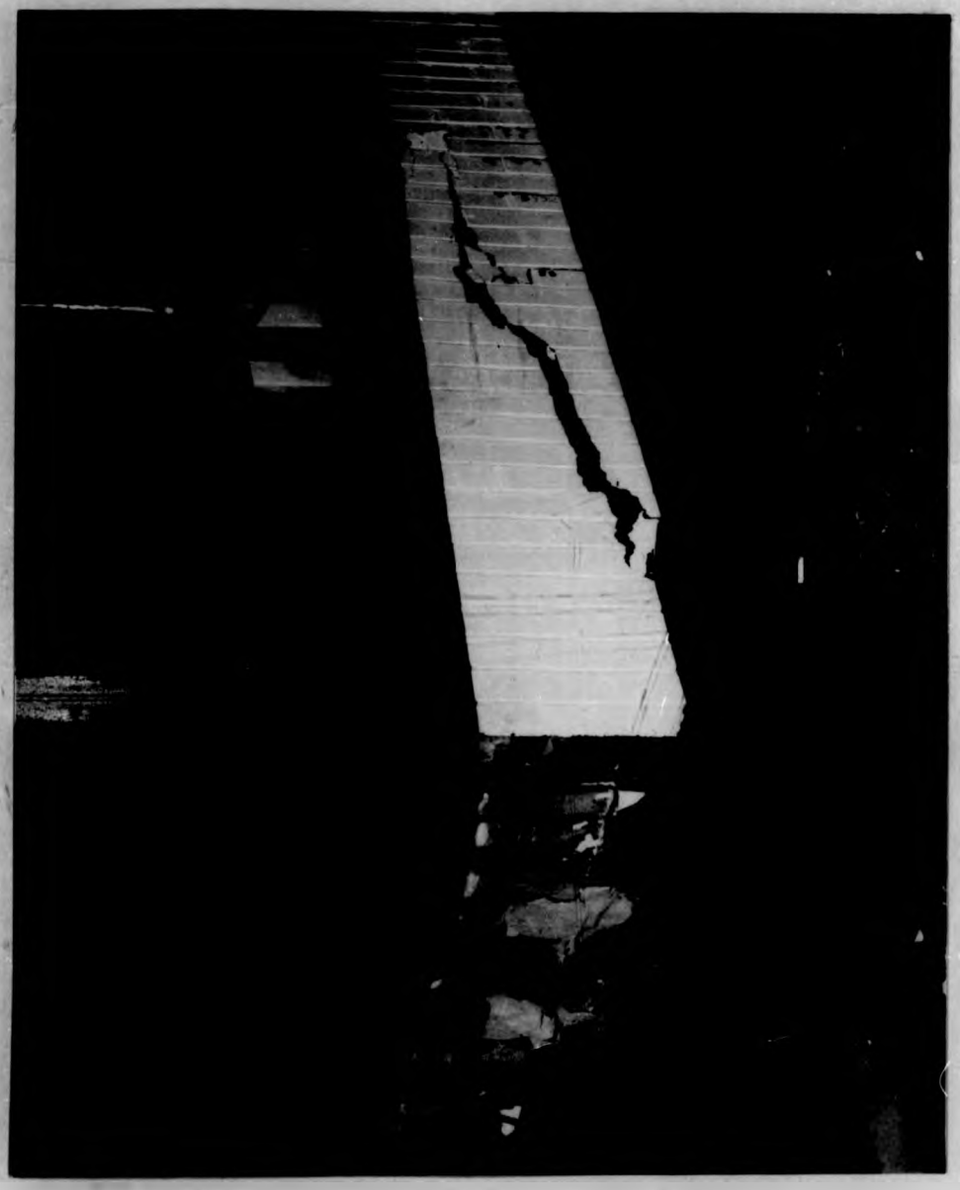

PLATE 5.2 Cracks in beam 2

PLATE 5.2 Cracks in beam 2

PLATE 5.3 Cracks in beam 5

PLATE 5.3 Cracks in beam 5

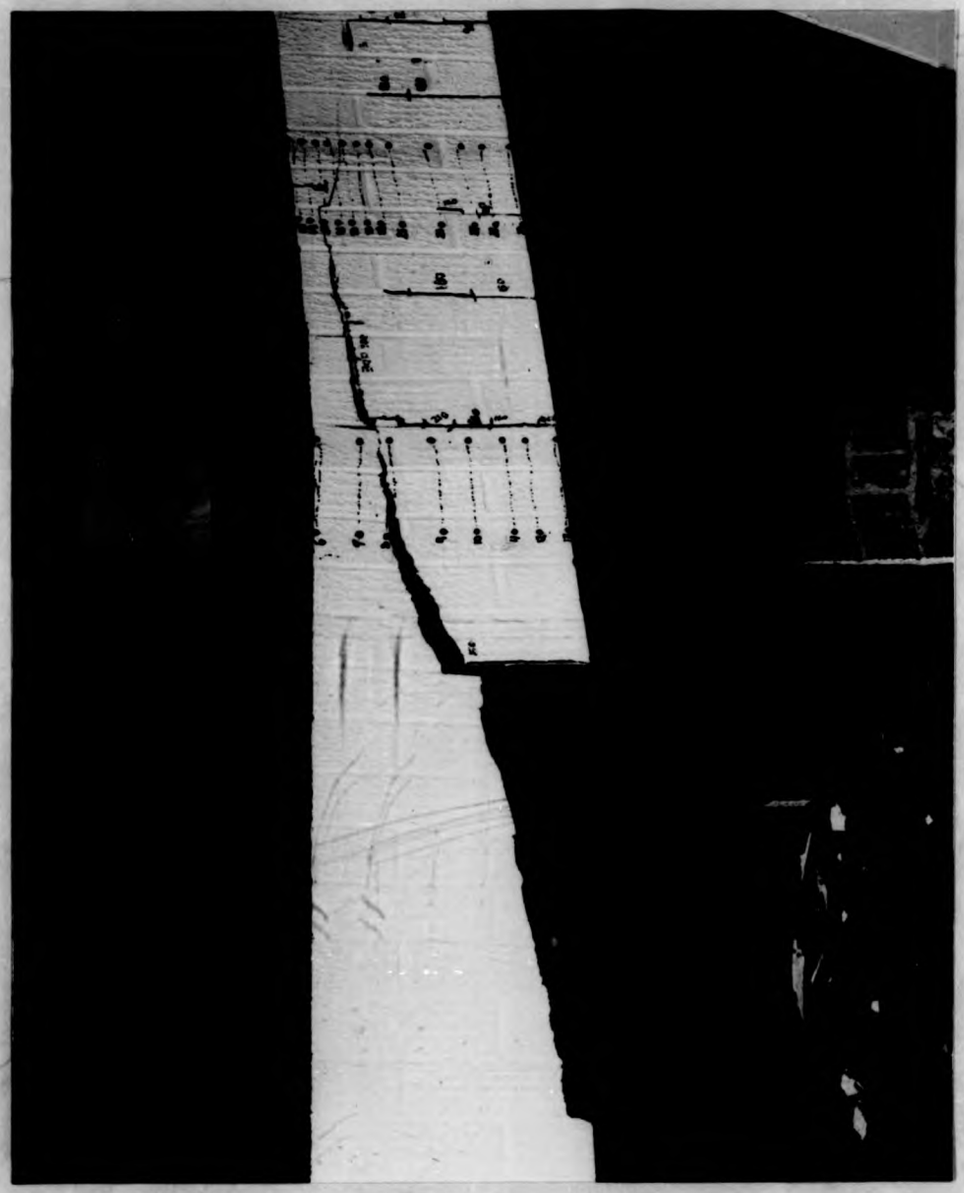

PLATE 5.4 Cracks in beam 8

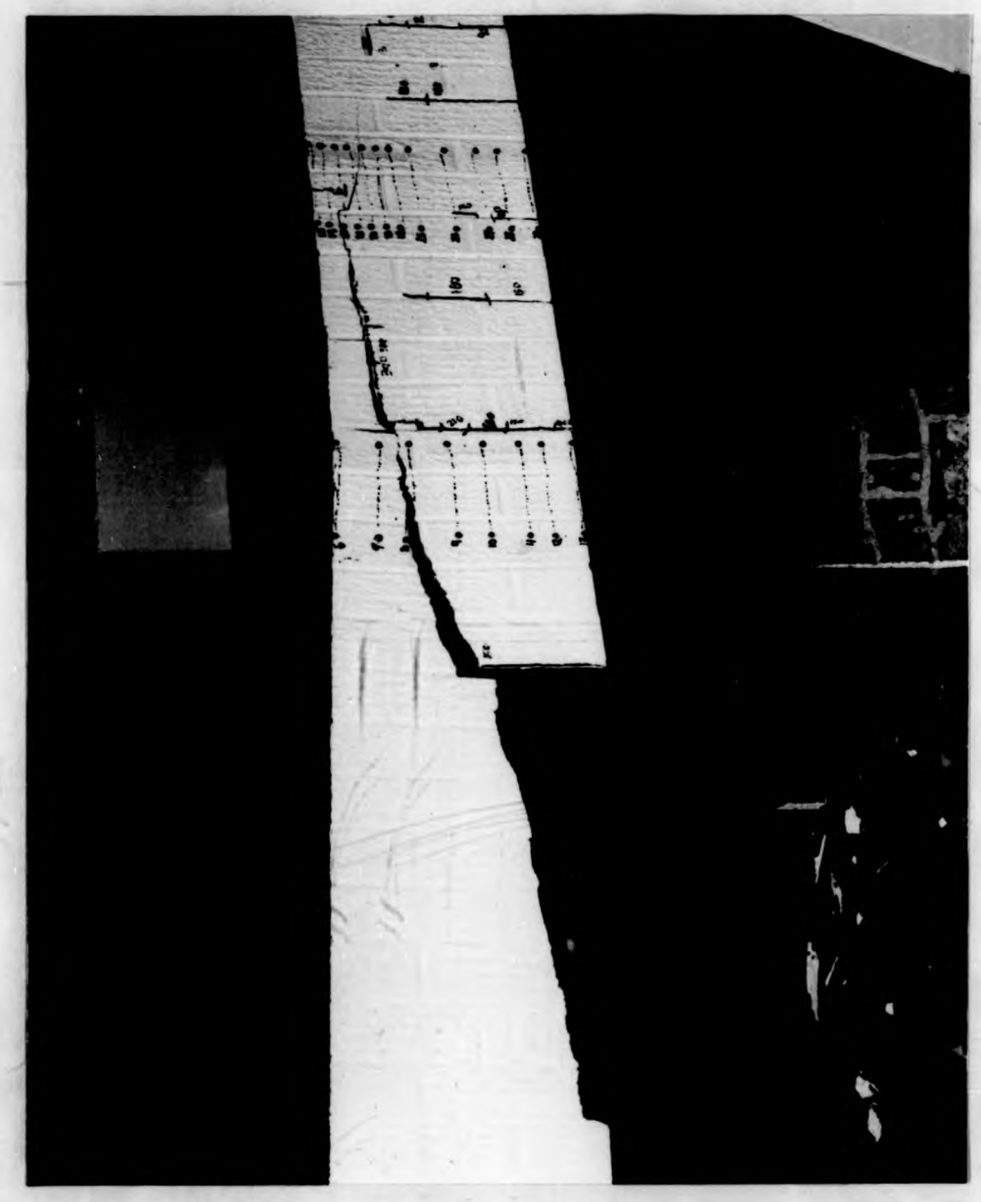

PLATE 5.4 Cracks in beam 8

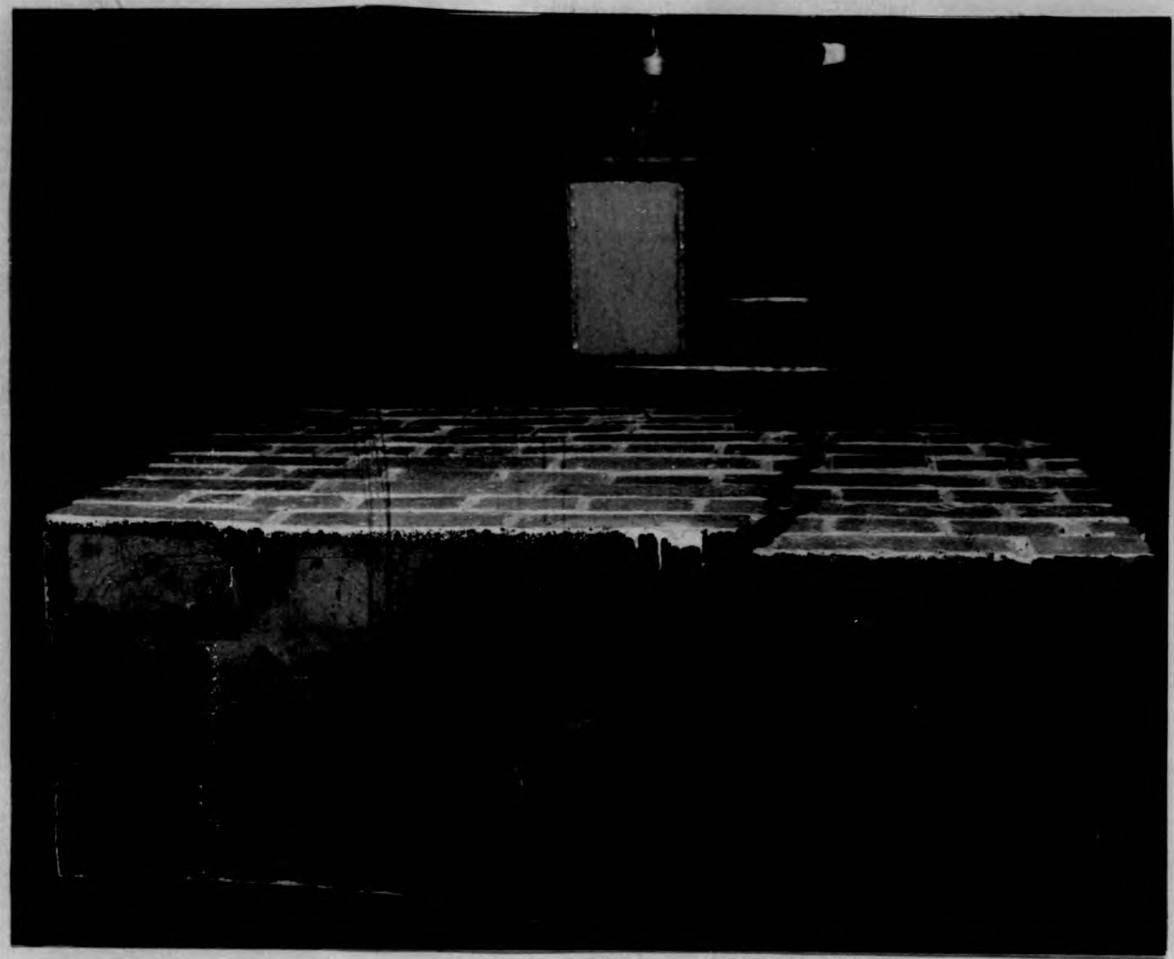

PLATE 5.6 Longitudinal crack along the pocket boundary of beam 12

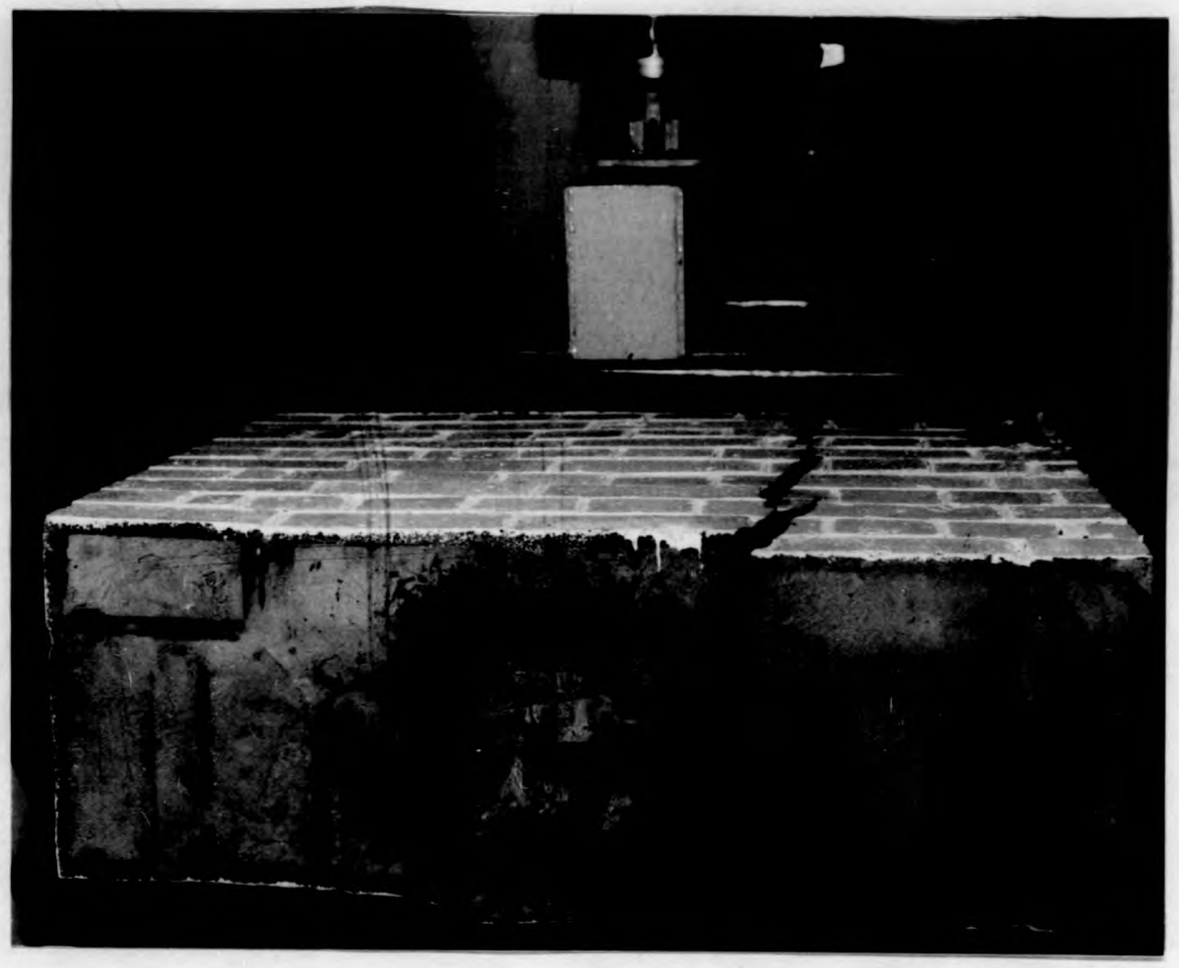

PLATE 5.6 Longitudinal crack along the pocket boundary of beam 12

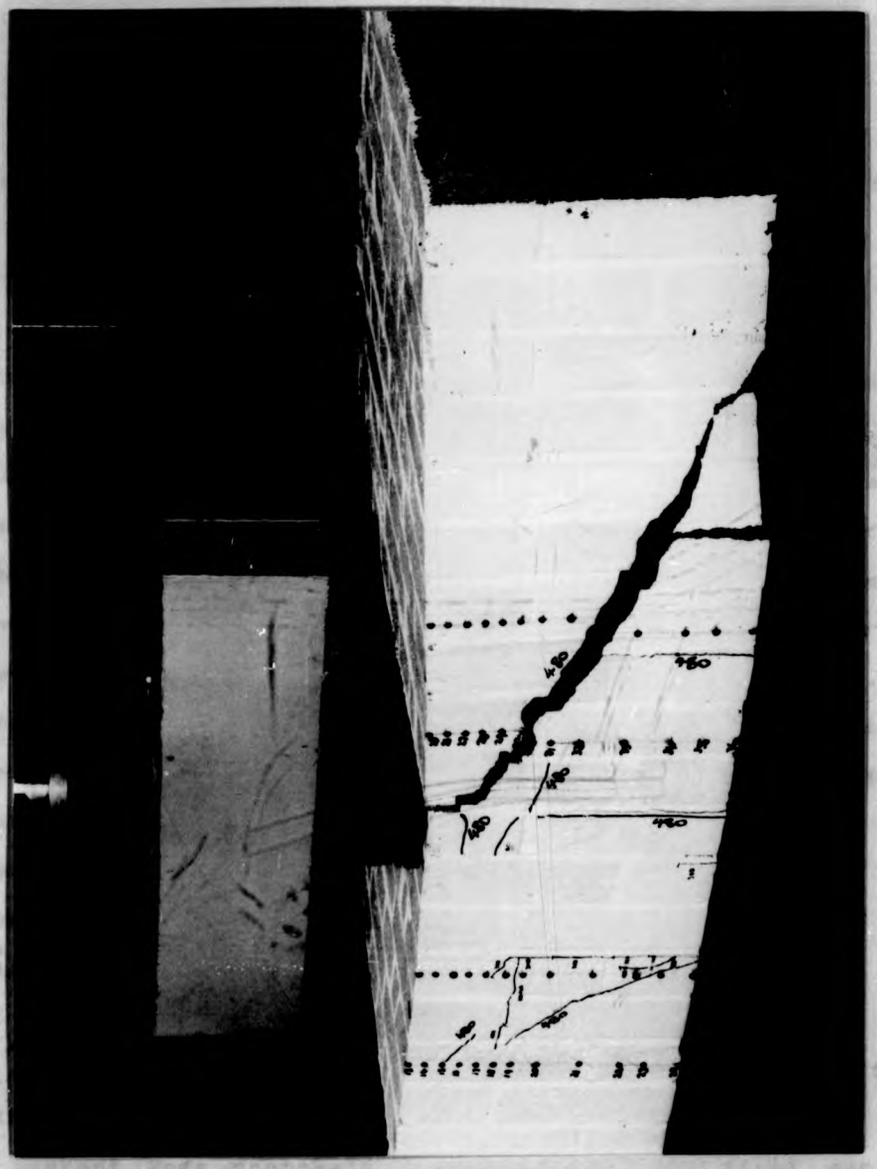

PLATE 5.5 cracks in beam 12

PLATE 5.5 cracks in beam 12

6. ANALYSIS OF EXPERIMENTAL RESULTS

6.1 Comparison against the requirements of the Draft Code

6.1.1 Serviceability limit state

There are two conditions which are usually examined in relation to serviceability requirements; the first is crack widths and the second is deflection at working loads.

Although crack width limits are used in the U.K. in reinforced concrete design[45] , they are not generally employed in the design of reinforced brickwork either in the UK or elsewhere. Essentially a crack width limit is an appearence criterion although it is often considered to be a durability requirement to prevent or delay corrosion of the reinforcement. However the relevance of this is currently being questioned [77]. The current proposals for the Draft Code are based on preventive measures whereby the type of reinforcement is selected for durability appropriate to the exposure condition of the member. Three types of protection to carbon steel are specified: none, a galvanised zinc coating of masses 460g/m^2 and 940 g/m^2 and an austenitic stainless steel coating at least 1mm thick.

The restriction of deflection under working loads is often for aesthetic reasons although it also serves to limit crack widths. The current Code proposals[78] are to limit the final deflection (including the effects of temperature, creep and moisture

movement) to height/80 for cantilevers and to span/250 for all other elements.

6.1.1.1 Crack widths

Due to the quantity of instrumentation and the restricted access, it was impractical to monitor crack widths in the retaining wall tests. Although the ends of the wall were accessible it is only the crack widths in the reinforced concrete (400mm away) that matter. Thus crack widths measured on the ends of the wall could be indicative only of the likely width at the pocket. For beams it was considered too dangerous to measure crack widths on the underside of the beam at the pocket. Consequently crack widths were not recorded specifically except where they occurred within strain gauge lengths.

In general the crack widths at working loads were small, usually in the range of 0.1mm to 0.2mm. They were estimated by assuming that all the measured strain was due to the formation of a single crack within the gauge length. This gave an overestimate of crack width since no allowance was made for the tensile strain in the uncracked brickwork and there may have been more than one crack.

The working load was determined by dividing the ultimate load by the global factor of safety appropriate to the failure mode. The three modes of failure and their global safety factors are:-

shear failure, $\gamma_f \gamma_{mv}$ = 1.6 x 2.0 = 3.2

compression of brickwork, $\gamma_f \gamma_{mm}$ = 1.6 x 2.0 = 3.2

yielding of steel, $\gamma_f \gamma_{ms}$ = 1.6 x 1.15 = 1.84

When a combined failure occurs, such as shear and steel yield, there will be two global safety factors. For analytical purposes the highest global safety factor was employed. Moreover the retaining walls were assumed to resist only live loads, hence $\gamma_f = 1.6$.

6.1.1.2 Deflection

The span/deflection ratio at working load has been analysed in two ways. The first way, method 1, assumed that the section was uncracked and ignored any stiffening due to the steel reinforcement. This Code proposal[78] suggests that the long term elastic modulus of brickwork of $450f_k$ should be used. However the wall and beam tests were of short duration thus the short term modulus $900f_k$ has been employed in the analysis.

Equation (6.1) based on elastic theory gives the relationship between the deflection at the end of a cantilever and the flexural rigidity, $E_b I_b$, for the load arrangement used in wall tests 2-6. For wall 1 the loading was slightly different and the factor changes from 1.775 to 1.738. This equation was derived by invoking the principle of superposition and is expressed in terms of bending moment at the base, M.

$$\Delta_{top} = \frac{M}{E_b I_b} 1.775 \times 10^6 \quad \text{mm} \qquad (6.1)$$

For the beams the deflection at the centre was evaluated using eqn.(6.2). where M is the maximum moment at the centre.

$$\Delta_{centre} = \frac{M L^2}{6 E_b I_b} \left(\frac{3}{4} - \left(\frac{a^2}{L^2} \right) \right) \qquad (6.2)$$

where a is the length of the shear span and L is the overall length of the beam.

Equations (6.1) and (6.2) were used to determine the deflection at working loads which are expressed as the predicted span/deflection ratio in column 2 of Table 6.1.

The second way, method 2, was also based on elastic theory and on the physical properties of the section. Deflections were evaluated using the flexural stiffness of a cracked section, $E_b I_{cr}$, by substituting the appropriate values in eqns (6.1) and (6.2). The second moment of area of a cracked section, I_{cr} in terms of brickwork units and assuming that brickwork has zero tensile strength is given by eqn (6.3)

$$I_{cr} = \frac{bn^2}{2} \left(d - \frac{n}{3} \right) \qquad (6.3)$$

where the neutral axis depth, n, is found from eqn. (6.4)

$$\left(\frac{n}{d} \right)^2 - \frac{2 A_s E_s}{b d E_b} \left(1 - \frac{n}{d} \right) = 0 \qquad (6.4)$$

The deflections were determined for $E_b=900f_k$ and $E_b=600f_k$ and were expressed in terms of predicted span/deflection ratios in columns 3 and 4 of Table 6.1 respectively.

In Table 6.1 the measured span/deflection ratios from the experimental results may be compared with those predicted using the two theoretical methods. It is clear that cracked section analysis gives the better predictions, and for beams always overestimated deflections whilst method 1 always underestimated deflections. For method 2 there was a small difference only between the results for the short term modulus $E=900f_k$ and $E=600f_k$, with the former giving the best predictions. For the walls it is impractical to make any comparison with the experimental results since the deflection included the effects of rotation of the steel base, see section 5.1.2.

The experimental span/deflection ratios of the beams were always within the proposed Code serviceability limit of span/250. If rotation of the base and slip of the anchorage are taken into account then it is likely that all the experimental results for the walls would have met the proposed requirement[78] of span/80 for the Draft Code.

A current requirement of the Draft Code is that the span/effective depth ratio of a cantilever with reinforcement quantities up to 0.5% should not exceed 18. There is no clear guidance for walls with greater quantities of reinforcement. However if it is assumed that this requirement applies to walls

TABLE 6.1 COMPARISON OF EXPERIMENTAL AND PREDICTED SPAN TO DEFLECTION RATIOS AT WORKING LOADS

Specimen		Span / deflection ratio				
		Method 1 E=900 f_k	Method 2 E=900 f_k	Method 2 E=600 f_k	Experimental	F.E. E=600 f_k
Wall	1	858	328	271	49	300
	2	442	296	242	104	288
	3	653	228	209	80	280
	4	1343	266	243	136	411
	5	992	192	164	109	210
	6	1119	217	176	54	118
Beam	1	2174	468	441	647	623
	2	1066	569	562	971	730
	3	3434	562	406	800	704
	4	4272	459	441	861	560
	5	5112	1296	730	1680	646
	6	2956	711	619	1700	850
	7	2792	833	734	2125	1156
	8	2430	708	659	1511	827
	9	2888	397	377	1046	540
	10	1278	363	293	850	397
	11	1020	641	529	1236	765
	12	2626	2010	1718	2400	--
	13	5794	1626	1462	2400	--
	14	6956	2108	2000	2400	--
	15	7098	2051	1816	2584	--

with greater percentages of reinforcement then the experimental results indicated that the limit on span/effective depth ratio is compatible with the serviceability requirement that limits the span/deflection ratio to span/250.

6.1.2 Ultimate limit state

For retaining walls the ultimate limit state is arguably more important than the serviceability limit state. Failures due to lack of stability of the wall or shear failures in the soil although important in the overall design are not considered in this study. Only the performance of the reinforced brickwork stem was subject to investigation.

At ultimate limit state there are two modes of failure, namely shear failure and flexural failure. The Draft Code requires both of these conditions to be checked independently using the design equations in section 2.3.

6.1.2.1 Flexure

The Draft Code contains two sets of design equations for flexure, namely those for rectangular sections and those for flanged sections. A requirement of the Code is that pocket walls should be treated as flanged members irrespective of their shape, see section 2.3. For analytical purposes the partial safety factors were set to unity; thus eqns (2.1-2.5) gave the theoretically predicted ultimate moments of resistance.

6.1.2.1.1 Walls

The material strengths of brickwork and steel were thought to have a major influence on the predicted moment capacities. Two sets of values were used in the analysis. These were the mean measured material strengths and the Code characteristic values taken from Table 2.2 for brickwork and Table 2.4 for steel. Table 6.2 compares the experimental results with the predicted moment capacities using the Code equations.

From Table 6.2 it is clear that the predictions are conservative for all walls except number 1. However the loading of wall 1 was stopped prematurely due to excessive deflections caused mainly by slip of the anchorage system. Thus the Code equations appear to be adequate.

When rectangular section analysis was compared with flanged section analysis, it was found that the former gave marginally better predictions, Table 6.2, bearing in mind that the walls represent extremes in parameters such as reinforcement percentage, brick strength and slenderness. This is consistent with the experimental evidence that these walls act as homogenous cantilevers; thus the Code should acknowledge this.

In practice flange section analysis uses a fixed lever arm independent of material properties which is an approximation that tends to underestimate the strength of lightly reinforced sections by about 25% [79] whilst overestimating the strength of

TABLE 6.2 COMPARISON OF WALL TEST RESULTS WITH CAPACITIES GIVEN BY CODE EQUATIONS

Wall	1	2	3	4	5	6
Failure moment (KN m)	412	503	222	221	254	224
Average shear stress at failure (N/mm^2)	1.07	0.96	0.41	0.41	0.78	0.68
Failure mode*	T	T+C	T	T	C	C
Predicted capacities based on code strengths						
M_{flex}, eqn(2.2) rectangular OR section (KNm)	1240	430	584	1208	196	196
M_{flex}, eqn (2.1) rectangular UR section (KNm)	512	404+	198	203‡	256+	223+
M_{flex}, eqn(2.5) flanged OR section (KNm)	923	331	426	881	208	208
M_{flex}, eqn(2.4) flanged UR section (KNm)	458	433	176	176	237	206
characteristic shear stress, f_k (N/mm^2)	0.53	0.53	0.39	0.39	0.59	0.57
Predicted capacities based on mean strengths						
M_{flex}, eqn(2.2) rectangular OR section (KNm)	930	379	557	1122	180	243
M_{flex}, eqn(2.1) rectangular UR section (KNm)	512	420+	208	212	272+	237+
M_{flex}, eqn(2.5) flanged OR section (KNm)	705	358	406	818	191	259
M_{flex}, eqn(2.4) flanged UR section (KNm)	477	452	184	184	251	219

Notes: * T = steel yield, C = brickwork crushed

\+ min lever arm of 0.75d used

‡ max lever arm of 0.95d used

OR = over-reinforced , UR = under-reinforced

heavily reinforced sections. Thus the Draft Code imposes an unrealistic restriction on the design of rectangular plan-shaped retaining walls, especially since many are likely to be lightly reinforced.

The strengths of under-reinforced sections were generally more accurately predicted than over reinforced sections. Furthermore when the mean measured strengths were inserted into the Code equations they gave better predictions for under reinforced sections than when the characteristic strengths were employed. The reverse was true for over-reinforced sections. This occurs because the tensile strength of the reinforcement may be more accurately defined than the flexural compressive strength of brickwork. In the case of an over-reinforced section the Code formulae were intended to give a conservative limit to the moment of resistance rather than exactly define a value. It is also relevant to observe that as yet there is no broad agreement on the type of test specimen which should be used to determine the compressive strength of brickwork in direct compression and the question of whether this value would apply to flexural compression is open. Research should be carried out to clarify this situation. Preferably it should concentrate on the suitability of small scale test specimens.

6.1.2.1.2 Beams

The beams were analysed as rectangular sections using eqns (2.1-2.3) thus treating them as homogenous sections. This is in

accordance with both the findings of section 6.1.2.1.1 and the experimental results. The accuracy of the Code equations was assessed from the moment ratio, M_{ult}/M_{flex}, Table 6.3, where the predicted flexural moment capacity based on Code characteristic strengths, M_{flex}, was the lesser value given in columns 3 and 4 Table 6.3. M_{ult} was the experimental ultimate moment capacity. In general the flexural failures were predicted accurately although they were slightly conservative. As all the beams failed either by yielding of the steel or shear it was not possible to comment in detail on the performance of eqn (2.2) which gives the flexural compressive strength of a member. However the result of beam 11 indicates that it might be conservative since the Code equations indicated that compressive failure of the brickwork should have occurred at 245kNm, whereas shear failure occurred at 281kNm.

The above points are considered to apply if the mean measured material strengths had been used in the analyses. For steel the characteristic tensile strength was less than the mean measured yield strength by 6%. Moreover all beams, except beam 11, were under-reinforced according to the Code equations, thus the steel strength was the governing factor in determining M_{flex}.

6.1.2.2 Shear

For the purposes of analysis the partial safety factor for shear γ_{mv} was set to unity in eqn (2.1) , hence the characteristic shear stress is also the predicted ultimate shear capacity of the

TABLE 6.3 COMPARISON OF BEAM TEST RESULTS WITH CAPACITIES PREDICTED BY CODE EQUATIONS

Beam No	Shear span ratio	Predicted moment capacities* brickwork M_{flex}+ (KNm)	steel M_{flex}+ (KNm)	shear M_{shear} (KNm)	Ultimate moment M_{ult} (KNm)	Moment ratios $\frac{M_{ult}}{M_{flex}}$	$\frac{M_{ult}}{M_{shear}}$	predicted failure mode++	failure mode++
1	5.09	733	163	175	170	1.04	0.97	T	T
2	5.00	273	236	208	240	1.01	1.15	S	T+S
3	4.75	856	103	165	117	1.13	0.70	T	T
4	3.93	790	98	126	129	1.31	1.02	T	T
5	2.00	756	98	60	123	1.25	2.05	S	T+S
6	5.09	740	262	208	305	1.16	1.46	S	T+S
7	5.28	680	394	221	326	0.82	1.47	S	S
8	5.18	565	254	202	264	1.04	1.30	S	T+S
9	5.00	604	98	153	121	1.23	0.79	T	T
10	5.18	256	93	148	121	1.30	0.81	T	T
11	5.28	245	318	220	281	1.14	1.27	S	S
12	2.00	254	226	77	132	0.58	1.71	S	S
13	2.00	559	253	77	208	0.82	2.70	S	S
14	1.89	783	273	84	172	0.63	2.04	S	S
15	1.96	727	396	78	257	0.65	3.29	S	S

Notes: * based on characteristic strengths given in draft code

+ the lesser value governs

++ T = tension failure of reinforcement S = shear failure

section.

6.1.2.2.1 Walls

From Table 6.2 it is clear that the Draft Code estimate of the ultimate shear strength of a section is too low for walls with large amounts of reinforcement. Indeed a design comparison[79] for walls 327mm thick and 3,4 and 5m high showed that shear was always the governing design criterion and that as the height and quantity of reinforcement increased the design shear load exceeded the design shear capacity by a rapidly increasing margin, Table 6.4.

Several reasons may be proposed for the inaccuracy of characteristic shear stresses in the Draft Code in relation to pocket-type walls. Firstly these values were derived from tests on grouted cavity beams where the probability of shear failure is greater because the brickwork leaves have a tendency to separate from the reinforced concrete core thereby precipitating failure. Secondly that the interaction of moment and shear and the relative proportions of each (shear span ratio) may affect the mode of failure. This aspect is considered in more detail in section 6.1.2.3.

6.1.2.2.2 Beams

To enable a direct comparison between shear and flexure the average shear stress was converted to an equivalent bending

TABLE 6.4 DESIGN COMPARISON TAKEN FROM REFERENCE 79

Wall height	required steel	proportion of reinforcement	required f_k value	design shear load *	design shear resistance of wall 1
(m)	(mm^2)	(% bd)	(N/mm^2)	(kN)	(kN)
3	1020	0.18	3.8	43.2	40
4	2418	0.43	9.0	76.8	48
5	4722	0.84	17.7	120.0	58

Note: * the design load was based on the pressure exerted on the wall by a dry cohesionless soil of specific density 18 kN/m^2 with an angle of repose of 30^o

moment, M_{shear}, using eqn (6.1)

$$M_{shear} = Va \qquad (6.1)$$

The predicted shear capacities using the Code characteristic shear strengths are given column 6, Table 6.3. If the shear moment ratio M_{ult}/M_{shear} is greater than the flexural moment ratio M_{ult}/M_{flex} then shear is the predicted mode of failure, Table 6.3. Figure 6.1 shows that in general the mode of failure of pocket-type sections was predicted accurately however the Code appears to be unduly conservative in its shear requirements.

From Figure 6.2 it is apparent that beams with low shear span ratios, a/d=2, fail at higher shear stresses than beams with larger shear span ratios. This behaviour is consistent with that found for other types of reinforced brickwork beams[16,80,81,82] and for reinforced concrete beams[83]. A detailed explanation of the failure mechanism is given elsewhere[83]. At present the Draft Code makes no allowance for the influence of shear span ratio in the range a/d=2-4, although it does permit the characteristic shear stress to be increased if a/d is less than 2.

Also indicated by Figure 6.2 is that the pocket-type beams which failed in shear performed better in general than grouted cavity construction. There was no discernable trend between shear resistance and brick strength, see beams 12,13, &14 and beams 6,8 &11 However an increase in the percentage of tensile

Figure 6.1 Comparison between predicted and actual failure modes

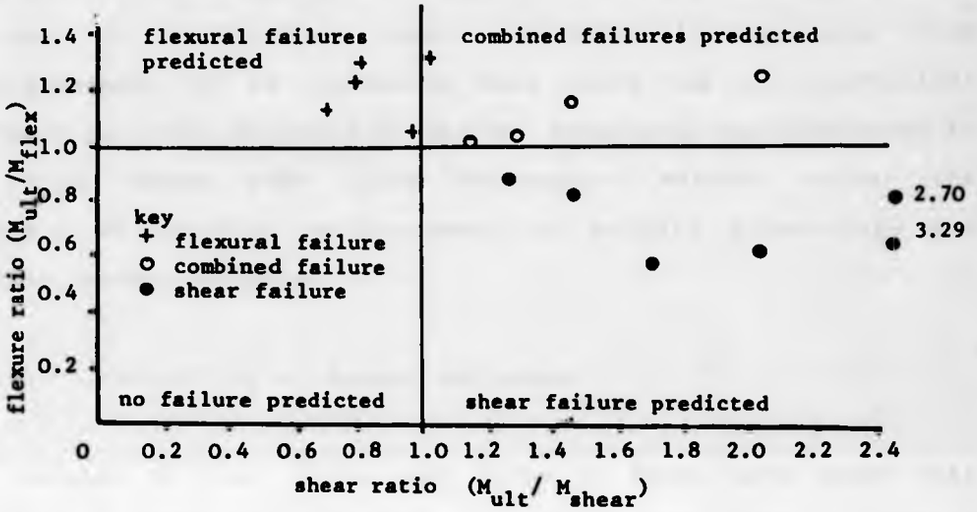

Figure 6.2 Comparison of the shear behaviour of pocket type sections with grouted cavity sections

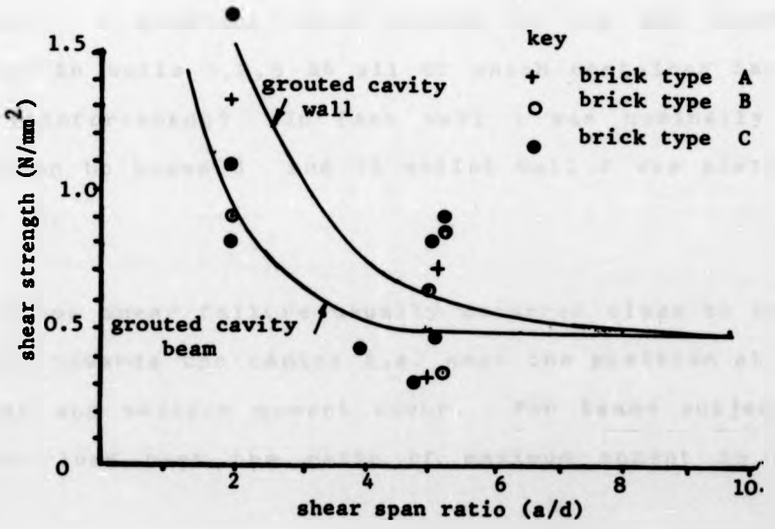

reinforcement did give an increase in the shear capacity of the section. This is illustrated by beams 7 and 15 which contained 1.4% reinforcement whose shear strengths were greater than beams 6 and 14 which were similar but contained only 0.9% reinforcement. It is considered that there was an insufficient increase in shear strength to justify proposing any amendments to the Code values that would distinguish between either the quantity of tensile reinforcement or between pocket-type and grouted cavity sections.

6.1.2.3 Interaction of moment and shear

The results of four point load tests on beams have shown that pocket-type sections may fail in shear albeit under a special circumstance namely they must contain large quantities of reinforcement. Furthermore as the shear span increased from 2 to 5 so the mode of failure change from shear to combined shear-flexure. This moment-shear interaction affects the behaviour of beams. A question which arises is why did shear failure not occur in walls 1,2,5 &6 all of which contained large quantities of reinforcement? In fact wall 1 was nominally an identical section to beams 8 and 13 whilst wall 2 was similar to beams 2 and 12.

In beams shear failure usually occurred close to the the loading point towards the centre i.e. near the position at which maximum shear and maximum moment occur. For beams subjected to a four point load test the ratio of maximum moment to maximum shear

equals the length of the shear span, a. For cantilever retaining walls the equivalent situation occurs at the base and thus the "effective" shear span is given by the ratio of moment to shear at the base. The ratio of effective shear span to effective depth or effective shear span ratio has been used in Table 6.5 as a basis for comparing the effect of the shear-moment interaction. These results plotted in Figs. 6.1 & 6.2 fit in with the overall pattern of the beam results.

From the results given in Table 6.5 arise several important implications for the design of pocket-type retaining walls. If the wall is heavily reinforced and is subjected to a loading condition that gives a small effective shear span then it may be prone to shear failure. In practice such a loading condition may be realised when the ground is compacted mechanically, see section 2.4. It should be noted that wall 1 met these conditions but did not fail in shear even though it had an effective shear span ratio of 2.72 . If a triangular pressure distribution is considered to be a reasonable design load on a retaining wall then the effective shear span ratio is h/3d, which for slender walls (h/d=18) approaches 6 whilst for stubby walls (h/d=9) is nearer to 3. Thus the experimental results suggest that a wall resisting a triangular pressure distribution is unlikely to fail in shear unless it is very stubby (h/d <3). Moreover the majority of earth retaining walls are likely to be lightly reinforced and therefore prone to flexural failure.

TABLE 6.5 INTERACTION OF MOMENT AND SHEAR IN CANTILEVER WALLS

Wall	Ratio of moment to shear (m)	effective shear span ratio	ultimate shear stress N/mm^2	moment ratio $\frac{M_{ult}}{M_{flex}}$	moment ratio $\frac{M_{ult}}{M_{shear}}$	predicted failure mode[2]
1+	0.975	3.54	0.77	-	-	-
1*	0.75	2.72	1.07	0.80	2.0[1]	S
2	0.975	3.70	0.96	1.24	1.81	S
3	0.975	3.37	0.41	1.12	1.05	T
4	0.975	3.37	0.41	1.08	1.05	T
5	0.975	5.83	0.78	1.30	1.32	T & S
6	0.975	5.83	0.68	1.14	1.19	S

Notes:
+ load cycle 2 - wall did not fail
* load cycle 3
1. based on rectangular section analysis results Table 6
2. S = shear, T = Steel yield

6.2 Finite element analysis

6.2.1 Modelling

The finite element program was used to analyse the walls and beams that failed in flexure in the experimental test programme. Beams 7 and 11 which failed in shear and had a shear span ratio of 5 were also analysed although it was realised that the plate bending element was incapable of detecting shear failure. These beams were analysed for their performance at serviceability limit state. Since the element was unable to take into account the out of plane shear stresses it was expected that the analysis would greatly underestimate deflections in beams with a short shear span. Indeed this proved to be the case for beam 5, consequently beams 12-15 were not analysed.

For each wall a coarse mesh was used except near to the base where a finer mesh was incorporated to pick up yielding of the reinforcement or crushing of the brickwork, Figure 6.3. This mesh was similar to that used successfully for the analysis of retaining walls whose results are given in chapter 4. A coarse mesh was used for the analysis of the beams, Figure 6.4, again this was similar to that adopted successfully for the analysis of beams in chapter 4. The quantity of reinforcement and its effective depth were the same as the experimental values.

The stress-strain characteristics of the materials were assumed to be linearly elastic-plastic as outlined in chapter 4.

Figure 6.3 Mesh used for the analysis of retaining walls

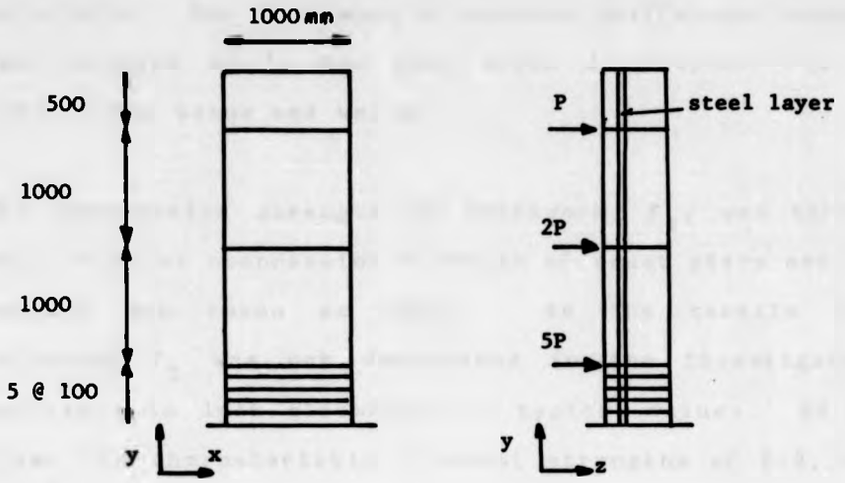

Figure 6.4 Mesh used for the analysis of pocket type beams

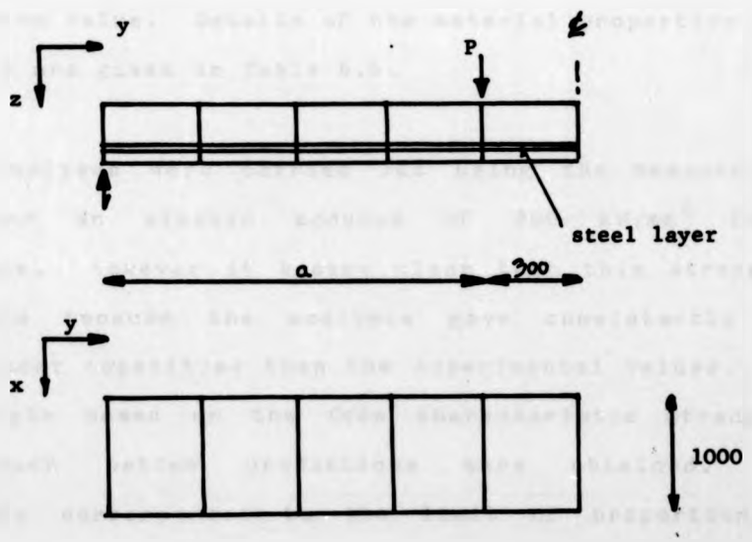

Concrete was assumed to have identical properties to the adjacent brickwork. For brickwork a tension stiffening response of β=8 was included as it has been shown in chapter 4 to give good results for beams and walls.

The compressive strength of brickwork, f_c, was taken from the mean uniaxial compression strength of squat piers and the elastic modulus was taken as $600f_c$. As the tensile strength of brickwork f_t was not determined in the investigation it was necessary to look elsewhere for typical values. BS.5628:Part 1 gives the characteristic flexural strengths of 0.4, 0.7 and 0.7 N/mm^2 for brickwork types A, B and C respectively. However for the analysis f_t was based on values obtained from another experimental study [62] that used brickwork types A and B but not type C. For type C, f_t was based on the mean properties of two brick types that had similar compressive strengths and water absorptions. Thus the tensile strength was considered to be a representative value. Details of the material properties used in the analysis are given in Table 6.6.

Initially analyses were carried out using the measured yield strength and an elastic modulus of 200 kN/mm^2 for the reinforcement. However it became clear that this strength was inappropriate because the analyses gave consistently higher ultimate moment capacities than the experimental values. When a yield strength based on the Code characteristic strength was employed much better predictions were obtained. This approximately corresponded to the limit of proportionabilty,

TABLE 6.6 FINITE ELEMENT ANALYSIS OF EXPERIMENTAL WALLS AND BEAMS: MATERIAL PROPERTIES AND RESULTS

Section	Brickwork			Reinforcement		Failure Moment (KNm)	
	f_b N/mm^2	f_t N/mm^2	E_b KN/mm^2	f_s N/mm^2	E_s KN/mm^2	FE*	expt.
Wall 1	16.1	0.92	9.66	425	200	528	412
2	6.9	0.61	4.14	425	200	384	503
3	8.4	0.61	5.04	425	200	216	222
4	16.8	0.92	10.08	425	200	240	221
5	8.1	0.61	4.86	425	200	216	254
6	9.0	0.61	5.40	425	200	216	224
Beam 1	60.2	1.01	36.1	425	200	185+	170
2	11.8	0.61	7.1	425	200	226	240
3	60.2	1.01	36.1	425	200	138	117
4	60.2	1.01	36.1	425	200	136	129
5	60.2	1.01	36.1	425	200	145	123
6	50.3	1.01	30.1	425	200	302	305
7	60.2	1.01	36.1	425	200	470	329
8	21.1	0.92	12.6	425	200	277	264
9	21.1	0.92	12.6	425	200	126	121
10	11.8	0.61	7.1	425	200	126	121
11	11.8	0.61	7.1	425	200	302	281

Notes: + a tolerance of ϕ_F = 0.005 was used to get this result

* finite element analysis where the load given is the last at which convergence was achieved

2100μs, in the reinforcement. The reason for this is probably that the test specimens had limited ductility due to breakdown of the reinforcement-concrete bond near ultimate load which prevented the measured yield stress from being attained. Indeed severe cracking and spalling of the concrete over the reinforcement occurred in the tests.

6.2.2 Serviceability limit state

The analytical load displacement relationship for each beam may be compared with the experimental curves in Figure 5.23. In general the finite element analysis underestimated deflection at high loads particularly for heavily reinforced sections whilst it overestimated deflections at low loads. This behaviour is in accordance with the assumed stress-strain curve for brickwork, Figure4.5 where the elastic modulus is less than the real value at low stresses and at high stresses the reverse applies. However the analytical load displacement relationship was in good agreement with the experimental curve except for beams 12-15 which had short shear spans (a/d=2) and were heavily reinforced The reasons for this are given in section 6.2.1.

For the walls a direct comparison was not made between the experimental and analytical deflections because the experimental values included the effects of base rotation. Since there was good agreement between the analytical and experimental results of the beams it may be assumed that this would have applied for walls had base rotation been excluded. Thus the analytical

displacements of the wall, Figure 6.5 were considered to be representative of the experimental values. Comparison of Figs 5.1 & 6.5 shows that the analytical curves follow the same general trends as the experimental curves.

At the seviceability load, defined in section 6.1.1.1, the analytical span deflection ratios were determined, Table 6.1. For beams the ratios compare favourably with the experimental values . However this did not apply to walls for the reasons outlined above. The analytical results for both walls and beams indicated that pocket-type sections met the proposed serviceabilty requirements of the Draft Code[78]. From Table 6.1 it is clear that method 2 based on the stiffness of a cracked section gave similar results to those obtained using finite element.

6.2.3 Ultimate limit state

The analysis gave good predictions of the ultimate moment capacity for walls 1,3,4 and 6 but relatively poor predictions for walls 2 and 5 where the experimental failure moment was underestimated by 25% and 15% respectively. Walls 2 and 5 were over-reinforced and in each analysis the brickwork started to crush at 60%-70% of the predicted failure moment. Hence it is probable that the brickwork compressive strengths, based on pier results used in these analyses were too low. Similar brickwork was used in walls 3 and 6 and in beams 2,10, and 11 but these had greater compressive strengths. This suggests that the pier test

Figure 6.5 Analytical load displacement relationships of retaining walls

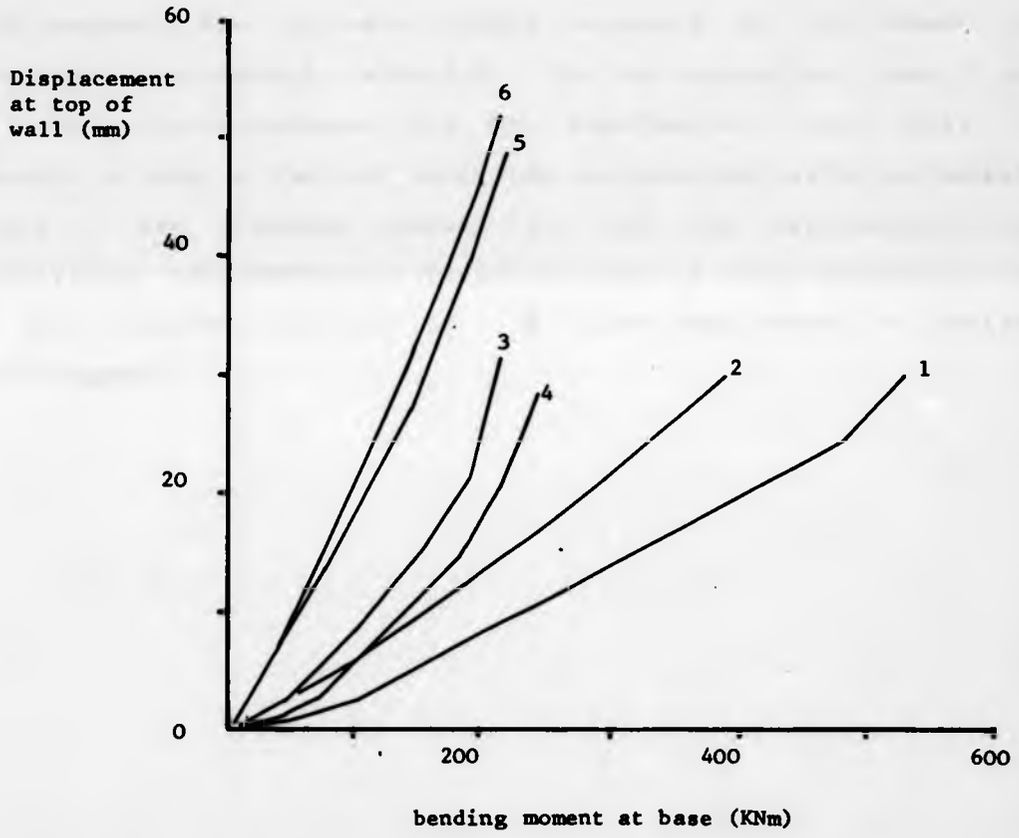

may not give a consistently reliable assessment of compressive strength. For the under-reinforced sections this is of little consequence since the ultimate moment capacity was primarily dependent on the yield stress of the reinforcement; of secondary importance were the compressive strength and elastic modulus of brickwork.

In general the ultimate moment capacity of the beams was predicted accurately, Table 6.6. The two exceptions, beams 7 and 11 were over-reinforced and the experimental beams failed in shear; a mode of failure which the anlysis was unable to detect. Beam 1 was slightly unusual in that the experimental and analytical load-deflection responses were in close agreement, but a much tighter tolerance of ϕ =0.005 was needed to achieve convergence.

7. PARAMETRIC SURVEY

7.1 General

In the previous chapter it has been shown that the results of the finite element analysis of pocket-type walls were in good agreement with the experimental results. However it was not possible to undertake an extensive experimental study because of the cost.

Non-linear finite element analysis was employed to carry out a parametric survey into the behaviour of pocket-type retaining walls. The variables selected for examination included pocket spacing, slenderness, section type (flanged or rectangular) and arching action of the brickwork panels. It is recognised that results given below are qualitative rather than quantitative since the analysis is a numerical procedure. It is unable to take into account out of plane shear stresses and it is confined to isotropic material properties. These aspects are considered to have little or no effect on the conclusions since out of plane shear failure was not observed in the experimental results of the walls but only with very heavily reinforced beams.

7.2 Procedure

Pocket walls were designed according to the Draft Code recommendations outlined in section 2.3. Each wall was designed to resist a triangular pressure distribution as might be

generated by a dry cohesionless soil. For the majority of walls a soil of specific density 18kN/m^3 and a 30^o angle of repose gave the requisite load . The exceptions were walls 1-4, 17-20, which were designed to retain a metalic ore of specific density 42.6 kN/m^3 and a 30^o angle of repose. A partial safety factor, γ_f of 1.6 was applied to the loads. For the design of the section the partial safety factors applied to the material strengths were for steel γ_{ms} = 1.15 and for brickwork γ_{mm} = 2.0. Hence the global safety factor was approximately $\gamma_f \gamma_{ms}$ or 1.84 for under-reinforced sections and γ_f x γ_{mm} or 3.2 (for over-reinforced sections).

Yield line analysis[84] was used to design the unreinforced panels that spanned between the pockets and off the base. The assumptions and equations for the loading conditions, are given in Appendix A3. The validity of applying yield line analysis to unreinforced brickwork is subject to debate[85] . However Haseltine and Moore[64] state that it forms the basis of design for uniformly loaded brickwork panels to BS.5628:Part 1[29]. Furthermore they indicated that it gave results which were compatible with experimental results. Thus by extending this argument it was thought that yield line analysis may also be applied to the design of panels subjected to a triangular pressure distribution.

The material strengths were chosen to be representative of those likely to be used in practice. Brickwork of medium compressive stength, f_k=15 N/mm^2, and a tensile strength f_t=1.0 N/mm^2

and steel reinforcement of yield strength f_y=425 N/mm^2 was adopted for the analyses. Linear elastic-plastic stress-strain characteristics were assumed for both brickwork and reinforcement, Figure 4.4. & 4.7 respectively.

Brickwork was assumed to obey the square yield criterion, Figure 4.6. Since there were large areas of unreinforced brickwork a non-tension stiffening response was included. For each analysis the element discretisation and load arrangement shown in Figure 7.1 was adopted. The triangular pressure distribution was approximated by a series of point loads applied at the levels indicated. Note that symmetry was invoked and only one half of the panel and one half of the pocket was analysed.

7.3 Results

In all 41 walls were analysed. Their dimensions and material properties are given in Table 7.1. For the purposes of determining the aspect ratio, α, (height to length ratio) of a panel the length was taken as the distance between the centreline of the pockets, l_p, Figure 7.1. Some additional analyses were undertaken to clarify certain issues raised by the survey. Details of these are given within the appropriate section of text.

A summary of the results is given in Table 7.2. The design moment at the base of the wall, M_d was made equal to the moment

Figure 7.1 Element discretisation and loading arrangement.

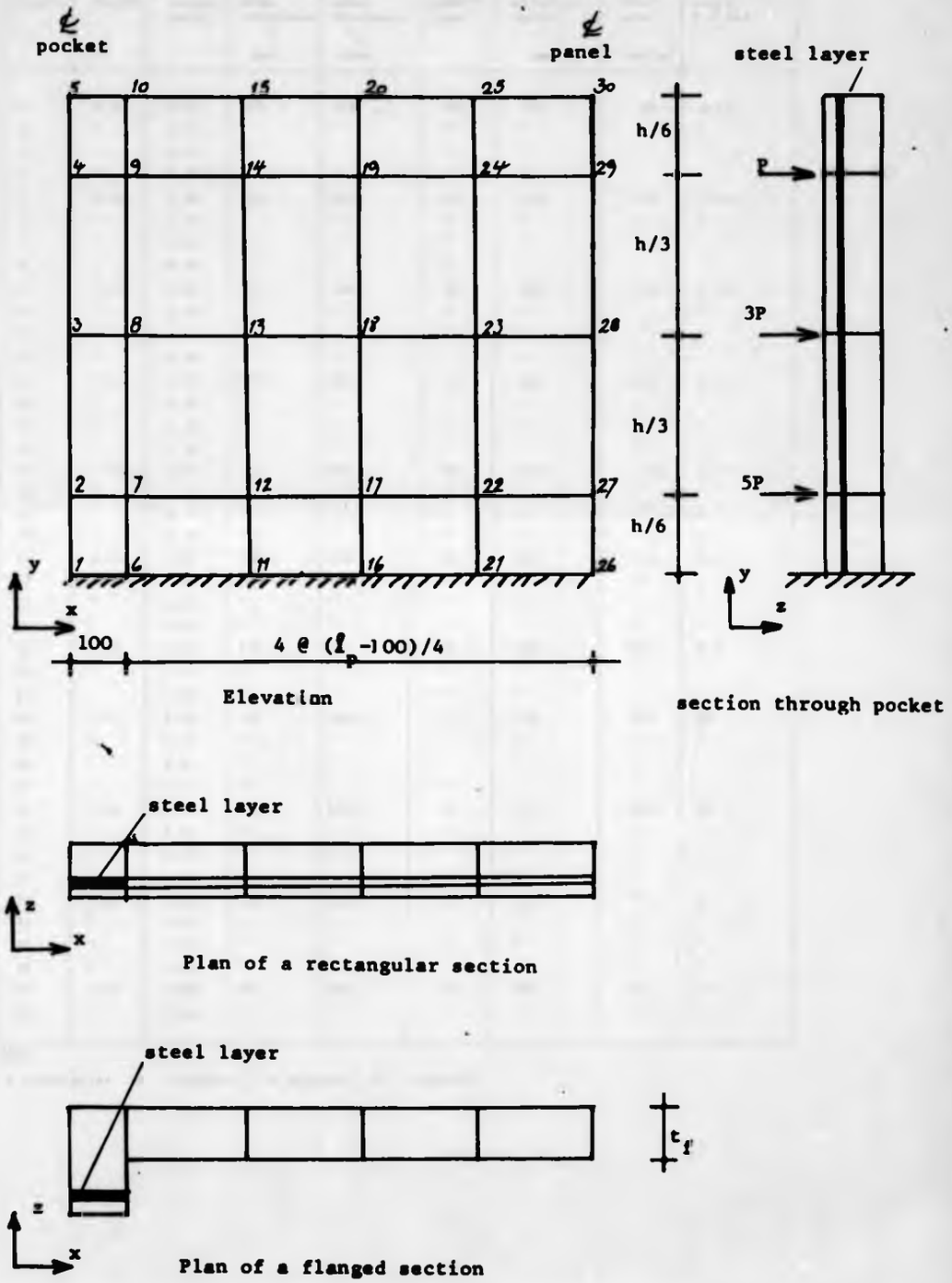

TABLE 7.1 DETAILS OF PARAMETRIC SURVEY.

Analysis No	Height (m)	Aspect ratio	stem thickness t (mm)	panel thickness t_f (mm)	panel* type	effective depth (mm)	steel area (mm^2/m)	steel $\Sigma A_s/bd$
1	2.25	2.25	215	215	RI	170	782	0.46
2	"	1.12	"	"	"	"	"	"
3	"	0.75	"	"	"	"	"	"
4	"	0.50	"	"	"	"	"	"
5	3.00	3.00	215	215	RI	170	782	0.46
6	"	1.00	"	"	"	"	"	"
7	"	0.66	"	"	"	"	"	"
8	"	0.50	"	"	"	"	"	"
9	3.00	3.00	330	330	RI	280	439	0.15
10	"	1.50	"	"	"	"	"	"
11	"	1.00	"	"	"	"	"	"
12	"	0.66	"	"	"	"	"	"
13	4.5	4.50	330	330	RI	280	1657	0.59
14	"	2.25	"	"	"	"	"	"
15	"	1.50	"	"	"	"	"	"
16	"	1.00	"	"	"	"	"	"
17	2.25	2.25	215	215	RE	170	782	0.46
18	"	1.12	"	"	"	"	"	"
19	"	0.75	"	"	"	"	"	"
20	"	0.50	"	"	"	"	"	"
21	3.00	3.00	330	330	RE	280	439	0.15
22	"	1.50	"	"	"	"	"	"
23	"	1.00	"	"	"	"	"	"
24	"	0.66	"	"	"	"	"	"
25	4.50	4.50	330	330	RE	280	1657	0.59
26	"	1.50	"	"	"	"	"	"
27	"	1.00	"	"	"	"	"	"
20	2.25	2.25	215	102.5	FI	170	920	NA
29	"	0.75	"	"	"	"	"	"
30	"	0.50	"	"	"	"	"	"
31	"	0.37	"	"	"	"	"	"
32	3.00	3.00	215	102.5	FI	170	920	NA
33	"	1.00	"	"	"	"	"	"
34	"	0.66	"	"	"	"	"	"
35	"	0.50	"	"	"	"	"	"
36	3.00	3.00	330	215	FI	280	556	NA
37	"	1.00	"	"	"	"	"	"
38	"	0.66	"	"	"	"	"	"
39	"	0.50	"	"	"	"	"	"
40	3.00	3.00	330	102.5	FI	280	508	NA
41	"	1.00	"	"	"	"	"	"

Note:

R = rectangular F = flanged I = interior E = exterior

TABLE 7.2 RESULTS OF PARAMETRIC SURVEY.

Analysis No.	M_d (KNm)	M_{panel} (KNm)	Finite element analysis			$\frac{M_{FE}}{M_d}$
			M_{yield} (KNm)	M_{ult} (KNm)	failure mode	
1	49.7	250	63	71	T+C	1.27
2	99	164	95	106	T+C	0.96
3	149	140	-	101	P	0.66
4	224	134	-	46	P	0.20
5	49.7	-	61	74	T	1.23
6	99	207	111	> 127	T+C	1.11
7	149	183	179	179	T+C	1.20
8	224	178	-	57	P	0.26
9	49.7	-	63	116	T	1.27
10	99	596	112	140	T	1.12
11	149	488	190	853	T	1.27
12	224	433	-	190	P	0.84
13	168	-	211	211	T+C	1.27
14	335	1180	401	401	T+C	1.19
15	503	894	720	720	T+C	1.43
16	745	732	-	470	P	0.63
17	49.7	156	-	31.6	P	0.63
18	99	101	-	42.7	P	0.43
19	149	91	-	50	P	0.33
20	224	86	-	46	P	0.20
21	49.7	-	63	116	T	1.27
22	99	370	-	84	P	0.84
23	149	305	-	95	P	0.63
24	224	280	-	152	P	0.67
25	168	-	211	211	T+C	1.25
26	503	555	-	216	P	0.43
27	745	458	-	234	P	0.31
28	49.7	57	-	71	C	1.42
29	149	32	-	50	P	0.33
30	224	30	-	39, 9	P	0.18
31	298	29	-	34.0	P	0.11
32	49.7	-	-	74	C	1.48
33	149	47	-	74	C+P	0.50
34	224	42	-	49.1	P	0.22
35	298	40	-	45.3	P	0.15
36	49.7	-	127	137	T+C	2.54
37	149	207	-	284	C	1.90
38	224	183	-	180	P	0.80
39	298	178	-	216	P	0.72
40	49.7	-	101	101	T+C	2.03
41	149	47	-	130	P	0.88

* T = steel yield C = brickwork crushing P = panel failure

of resistance of the stem using eqns (2.1)-(2.3) for rectangular sections and eqns (2.4) and (2.5) for flanged sections. This may be compared with the yield moment, M_y and the ultimate moment, M_{ult} as determined from the finite element analysis, where M_y is the moment at the base when the steel started to yield; M_{ult} is the highest moment at the base at which convergence was achieved. In some analyses there was considerable ductility between yield and collapse. This is contrary to practical experience where other factors such as breakdown of the reinforcement-concrete bond occurs which severely restricts ductility. For this reason the analytical collapse moment M_{fe} was assumed to be the lesser of M_y and M_{ult}. In practice M_{fe} was equal to M_y only when steel yield occurred prior to collapse. The moment of resistance of the panels was determined from the yield line approach outlined in Appendix A3. This was converted to the equivalent moment at the base of the wall M_{panel} and is given in Table 7.2.

The majority of walls were designed to develop flexural failure of the stem before panel failure occurred; that is M_{panel} was designed to be greater than M_d. Finite element analysis indicated that this may not apply in some cases. Reasons for this are discussed below.

7.3.1 Rectangular sections

A pocket-type retaining wall will contain many panels of brickwork spanning between the pockets, Figure 7.2. The interior

Figure 7.2 Types of panels in pocket wall

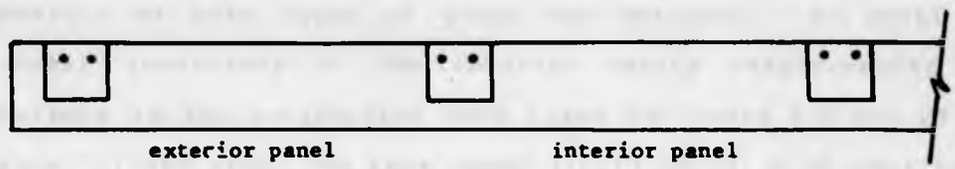

Figure 7.3 Arching action.

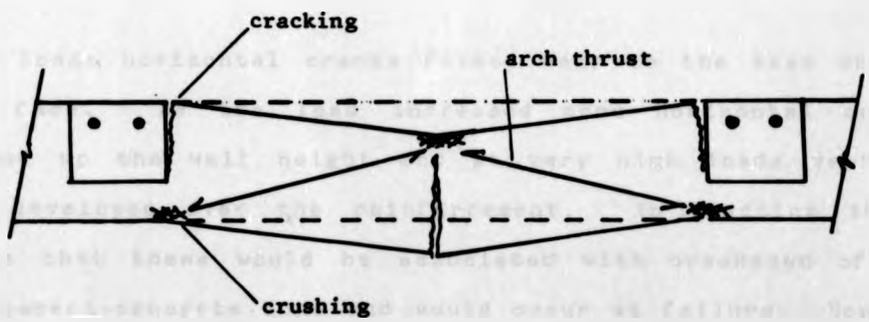

panels may be expected to arch between the pockets since the adjacent panels should provide buttressing resistance Figure 7.3. For the exterior panels or those adjacent to a movement joint this does not apply and it is unlikely that the end pocket will have sufficient inplane stiffness to resist arching forces. The behaviour of both types of panel was analysed. To model the boundary conditions of the interior panels displacements and rotations in the x-direction were fixed for nodes 2-5 and 27-30, Figure 7.1 and along the base nodes 1,6,11,16,21, & 26 were fully fixed. For exterior panels symmetry does not exist because the end pocket has no restraint whilst the interior pocket has inplane restraint. Thus to model it correctly the whole panel needs to be analysed. For simplicity the exterior panel was assumed to be symmetrical with zero end restraint, hence the same conditions apply as for interior panels, with the exception that nodes 2-5 were free. This is considered to be a conservative approach.

7.3.1.1 Interior panels.

At low loads horizontal cracks formed near to the base on the loaded face. As the load increased more horizontal cracks developed up the wall height and at very high loads vertical cracks developed over the reinforcement. In practice it is probable that these would be associated with breakdown of the reinforcement-concrete bond and would occur at failure. However in the analysis collapse occurred when either the stem or the panel failed in flexure. Stem failure was either due to

brickwork crushing, usually in the immediate vicinity of the pocket or due to the reinforcement reaching its yield stress. Occasionally both events occurred simultaneously. When the brickwork was highly stressed but before crushing vertically inclined cracks formed over the pocket, close to the base on the unloaded face. These were also present when panel failure occurred. Unfortunately the analysis was unable to follow the cracking sequence up to collapse. To achieve this displacement control rather than load control is required.

Figure 7.4 shows profiles of relative lateral displacement of a typical interior panel prior to collapse of the panel. At each height the relative displacement was evaluated as the difference between displacement at the point under consideration and displacement at the centreline of the pocket . From the profiles it is clear that the panel acted as if it were fixed at the pocket for the full height. The greatest relative displacements occurred in the lower part of the wall and it is probable that this is associated with the load distribution.

The results of the analyses of the interior panels are compared by using a non-dimensional parameter, form in Figure7.5. When the moment ratio, M_{fe}/M_d, is greater than unity the analytical results indicate that the Code is conservative. For convenience the results were grouped together according to their slenderness ratio and percentage of tensile reinforcement. It is clear that both these parameters had a small effect on the relative strength of the walls. However the greatest effect was

Figure 7.4 Deflection profiles at various heights for a typical interior panel.

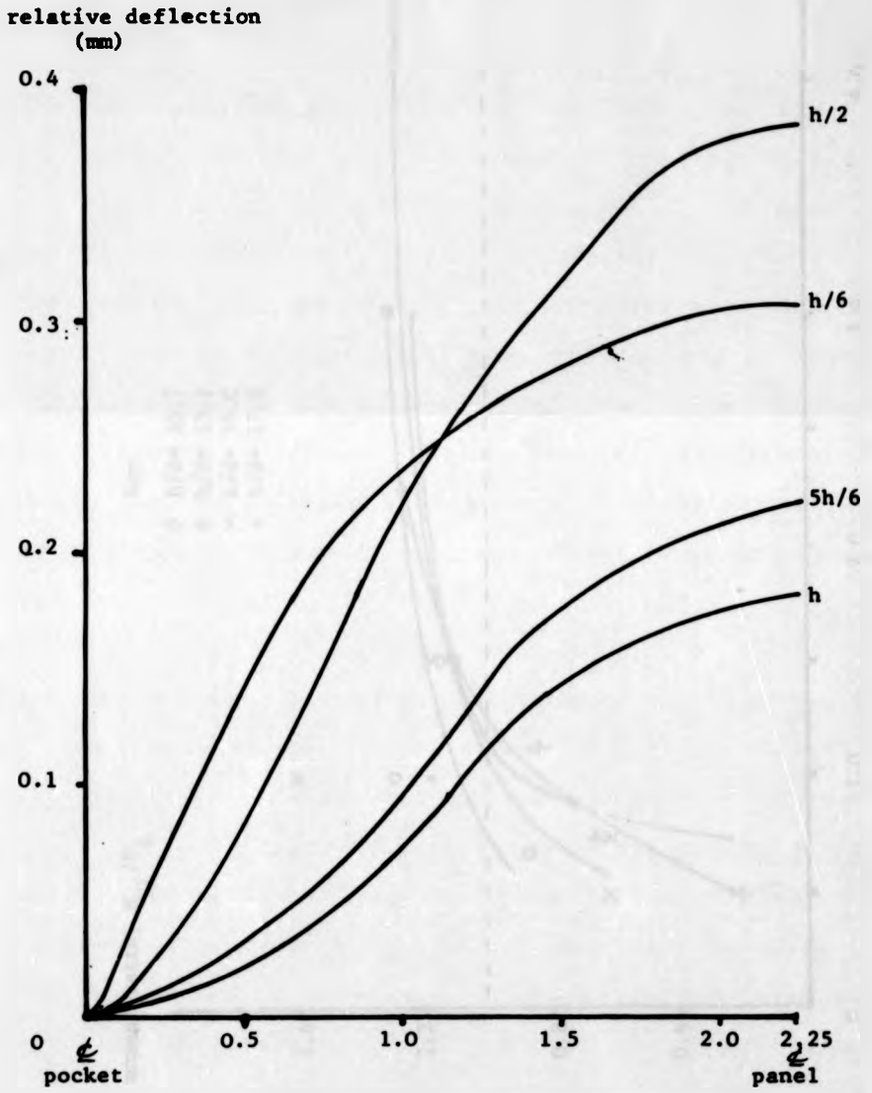

Figure 7.5 Moment ratio vs aspect ratio for interior panels.

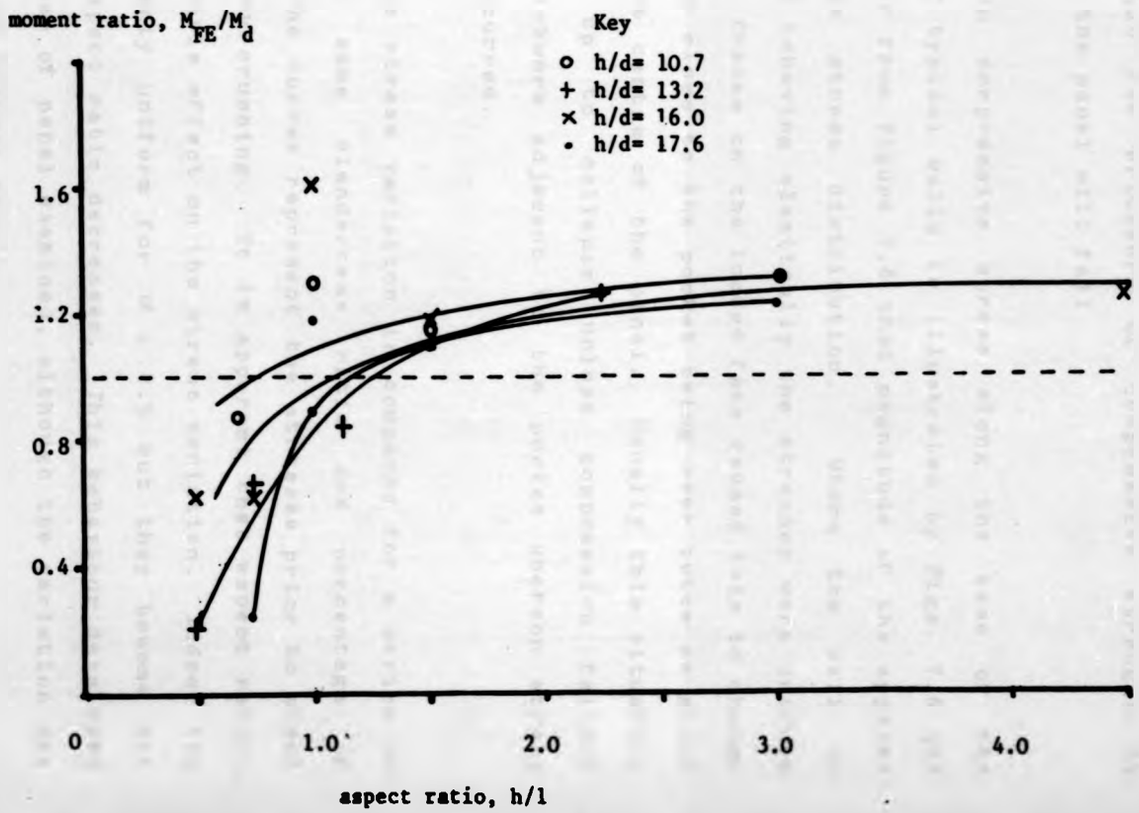

exerted by the aspect ratio, α, of the panel. Indeed the results indicate that for the design moment capacity of the reinforced pocket, M_d, to be reached or exceeded the aspect ratio must be greater than 1.25 for brickwork of compressive strength 15 N/mm^2, otherwise the panel will fail.

The variation in compressive stress along the base of the unloaded face of typical walls is illustrated by Figs. 7.6 and 7.7. It is clear from Figure 7.6 that magnitude of the applied load affects the stress distribution. Where the wall is uncracked and is behaving elastically the stresses were uniform along the wall. Cracks on the loaded face caused this to change with the stresses close to the pocket being over twice as great as those near the centre of the panel. Usually this situation was maintained up to collapse unless compression failure developed in brickwork adjacent to the pocket whereon stress redistribution occurred.

In Figure 7.7 the stress variation is compared for a series of walls with the same slenderness ratio and percentage of reinforcement. The curves represent the stresses prior to steel yield or brickwork crushing. It is apparent that aspect ratio, α, has a considerable effect on the stress variation. Indeed the stresses are nearly uniform for α = 4.5 but they become non uniform as the aspect ratio decreases. This behaviour developed for all thicknesses of panel examined, although the variation was more pronounced for thinner panels.

figure 7.6 A typical example of the variation in compressive stress along the wall base

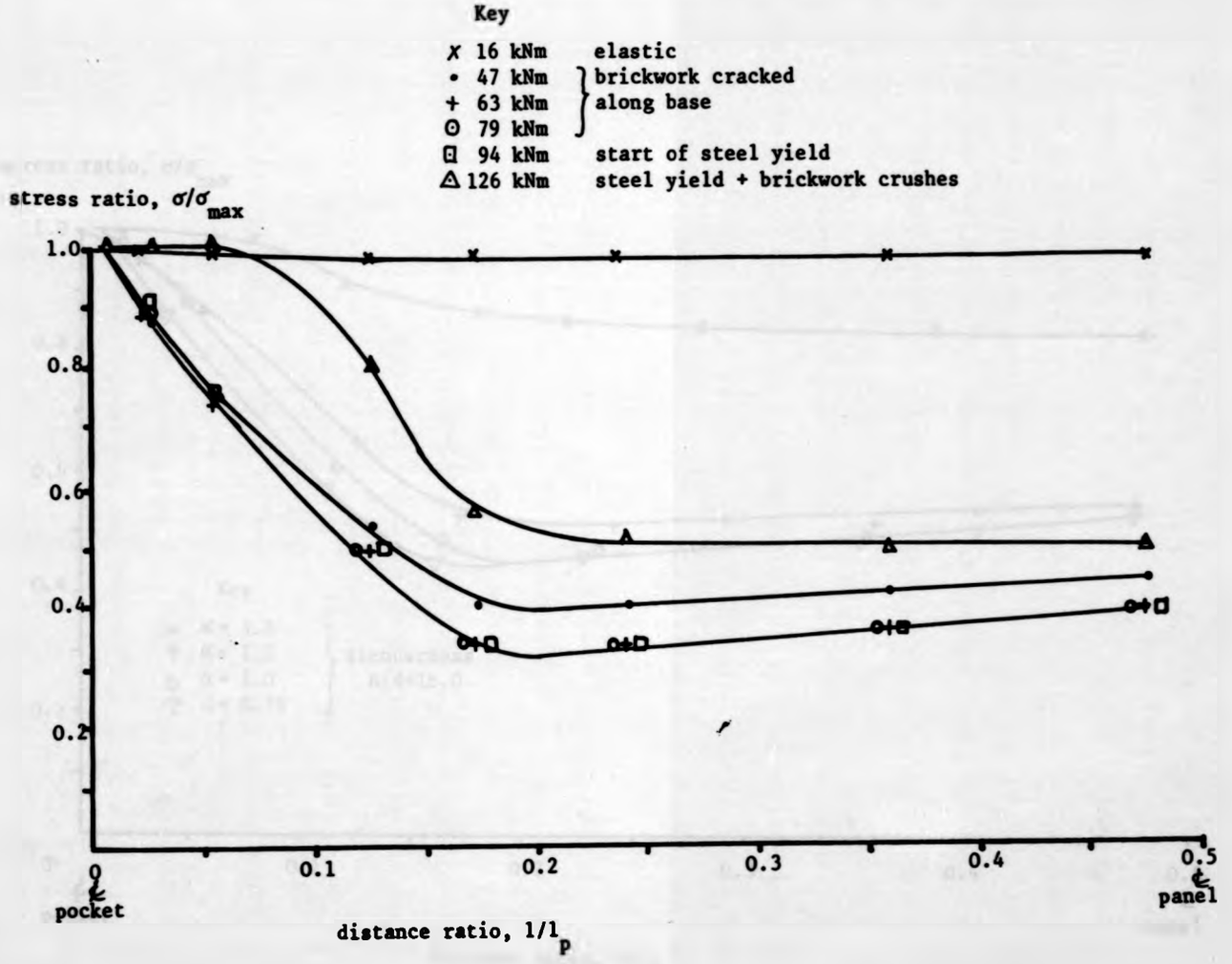

Figure 7.7 Variation of compressice stress along the base for a series of walls.

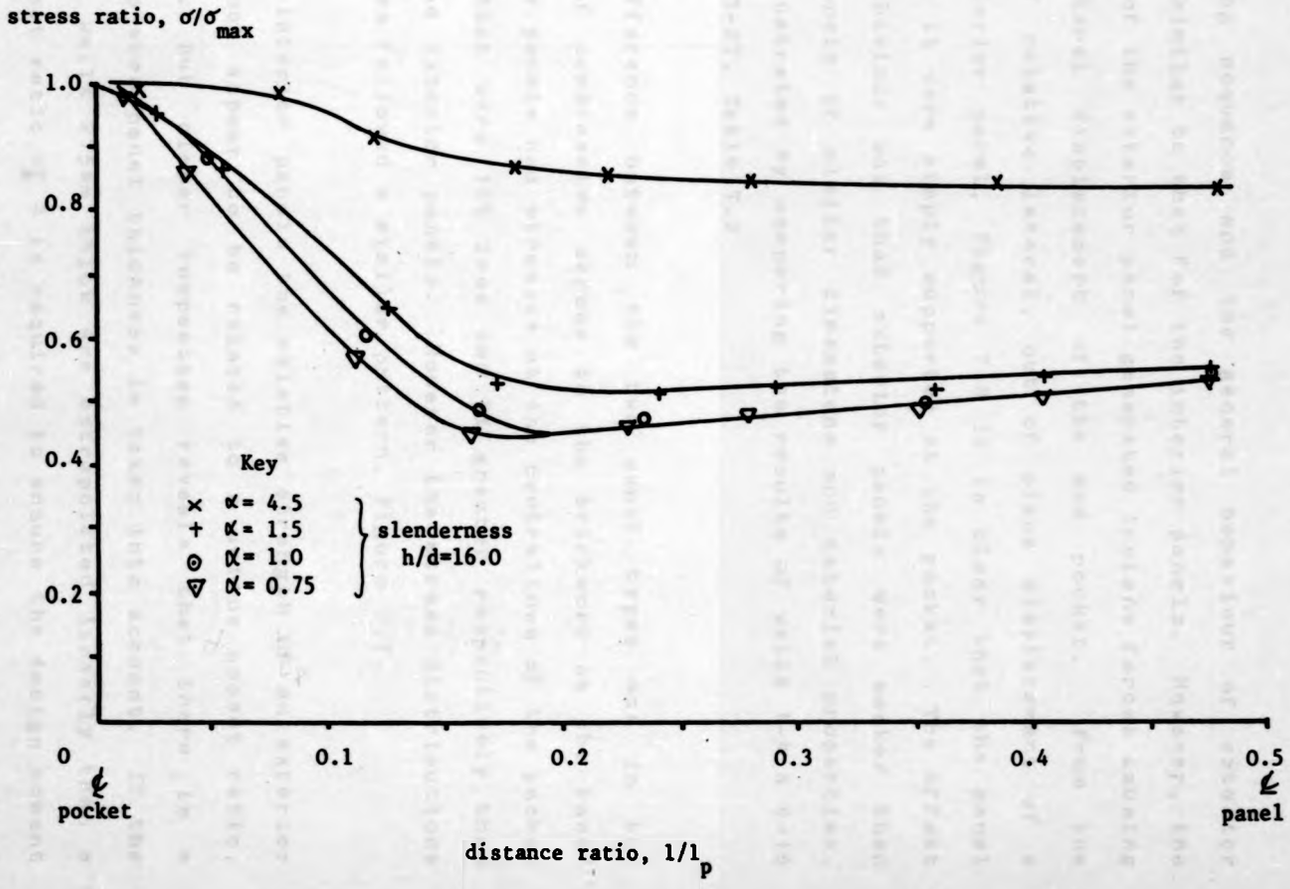

7.3.1.2 Exterior panels

The cracking sequence and the general behaviour of exterior panels was similar to that for the interior panels. However, the deflection of the exterior panel generated inplane forces causing inplane lateral displacement of the end pocket. From the profiles of relative lateral, out of plane displacement of a typical exterior panel, Figure 7.8 it is clear that the panel acted as if it were simply supported at the pocket. The effect of this behaviour was that exterior panels were weaker than interior panels of similar dimensions and material properties. This is illustrated by comparing the results of walls 1-4 & 9-16 and walls 17-27, Table 7.2

Another difference between the two panel types was in the magnitude of compressive stress in the brickwork at the base. The interior panels had stresses at the centrelines of the pocket and panel that were 15% less and 5% greater respectively than those in the exterior panels. However the stress distributions of both types followed a similar pattern, Figure 7.7.

Unlike the interior panels the relative strength of an exterior panel did not appear to be related to a unique aspect ratio, Figure 7.9. But closer inspection reveals that there is a relationship when panel thickness is taken into account. If the results for walls 215mm thick are extrapolated linearly then a minimum aspect ratio of 4 is required to ensure the design moment is reached. For 327mm thick walls, the minimum ratio is 2.5.

Figure 7.8 Deflection profiles at various heights for a typical exterior wall.

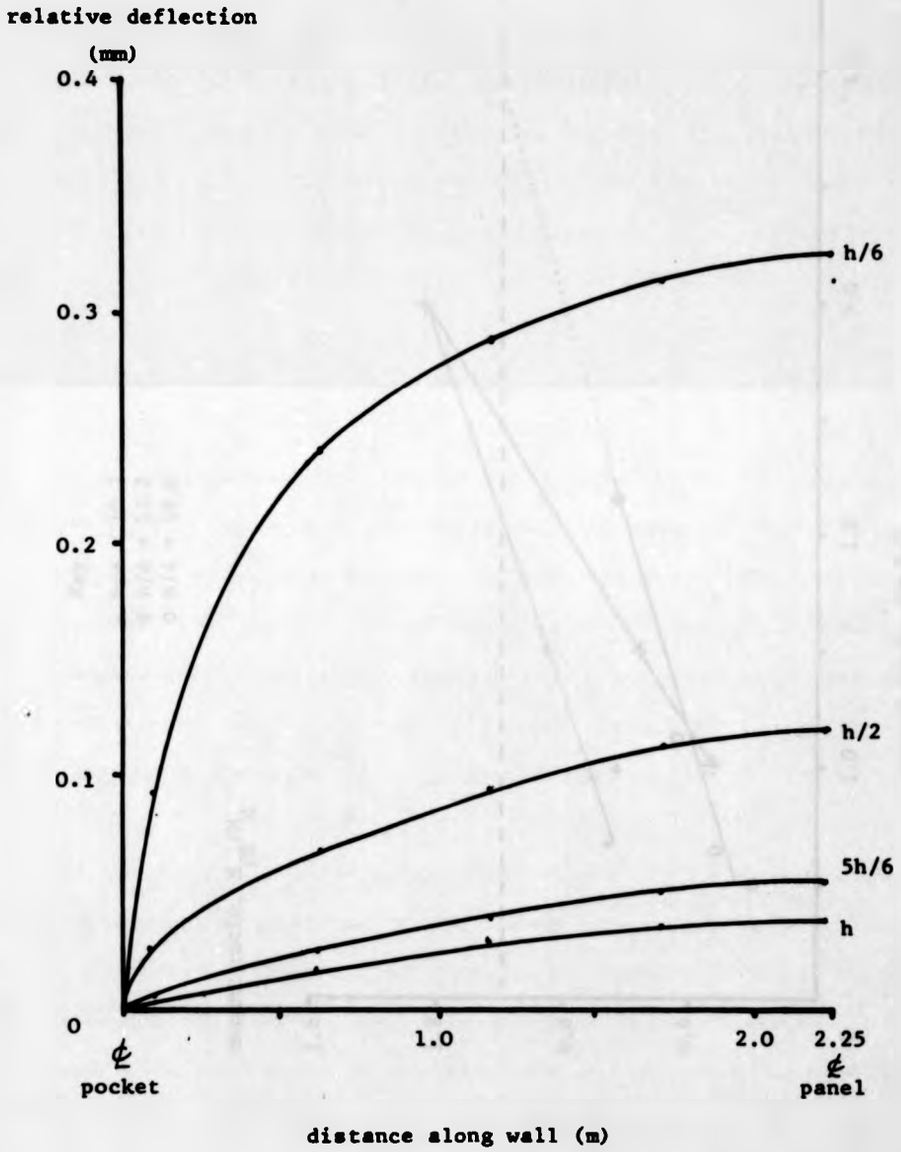

Figure 7.9 Moment ratio vs aspect ratio for exterior panels.

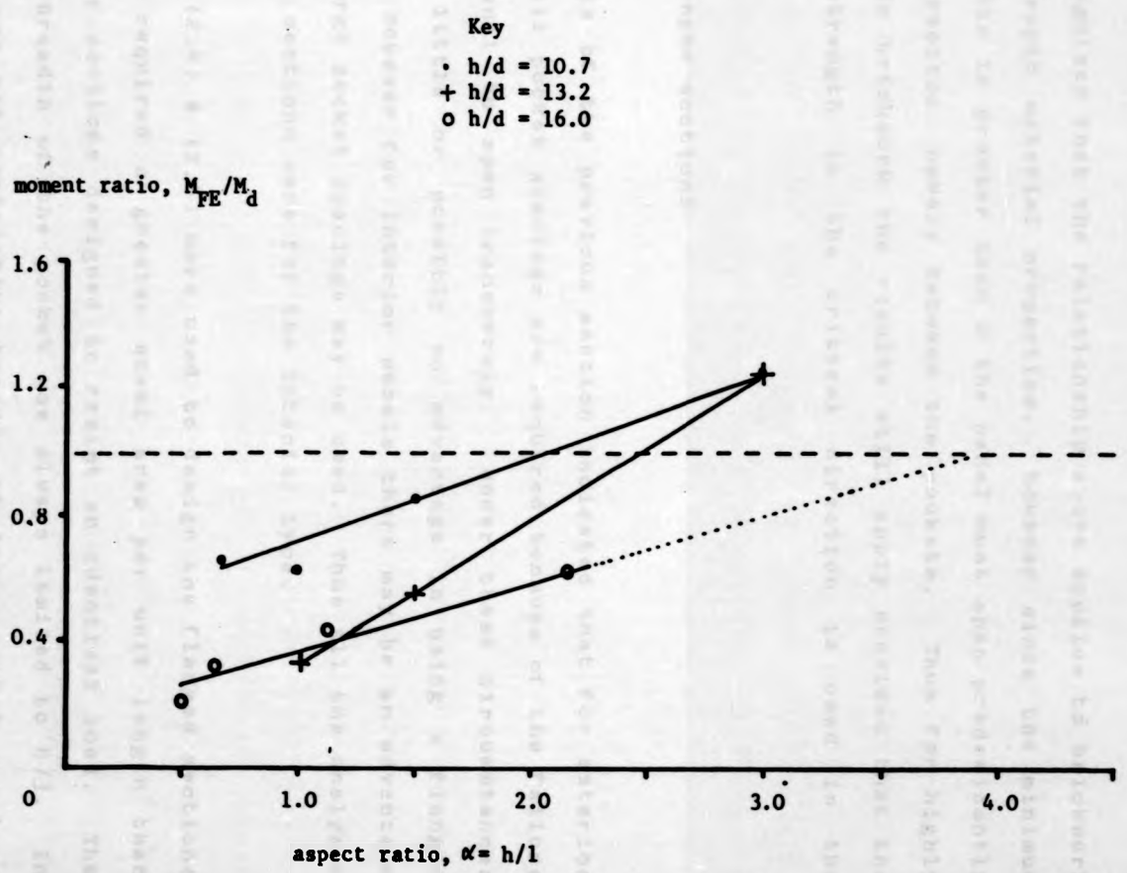

Figure 7.9 Moment ratio vs aspect ratio for exterior panels.

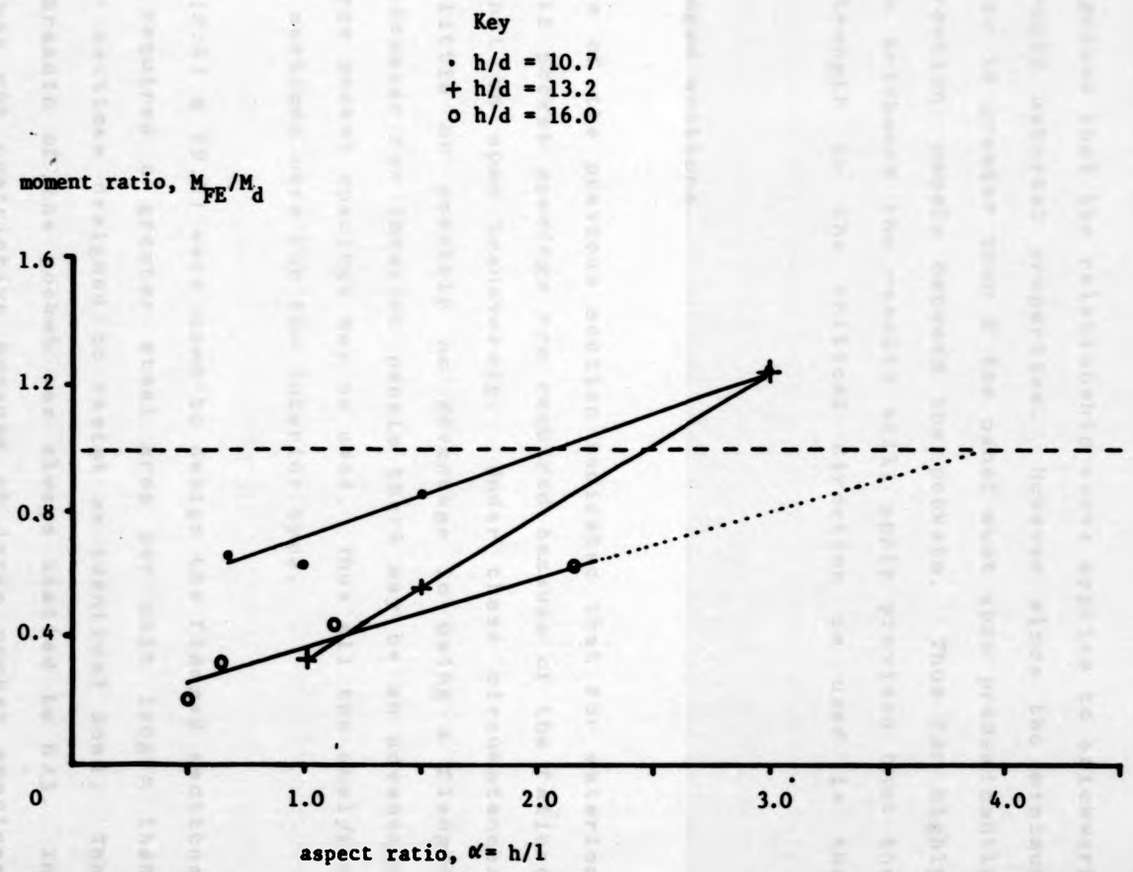

Thus it appears that the minimum aspect ratio is inversely proportioned to panel thickness for brickwork of a particular tensile strength. Slenderness has only a minor effect.

It is recognised that the relationship above applies to brickwork with isotropic material properties. However since the minimum aspect ratio is greater than 2 the panel must span predominantly in one direction, namely between the pockets. Thus for highly anisotropic brickwork the results still apply provided that the tensile strength in the critical direction is used in the analysis.

7.3.2 Flanged sections

The results of the previous section indicated that for exterior panels small pocket spacings are required because of the failure of the panel to span transversly. Under these circumstances there is little or possibly no advantage in using a flanged section. However for interior panels there may be an advantage because large pocket spacings may be used. Thus all the analyses on flanged sections were for the interior type.

Equations (2.4) & (2.5) were used to design the flanged sections and these required a greater steel area per unit length than rectangular sections designed to resist an identical load. The effective breadth of the pocket was always limited to h/3. In fact this was not restrictive because at large pocket spacings panel failure occurred before the brickwork crushed, Table 7.2.

Where crushing occurred the failure moment, M_{fe} , was close to or greater than the design moment. Hence the Draft Code design method is conservative. For brickwork with a lower compressive strength this may not apply.

Another aspect of the Code design method is that it is idiosyncratic for under-reinforced sections since a reduction in the flange thickness will lead to a reduction in the steel area for a given design moment. For instance compare walls 36 & 37 with 40 & 41 in Table 7.1. This anomaly arises because the lever arm is dependent on the flange thickness and effective depth with no account taken of material strengths. In practice this usually leads to an underestimate of the lever arm and thus it is a conservative design approach.

Presented in Figure 7.10 are the analytical results for flanged sections. These were grouped according to their slenderness ratio, panel thickness and percentage of tensile reinforcement. For each group the minimum aspect ratio required to ensure the design moment is reached was noted. Unlike interior panels in a rectangular section there was no definitive minimum aspect ratio. The reason for this is that the vertical or longitudinal shear stresses were great enough to cause cracks to form along the pocket boundary which lead to premature flexural failure of the panel. In addition walls which are very slender with low aspect ratios fail by localised crushing of the brickwork in the vicinity of the pocket.

Figure 7.10 Moment ratio vs aspect ratio for flanged sections.

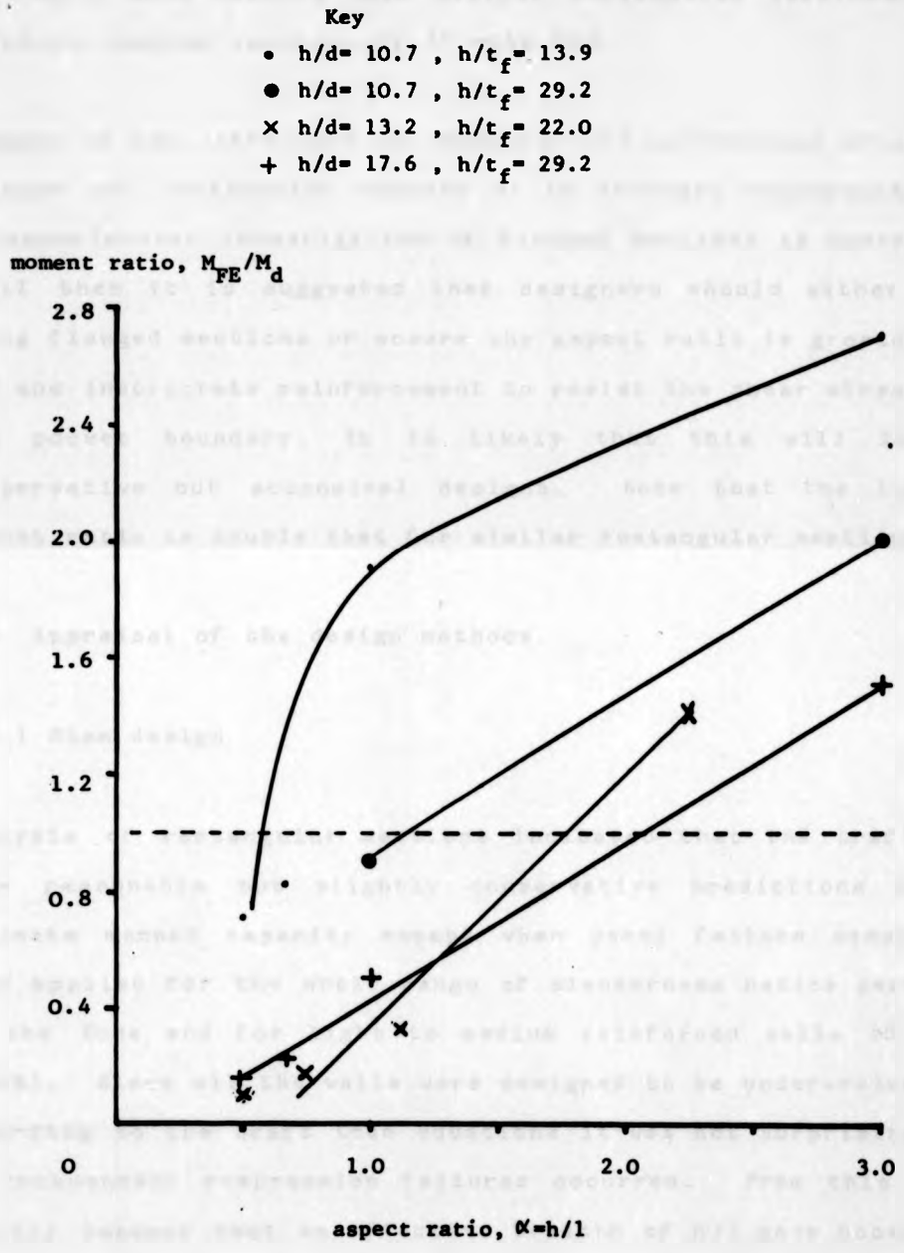

These results for flanged sections indicate that panel failure may occur more readily than similar rectangular sections. For instance compare analyses 32-35 with 5-8.

Because of the difference in behaviour and performance of similar flanged and rectangular sectons it is strongly recommended that an experimental investigation of flanged sections is undertaken. Until then it is suggested that designers should either avoid using flanged sections or ensure the aspect ratio is greater than 2.5 and incorporate reinforcement to resist the shear stresses at the pocket boundary. It is likely that this will lead to conservative but economical designs. Note that the limiting aspect ratio is double that for similar rectangular sections.

7.4 Appraisal of the design methods

7.4.1 Stem design

Analysis of rectangular sections indicated that the Draft Code gave reasonable but slightly conservative predictions of the ultimate moment capacity except when panel failure occurred . This applied for the whole range of slenderness ratios permitted by the Code and for light to medium reinforced walls (0.15% - 0.60%). Since all the walls were designed to be under-reinforced according to the Draft Code equations it was not surprising that no independent compression failures occurred. From this it is tacitly assumed that an effective breadth of h/3 gave acceptable results for sections with light to medium quantities of

reinforcement. This may not apply for more heavily reinforced sections.

In the majority of cases the analysis of flanged sections indicated that collapse of the panel occurred. But flexural failure of the stem usually developed when the aspect ratio of the panel was greater than 2.5. Of the flexural failures several were due to localised crushing of the brickwork at the base of the stem, although according to the Draft Code these were all under- reinforced. However the Code was always very conservative because the lever arm was greatly underestimated.

Presented in Figures 7.11 & 7.12 are the load-deflection responses of several series of walls, each with a different slenderness ratio. Deflection is expressed in non-dimensional terms where the denominator Δ_{serv} is the Code serviceability limit on deflection (=h/80). For design purposes the serviceability moment Δ_{serv} was defined as the design moment divided by the product of the relevant partial safety factors for load and material. Since the sections were under-reinforced then eqn. (7.1) applied.

$$M_{serv} = \frac{M_d}{\gamma_{ms}\gamma_f} \qquad \ldots.(7.1)$$

The analysis indicated that pocket-type construction easily meets the serviceability deflection requirements of the Draft Code.

Figure 7.11 Deflection ratio vs moment ratio for a series of walls of slenderness h/d = 13.2.

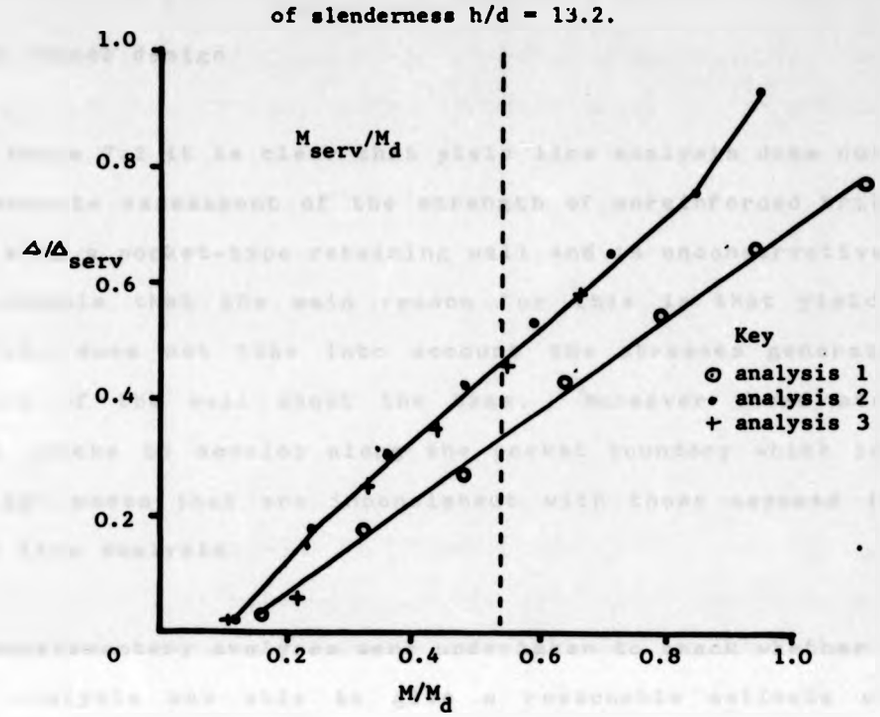

Figure 7.12 Deflection ratio vs moment ratio for a series of walls of slenderness h/d = 17.6.

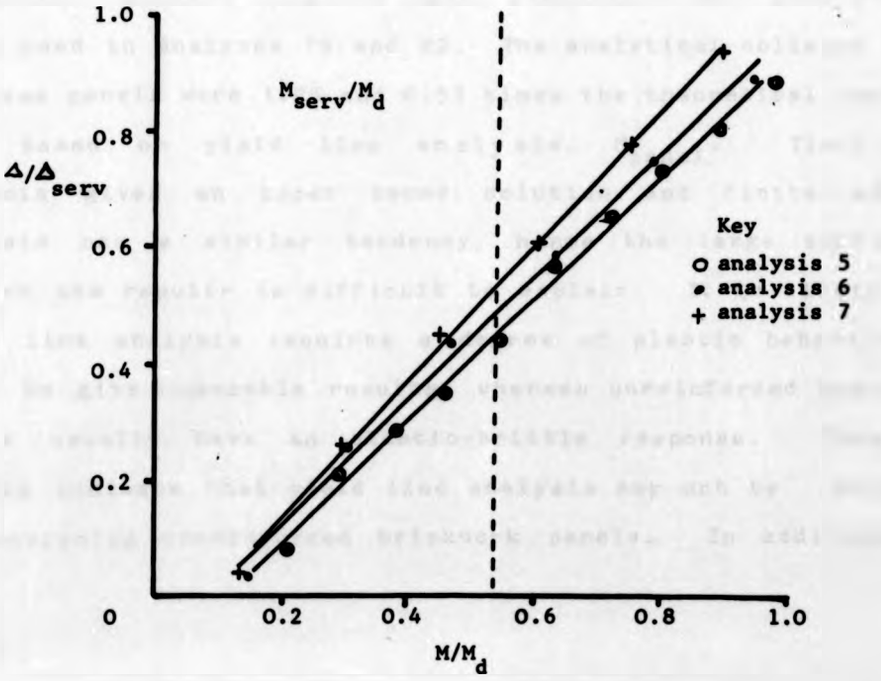

7.4.2 Panel design

From Table 7.2 it is clear that yield line analysis does not give an accurate assessment of the strength of unreinforced brickwork panels in a pocket-type retaining wall and is unconservative. It is probable that the main reason for this is that yield line analysis does not take into account the stresses generated by flexure of the wall about the base. Moreover these stresses cause cracks to develop along the pocket boundary which induces collapse modes that are inconsistent with those assumed in the yield line analysis.

Two supplementary analyses were undertaken to check whether yield line analysis was able to give a reasonable estimate of the strength of unreinforced brickwork panels. These had simple supports at the edge and were fixed at the base. Material properties, applied load and panel dimensions were identical to those used in Analyses 19 and 22. The analytical collapse loads of these panels were 1.25 and 0.51 times the theoretical collapse load based on yield line analysis, M_{panel}. Yield line analysis gives an upper bound solution and finite element analysis has a similar tendency, hence the large difference between the results is difficult to explain. It is likely that yield line analysis requires a degree of plastic behaviour in order to give reasonable results, whereas unreinforced brickwork panels usually have an elastic-brittle response. Thus the results indicate that yield line analysis may not be suitable for analysing unreinforced brickwork panels. In addition the

results confirm that flexure of the panel about the base causes a reduction in the strength, which in these cases was by a factor of 2.25. This may be of considerable importance in the design of unreinforced panels which are built into portal frame structures that sway thus these type of panels merit a detailed investigation. However this is outside the scope of the present investigation.

For interior panels an alternative design approach is to assume that they arch between the pockets and to design them in accordance with cl. 36.4.4 BS.5628:Part 1[29] . By inspection this approach also will be unsatisfactory since the collapse mode is not consistent with the arching mechanism, although small arching forces did develop.

It is clear that at present panels in pocket-type construction cannot be designed satisfactorily . But this should not deter designers since it has been shown that rules for the sizing of panels can be derived from the analysis for a given set of material properties and loading. Obviously much development work still needs to be done and experimental confirmation is required.

7.5 Design recommendations

The recommendations below are based solely on the results of the parametric survey. As such they are qualitative and they require experimental verification . Since the survey was confined to one type of brickwork with medium tensile and compressive strengths

care must be taken if these recommendations are applied to brickwork with different properties.

1. The reinforced stem should be designed to cantilever from the base and transmit all the load on the pocket wall to the base.

2. The effective width of the stem should be taken as the lesser of h/3 or l_p.

3. Brickwork panels should not be designed using yield line analysis or for arching action but should follow the sizing given below.

4. Exterior panels should be part of a rectangular section and have an aspect ratio greater than 2.5 and 4 for wall thicknesses 330mm and 215mm respectively.

5. Interior panels that are part of a rectangular section should have an aspect ratio greater than 1.25. This applies for walls of any slenderness.

6. Preferably flanged sections should be analysed by non-linear finite element technique. If this is not practical then the interior panels should have an aspect ratio greater than 2.5 . If lower aspect ratios are deemed necessary then reinforcement should be provided to prevent shear failure along the pocket panel boundary. Flanged sections are not normally considered to be suitable for exterior panels.

8. SUMMARY, CONCLUSIONS AND SUGGESTIONS FOR FURTHER WORK

8.1 Summary and conclusions

From the literature survey it is clear that reinforced brickwork pocket-type retaining walls are a well established form of construction in the USA, however only a small number have been built in the UK. This is surprising since cost studies have consistently indicated that pocket-type construction is more economical than fair-faced reinforced concrete walls. Over the last decade much information regarding the design of reinforced brickwork has been published, but perhaps the most important publication has been the Draft Code for Reinforced Masonry[3]. Its recommendations concerning pocket-type construction have been examined in relation to the results of an experimental research programme.

Two inconsistencies in the Draft Code requirements relating to the shear and flexural design equations were found. Both the breadth and flange thickness are defined ambiguously. The proposed remedy is to define the former as the effective width and the latter as the thickness of masonry between the ribs. Further aspects of the Draft Code are considered below.

The method and results of an experimental research programme into the structural performance of pocket-type constructions is described. In all six full size walls were tested, all of which failed in flexure either due to yielding of the steel or the

brickwork crushing but with no signs of shear failure. Although horizontal arching between the reinforced pockets was expected there was no indication that this took place. It was noted that the relationship between bending moment and shear force affects the behaviour of the wall in a similar manner to shear span ratio in beams. More work is required on this aspect since it could have important consequences in the design of retaining walls supporting mechanically compacted fill or surcharge loads.

In addition fifteen beams were tested, all of which failed either by yielding of the steel or in shear. Although there were no compression failures there were some signs of crushing under the load points after shear failure had occurred. The brickwork strains were uniform across the compression face which suggests that no shear lag effects were present. In many of the beams which failed in shear longitudinal cracks developed over the pocket boundary immediately prior to failure. If shear reinforcement in the form of rectangular links which cross the pocket boundary had been used then both shear failure and longitudinal cracking may have been prevented. Shear failure usually occurred in heavily reinforced sections.

Comparison of the experimental results with the Draft Code indicated that rectangular section analysis gave better predictions than flanged section analysis for the rectangular sections. This is consistent with the experimental evidence, thus the Draft Code should acknowledge this. In practice flanged section analysis uses a fixed lever arm, independent of material

properties, which is an approximation that tends to underestimate the strength of lightly reinforced sections by up to about 25% whilst over estimating the strength of heavily reinforced sections. Thus the Draft Code imposes an unrealistic restriction on the design of rectangular-plan-shaped retaining walls, especially since many are lightly reinforced.

The failure loads of under-reinforced sections are generally better predicted by the Draft Code equations than those for over-reinforced sections. When the measured material strengths rather than values from the Draft Code were used in the analysis better predictions for under-reinforced sections were obtained, whilst for over-reinforced sections the reverse was true. In part, this is because the tensile strength of reinforcement may be more readily defined than the flexural compressive strength of brickwork. Also the lever arm may be more accurately assessed for under-reinforced sections. But in the case of an over-reinforced wall the Draft Code formulae are intended to provide a conservative limit to the moment of resistance rather than exactly define a value. It is also relevant to observe that as yet there is no broad agreement on the test specimen that should be used to determine the compressive strength of brickwork in direct compression and the question of whether this value would apply to flexural compression is open. The experimental results indicate that a four course high one brick square prism capped with 12mm thick fibre board may be a suitable small scale specimen.

In general pocket-type beams which failed in shear performed better than grouted cavity construction. There was no discernible trend between brick strength and shear resistance, however an increase in the percentage of tensile reinforcement did give an increase in the shear capacity of the section. It is clear that beams with low shear span ratios failed at greater shear stresses than those with high shear spans. This behaviour is consistent with that found in other types of reinforced brickwork and reinforced concrete beams. Design for shear to the Draft Code recommendations is unduly conservative primarily because the characteristic shear strengths are too low but also because the partial safety factory for shear is relatively high. Any revision of the Draft Code figures for shear strength should reflect the fact that shear span ratio has an important effect on the shear capacity of a pocket-type section. The Code already recognises the effect of the percentage of tensile reinforcement.

Concurrent with the experimental work a non-linear finite element program was developed to analyse pocket-type walls. A review of the literature revealed that little is known about the uniaxial stress-strain relationships of brickwork in directions other than on the bedface or about the biaxial behaviour. However there was enough information to justify using a square failure criterion although brickwork is known to be anisotropic. Brickwork was assumed to be linear elastic-plastic under uniaxial compression and linear elastic-brittle under uniaxial tension. An average elastic modulus of $600f_c$ was found to be adequate. Reinforcement was modelled as an elastic plastic material. In

some analyses a tension stiffening response was used to model degradation in stiffness due to crack formation in a reinforced brickwork structure.

Initially the finite element program was used to analyse a variety of test problems to examine its performance in relation to experimental results. The results indicated that it was able to analyse satisfactorily the load deflection response of one-way and two-way reinforced concrete slabs, reinforced brickwork retaining walls, two-way unreinforced brickwork panels and arching action in one-way brickwork panels. The analysis was not suitable for very lightly reinforced two way brickwork panels since tensile membrane action developed. It might have been expected that the simplified material properties assumed in the analyses woud lead to poor results. However this did not apply because the non-linear behaviour was primarily due to cracking, and was thus dependent mainly on the tensile strength.

Perhaps the main drawback of the finite element analysis was that it was unable to take into account out of plane shear stresses, thus it could not detect shear failure in beams. Fortunately the experimental results indicated that a pocket-type retaining wall was unlikely to fail in shear even when heavily reinforced.

The finite element program was developed primarily to investigate the effects of various parameters on the behaviour of pocket-type walls. Cost considerations prevented an experimental study. The parameters selected for examination were slenderness, pocket

some analyses a tension stiffening response was used to model degradation in stiffness due to crack formation in a reinforced brickwork structure.

Initially the finite element program was used to analyse a variety of test problems to examine its performance in relation to experimental results. The results indicated that it was able to analyse satisfactorily the load deflection response of one-way and two-way reinforced concrete slabs, reinforced brickwork retaining walls, two-way unreinforced brickwork panels and arching action in one-way brickwork panels. The analysis was not suitable for very lightly reinforced two way brickwork panels since tensile membrane action developed. It might have been expected that the simplified material properties assumed in the analyses woud lead to poor results. However this did not apply because the non-linear behaviour was primarily due to cracking, and was thus dependent mainly on the tensile strength.

Perhaps the main drawback of the finite element analysis was that it was unable to take into account out of plane shear stresses, thus it could not detect shear failure in beams. Fortunately the experimental results indicated that a pocket-type retaining wall was unlikely to fail in shear even when heavily reinforced.

The finite element program was developed primarily to investigate the effects of various parameters on the behaviour of pocket-type walls. Cost considerations prevented an experimental study. The parameters selected for examination were slenderness, pocket

spacing, panel thickness, percentage of reinforcement and arching action in panels. It has a further advantage in that trends in behaviour are not disguised by variation in brickwork properties. Both rectangular and flanged sections were analysed. Brickwork properties were kept unchanged for each analysis. Some of the results obtained from this parametic survey are given below in the form of design recommendations. These are qualitative and they require experimental verification.

The reinforced stem should be designed to cantilever from the base and transmit all the load on the pocket wall to the base. Analysis has indicated that the effective width of the stem should be taken as the lesser of h/3 or l_p . Two-way action will develop in the brickwork panels that span between the pockets, however careful consideration must be given to the sizing of the panels. This is dependent on their positions relative to the end of the wall and section type. For rectangular sections external panels should have an aspect ratio greater than 2.5 and 4 for wall thicknesses 330mm and 215mm respectively, whilst interior panels should have an aspect ratio greater than 1.25. This recommendation will allow designers plenty of scope to increase pocket spacing above 1.0m commonly used. Flanged sections are not considered suitable for exterior panels whilst for interior panels it is recommended that they should have an aspect ratio greater than 2.5. The analysis clearly indicates that on no account should panels be designed using yield line analysis or arching formulae because these are unconservative design methods.

8.2 Suggestions for further work

The suggestions for further work are given below are listed in order of priority. Only the most important aspects are included.

1. It is necessary to test a slender pocket-type wall to confirm that this construction meets the serviceability deflection requirements of the Code.

2. Verification of the parametric survey results is required for rectangular sections with exterior and interior panels. More precisely the limiting panel aspect ratio and mode of failure need to be studied experimentally. At least one wall in each category should be tested preferably with the limiting aspect ratio.

3. Pending the outcome of suggestion 2 further parametric surveys will be required to provide a set of design rules to cover all the likely combinations of material properties, wall sizes and loading conditions. This work should concentrate on determining limiting aspect ratios.

4. A cost benefit analysis into the relative merits of rectangular and flanged sections should be undertaken. The result is not obvious since aspect ratio and different design formulae in the Draft Code obscure the issue.

5. An extensive experimental investigation into the failure modes

of flanged sections would be informative. The parameters that merit particular attention are flange thickness, aspect ratio, slenderness and brickwork properties.

In addition the following points indicate how the finite element analysis could be improved.

1. The analysis should take account of out of plane shear stress. This could be achieved by using a Mindlin plate element or by modifying the current analysis. However if the latter approach was adopted it would require computation of the shear stresses from the change in direct stresses through the depth of the element and it would give a linear variation. This would only be an approximation to the actual variation in shear stress. A Mindlin plate would give a non-linear variation in shear stress and thus is more suitable.

2. Better material constitutive relationships are needed. This requires further research into the uniaxial and biaxial stress-strain behaviour of brickwork.

3. From the outcome of point 2 it should be possible to incorporate a better failure criterion for brickwork, especially in the tension-compression zone.

REFERENCES

1. British Standards Institution., CP111:1970 "Structural recommendations for load-bearing walls", London

2. Brebner A, "Notes on reinforced brickwork tests, theory and actual construction of reinforced brickwork in India", Gov.India Public Works Dept. Tech Paper No 38 (2vols), Gov Printing Office, India, 1923.

3. British Standards Institution "Draft for Public Comment (BS:5628:Part 2) "The structural use of masonry:Part 2 reinforced and prestressed masonry" London May 1981

4. Tellett J "A review of the literature on reinforced brickwork" (unpublished) British Ceramic Research Assocn.1983

5. Grogan J C & Plummer H C "Reinforced brick masonry retaining walls" Structural Clay Products Institute, Washington DC 1965

6. British Standards Institution CP114:1969 "The Structural use of reinforced concrete in buildings" London

7. Haseltine B A and Tutt J N "Brickwork retaining walls" Brick Development Assocn." August 1977

8. Structural Ceramic Advisory Group "Design guide for reinforced and prestressed clay brickwork" British Ceramic Research Assocn. Spec. Publ. 91 1977

9. Maurenbrecher A H P and Foster D "Design of a prestressed brickwork water tank" Structural Clay Products Ltd. SCP9 Hertford 1975

10. Maurenbrecher A H P, Bird A B Sutherland R J M & Foster D "Reinforced brickwork vertical cantilevers:1" Structural Clay Products Ltd, SCP10 Hertford 1976

11. Maurenbrecher A H P, Bird A B, Sutherland R J M & Foster D "Reinforced brickwork vertical cantilevers: 2" Structural Clay Products Ltd. SCP11 Hertford 1976

12. Bird A B "Reinforced brickwork windmill tower" Structural Clay Products Ltd. edited by D Foster SCP12 Hertford 1976

13. Maurenbrecher A H P "Reinforced brickwork pocket-type retaining wall" Structural Clay Products Ltd SCP13 edited by D Foster Hertford 1977

14. Foster D "Reinforced brickwork retaining walls - long term tests" Structural Clay Products Ltd SCP14 Hertford 1979

15. Johnson G D "Reinforced Brickwork retaining walls - design guide" Structural Clay Products Ltd SCP15 Hertford 1979

16. Sinha B P "Reinforced Brickwork grouted cavity shear tests" Structural Clay Products Ltd SCP16 edited by D Foster Hertford 1979

17. Brick and Tile Service Inc. " R.B.M. retaining walls" Bric and Tile Service, Greensboro, North Carolina

18. Abel C R and Cochran M R "A reinforced brick masonry retaining wall with reinforcement in pockets" SIBMAC Proceedings, edited by H W H West and K H Speed British Ceram. Res. Assoc. Stoke on Trent 1971

19. Sutherland R J M, private correspondence, 1981

20. Sutherland R J M "Reinforced masonry cantilever construction"reinforced and prestressed masonry, Proc. of Conf. held on 5 May 1982, Thomas Telford Ltd. London

21. Bell S, private correspondence 1982

22. Drinkwater J P and Bradshaw R E "Reinforced and prestressed masonry in agriculture", Reinforced and Prestressed Masonry, Proc. of Conf. held on 5 May 1982 Thomas Telford Ltd London

23. Drinkwater J P, private correspondence 1982

24. Filippi H "Brick Engineering - Reinforced brick masonry principles of design and construction" Brick Manufacturers Association of America Vol.3 1933

25. Plummer H and Blume J "Reinforced brick masonry and lateral force design" Washington DC Structural Clay Products Institute 1953

26. Sutherland R J M "Brick and block masonry in engineering" Proc. Instn. Civ. Engs. Part 1 (70) pp.31-63 Feb. 1981

27. British Standards Institution BS1146:1943 "Reinforced brickwork" London

28. British Standards Institution CP121:Part 1:1973 "Walling" London

29. British Standards Institution BS5628:Part 1:1978 "Structural use of masonry, unreinforced" London

30. Edgell G J, private correspondence 1983

31. Hambly E C "Bridge Foundations and substructures" Building Research Establishment report, HMSO London 1979

32. Coulomb C A "Essai sur une application des regles de maximis et minimis a quelques problems des statique relatifs a l'architecture" Mathematical Memoires presented to the Academie Royale des Sciences, Paris 1773

33. Rankine W J H "Theory on the stability of loose earth based on the ellipse of stresses" Phil.Trans. Royal Soc. 147,1857

34. Civil Engineering Codes of Practice Joint Committee, CP2:1951 "Earth retaining structures", Inst. Struct. Engrs. London

35. Broms. B B & Ingelson I "Earth pressure against the abutment of a rigid frame bridge" geotechnique, 21,no.1, p.15-28,1971

36. Sims F A & Jones J F "Comparison between theoretical and measured earth pressures acting on a large motorway retaining wall" J Inst. Highway Engrs, 26, Dec.1974 pp 26-29

37. Coyle H M Bartoskewitz R E Milberger L J & Butler H D "Field measurements of lateral earth pressures on a cantilever retaiing wall" Transportation Res. Rec. 517 pp 16-74

38. Ingold T S "Performance of a retaining wall with deep foundations, Ground Eng. 10, No.2, pp 24-25 March 1977

39. Ingold T S " The effects of compaction on retaining walls Geotechnieque, 29, No 3 pp 265-283 1979

40. Ingold T S "Lateral earth pressures - a reconsideration" Ground Eng. 13, No4 pp 39-43 May 1980

41. Strucutral Ceramics Advisory Group "Model specification for load bearing clay brickwork" SP 56:1980, British Ceramic Research Associaton, Stoke on Trent, 1980 (revision)

42. British Standards Institution BS3921:1974 "Clay bricks and Blocks",London

43. British Standards Institution BS12:1978 "Specification for ordinary and rapid hardening Portland cement", London

44. British Standards Institution, BS890:1972 "Building Limes" London

45. British Standards Institution CP110:Part 1:1972 "The structural use of concrete",London

46. British Standards Institution BS1200:1976 " Building sands" London

47. British Standards Institution BS4449:1978 "Specification for hot rolled steel bars for the reinforcement of concrete" London

48. Stafford Smith B & Carter C "Distribution of stresses in masonry walls subjected to vertical loading" Proc.2nd Int. Brick Masonry Conf. Stoke on Trent,1970,Edited by West H W H and Speed K.

49. Khoo C L & Hendry A W "A failure criterion for brickwork in axial compression" Brit. Ceram R A,Tech. Note 179,Feb 1972

50. Page A W "A non-linear analysis of the composite action of masonry walls on beams" Proc. Instn Civ.Engrs. Part 2,vol.67 March 1979

51. Samarasinghe W, Page A W & Hendry A W "A finite element model for the inplane behaviour of brickwork" Proc. Instn.Civ.Engrs Part 2,vol 73,March 1982

52. Rahman M A & Sawko F "Shear lag effect in brick diaphragm walls subjected to wind pressure" Int. J Masonry Constr. Vol 1, No 1,March 1980

53. Page A W "A biaxial failure criterion for brick masonry in the tension-tension range" Int. J. Masonry Constrc. Vol 1 No 1, March 1980

54. Phillips D V & Zienkiewicz O C "Finite element non-linear analysis of concrete structures" Proc.Instn.Civ Engrs. Part2, Vol.61,pp59-88,March 1976

55. Crisfield M A "Iterative sclution procedures for linear and non-linear structural analysis" Transport and Road Research Laboratory, Report 900, Crowthorne,1979

56. Crisfield M A "Variable step lengths for non-linear structural analysis" Transport and Road Research Laboratory, Report 1049,Crawthorn,1982

57. Powell B & Hodgkinson H R "Determination of stress-strain relationships for brickwork" Proc. 4th Int. Brick Masonry Conf., Bruges,1976

58. Edgell G J "Stress-strain relationships for brickwork-their application in the theory of unreinforced slender members " British Ceramic Research Association, Technical Note 313, Stoke on Trent,1980

59. Hodgkinson H R & Davies S "The stress-strain relationships of brickwork when stressed in directions other than normal to the bed face" Proc. 6th Int. Brick Masonry Conf., Rome,1982

60. Pedreschi R F "A study of the behaviour of post-tensioned brickwork beams" PhD. Thesis, Edinburgh, 1983

61. Dhanasekar M, Page A W & Kleenman P W "The elastic properties of brick masonry" International Journal of Masonry Construction, Vol.2,No 4, 1982

62. West H W H "The flexural strength of clay masonry determined from wallette specimens" British Ceramic Research Assocn. Technical Note 247, Stoke on Trent, 1976

63. Sinha, B P & Hendry A W "Tensile strength of brickwork specimens," British Ceramic Research Assocn. Technical Note 219, Stoke on Trent,1974

64. Haseltine B A & Moore J F A "Handbook to BS5628:Strutural Use of Masonry" Brick Development Associaton, Windsor,1980

65. Page A W "The biaxial compressive strength of brick masonry" Proc. Instrn of Civ. Engrs,Part 2,Vol 2,pp 893-906, 1981

66. Samarasinghe W & Hendry A W "Strength of brickwork under biaxial stress" Proc 7th International load bearing Brickwork Symposium,London,1980

67. Edgell G J, Tellett J & Hodgkinson H R "The buttressing resistance of lightly loaded partition walls" Proc. 6th International Brick Masonry Conference, Rome,1982

68. Kupfer H, Hilsdorf H K & Rusch H "Behaviour of concrete under biaxial stresses" Journal American Concrete Institute, Vol.66,No.8,pp656-666, August 1969

69. Hand F R, Pecknold D A & Schnobrich W C " A layered finite element analysis of reinforced concrete plates and shells" University of Illinois 1972

70. Moffatt K R & Lim P T K "Finite element analysis of composite box girder bridges having complete or incomplete interaction" Proc. Instn. Civ. Engrs Part 2, vol.61,pp 1-22, March 1976

71. Ziekiewicz O C "The finite element method" 3rd edition McGraw Hill London 1977

72. Cope R J & Rao P V "A two stage procedure for the non-linear analysis of slab bridges" Proc. Instn Civ.Engrs. Part 2 Vol 75, pp 671-688, December 1983

73. Jain S C & Kennedy J B "Yield criterion for reinforced concrete slabs" Journal of the Structural Division of American Society of Civil Engineers, Vol 99,No.ST7,Proc. paper 10409,pp 631-644, March 1974

74. Jofreit J C & McNiece G M "Finite element analysis of reinforced concrete slabs " Journal of the Structural Division of American Society of Civil Engineers Vol 97,ST3 pp785-806,March 1971

75. Johnson G D "Reinforced brickwork: Lateral resistance with bed joint reinforcement" Structural Clay Products Ltd, edited by D Foster, SCP18, Hertford,1982

76. Hodgkinson H R, Haseltine B A and West H W H "Preliminary tests on the effect of arching in laterally loaded walls" British Ceamic Res. Assoc., Tech. Note 250, January 1976.

77. Beeby A W "What are crack width limits for?" Concrete pp 31-33, Wexham Springs, July 1978

78. Edgell G J "Private communication" July 1983

79. Edgell G J, Tellett J and West H W H "Research into the behaviour of reinforced brickwork pocket-type retaining walls" 3rd North American Masonry Symposium, Augsut 1982

80. Suter G T and Hendry A W "The shear strength of reinforced brickwork beams" Structural Engineer, Vol 53, No 6,1975

81. Suter G T and Keller H "Shear strength of grouted reinforced masonry beams" Proc. 4th Int. Brick Masonry Conference, Brugge, 1976

82. Tellett J and Edgell G J "The shear strength of reinforced calcium silicate beams" British Ceramic Res. Assoc., Tech Note 332, 1982

83. Kani G N J "The riddle of shear failure and its solution" Journal of the American Conrete Institute , Vol 61, No4, p441, 1964

84. Jones L L and Wood R H "Yield-line analysis of slabs" Chatto and Windus, London 1967

85. Baker L R "Lateral loading of masonry panels- A state of the art report" Presented at symposium on Loadbearing brickwork held in Bombay, pp20, November 1981

APPENDIX A1

Formulation of the Element Stiffness Matrix

The element stiffness matrix, $[K^e]$ is composed from the material proprety matrix [D] and the [B] matrix which relates noctal displacements to internal strains. Each matrix is considered in turn. The element stiffness matrix is given by

$$[K^e] = \iint [B]^T [D] [B] \quad dx\, dy$$

The eccentric plate bending element has four corner nodes each having six degrees cf freedom, namely three displacements and three rotations that are related to the displacement functions, and when collected tcgether for the whcle element the resulting twenty four equaticns may be summarised by

$$\{\delta^e\} = [C]\{\alpha\}$$

or

$$\{\alpha\} = [C]^{-1}\{\delta^e\}$$

where $[C]^{-1}$ is a 24x24 matrix whose terms are given in reference[70] and are dependent upon the dimensions of the element. From consideration of the relationship between internal element strains, $\{\varepsilon\}$, and nodal displacements, $\{\delta^e\}$, a matrix [B] is found viz:

$$\{\varepsilon\} = [B]\{\delta^e\}$$

$$\{\varepsilon\} = [Q][C]^{-1}\{\delta^e\}$$

hence $[B] = [Q]\,[C]^{-1}$

The [C] matrix is independent of the position within the element whereas [Q] matrix whose terms are given in Table 2.7 is not. Thus the selection of points at which [Q] is evaluated is of prime importance in determining the strains accurately (see section 7.4.5)..

Consider the element shown in Fig. 4.8 in which the nodes i j k l are located on the reference surface and the top surface of the element is a distance, z, from the reference surface. If u_o v_o & w_o are the nodal displacements then the corresponding values of a point P on the top surface of the element are given by

$$u = u_o - z \frac{dw_o}{dx}$$

$$v = v_o - z \frac{dw_o}{dy}$$

$$w = w_o$$

These expressions may be differentiated to give expressions for strain within an element as

$$\begin{bmatrix} \varepsilon_x \\ \varepsilon_y \\ \gamma_{xy} \end{bmatrix} = \begin{bmatrix} 1 & 0 & 0 \\ 0 & 1 & 0 \\ 0 & 0 & 1 \end{bmatrix} \begin{bmatrix} \frac{\partial u_o}{\partial x} \\ \frac{\partial v_o}{\partial y} \\ \frac{\partial u_o}{\partial y} + \frac{\partial v_o}{\partial x} \end{bmatrix} + \begin{bmatrix} 1 & 0 & 0 \\ 0 & 1 & 0 \\ 0 & 0 & 1 \end{bmatrix} \begin{bmatrix} -z\frac{\partial^2 w_o}{\partial x^2} \\ -z\frac{\partial^2 w_o}{\partial y^2} \\ -2z\frac{\partial^2 w_o}{\partial x \partial y} \end{bmatrix}$$

Implicit in the relationships above are the following assumptions

(i) plane sections remain plane

(ii) the strains and deforations are small compared with element thickness

(iii)the plate element has a constant thickness

Assumption (i), usually known as kirchoff's law, strictly is not correct, though for elastic materials the error introduced is negligible provided assumptions (ii) applies. Kirchoff's law enables strains to be determined at any surface.

The strains and the curvatures are related to the stresses by the material property matrix [D], the terms of which are derived from consideration of the material properties (see section 7.3).

The relationships are

$$\{\sigma\} = [D]\{\varepsilon\} + [D]\{-z\chi\}$$

or in more detail as:

$$\begin{bmatrix} \sigma_x \\ \sigma_y \\ \tau_{xy} \end{bmatrix} = \begin{bmatrix} C_{11} & C_{12} & 0 \\ C_{21} & C_{22} & 0 \\ 0 & 0 & C_{33} \end{bmatrix} \begin{bmatrix} \varepsilon_{xo} \\ \varepsilon_{yo} \\ \gamma_{xyo} \end{bmatrix} + \begin{bmatrix} C_{11} & C_{12} & 0 \\ C_{21} & C_{22} & 0 \\ 0 & 0 & C_{33} \end{bmatrix} \begin{bmatrix} -z\chi_{xo} \\ -z\chi_{yo} \\ -2z\chi_{xyo} \end{bmatrix}$$

where $C_{11} = C_{22} = E/(1-\nu^2)$

$C_{12} = C_{21} = \nu E/(1-\nu^2)$

$C_{33} = E(1-\nu)/(2-2\nu^2)$

Integration of these relationships over the depth of the element gives the stress resultants (i.e. forces and moments per unit length across the elements) as:

$$\begin{Bmatrix} N \\ M \end{Bmatrix} = [D] \begin{Bmatrix} \varepsilon \\ \chi \end{Bmatrix}$$

or in more detail as

$$\begin{bmatrix} N_x \\ N_y \\ N_z \\ M_x \\ M_y \\ M_{xy} \end{bmatrix} = \begin{bmatrix} R_{11} & R_{12} & 0 & T_{11} & T_{12} & 0 \\ R_{21} & R_{22} & 0 & T_{21} & T_{22} & 0 \\ 0 & 0 & R_{33} & 0 & 0 & T_{33} \\ T_{11} & T_{12} & 0 & S_{11} & S_{12} & 0 \\ T_{21} & T_{22} & 0 & S_{21} & S_{22} & 0 \\ 0 & 0 & T_{33} & 0 & 0 & S_{33} \end{bmatrix} \begin{bmatrix} \varepsilon_{xo} \\ \varepsilon_{yo} \\ \gamma_{xyo} \\ \chi_{xo} \\ \chi_{yo} \\ \chi_{xyo} \end{bmatrix}$$

where the terms within the [D] matrix are related to the thickness of the element or station $(Z_2 - Z_1)$ as given below

$$R_{ij} = C_{ij}\,(Z_2 - Z_1)$$
$$T_{ij} = C_{ij}\,(Z_2^2 - Z_1^2)/2$$
$$S_{ij} = C_{ij}\,(Z_2^3 - Z_1^3)/3$$

For the special case where the reference surface coincides with the mid surface of the element $T_{ij} = 0$ and the relationships above reduce to the usual stress strain relationship for a concentric plate bending element in which the extensional and flexural behaviour are assumed to occur independently. Generally the reference surface does not coincide with the mid surface of the element therefore the extensional and flexural behaviour are coupled for the eccentric plate bending element.

APPENDIX A2

A Reconsideration of the deflections in the retaining wall tests

When the retaining walls tested experimentally were analysed using the finite element technieque it was found that there was reasonable agreement between measured and theoretical strains. However the theoretical deflections were less than half the measured deflections. This in itself was not sufficient reason to examine the discrepancy in any detail because the analysis contains many assumptions. Analysis of the pocket type beams that failed flexurally indicated that there was good agreement between the measured and theoretical strains and deflections. Furthermore the analysis had been shown to give acceptable results for a variety of test problems, chapter 4. Thus the experimental deflections of the walls were probably suspect and in need of reconsideration.

Wall 6, although failed, was still intact and able to carry quite large loads. From tests on this wall it was discovered that the steel base which acted as a foundaton was subject to rotation. This rotation increased the deflection measured at the top of the wall. Having established that not all the measured deflection was due to flexure of the wall a replica wall was built with the specific intention of determining other sources of extraneous movement and its effect on deflection of the walls.

Two sources of movement which caused additional lateral

deflection of the wall were identified. These were base rotation and vertical movement of the reinforcement anchorage plate relative to the base. In both cases they were assumed to increase linearly with applied moment.

Rotation of the base was dependent on how tightly the base is bolted to the floor. Moreover any changes in air temperature would cause the tightness of the bolts to change: this effect is impossible to quantify. Before wall 6 was demolished it was established that base rotation caused a lateral displacement at the top of the wall of 17mm; this assumes rigid body movement of the steel base about its compression edge. For the replicate wall only 7mm deflection at 240 KNm was attributeable to base rotation. It was assumed that these values increase linearly with applied load and were the upper and lower limits. In Table A.2 the mean value was used to find the estimated "true" deflections and the likely range.

Figure A.2 shows the details of the connection of the anchorage plate to the steel base. The anchorage was bolted to the base through slotted clearance holes with a large flat washer and a tapered washer spanning the hole. The 'T' shaped anchorage was made from 25 mm mild steel plates butt welded together which caused some distortion of the anchorage. Most of the movement of the anchorage is attributed to straightening out of the distortion although some may be due to slackness of the bolted connection. Upward movement of the anchorage would cause the crack at the base of the wall to widen thereby allowing greater

deflection of the wall. The displacement of the top of the wall due to movement of the anchorage was calculated assuming rigid body rotation of the wall about the tip of the crack and the length of the crack was determined from the neutral axis depth. At 240 KNm 2mm upward movement occurred which gave an approximate value that was assumed arbitrarily to vary by 25%.

The estimated "true" deflections of walls 2-6 are given in Table A.2 where they agree reasonably with those predicted by finite element analysis. Exceptions to this are the heavily reinforced slender walls which were subject to extensive crushing of the brickwork. Under these circumstances it is likely that the stiffness of the brickwork may have been over estimated in the analysis. A further possibility is that localised deformation of the steel base occurred under the compressive face of the wall although this is considered unlikely.

It is concluded that if deflections are considered important then tests on walls 1 and 5 should be repeated to established the actual deflection behaviour but with several modifications to the experimental procedure. Firstly the walls should be built off a reinforced concrete base and secondly the deflections should be measured relative to the base, not the floor as in the present investigation.

Figure A2 Anchorage Arrangement (Section)

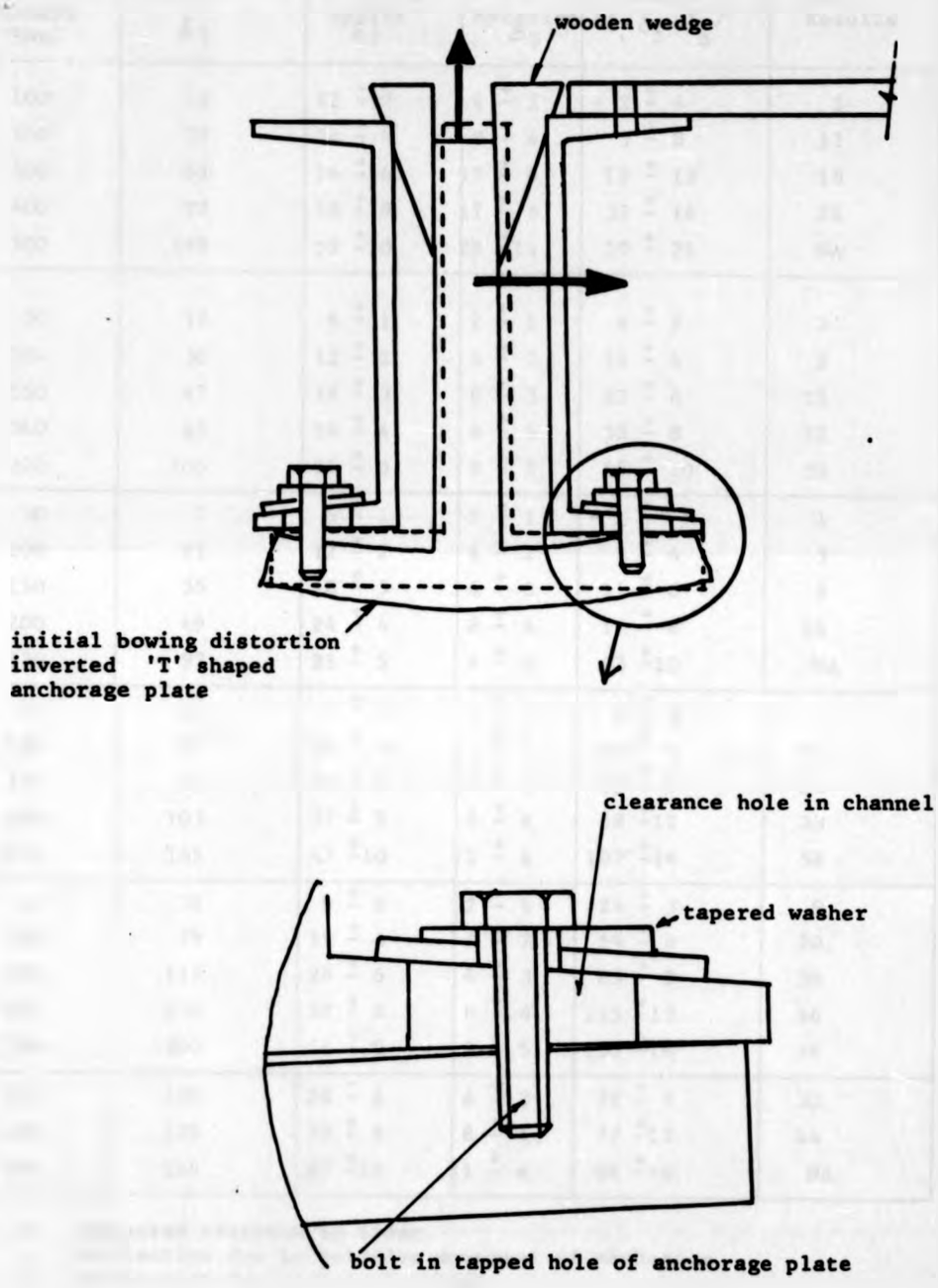

TABLE A.2 COMPARISON OF MEASURED, ESTIMATED AND PREDICTED DEFLECTIONS AT THE TOP OF THE WALL

Wall No	Applied Bending Moment (KNm)	Deflections (mm)				
		Experimental[1] δ_1	Anchorage[2] uplift δ_2	Base[3] Rotation δ_3	Estimated $(\delta_1-\delta_2-\delta_3)$	F.E Results
2	100	14	12 ± 2	4 ± 2	- 2 ± 4	5
	200	37	24 ± 4	8 ± 4	5 ± 8	11
	300	61	36 ± 6	13 ± 6	12 ± 12	18
	400	97	48 ± 8	17 ± 8	32 ± 16	26
	500	140	59 ±10	22 ±11	59 ± 21	NA
3	50	12	6 ± 1	2 ± 1	4 ± 2	3
	100	30	12 ± 2	4 ± 2	14 ± 4	8
	150	47	18 ± 3	6 ± 3	23 ± 6	15
	200	65	24 ± 4	8 ± 4	33 ± 8	22
	220	100	25 ± 5	9 ± 5	66 ± 10	32
4	50	7	6 ± 1	2 ± 1	- 1 ± 1	1
	100	21	12 ± 2	4 ± 2	5 ± 4	3
	150	35	18 ± 3	6 ± 3	11 ± 6	9
	200	49	24 ± 4	8 ± 4	17 ± 8	16
	220	97	25 ± 5	9 ± 5	63 ±10	NA
5	50	14	9 ± 2	2 ± 1	3 ± 3	7
	100	37	19 ± 4	4 ± 2	14 ± 6	16
	150	69	28 ± 6	6 ± 3	35 ± 9	24
	200	103	37 ± 8	8 ± 4	58 ±12	33
	250	165	47 ±10	11 ± 6	107 ±16	54
6	50	35	9 ± 2	2 ± 1	24 ± 3	9
	100	79	19 ± 4	4 ± 2	54 ± 6	20
	150	117	28 ± 6	6 ± 3	83 ± 9	30
	200	170	37 ± 8	8 ± 4	125 ±12	44
	220	200	41 ± 9	9 ± 5	150 ±14	56
7	150	106	28 ± 6	6 ± 3	72 ± 9	30
	200	122	37 ± 8	8 ± 4	77 ±12	44
	250	144	47 ±10	11 ± 6	86 ±16	NA

Notes: 1. measured relative to floor
2. deflection due to relative movement of anchorage
3. deflection due to base rotation

APPENDIX A.3

Yield line Analysis of Panel Carrying 3 Line loads

1. Interior Panels

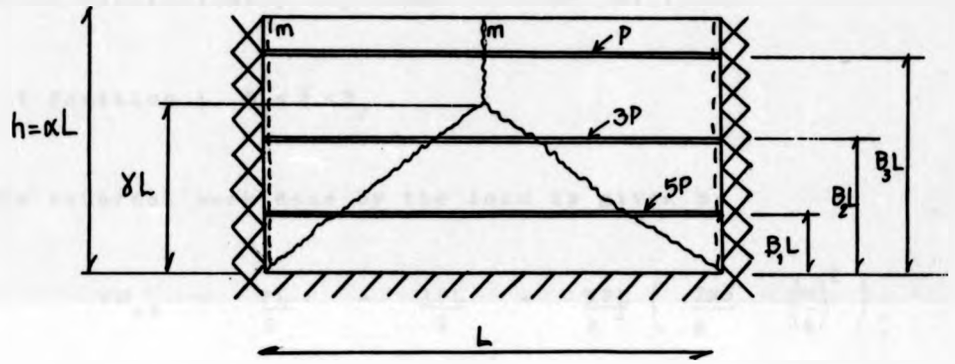

The loads used in the parametric survey were

P	applied at	5h/6	or B_3L
3P	"	h/2	or B_2L
5P	"	h/6	or B_1L

where P is the load per unit length

The boundary conditions assumed for an interior panel were fixity at three sides and free at the top.

The moment of resistance, for the vertical yield lines was m per unit length and for the horizontal lines μm per unit length, where μ is the orthogonal strength ratio. The internal work done

by the yield lines is

$$WD_{int} = m(\mu + 8\alpha\gamma) \qquad (A3.1)$$

The external work done by the loads is dependent on the bifurcation point of the yeild line in the centre of the panel which theoretically may occur in four positions

1.1 Position 1, $B_1 < \gamma < B_2$

The external work done by the load is given by

$$WD_{ex} = \frac{PL}{2} + \frac{3PL}{2} + \frac{5PL}{2}\left(\frac{2\alpha\gamma}{6} - \left(\frac{\alpha}{6}\right)^2\right)$$

$$= \frac{PL}{72\gamma^2}\left(\frac{144\gamma^2 - 5\alpha^2 + 60\gamma\alpha}{\mu + 8\gamma\alpha}\right) \qquad (A3.2)$$

For equilibrium the internal and external work must be equal. Thus equating eqns (A3.1) and (A3.2) and rearranging gives the work equation

$$m = \frac{PL}{72\gamma}\left(\frac{144\gamma^2 - 5\alpha^2 + 60\gamma\alpha}{\mu + 8\gamma\alpha}\right) \qquad (A3.3)$$

$\partial m / \partial \gamma = 0$ for maximum m

$$\frac{144\gamma^2 - 5\alpha^2 + 60\gamma\alpha}{72\mu\gamma + 576\gamma^2\alpha} = \frac{288\gamma + 60\alpha}{72\mu + 1152\gamma\alpha} \qquad (A3.4)$$

This eventually leads to a quadratic equation in terms of X, the solution of which is

$$\gamma = \frac{10\alpha^3 \pm \sqrt{100\alpha^6 + 150\mu\alpha^4 - 45\mu^2\alpha^2}}{120\alpha^2 - 36\mu} \qquad \text{(A3.5)}$$

A similar procedure is followed for each position of the yield line. Below only the work equation and the quadratic equation is given.

1.2 Position 2, $B_2 < \gamma < B_3$

the work equation is

$$m = \frac{PL}{18\gamma}\left(\frac{9\gamma^2 + 42\gamma\alpha - 8\alpha^2}{\mu + 8\gamma\alpha}\right) \qquad \text{(A3.6)}$$

and for a maximum m, γ is

$$\gamma = \frac{64\alpha^3 + \sqrt{4096\alpha^6 + 2688\mu\alpha^4 - 72\mu^2\alpha^2}}{336\alpha^2 - 9\mu} \qquad \text{(A3.7)}$$

1.3 Position 3, $B_3 < \gamma < \alpha$

the work equation is

$$m = \frac{PL}{24\gamma}\left(\frac{76\gamma\alpha - 19\alpha^2}{\mu + 8\gamma\alpha}\right) \qquad (A3.8)$$

and for a maximum m, γ is

$$\gamma = \frac{2\alpha \pm \sqrt{4\alpha^2 + 2\mu}}{8} \qquad (A3.9)$$

1.4 Position 4, $\alpha < \gamma$

For this case the bifurcation point is imaginary since it occurs above the panel. This requires another set of length parameters and a redefinition of the internal work equation.

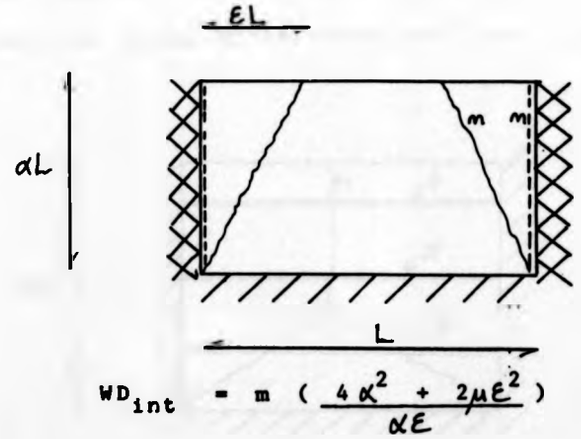

$$WD_{int} = m\left(\frac{4\alpha^2 + 2\mu\varepsilon^2}{\alpha\varepsilon}\right) \qquad (A3.10)$$

and the external work done is

$$WD_{ex} = \frac{PL}{12\alpha^2}\left(38\alpha^2 + 19\varepsilon\alpha^2\right) \qquad (A3.11)$$

and the work equation is

$$m = \frac{PL\varepsilon}{12\alpha}\left(\frac{38\alpha^2 - 19\alpha^2\varepsilon}{4\alpha^2 + 2\mu\varepsilon^2}\right) \qquad (A3.12)$$

for a maximum m, $\partial m/\partial\varepsilon = 0$

$$\frac{38\alpha^2\varepsilon - 19\alpha^2\varepsilon^2}{4\alpha^2 + 2\mu\varepsilon^2} = \frac{38\alpha^2 - 38\alpha^2\varepsilon}{4\mu\varepsilon}$$

This eventually gives a quadratic in ε, the solution of which is

$$\varepsilon = \frac{\alpha^2 \pm\sqrt{\alpha^4 + 2\mu\alpha^2}}{\mu} \qquad (A3.13)$$

2. Exterior Panels

The boundary conditions assumed for an exterior panel were simple supports along three sides and free along the top

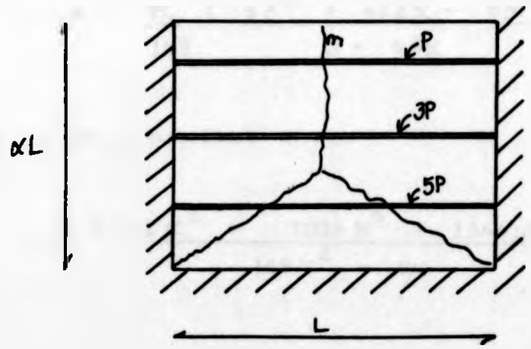

by inspection the internal work done is

$$WD_{int} = m \left(\frac{\mu + 4\gamma\alpha}{\gamma} \right) \qquad (A3.14)$$

And as before there are four cases to consider

2.1 Position 1, $B_1 < \gamma < B_2$

the work equation is

$$m = \frac{PL}{72\gamma} \left(\frac{144\gamma^2 - 5\alpha^2 + 60\gamma\alpha}{\mu + 4\gamma\alpha} \right) \qquad (A3.15)$$

and it is a maximum when

$$\gamma = \frac{5\alpha^3 \pm \sqrt{25\alpha^6 + 75\mu\alpha^4 - 45\mu^2\alpha^2}}{60\alpha^2 - 36\mu} \qquad (A3.16)$$

2.2 Position 2, $B_2 < \gamma < B_3$

the work equation is

$$m = \frac{PL}{18\gamma} \left(\frac{9\gamma^2 + 42\gamma\alpha - 8\alpha^2}{\mu + 4\gamma\alpha} \right) \qquad (A3.17)$$

and it is a maximum when

$$\gamma = \frac{32\alpha^3 + 1024\alpha^6 + 1344\mu\alpha^4 - 72\mu^2\alpha^2}{168\alpha^2 - 9\mu} \qquad (A3.18)$$

2.3 Position 3, $B_3 < \gamma < \alpha$

the work equation is

$$m = \frac{PL}{24\gamma}\left(\frac{76\gamma\alpha - 19\alpha^2}{\mu + 4\gamma\alpha}\right) \qquad \text{(A3.19)}$$

and it is a maximum when

$$\gamma = \frac{\alpha \pm \sqrt{\alpha^2 + \mu}}{4} \qquad \text{(A3.20)}$$

2.4 Position 4, $\alpha < \gamma$

the internal work equation is

$$WD_{int} = m\left(\frac{2\alpha^2 + 2\mu\varepsilon^2}{\alpha\varepsilon}\right) \qquad \text{(A3.21)}$$

hence the work equation is

$$m = \frac{PL\varepsilon}{24\gamma}\left(\frac{38\alpha^2 - 19\alpha\varepsilon^2}{\alpha^2 + \mu\varepsilon^2}\right) \qquad \text{A3.22)}$$

and it is a maximum when

$$\varepsilon = \frac{\alpha^2 \pm \sqrt{\alpha^4 + 4\mu\alpha^2}}{2\mu} \qquad \text{A3.23)}$$

3. Bending moment coefficients

The equations have been evaluated and a series of bending moment coefficients are given in Table A.3. It should be noted that if

the length coefficient δ or ε lay outside the range appropriate to the bifucation point the coefficients were ignored. Where there were two acceptable bending moment coefficients the lower was deemed to apply since this would give the lowest upper bound.

As this analysis was employed in assessing the performance of brickwork with isotropic properties the orthogonal ratio, μ, is equal to unity and only values for this case are given in Table A.3

4. Panel strength

The moment of resistance of a panel is equal to the produce of the tensile strength and the elastic modulus

$$\text{ie} \quad f_t \frac{ht^2}{6} \qquad \text{(A3.24)}$$

This may be equated with the moment on the panel which is dependent on the boundary conditions of the panel and the applied load

$$\text{ie} \quad f_t \frac{ht^2}{6} = P\,lh\lambda \qquad \text{(A3.25)}$$

Where λ is the bending moment coefficient and 9P is the total load per unit length. The relationship between the moment at the base and the total applied load is given by

$$M = \frac{19}{6} P l h \qquad (A3.26)$$

Eliminating P from eqns (A3.25) and (A3.26) gives the moment capacity of the panel in terms of the moment at the base of the retaining wall.

$$\text{ie} \quad M_{panel} = 0.5277 f_t \frac{ht^2}{\lambda} \qquad (A3.27)$$

Table A3.1 Bending moment coefficents for panels in a pocket type wall.

Aspect ratio	Interior Panels	Exterior Panels
0.25	0.435	0.674
0.50	0.410	0.638
0.75	0.392	0.604
1.00	0.353	0.564
1.25	0.316	0.515
1.50	0.289	0.466
1.75	0.262	0.423
2.00	0.239	0.384
2.25	0.219	0.351

APPENDIX A4

STRESS - STRAIN CURVES FOR THE REINFORCEMENT

Typical stress-strain curve for a 16ϕ bar

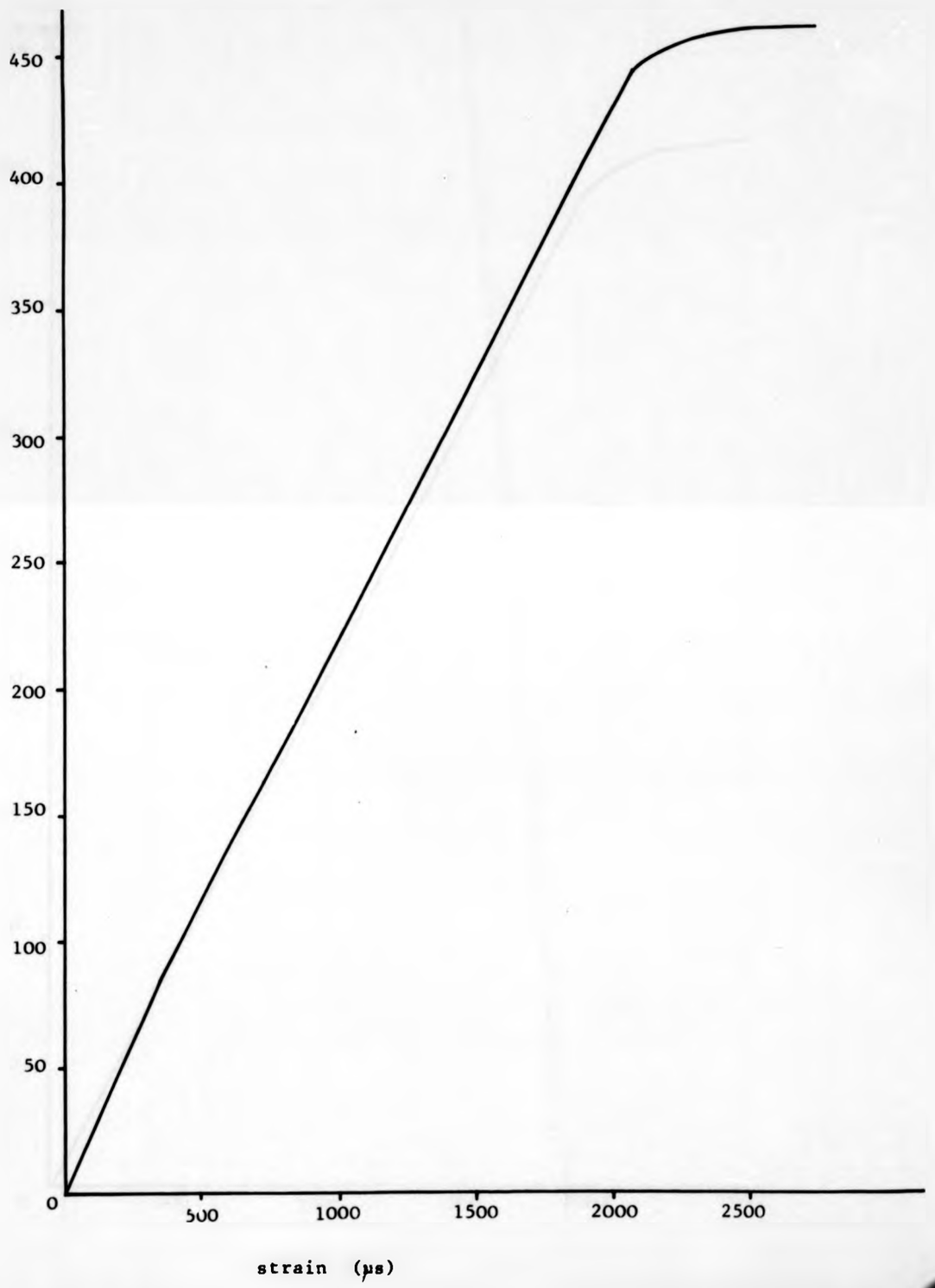

Typical stress-strain curve for a 25ϕ bar

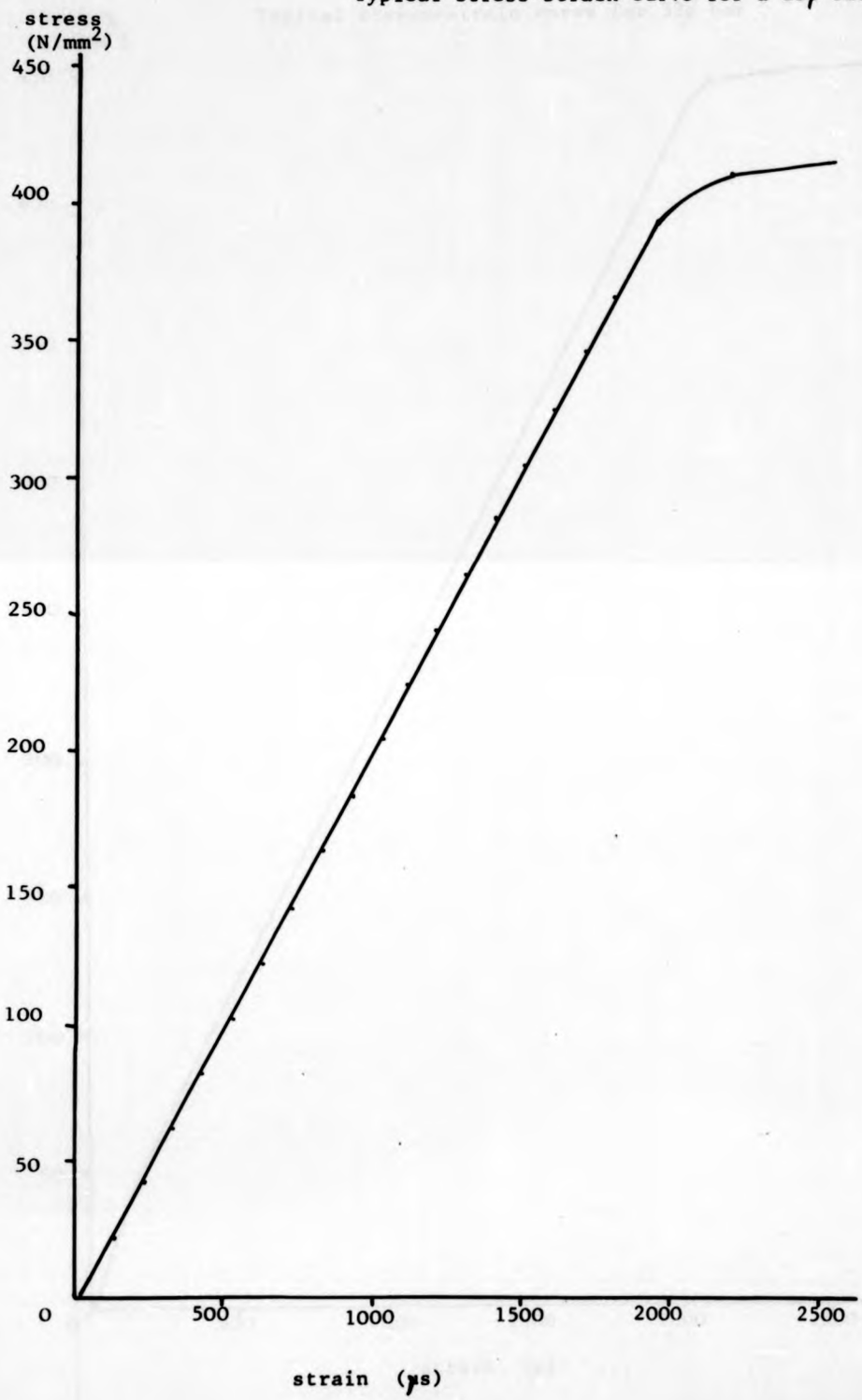

Typical stress-strain curve for 32ϕ bar